

Studies on Bio-Oxygenated Fuelled Stationary C.I. Engine

Ph.D. Thesis

ASHISH NAYYAR

ID No. 2011RME7142



DEPARTMENT OF MECHANICAL ENGINEERING
MALAVIYA NATIONAL INSTITUTE OF TECHNOLOGY JAIPUR, INDIA

April, 2018

Studies on Bio-Oxygenated Fuelled Stationary C.I. Engine

*Submitted in
fulfillment of the requirements for the degree of*

Doctor of Philosophy

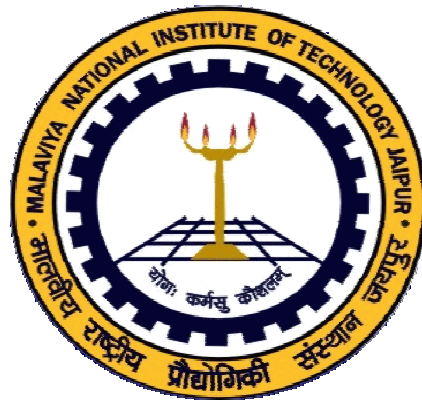
by

Ashish Nayyar

ID: 2011RME7142

Under the supervision of

Prof. Dilip Sharma and Prof. S. L. Soni



DEPARTMENT OF MECHANICAL ENGINEERING

MALAVIYA NATIONAL INSTITUTE OF TECHNOLOGY JAIPUR, INDIA

April, 2018

© Malaviya National Institute of Technology Jaipur, 2018
All rights reserved.

Dedicated to

My Family



**DEPARTMENT OF MECHANICAL ENGINEERING
MALAVIYA NATIONAL INSTITUTE OF TECHNOLOGY, JAIPUR**

Certificate

This is to certify that the thesis entitled '**Studies on Bio-Oxygenated Fuelled Stationary C.I. Engine**' being submitted by **Mr. Ashish Nayyar (2011RME7142)** is a bonafide research work carried out under our supervision and guidance in fulfillment of the requirement for the award of the degree of **Doctor of Philosophy** in the Department of Mechanical Engineering, Malaviya National Institute of Technology, Jaipur, India. The matter embodied in this thesis is original and has not been submitted to any other University or Institute for the award of any other degree.

(Dr. Dilip Sharma)

Professor

Department of Mechanical

Engineering

MNIT Jaipur

(Dr. S. L. Soni)

Professor

Department of Mechanical

Engineering

MNIT Jaipur

Place: Jaipur

Date: 19:04:2018

DECLARATION

I, **Ashish Nayyar**, declare that this thesis titled, “**Studies on Bio-Oxygenated Fuelled Stationary C.I. Engine**” and the work presented in it, are my own. I confirm that:

- This work was done wholly or mainly while in candidature for a research degree at this university.
- Where any part of this thesis has previously been submitted for a degree or any other qualification at this university or any other institution, this has been clearly stated.
- Where I have consulted the published work of others, this is always clearly attributed.
- Where I have quoted from the work of others, the source is always given. With the exception of such quotations, this thesis is entirely my own work.
- I have acknowledged all main sources of help.
- Where the thesis is based on work done by myself, jointly with others, I have made clear exactly what was done by others and what I have contributed myself.

Date: April 19, 2018

Ashish Nayyar

(2011RME7142)

Acknowledgement

It gives me immense pleasure to express my sincere thanks to my supervisors, Respected Prof. S. L. Soni and Prof. Dilip Sharma, Department of Mechanical Engineering, Malaviya National Institute of Technology Jaipur, for their valuable guidance, encouragement and help. I would be thankful to them throughout my life.

I would also like to thank members of my doctoral guidance committee, Dr. G. D. Agarwal, Dr. Madhu Agarwal and Dr. N. Rohatgi for their valuable suggestions and cooperation throughout the course of study. I am also thankful to Prof. Awadhesh Kumar Bhardwaj, Convener-DPGC and Prof. G. S. Dangayach, Head-Department of Mechanical Engineering.

My sincere thanks to Dr. Manu Augustine, Dr. Bhuvnesh Bhardwaj, Dr. Alok Mathur, Dr. N. K. Banthiya, Mr. Naveen K. Sain, Mr. Inzamam Ulhaque, Mr. Sudhir Pathak, Mr. Ankit Agarwal, Mr. Dinesh Kumar Sharma, Mr. Chandan Gupta and Mr. Dinesh L. Gupta without whose help it would have been difficult to complete my thesis writing.

I am grateful to Mrs. Rachna Meel, Registrar SKIT, Mr. Jaipal Meel, Director SKIT and Dr. S. L. Surana, Director (Academics) SKIT for their cooperation and support.

I am also grateful to my parents, in-laws and brothers for their support, good wishes and blessings for my successful completion of research work.

I am grateful to my wife Mrs. Rimple Nayyar for her understanding and moral support during this period. I appreciate her patience, encouragement and the pains taken in looking after the entire family.

I am glad to express my sincere thanks to my little son Harshil and niece Kanan who have helped me to ease the pressure of the last crucial phase of work with their cheerful company.

Last, but not the least, I wish to express my gratefulness to all my friends, relatives, colleagues and students for their support, assistance and encouragement.

Thank you all.

Place: Jaipur

Date: April 19, 2018

(Ashish Nayyar)

Abstract

Environmental pollution is increasing rapidly due to emissions produced by burning of fossil fuels in internal and external combustion engines. The use of internal combustion (I.C.) engines has been increased in mobile as well as in stationary applications. Diesel engines are the main source of smoke and NO_x emissions. The use of biofuel and oxygenated additives in diesel is one of the potential solutions. Improved fuel can be used in new as well as in old engines with minor modifications or without any modification at all.

Vegetable oils, biodiesels, alcohols and many other compounds are compatible with diesel engines. This study explores the possibility of using ternary blends of additives, n-butanol and diesel in compression ignition (C.I.) engines to control emissions of smoke and NO_x. The main focus of this thesis is to determine suitable additives for oxygenated biofuel-diesel blends for improved engine performance and reduced emissions (particularly smoke and NO_x). Further, the study also aims to develop mathematical models to predict engine performance and emissions for the suggested ternary blend.

To achieve the stated objectives in a structured fashion, an experimental investigation was done on a small size, single cylinder, four stroke, constant speed, water cooled, direct injection variable compression ratio (VCR) diesel engine. The bio-oxygenated fuel used in the present work is n-butanol. The optimized n-butanol-diesel blend (BU20) was taken as base fuel to investigate the effects of nitromethane (NM), 2-Methoxy-ethyl-ether/Diglyme (DGM) and Diethylether (DEE) on performance and emissions of the engine. Different concentrations of n-butanol-diesel blends were prepared to range from 10%-25% on a volume basis (v/v) and were designated as BU10, BU15, BU20, BU25 (The numerals indicating the percentage of n-butanol in the blend). NM-BU20 blends were prepared to range from 1-3% (v/v) and were designated as NM1BU20, NM2BU20, and NM3BU20. DGM-BU20 and DEE-BU20 blends were prepared to range from 5-20% (v/v) and were designated as DGM5BU20, DGM10BU20, DGM15BU20, DGM20BU20 and DEE5BU20, DEE10BU20, DEE15BU20 and DEE 20BU20.

Investigations were performed in four stages. In the first stage, tests were performed using diesel only (B0) to obtain baseline data involving the optimal settings of compression ratio, injection timing and injection pressure. In the second stage, tests were

performed with n-butanol-diesel blends on the optimum engine settings as obtained in the first stage. From this set of data, the optimum blend (which eventually turned out to be BU20) was selected. In the third stage, tests were performed with varying compression ratios, injection timings and injection pressures to optimize these operating parameters for BU20. In the fourth stage, tests were conducted with NM-BU20, DGM-BU20 and DEE-BU20 blends. An overall comparison of all tested fuels was done to find the most suitable ternary bio-oxygenated fuel for optimum engine performance and emissions.

With mathematical modeling, reduced quadratic and cubic models were obtained to predict the optimum values of engine operating parameters with BU20 and blending ratios of different additives for desired values of outputs.

With n-butanol-diesel blends, the optimum performance and emissions of the engine was observed with BU20 at a higher compression ratio of 19.5 under similar operating conditions. For all NM-BU20 blends, BSFC was higher and BTE improved slightly in comparison to BU20. Smoke & CO were reduced by 28.8% & 6.3% and NO_x & HC emissions were increased by 9.55% & 33.33% respectively for NM1BU20 as compared to BU20 at full load condition. For all DGM-BU20 blends, BSFC was higher as compared to BU20. Smoke & NO_x were reduced by 28.57% & 9.55% and CO & HC emissions were increased by 38.23% & 38.88% respectively for DGM15BU20 as compared to BU20 at full load condition. The change in BSFC was negligible with blending of DEE in BU20. Smoke & NO_x reduced by 9.52% & 8.53%; while CO & HC increased by 14.7% and 55.55% for DEE10BU20 as compared to BU20 at full load condition.

An overall comparison of BU20, NM1BU20, DGM15BU20 and DEE10BU20 revealed that DGM15BU20 showed better results of performance and emissions. BSFC and BTE of DGM15BU20 were higher as compared to diesel by 11.8% and 8.8% respectively at full load condition. For DGM15BU20, smoke & NO_x were lesser by 66.9% & 21.9% and CO & HC were more by 30.6% & 47.1% respectively as compared to diesel at full load condition. The ternary blend of Diglyme-n-butanol-diesel (DGM15BU20) was concluded to be the best blended fuel amongst all the tested blends for the experimental C.I. engine. It can also be quite confidently stated that this fuel could contribute well towards a cleaner environment in near future.

Contents

Certificate.....	iv
Declaration.....	v
Acknowledgement	vi
Abstract.....	vii
Contents	ix
List of Figures	xiv
List of Tables.....	xxi
Nomenclature.....	xxiv
Chapter 1.....	1
Introduction	1
1.1 Introduction	1
1.2 Energy demand and perspectives.....	2
1.3 Oil demand and perspectives	3
1.4 Emissions characteristics of internal combustion engines	8
1.4.1 Types of emissions from diesel engines	9
1.4.2 Growth of mobile engines in India	11
1.4.3 Stationary diesel engines.....	11
1.5 Air pollution in India	12
1.6 Diesel emissions and human health solutions.....	13
1.7 Need of alternative fuels/biofuels and additives	14
1.8 Limitations of biofuels.....	15
1.9 Alcohol as alternative fuel	16
1.9.1 Advantages of alcohols	17
1.9.2 Limitations of alcohol.....	17
1.9.3 Use of alcohols in C.I. engines	18
1.10 Addition of nitrogenated and oxygenated additives:	19
1.11 Compatibility with engine operation and material.....	20
1.12 Outline of the Thesis.....	22

Chapter 2.....	23
Literature Review	23
2.1 Vegetable oil as C.I. engine fuel:	24
2.2 Biodiesel as C.I. engine fuel:	26
2.3 Alcohols as C.I. engine fuels:	29
2.3.1 Methanol and Ethanol	30
2.3.2 N-butanol:	33
2.4 Other oxygenated additives as C.I. engine fuel:.....	44
2.4.1 Nitromethane.....	47
2.4.2 2-Methoxyethyl ether/Diglyme (DGM)	49
2.4.3 Diethylether.....	51
2.5 Motivation and research gap.....	55
2.6 Objectives	57
2.7 Research procedure and methodology	57
Chapter 3.....	59
Experimental Set-Up and Procedure	59
3.1 Test engine	59
3.2 Test installation description	59
3.3 Emission measurements.....	63
3.3.1 AVL Smoke-meter (Austria, Model: 437C).....	63
3.3.2 Exhaust gas analyzer (AVL India, Model: 444N).....	64
3.4 Fuel Preparation.....	65
3.5 Experimental procedure	67
3.6 Uncertainty in measurement	67
3.7 Development of prediction models	68
Chapter 4.....	71
Experimental Results and Discussions.....	71
4.1 Optimization of engine operating parameters with diesel (B0)	71
4.2 Performance and emissions characteristics of the engine using n-butanol-diesel blends:	76

4.2.1 Analysis of pressure-crank angle diagram for n-butanol-diesel blends	77
4.2.2 Determination of optimum blend of n-butanol-diesel	78
4.2.3 Modeling for n-butanol-diesel blends	78
4.2.3.1 Diagnosis of data for analysis of variance n-butanol-diesel blends.....	79
4.2.3.2 ANOVA for response surface model for n-butanol-diesel blends	83
4.2.3.3 Comparison of observed and estimated responses	91
4.2.4 Performance of engine using n-butanol diesel blends.....	93
4.2.4.1 Brake specific fuel consumption (BSFC).....	93
4.2.4.2 Variation of brake specific energy conversion	96
4.2.4.3 Brake thermal efficiency	97
4.2.5 Emissions of engine using n-butanol blends	100
4.2.5.1 Variation of Smoke	100
4.2.5.2 Variation of NOx.....	102
4.2.5.3 Variation of CO	105
4.2.5.4 Variation of HC	107
4.2.6 Validation and optimization of responses	109
4.3 Optimization of engine operating parameters for BU20 (Third Phase):	111
4.3.1 Development of prediction models with BU20	111
4.3.1.1 Diagnosis of data for analysis of variance for BU20.....	114
4.3.1.2 ANOVA for response surface model for BU20	117
4.3.2 Performance of engine using BU20 with varying parameters	124
4.3.2.1 Brake specific fuel consumption (BSFC).....	124
4.3.2.2 Brake thermal efficiency	125
4.3.3 Emissions of engine using BU20 with varying operating parameters	127
4.3.3.1 Variation of Smoke	127
4.3.3.2 Variation of NOx.....	128
4.3.3.3 Variation of CO	129
4.3.3.4 Variation of HC	130
4.3.4 Validation and optimization of response.....	131
4.4 Comparison of performance and emissions characteristics of diesel and BU20	132
4.5 Performance and emissions characteristics of the engine using nitromethane-n-butanol-diesel blends:	133
4.5.1 Determination of optimum blends of nitromethane-n-butanol (20%)-diesel (NM-BU20):	133

4.5.2 Modeling for NM-BU20 blends	134
4.5.2.1 Diagnosis of data for analysis of variance for NM-BU20 blends	135
4.5.2.2 ANOVA for response surface model for NM-BU20 blends.....	138
4.5.2.3 Comparison of observed and estimated responses for NM-BU20 blends	144
4.5.3 Performance of engine using nitromethane-n-butanol-Diesel (NM-BU20) blends.....	146
4.5.3.1 Brake specific fuel consumption (BSFC)	146
4.5.3.2 Brake thermal efficiency	148
4.5.4 Emissions of engine using nitromethane-n-butanol-diesel (NM-BU20) blends.....	150
4.5.4.1 Variation of Smoke.....	150
4.5.4.2 Variation of NO _x	151
4.5.4.3 Variation of CO	152
4.5.4.4 Variation of HC	154
4.5.5 Validation and optimization of responses	156
4.6 Performance and emissions characteristics of the engine using diglyme-BU20 blends:	157
4.6.1 Determination of optimum blend of diglyme-BU20 (DGM-BU20)	158
4.6.2 Modeling for diglyme-n-Butanol (20%)-diesel (DGM-BU20) blends.....	158
4.6.2.1 Diagnosis of data for analysis of variance for DGM-BU20 blends	159
4.6.2.2 ANOVA for response surface model for DGM-BU20 blends.....	162
4.6.2.3 Comparison of observed and estimated responses for DGM-BU20 blends.....	169
4.6.3 Performance of engine using DGM-BU20 blends	170
4.6.3.1 Brake specific fuel consumption (BSFC)	170
4.6.3.2 Brake thermal efficiency	173
4.6.4 Emissions of engine using DGMBU20 blends.....	174
4.6.4.1 Variation of Smoke.....	174
4.6.4.2 Variation of NO _x	176
4.6.4.3 Variation of CO	178
4.6.4.4 Variation of HC	179
4.6.5 Validation and optimization of responses	181
4.7 Performance and emissions characteristics of the engine using diethylether-BU20 blends.....	182
4.7.1 Determination of optimum blend of diethylether-BU20	183
4.7.2 Modeling for diethylether-n-butanol-diesel (DEE-BU20) blends.....	183
4.7.2.1 Diagnosis of data for analysis of variance for DEE-BU20 blends.....	184
4.7.2.2 ANOVA for response surface model for DEE-BU20 blends	187

4.7.2.3 Comparison of observed and estimated responses for DEE-BU20 blends	193
4.7.3 Performance of engine using diethylether-n-butanol-diesel (DEE-BU20) Blends	195
4.7.3.1 Brake specific fuel consumption (BSFC)	195
4.7.3.2 Brake thermal efficiency	197
4.7.4 Emissions of engine using diethylether-n-butanol-diesel (DEE-BU20) blends	199
4.7.4.1 Variation of Smoke	199
4.7.4.2 Variation of NO _x	201
4.7.4.3 Variation of CO	203
4.7.4.4 Variation of HC	204
4.7.5 Validation and optimization of responses	206
4.8 Comparison of performance and emissions of BU20, NM1BU20, DGM15BU20 and DEE10BU20 blends.....	207
4.8.1 Heat release rate for BU20, NM1BU20, DGM15BU20 and DEE10BU20 blends	207
4.8.2 Comparison of performance of BU20, NM1BU20, DGM15BU20 and DEE15BU20 blends ..	208
4.8.3 Comparison of emissions of BU20, NM1BU20, DGM15BU20 and DEE10BU20 blends	210
4.8.4 Smoke-NO _x trade-off for BU20, NM-BU20, DGM-BU20 and DEE-BU20 blends	214
4.9 Comparison of performance and emissions of DGM15BU20 with diesel.....	215
4.10 Economic analysis of blended fuel	215
Chapter 5.....	217
Conclusions and Future Scope	217
5.1 Conclusions	217
5.2 Future Scope	220
References	221
Appendix-A	238
Appendix-B	239
Appendix-C	240
Brief bio-data.....	242
Publications.....	243

List of Figures

F. No.	Title	Page No.
1.1	Total final consumption of energy by sectors in Modern Scenario	2
1.2	Primary energy supply (MTOE) and percentage share under Modern Scenario	3
1.3	World oil demand and price by scenario	4
1.4	Share of fuel in transportation (Modern Scenario)	6
1.5	Fuel demand by various transport sectors in India under New Policy Scenario	7
1.6	Transportation fuel demand for passenger transportation in India in new policy scenario	8
1.7	Energy demand by fuel type in different sectors of India	12
3.1 (a)	Schematic of engine set-up	60
3.1 (b)	Schematic of engine set-up	61
3.2	Actual engine set-up	61
3.3	AVL smoke-meter	62
3.4	AVL exhaust gas analyzer	64
4.1	Effect of engine operating parameters on BSFC	73
4.2	Effect of engine operating parameters on BTE	74
4.3	Effect of engine operating parameters on smoke	74
4.4	Cylinder pressure vs. crank angle diagram (at 100% rated power)	76
4.5 (a)	Plot of normal % probability vs. internal studentized residuals for BSFC & BSEC	79
4.5 (b)	Plot of internal studentized residuals vs. predicted response for BSFC & BSEC	80
4.6 (a)	Plot of normal % probability vs. internal studentized residuals for BTE	80
4.6 (b)	Plot of internal studentized residuals vs. predicted response for BTE	80
4.7 (a)	Plot of normal % probability vs. internal studentized residuals for smoke	81
4.7 (b)	Plot of internal studentized residuals vs. predicted response for smoke	81

4.8 (a)	Plot of normal % probability vs. internal studentized residuals for NO _x	81
4.8 (b)	Plot of internal studentized residuals vs. predicted response for NO _x	81
4.9 (a)	Plot of normal % probability vs. internal studentized residuals for CO	82
4.9 (b)	Plot of internal studentized residuals vs. predicted response for CO	82
4.10 (a)	Plot of normal % probability vs. internal studentized residuals for HC	82
4.10 (b)	Plot of internal studentized residuals vs. predicted response for HC	82
4.11	Plot of actual values vs. predicted values for (a) BSFC (b) BTE	91
4.12	Plot of actual values vs. predicted values for (a) Smoke (b) NO _x (c) CO (d) HC	92
4.13	Variation of BSFC with engine load for n-butanol-diesel blends	93
4.14	Variation in BSFC due to combined effect of load and n-butanol blending	94
4.15	Variation in BSFC with load and n-butanol-diesel blends at minimum and maximum values	94
4.16	Variation of BSEC with engine load for n-butanol-diesel blends	95
4.17	Variation of BSFC and BSEC for different n-butanol-diesel blends at full load condition	96
4.18	Variation of BTE with engine load for diesel and n-butanol-diesel blends	97
4.19	Variation in BTE due to combined effect of load and n-butanol blending	98
4.20	Variation in BTE with load and n-butanol-diesel blends at minimum and maximum values	98
4.21	Variation in smoke for n-butanol blends	99
4.22	Variation in smoke due to combined effect of load and n-butanol blending	100
4.23	Variation in smoke with load and n-butanol-diesel blends at minimum and maximum values	100
4.24	Variation in NO _x for n-butanol blends	101
4.25	Variation in NO _x due to combined effect of load and n-butanol blending	102
4.26	Variation in NO _x with load and n-butanol-diesel blends at minimum and maximum values	102
4.27	Smoke-NO _x trend for n-butanol diesel blends	103
4.28	Variation in CO for n-butanol blends	104

4.29	Variation in CO due to combined effect of load and n-butanol blending	105
4.30	Variation in CO with load and n-butanol-diesel blends at minimum and maximum values	105
4.31	Variation in HC for n-butanol blends	106
4.32	Variation in HC due to combined effect of load and n-butanol blending	107
4.33	Variation in HC with load and n-butanol-diesel blends at minimum and maximum values	107
4.34	Performance and emission of n-butanol diesel blends (100% rated power)	108
4.35 (a)	Plot of normal % probability vs. internal studentized residuals for BSFC	113
4.35 (b)	Plot of internal studentized residuals vs. predicted response for BSFC	113
4.36 (a)	Plot of normal % probability vs. internal studentized residuals for BTE	114
4.36 (b)	Plot of internal studentized residuals vs. predicted response for BTE	114
4.37 (a)	Plot of normal % probability vs. internal studentized residuals for smoke	114
4.37 (b)	Plot of internal studentized residuals vs. predicted response for smoke	114
4.38 (a)	Plot of normal % probability vs. internal studentized residuals for NO _x	115
4.38 (b)	Plot of internal studentized residuals vs. predicted response for NO _x	115
4.39 (a)	Plot of normal % probability vs. internal studentized residuals for CO	115
4.39 (b)	Plot of internal studentized residuals vs. predicted response for CO	115
4.40 (a)	Plot of normal % probability vs. internal studentized residuals for HC	116
4.40 (b)	Plot of internal studentized residuals vs. predicted response for HC	116
4.41 (a)	BSFC at different CRs, injection timings and injection pressures for BU20	123
4.41 (b)	BSEC at different CRs, injection timings and injection pressures for BU20	124
4.42	BTE at different CRs, injection timings and injection pressures for BU20	124
4.43	Variation in BTE due to combined effect of (a) CR and injection Pressure and (b) Injection Timing and Injection Pressure for BU20	125
4.44	Smoke emission at different CRs, injection timings and injection pressures for BU20	126
4.45	Variation in smoke due to combined effect of (a) CR and injection Timing and (b) Injection Pressure and Injection Timing for BU20	127

4.46	NO _x emission at different CRs, injection timings and injection pressures for BU20	128
4.47	Variation in NO _x due to combined effect of (a) CR and injection Timing and (b) Injection Pressure and Injection Timing for BU20	128
4.48	CO emission at different CRs, injection timings and injection pressures for BU20	129
4.49	Variation in CO due to combined effect of CR and injection Pressure for BU20	129
4.50	HC emission at different CRs, injection timings and injection pressures for BU20	130
4.51	Comparison of diesel and BU20 performance and emissions	131
4.52 (a)	Plot of normal % probability vs. internal studentized residuals for BSFC	134
4.52 (b)	Plot of internal studentized residuals vs. predicted response for BSFC	134
4.53 (a)	Plot of normal % probability vs. internal studentized residuals for BTE	135
4.53 (b)	Plot of internal studentized residuals vs. predicted response for BTE	135
4.54 (a)	Plot of normal % probability vs. internal studentized residuals for smoke	135
4.54 (b)	Plot of internal studentized residuals vs. predicted response for smoke	135
4.55 (a)	Plot of normal % probability vs. internal studentized residuals for NO _x	136
4.55 (b)	Plot of internal studentized residuals vs. predicted response for NO _x	136
4.56 (a)	Plot of normal % probability vs. internal studentized residuals for CO	136
4.56 (b)	Plot of internal studentized residuals vs. predicted response for CO	136
4.57 (a)	Plot of normal % probability vs. internal studentized residuals for HC	137
4.57 (b)	Plot of internal studentized residuals vs. predicted response for HC	137
4.58	Plot of actual values vs. predicted values for (a) BSFC and (b) BTE	144
4.59	Plot of actual values vs. predicted values for (a) Smoke (b) NO _x (c) CO and (d) HC	144
4.60 (a)	Variation of BSFC with engine load for NM-BU20 blends	146
4.60 (b)	Variation of BSEC with engine load for NM-BU20 blends	146
4.61	Variation in BSFC with NM-BU20 blends at medium and full load	147
4.62	Variation of BTE with engine load for NM-BU20 blends	148

4.63	Variation in BSFC with NM-BU20 blends at medium and full load	148
4.64	Variation in smoke for NM-BU20 blends	149
4.65	Variation in smoke due to combined effect of load and NM blending	149
4.66	Variation in NO _x for NM-BU20 blends	150
4.67	Variation in NO _x due to combined effect of load and NM blending	151
4.68	Variation in CO for NM-BU20 blends	152
4.69	Variation in CO with NM-BU20 blends at medium and full load	152
4.70	Variation in HC for NM-BU20 blends	153
4.71	Variation in HC with NM-BU20 blends at medium and full load	154
4.72	Performance and emission of NM-BU20 blends (100% rated power)	155
4.73 (a)	Plot of normal % probability vs. internal studentized residuals for BSFC	159
4.73 (b)	Plot of internal studentized residuals vs. predicted response for BSFC	159
4.74 (a)	Plot of normal % probability vs. internal studentized residuals for BTE	159
4.74 (b)	Plot of studentized internal residuals vs. predicted response for BTE	159
4.75 (a)	Plot of normal % probability vs. internal studentized residuals for smoke	160
4.75 (b)	Plot of internal studentized residuals vs. predicted response for smoke	160
4.76 (a)	Plot of normal % probability vs. internal studentized residuals for NO _x	160
4.76 (b)	Plot of internal studentized residuals vs. predicted response for NO _x	160
4.77 (a)	Plot of normal % probability vs. internal studentized residuals for CO	161
4.77 (b)	Plot of internal studentized residuals vs. predicted response for CO	161
4.78 (a)	Plot of normal % probability vs. internal studentized residuals for HC	161
4.78 (b)	Plot of internal studentized residuals vs. predicted response for HC	161
4.79	Plot of actual values vs. predicted values for (a) BSFC (b) BTE	168
4.80	Plot of actual values vs. predicted values for (a) Smoke (b) NO _x (c) CO (d) HC	169
4.81 (a)	Variation of BSFC with engine load for Diglyme-BU20 blends	170
4.81 (b)	Variation of BSEC with engine load for Diglyme-BU20 blends	171

4.82	Variation in BSFC due to combined effect of load and Diglyme blending	171
4.83	Variation of BTE with engine load for Diglyme-BU20 blends	172
4.84	Variation in BTE due to combined effect of load and Diglyme blending	173
4.85	Variation in smoke for Diglyme-BU20 blends	173
4.86	Variation in smoke due to combined effect of load and Diglyme blending	174
4.87	Variation in NO _x for Diglyme-BU20 blends	175
4.88	Variation in NO _x due to combined effect of load and Diglyme blending	176
4.89	Variation in CO for Diglyme-BU20 blends	177
4.90	Variation in CO due to combined effect of load and Diglyme blending	178
4.91	Variation in HC for Diglyme-BU20 blends	178
4.92	Variation in HC due to combined effect of load and Diglyme blending	179
4.93	Performance and emission of Diglyme-BU20 blends (100% rated power)	180
4.94 (a)	Plot of normal % probability vs. internal studentized residuals for BSFC	184
4.94 (b)	Plot of internal studentized residuals vs. predicted response for BSFC	184
4.95 (a)	Plot of normal % probability vs. internal studentized residuals for BTE	184
4.95 (b)	Plot of internal studentized residuals vs. predicted response for BTE	184
4.96 (a)	Plot of normal % probability vs. internal studentized residuals for smoke	185
4.96 (b)	Plot of internal studentized residuals vs. predicted response for smoke	185
4.97 (a)	Plot of normal % probability vs. internal studentized residuals for NO _x	185
4.97 (b)	Plot of internal studentized residuals vs. predicted response for NO _x	185
4.98 (a)	Plot of normal % probability vs. internal studentized residuals for CO	186
4.98 (b)	Plot of internal studentized residuals vs. predicted response for CO	186
4.99 (a)	Plot of normal % probability vs. internal studentized residuals for HC	186
4.99 (b)	Plot of internal studentized residuals vs. predicted response for HC	186
4.100	Plot of actual values vs. predicted values for (a) BSFC (b) BTE	193
4.101	Plot of actual values vs. predicted values for (a) Smoke (b) NO _x (c) CO (d) HC	193

4.102 (a)	Variation of BSFC with engine load for Diethylether-BU20 blends	195
4.102 (b)	Variation of BSEC with engine load for Diethylether-BU20 blends	195
4.103	Variation in BSFC with diethylether blending at medium and full load	196
4.104	Variation of BTE with engine load for Diethylether-BU20 blends	197
4.105	Variation in BTE with diethylether blending at medium and full load	198
4.106	Variation in smoke for Diethylether-BU20 blends	199
4.107	Variation in smoke due to combined effect of load and Diethylether blending	199
4.108	Variation in NO _x for Diethylether-BU20 blends	200
4.109	Variation in NO _x due to combined effect of load and Diethylether blending	201
4.110	Variation in CO for Diethylether-BU20 blends	202
4.111	Variation in CO with diethylether blending at medium and full load	203
4.112	Variation in HC for Diethylether-BU20 blends	203
4.113	Variation in HC with diethylether blending at medium and full load	204
4.114	Performance and emission of Diethylether-BU20 blends (100% rated power)	205
4.115	Comparison of heat release rate of different blended fuels	207
4.116 (a)	Variation of BSFC with engine load for different blended fuels	208
4.116 (b)	Variation of BSEC with engine load for different blended fuels	208
4.117	Variation of BTE with engine load for different blended fuels	209
4.118	Variation of smoke with engine load for different blended fuel	210
4.119	Variation of NO _x with engine load for different blended fuels	210
4.120	Variation of CO with engine load for different blended fuels	211
4.121	Variation of HC with engine load for different blended fuels	211
4.122	Comparison of BSFC and BTE at full load for different blended fuels	212
4.123	Comparison of smoke, NO _x , HC and CO at full load for different blended fuels	212
4.124	Smoke-NO _x Trade-off for different blended fuels	213
4.125	Comparison of performance and emissions for diesel and DGM15BU20	214

List of Tables

T. No.	Title	Page No.
1.1	Oil and total liquids demand by scenario	5
1.2	World oil demand by sector under New Policy Scenario	5
2.1	Literature review with various blends of n-butanol, biodiesel and other oxygenated additives in diesel	40
3.1	Specification of test-engine	58
3.2	Specifications of test set-up and formulae used to calculate different quantities	59
3.3	Specifications of AVL 437C smoke meter	62
3.4	Specifications of exhaust gas analyzer	63
3.5	Properties of diesel, n-butanol and additives	65
3.6	Uncertainty of various parameters	66
4.1	Parameters levels as per L16 orthogonal array based Taguchi design	70
4.2	Design layout and experimental results for diesel	71
4.3	Response table for means	72
4.4	Results for diesel (B0) at full load condition	75
4.5	Parameters and their levels according to Factorial design for n-butanol-diesel blends.	77
4.6	Design layout and experimental results for n-butanol-diesel blends	78
4.7	Reduce analysis of variance table and interaction fit for BSFC	83
4.8	Reduce analysis of variance table and interaction fit for BTE	85
4.9	Reduce analysis of variance table and interaction fit for Smoke	87
4.10	Reduce analysis of variance table and interaction fit for NO _x	88
4.11	Reduce analysis of variance table and interaction fit for CO	89
4.12	Reduce analysis of variance table and interaction fit for HC	90
4.13	Maximum and minimum limits for each response to optimize performance and emissions	109

4.14	Optimum conditions of load and blend and their predicted results	109
4.15	Parameters and their levels according to Factorial design for BU20	111
4.16	Design layout and experimental results for BU20	111
4.17	Reduce analysis of variance table and interaction fit for BSFC response	117
4.18	Reduce analysis of variance table and interaction fit for BTE response	118
4.19	Reduce analysis of variance table and interaction fit for smoke response	119
4.20	Reduce analysis of variance table and interaction fit for NO _x response	120
4.21	Reduce analysis of variance table and interaction fit for CO response	121
4.22	Reduce analysis of variance table and interaction fit for HC response	122
4.23	Optimum conditions of blends and their predicted responses for BU20	131
4.24	Parameters and their levels according to Factorial design for NM-BU20 blends	133
4.25	Design layout and experimental results for NM-BU20 blends	133
4.26	Reduced analysis of variance table and interaction fit for BSFC	138
4.27	Reduce analysis of variance table and interaction fit for BTE	139
4.28	Reduce analysis of variance table and interaction fit for Smoke	140
4.29	Reduce analysis of variance table and interaction fit for NO _x	141
4.30	Reduce analysis of variance table and interaction fit for CO	142
4.31	Reduce analysis of variance table and interaction fit for HC	143
4.32	Maximum and minimum limits for each response to optimize performance and emissions for NM-BU20 blends	156
4.33	Optimum conditions of load and blend and their predicted results for NM-BU20 blends	156
4.34	Parameters and their levels according to Factorial design for Diglyme-BU20 blends	157
4.35	Design layout and experimental results for Diglyme-BU20 blends	158
4.36	Reduce analysis of variance table and interaction fit for BSFC	162
4.37	Reduce analysis of variance table and interaction fit for BTE	163

4.38	Reduce analysis of variance table and interaction fit for Smoke	164
4.39	Reduce analysis of variance table and interaction fit for NO _x	165
4.40	Reduce analysis of variance table and interaction fit for CO	166
4.41	Reduce analysis of variance table and interaction fit for HC	167
4.42	Maximum and minimum limits for each response to optimize performance and emissions	181
4.43	Optimum conditions of load and blend and their predicted results	181
4.44	Parameters and their levels according to factorial design for DEE-BU20 blends	182
4.45	Design layout and experimental results for DEE-BU20 blends	183
4.46	Reduce analysis of variance table and interaction fit for BSFC	187
4.47	Reduce analysis of variance table and interaction fit for BTE	188
4.48	Reduce analysis of variance table and interaction fit for Smoke	189
4.49	Reduce analysis of variance table and interaction fit for NO _x	190
4.50	Reduce analysis of variance table and interaction fit for CO	191
4.51	Reduce analysis of variance table and interaction fit for HC	192
4.52	Maximum and minimum limits for each response to optimize performance and emissions	206
4.53	Optimum conditions of load and blend and their predicted results	206
4.54	Cost analysis of diesel, BU20 and DGM15BU20	215

Nomenclature

ANOVA	Analysis of variance
BU20	n-butanol20% (v/v)-diesel blend
BSEC	Break specific energy consumption (kj/kWh)
BSFC	Break specific fuel consumption (kg/kWh)
BTE	Break thermal efficiency (%)
C.I./CI	Compression Ignition
CA btdc	Crank angle before top dead centre
CN	Cetane number
CNG	Compressed natural gas
CO	Carbon monoxide
CO ₂	Carbon dioxide
CR	Compression ratio
DEE	Diethylether
DGM	2-Methoxy ethyl ether /Diglyme
DI	Direct injection
DOE	Design of experiments
EGR	Exhaust gas recirculation
HC	Hydrocarbons
HSU	Hartridge smoke unit
I.C./IC	Internal Combustion
Inj. Pr.	Injection pressure
Inj.T.	Injection timing
LNG	Liquid nitrogen gas

LPG	Liquid petroleum gas
Mb/d	million barrels per day
MTOE	Million tonne of oil equivalent
NO _x	Oxides of nitrogen
p.a.	per annum
PM	Particulate matter
Prob.	Probability
S.I./SI	Spark ignition
SFC	Specific fuel consumption (kg/kWh)
TC	Turbo charged
UHC	Unburned hydrocarbons

Symbols

%	Percentage
°	Degree
bp/BP	Break power of engine
C	Carbon
C _v	Calorific value
CV	Coefficient of variation
F	Mean Square for the term divided by the Mean Square for the Residual
H	Hydrogen
kW	Kilowatt
η	efficiency
MJ/kg	Mega joules per kilogram
Nm	Newton-meter

p-value	probability value
R^2	multiple correlation coefficient
T	Brake torque (Nm)
vs.	versus
ρ	Density (kg/m^3)

Subscripts

b	blending
f	fuel
v	value
x	1/2/33

Chapter 1

Introduction

1.1 Introduction

Energy is needed as an essential driving force to perform daily social and industrial activities and for development. The energy consumption of world is continuously on the rise with automation of services and processes because of luxurious life and faster means of transportation. Energy consumption at all levels, primary and secondary, is increasing continuously with development and increasing population. Though this looks like an expected turn of events with an ever changing and evolving society that is more and more dependent on the industry; there is another facet that everybody wishes to ignore. That is the parallel increase of hazardous emissions. A treatise on energy cannot be devoid of a serious discussion on emissions and its ramifications on the environment.

This chapter aims to present a scenario of near future wherein it is projected that there will be enormous rise in emissions along with a drastic rise in consumption of fossil fuels. The fossil fuels are limited and several economical and political issues have to be dealt with before its production and import/export. Share of diesel in total oil consumption worldwide is greater than gasoline. The blending of biofuels with diesel provides a reasonable solution of cost and pollution issues. This study strives to highlight the fact that the blending of n-butanol with diesel has several advantages over vegetable oil, biodiesel and methanol/ethanol. After literature review it is concluded that the expected levels of smoke and nitrogen oxides (NO_x) emissions have not been achieved yet with n-butanol-diesel blends. In most of the experimental studies involved in finding expected levels of smoke and NO_x , different additives were used for blending in diesel. As stated earlier, the results have not been very encouraging. This thesis therefore looks at the possibility of ternary blends to control emission of smoke and NO_x . The engine operating parameters were optimized for n-butanol-diesel blends and an optimum ternary blend was found at that specific engine setting. The main focus of this thesis is to determine suitable additives for oxygenated biofuel-diesel blends for improved engine performance and reduced emissions (particularly smoke and NO_x), and to develop a

mathematical model to predict engine performance and emissions for the suggested ternary blend.

1.2 Energy demand and perspectives

International Energy Agency (IEA) has developed different energy scenarios on the basis of worldwide data of energy production & consumption, policies, opportunities, and challenges. It is estimated that consumption of all recent fuels will see a rapid rise till 2040 under the New Policies Scenario. Oil demand is expected to increase to 103.5 million barrels per day (Mb/d) by the year 2040; whereas gas consumption is projected to increase by approximately 50%. It is estimated that renewable energy will increase by 60% in power sector by 2040. To achieve targets of energy production with reduced emissions in Decarbonization scenario (keeping below the 2°C climate change limit) the renewable energy sector would have to increase its share in all the sectors of energy generation. Natural gas and electricity are being forced to increase their part in total energy consumption worldwide. Yet, oil remains pivotal in energy security [1].

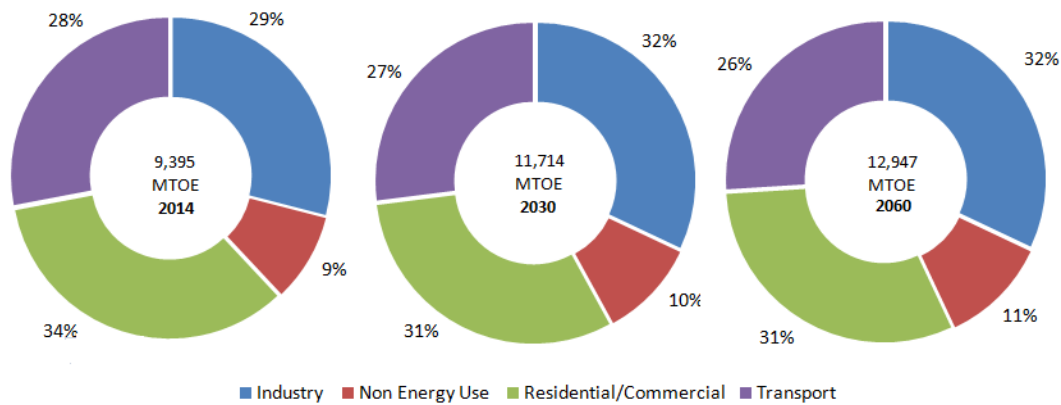


Fig. 1.1 Total final consumption of energy by sectors in Modern Scenario [2]

Fig. 1.1 shows consumption of energy sector-wise. It can be observed from Fig.1.1 that total final energy consumption is expected to go up by 25% from 2014 to 2030 with an average growth rate of 1.4% p.a. The upward force on consumption growth is mainly driven by a growth in industrial activity, increasing transport demand and an ease of energy access, which raises residential and commercial energy consumption. Technology improvements disrupt traditional energy systems, but boost up the efficiency of the systems in use. It is expected to slow down the final consumption rate drastically after

2030, decreasing to 0.3% p.a. (per annum) and settling at 12,947 MTOE (million tonnes of oil equivalent) in 2060. This is only 38% higher than the consumption of 2014 [2].

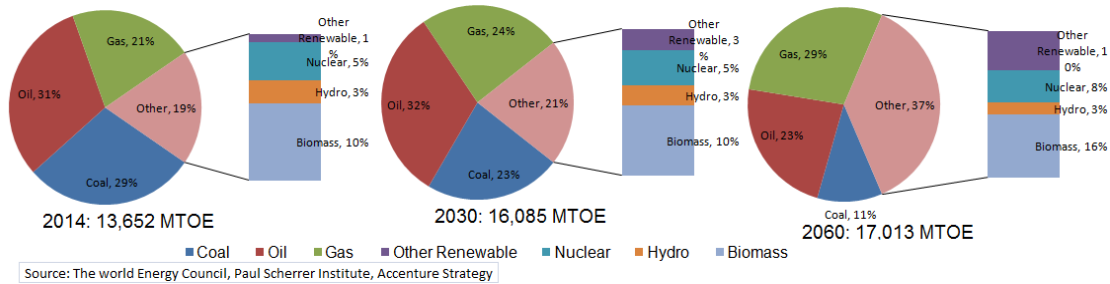


Fig. 1.2 Primary energy supply (MTOE) and percentage share under Modern Scenario

Fig.1.2 exhibits the world primary energy supply by different sources under Modern Scenario. It can be observed that total primary energy supply is expected to grow at a rate of 1.0% from 2014 to 2030 and will be 16,085 MTOE. The share of oil will increase from 31% to 32% in 2030 and is projected to be 23% in 2060 of total energy supply. It is to be noted that share of oil is always dominant in total primary energy supply [2]. To fulfil the increased energy demand and to control emissions simultaneously is the prime requirement of the current world. It is required that energy be available and be used with minimum environmental impact; with safety; and at affordable prices.

1.3 Oil demand and perspectives

Rapid economic growth, globalization, and freedom of mobility result in high volumes of air traffic, freight, and car-ownership. As a result, energy in the transport sector is expected to increase at a rate of 1.2% per annum (p.a.) from 2014 to 2030. In specific, demand for petroleum-based transportation fuels is stipulated to increase at a rate of 1.0% p.a. till 2030. However, the demand for petroleum fuels is predicted to decline at a rate of 0.5% p.a. beyond 2030 because of an increased share of renewable fuels and growth of electric vehicles (EV). Seeing the influence of growing income, new technology and consumer awareness, light-duty vehicles are projected to grow 2.7 times by 2060. By 2060, biofuels would capture almost 16% of transport fuel demand, indicating an enhancement of nearly 4.9% of its current usage by 2030 [1], [2].

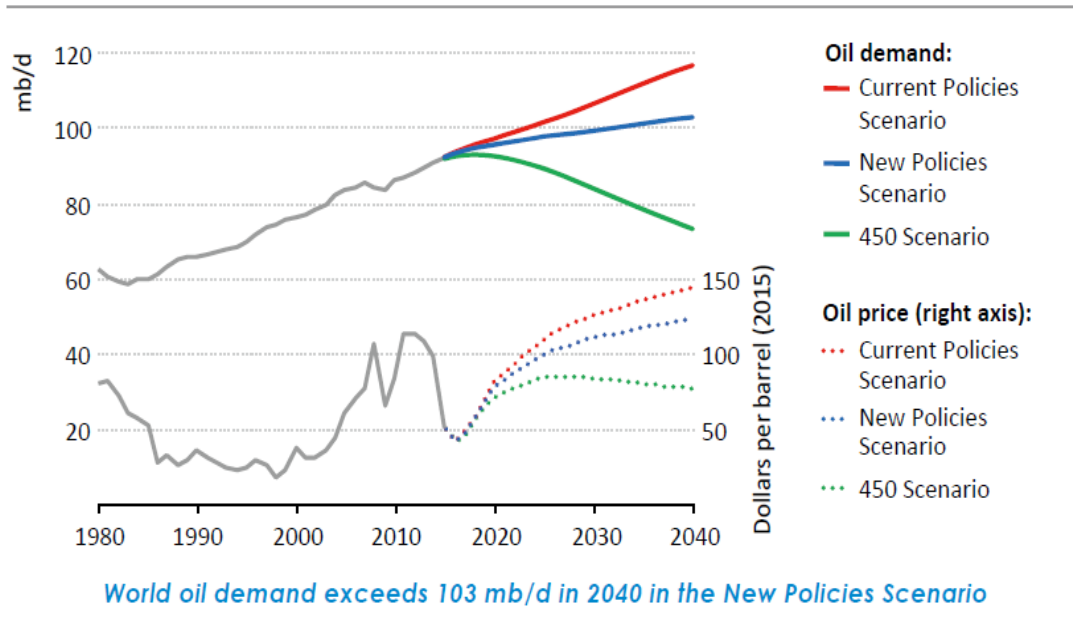


Fig. 1.3 World oil demand and price by scenario [1]

Fig. 1.3 shows predicted oil demand and price by following different scenarios. It can be observed that other than decarbonization scenario (i.e. 450 Scenario), the demand and price of oil show an increasing trend up to 2040. The increasing demand is mainly concentrated in transport and petrochemical sectors, which accounts for approximately three-fourth of the total oil consumption by 2040, which is two-thirds currently. The factors like population growth and technology advancement are taken into account to project these data. The production of oil by OPEC and non-OPEC countries and political issues also influence the oil supply and international prices. New production sites, heavy investment for relatively hard-to-access sites and geopolitical risks are also playing important roles in deciding oil supply and energy security throughout the world.

Table 1.1 Oil and total liquids demand by scenario (Mb/d)[1]

			<u>New Policies</u>		<u>Current Policies</u>		<u>450 Scenario</u>	
	2000	2015	2025	2040	2025	2040	2025	2040
OECD	45	41.5	37.3	29.8	38.5	34.6	34.4	20.7
Non-OECD	26.3	43.6	52.2	62.5	53.9	69.9	48.4	46.4
Bunkers*	5.4	7.4	8.8	11.2	9.4	12.6	7.1	6.2
World Oil	76.7	92.5	98.2	103.5	101.9	117	89.9	73.2
Share of non-OECD	34%	47%	53%	60%	53%	60%	54%	63%
World biofuels**	0.2	1.6	2.5	4.2	2.2	3.6	4	9
World total liquids	76.9	94.1	100.8	107.7	104.1	120.6	93.9	82.2

*Includes international marine and aviation fuel. ** Expressed in energy-equivalent volumes of gasoline and diesel.

Table 1.1 shows oil demand projected from 2000-2040. It can be observed that in this projection, the rate of increment in total liquid demand is higher in comparison to fossil fuels. This is because of an increased share of biofuels in future. The demand for oil and total liquid can be seen to decrease in decarbonization scenario by 2040.

Table 1.2 World oil demand by sector under New Policy Scenario[1]

	2000		2015		2040		2015-2040		Ease of substitution
	Mb/d	%	Mb/d	%	Mb/d	%	Change CAAGR*		
Transport	39	51%	51.7	56%	60.5	58%	8.8	0.60%	
Passenger Vehicles	18.2	24%	23.9	26%	24.6	24%	0.8	0.1%	Medium
Maritime	3.7	5%	5	5%	6.2	6%	1.3	0.90%	Medium
Freight	11.9	16%	16.3	18%	19.7	19%	3.4	0.80%	Low
Aviation	4.6	6%	5.8	6%	9.3	9%	3.5	1.90%	Low
Industry	14.4	19%	17	18%	22.7	22%	5.7	1.20%	
Steam and Process heat	6.1	8%	5.8	6%	6.5	6%	0.8	0.50%	High
Petrochemical feedstocks	8.1	11%	10.7	12%	15.7	15%	4.9	1.50%	Low
Buildings	7.7	10%	7.6	8%	6	6%	-1.6	-1.00%	Medium
Power generation	6.1	8%	5.4	6%	2.9	3%	-2.4	-2.40%	High
Other**	9.4	12%	10.8	12%	11.3%	11%	0.5	0.20%	
Total	76.7	100%	92.5	100%	103.5	100%	11.0	0.50%	

*Compound average annual growth rate. ** Include agriculture, transformation, other non energy use

Table 1.2 shows that oil demand in transport and industry is expected to increase up to 2040 significantly; while in power generation and building, it is expected to decrease. However, in agriculture and other sectors, the demand of oil is not foreseen to vary too much till 2040 [1]. Fig. 1.4 summarizes the predicted global fuel transition in transport from 2014 to 2060. For running mobile engines, oil will remain as the main source of energy up to 2030. However by 2060, a decline of 25% is expected in oil demand.

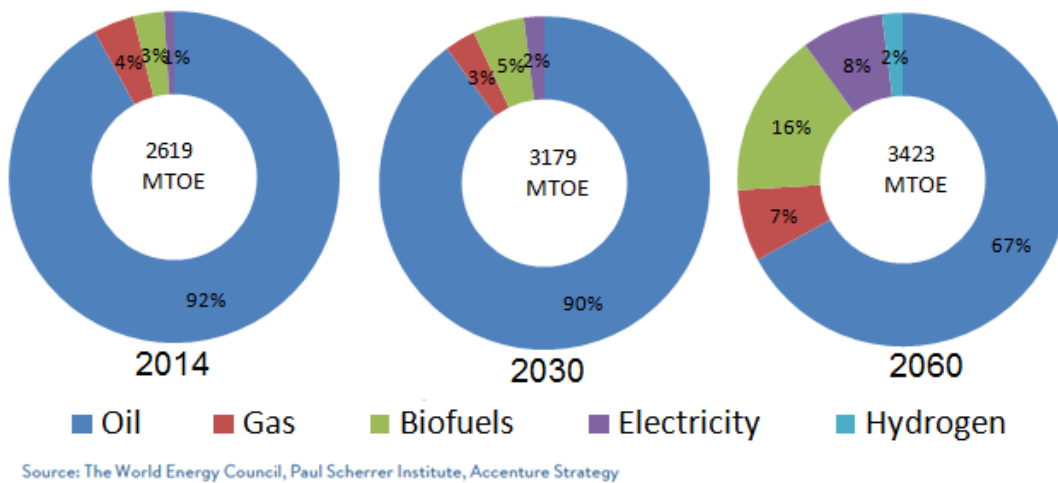


Fig.1.4 Share of fuel in transportation (Modern Scenario)[2]

Energy use in India's transport sector, at 75 MTOE in 2013, accounted for 14% of final energy consumption and was much lower than the share of many other countries. However, with an almost consistent growth rate averaging 6.8% per year since 2000, it has become the fastest-growing of all the end-use sectors. Approximately 90% of engines used in road transport are powered by fossil oil.

In the current scenario, all the indicators point to significant potential for increase in oil demand. For instance, passenger vehicle ownership at less than 20 vehicles per 1000 inhabitants is much lower than the world average. As another example, the use of energy per capita for transportation purposes is one-sixth of the world average. Further, the number of flights, at 0.07 trips per capita, is well below that of other emerging economies. In the New Policies Scenario, energy demand in transport sector is projected to be higher than all other sectors and the transport fuel demand in India is expected to reach 280 MTOE by 2040, mainly because of road transport (Fig.1.5).

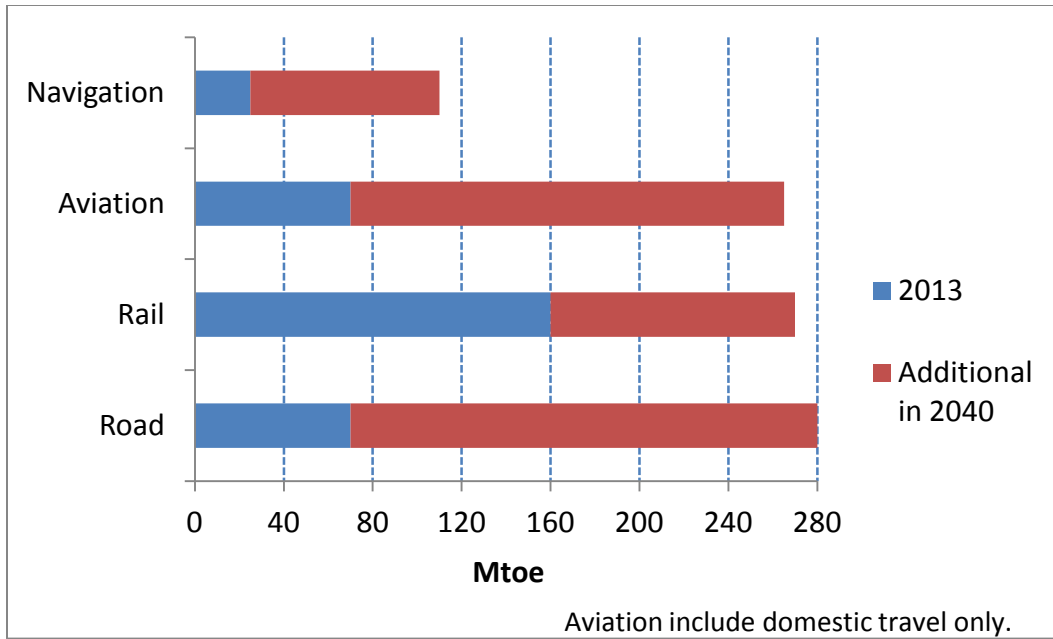


Fig.1.5 Fuel demand by various transport sectors in India under New Policy Scenario [3]

Previously, India's transport sector was dominated by rail, and roads carried only 15% of the passenger movement and 14% of freight [4], however, today the picture is changed. Transport in India is now mainly dominated by road transport, which accounts for 86% of passenger and almost two-thirds of freight movement. Therefore, road transport fuel demand had increased rapidly to 68 MTOE in 2013; around 60% of which was used for passenger transport. Passenger cars still play a relatively minor role in India's overall transport system, partly because much individual travel is made by collective modes of road transport (i.e. buses) and partly because of the high level of use of two and three-wheelers. In future projections this changes; with the share of passenger cars increasing sharply by 2040, by which time they would be accounting for 54% of road fuel demand for personal transport, as car ownership rises to a nationwide 175 vehicles per 1000 inhabitants Fig.1.6 [3].

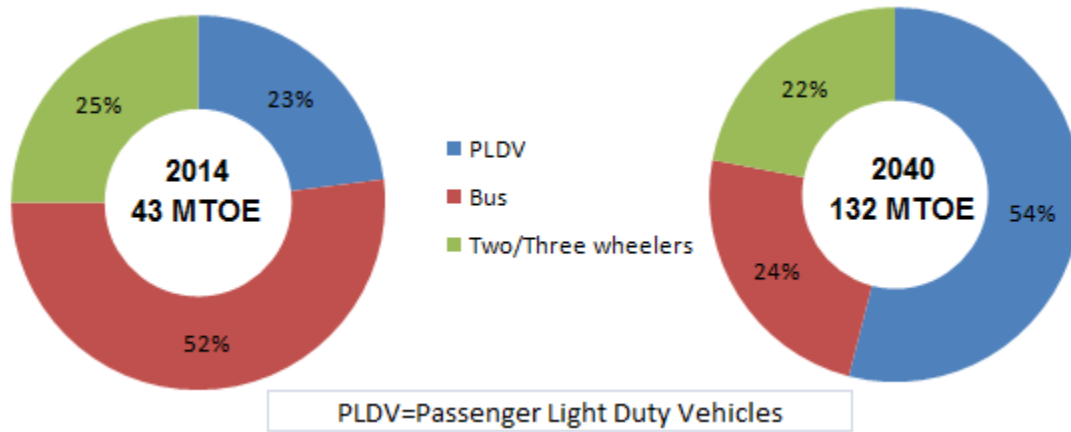


Fig.1.6 Transportation fuel demand for passenger transportation in India in new policy scenario[3]

1.4 Emissions characteristics of internal combustion engines

Worldwide, cars, trucks, buses, and other motor vehicles continue to have a key role in causing air pollution. These vehicles are major sources of carbon monoxide (CO), volatile organic compounds (VOCs) and nitrogen oxides, the precursors to tropospheric depletion of ozone, acid rain, and particulate matter (PM) in urban areas. Air pollutants are divided into two categories: (i) primary, if directly emitted into the environment by a stationary or mobile source; and (ii) secondary, if formed in the environment due to physical and chemical reactions such as hydrolysis, oxidation, or photochemistry. The primary pollutants that are emitted from automobiles are CO, hydrocarbons (HC), oxides of sulfur (SO_x), NO_x, PM including dust and smoke, and other VOCs. Secondary pollutants from automobile include NO_x, various photochemical oxidants (including ozone), secondary particulate matter and acid rain. Carbon dioxide has no direct adverse effects on human health or public welfare, but its build-up contributes to the enhancement of the greenhouse effect. Automobile pollution has increased severely in the last four decades. Pollution of the environment has been happening since many decades; but in recent years, transportation has made a major contribution. Since the industrial revolution, the atmospheric pollution generated by industry and society has increased. In last few decades, the industrial and domestic emissions have reduced in developed countries because of technology innovations and strict legislation. Meanwhile, use of the automobiles has increased rapidly with the result that I.C. engines are now a main source of pollution, particularly in the urban areas[5].

Due to social factors and opportunities of employments, population has increased in the urban areas; particularly in Asia and South America. This trend of population growth results in increased traffic and pollution in cities. Automobile vehicles are major emission sources of air pollutants all over the world. For example, in Europe prior to the adoption of the Euro 3 / Euro 4 equipment, the vehicles were major sources of emissions. In dense urban areas, vehicles are the major source of PM emission. Road vehicles currently account for 74% of nitrogen oxides and 94% of black smoke emissions in London. Diesel alone accounts for 32% and 87% of total emissions (43% and 92% of vehicle emissions) for these two pollutants respectively.

1.4.1 Types of emissions from diesel engines

1. Hydrocarbons (HC): Unburned hydrocarbons are the result of incomplete combustion and leakage of fuel vapor from the fuel tank and fuel pump. When using fuels other than diesel, some HC species are also produced during combustion. These pollutants react with nitrogen oxides in the presence of sunlight to form ground level ozone, a primary ingredient in smog. Ozone is desirable in the upper atmosphere, but in the lower environment, this gas irritates the respiratory system, causing coughing, choking, and reduced lung capacity.

2. Nitrogen oxides (NO_x): High temperature is the main reason of NO_x production. At elevated temperature, Nitrogen reacts with O₂ and forms NO and NO₂. These pollutants cause lung irritation and weaken the body's defenses against respiratory infections such as pneumonia and influenza. Additionally, they support the formation of ground level ozone and particulate matter.

3. Carbon monoxide (CO): CO is a colorless, odorless, and highly toxic gas, with a density close to that of air. It can have injurious effects on health because it interferes with the absorption of oxygen by red blood cells. This may lead to increased morbidity, adversely affect fertility, and reduces worker productivity. CO is especially a problem in urban areas where it assists in the formation of photochemical smog and surface ozone with other pollutants. Carbon monoxide results from the incomplete combustion of fuel and is emitted directly from tailpipes of vehicles. Incomplete combustion is most likely to occur at low air-to-fuel ratios in the engine. These conditions are very common in diesel

engines where fuel-air mixture is heterogeneous, especially at the time of vehicle starting when the air supply is reduced (choked), and at higher altitudes where less amount of oxygen is available for combustion because of the lower density of air.

As per available data, carbon monoxide is a pollutant closely related with emissions from automobile vehicles. Around 90% of all CO emission in developed countries originate from the transport sector, and about 85% of that total is associated with I.C. engines use. In many urban areas around the world, the contribution from automobile vehicles of carbon monoxide pollution can exceed 90% of the total. In urban areas, where population density is the highest, motor vehicles are responsible for about 98% of all emissions of carbon monoxide. The figure reaches to 100% in many densely populated areas[6].

4. Sulfur dioxide (SO_2): Power plants and motor vehicles create this pollutant by burning sulfur-containing fuels, especially diesel. Sulfur dioxide can react in the atmosphere to form fine particles and poses the largest health risk to young children and asthmatics.

5. Particulate matter (PM): Particulate matter or smoke is created during the incomplete combustion and thermal cracking of diesel fuel. Fine particles of less than 0.1 microns present the most serious threat toward human health, as they can penetrate deep into lungs. PM is a primary pollutant, while it forms secondary pollutants when combined with hydrocarbons, nitrogen oxides, and sulfur dioxides. Diesel exhaust is a major contributor to PM pollution.

6. Greenhouse gas: Carbon dioxide is a normal end-combustion product of every fuel containing carbon (biomass, wood, coal and its variants, oil and petroleum derivatives) and a product of aerobic metabolism (respiration). On the other hand, it is reconverted to carbonaceous solids by the chlorophyll in plants. Estimates suggest that about 15% of the world's total emission of CO_2 (contributed by humans) is generated by motor vehicles, and in some OECD (Organization for economic co-operation and development) countries the figure may even reach up to 70%. Cars and trucks contribute approximately one-fifth of the United States' total pollution that is directly related to global warming. Since CO_2 is a natural constituent of air, it is not strictly considered as a pollutant. The gas has no direct detrimental effect on human health.

1.4.2 Growth of mobile engines in India

After the onset of globalization, the automobile sector has brought a significant transformation in the Indian economy. Today, almost every global auto manufacturer has set up facilities in the country. The manufacturing of automobile vehicles in India rose at a very high pace in last few decades. Now, India is one of the largest producers of automobiles in the world.

Passenger vehicle sales in India were highest in 2016-17, with a record growth of 9.23 per cent. At the end of the financial year 2017, domestic passenger vehicles' (PV) sales were at 30,46,727 units against 27,89,208 in the previous year, according to data released by the Society of Indian Automobile Manufacturers (SIAM).

In the year 2016-17, total sales of utility vehicles were 7,61,997 units against 5,86,576 units in the previous year with a growth of 29.91%. Car sales during the year 2016-17 grew 3.85% to 21,02,996 units from 20,25,097 units in the previous year. Motorcycle and Scooter sales increased by 3.68% and 11.39% respectively in the year 2016-17 as compared to previous year [7].

1.4.3 Stationary diesel engines

Diesel engines are widely used in industries, buildings, small power plants, pumping operations, agriculture and earth moving equipment. Diesel-engines having capacities ranging from 1 kW to 100 kW have been used in domestic generators and 100kw to 5000 kW commercial and industrial generators. In continuous operating pumps (e.g., in oil pipelines and water distribution systems), diesel engines are very popular.

In India, small diesel engines (up to 5 kW) are very popular in the agriculture field. They are used for running water pumps, grass cutting, cutting of feed for cattle and many other purposes. These engines are easily available at competitive prices in local markets.

Fig.1.7 Shows energy demand by fuel in different sectors in India [3]. It can be seen that industry, buildings and agriculture are using enough amount of fossil oil. Mainly stationary diesel engines are used in these areas. About 13% of the total diesel consumption in India is shared by agriculture sector. The share of industry and other applications is 17 percent. Out of this the industry consumed 9.02%, mobile towers

consumed 1.54% and others (gensets for non-industrial purposes, civil construction, etc.) consumed 6.45% [8]

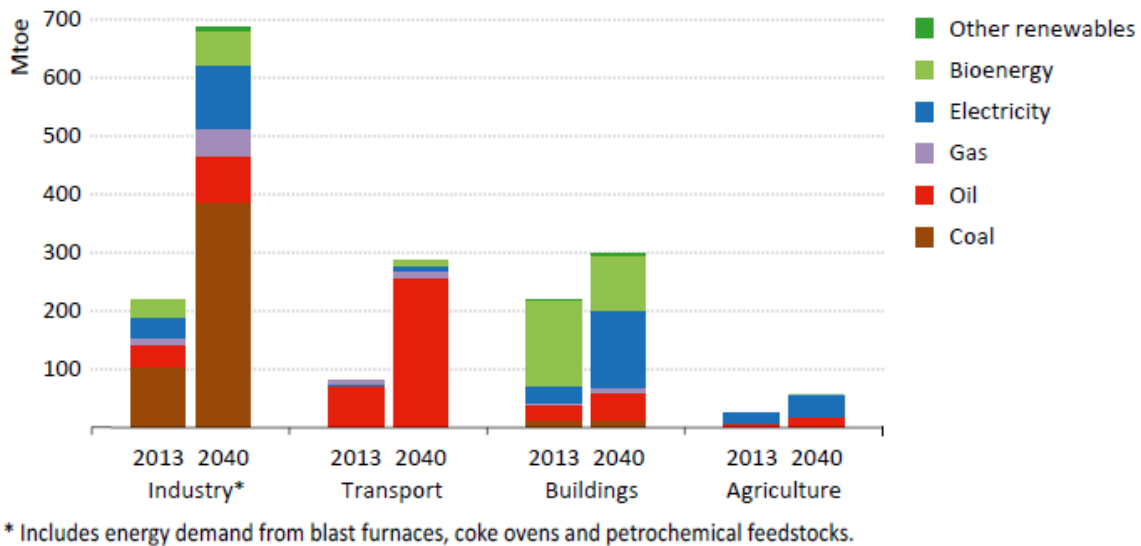


Fig.1.7. Energy demand by fuel type in different sectors of India [8]

1.5 Air pollution in India

The increased use of I.C. engines in automobile and in agriculture sector is contributing a lot to air pollution. Most of the car brands using petrol now have diesel versions, which are much more polluting as compared to their petrol versions. As per estimates, more than 50% of the cars on the roads are going to be powered by diesel by 2020.

According to a Greenpeace India report, India overtook China in the number of deaths caused by air pollution in 2016. Analyzing the Global Burden of Disease (GBD) data compiled by the Institute for Health Metrics and Evaluation at the University of Washington in Seattle, India had 3,283 premature deaths due to ambient air pollution every day, as opposed to China's 3,233 per day. The number of deaths per day due to air pollution in India has risen from 2,139 per day in 1990 to 3,238 in 2015 [9].

International Energy Agency (IEA) estimated in its special report that the global number will increase significantly, touching 7.5 million in 2040, unless the energy sector takes tough steps towards control of emissions from automobiles [10].

In recent years, air pollution has reached critical limits and the air quality in most Indian cities has failed to meet safe levels as per WHO (World Health Organization) standards.

The levels of PM_{2.5} and PM₁₀ (Air-borne particles smaller than 2.5 and 10 micrometers in diameter respectively) as well as the concentration of dangerous carcinogenic substances such as Sulfur Dioxide (SO₂) and Nitrogen Dioxide (NO₂) have reached alarming levels in most of the Indian cities.

According to WHO, Delhi is at top position in the list of most polluted cities across the world. Among the world's 20 most polluted cities in the world, 13 are from India. India is in the group of countries that has the highest particulate matter (PM) levels. Its cities have the highest levels of PM₁₀ and PM_{2.5}. At the level of more than 150 micrograms, Delhi has the highest level of airborne particulate matter PM_{2.5}, which is considered most harmful. These figures are six times more than the WHO safe limit of 25 micrograms. The main reasons of so much air pollution in India are ineffective, inefficient and bad networked transport systems, deficiency of fast and cost effective intra-city railway networks, huge population with resultant huge number of vehicles, faulty traffic management systems, lack of tough enforcement of emissions norms, older vehicles, substandard technology, automobiles with faulty engines and lack of engine maintenance etc.

1.6 Diesel emissions and human health solutions

The human health problems associated with diesel emissions can only be controlled by reducing these emissions. Both national and state governments have taken steps to reduce diesel emissions. However, more efforts are needed.

- **Improved design and modified engine standards:** New engine designs with more efficient combustion and fewer emissions are results of the electronic controlled fuel systems and latest emission trapping technology.
- **Retrofitting:** New emissions standards can only be applied to vehicles fitted with new engines, not to diesel engines that are already in operation. There are many high polluting diesel trucks, buses, and off-road equipment that will continue to run on the roads because of lagging emission standards and durability of diesel engines. Retrofitting these diesel vehicles and equipment with advanced emission control devices can effectively control harmful tailpipe emissions.

- **Cleaner Fuels:** Lower sulfur diesel fuel allows the use of advanced emission control technologies, which when combined, can reduce emissions more than 85 percent. Besides, the bio fuels, Hydrogen, LPG, LNG, Natural Gas, CNG and bio gas can be used in diesel engines to reduce emissions. There is a trade-off between engine efficiency and particular types of emissions. The selection of a particular type of alternative fuel will be on the basis of its local availability, engine compatibility, and cost.

1.7 Need of alternative fuels/biofuels and additives

Emissions from diesel engines can be controlled by improvement in engine design, by optimizing operating parameters, retrofitting, after-treatments and by improving the fuel properties. The engine design can be improved in newly built engines only; not in old engines. Electric vehicles and fuel cell operated vehicles are also specially designed in accordance with the input source of energy. The operating parameters are generally pre-optimized for particular applications and for petroleum fuels. However, after introducing additional enhancements like after burner and particulate filter etc. the engines become comparatively costlier and are generally used for a particular type of emission only. Exhaust Gas Recirculation (EGR) reduces NO_x emission; but at the same time, thermal efficiency gets deteriorated.

In current study, our focus is on fuel modification. Improved fuel can be used for both old as well as new engine and cost can be controlled by proper selection of fuel. The physical and chemical properties of fuel can also be controlled by blending or by some processing.

Biofuels (alternative fuels) are liquid fuels that are made from plant or animal-based sources called "biomass." Biomass includes plants, crops, seeds, waste from vegetable oil extraction, algae, animal waste and all that is produced naturally. Non-food based biofuels such as cellulosic biofuels are made from non-edible seeds or farm waste having huge potential to reduce oil consumption and emissions. For example, cellulose based ethanol is capable of reducing global warming and emissions by 90% as compared to fossil fuels. Alternative fuels are non-petroleum, biodegradable and pertain to energy security. The factors like availability, performance, non-polluting, and cost-effectiveness play major roles in the acceptance of any new fuel in the society. Alternative fuels

contain vegetable oils, biodiesels, and other organic and inorganic compounds. Edible and non-edible vegetable oils can directly mix with diesel or can be converted into biodiesel by transesterification process. Emulsions of vegetable oils with diesel have also been studied by various researchers.

Using biodiesel reduces greenhouse gas emissions because carbon dioxide released from biodiesel combustion is offset by the carbon dioxide absorbed from growing feed-stocks used to produce the fuel. Life cycle analysis conducted by Argonne National Laboratory found that use of biodiesel without blending (BU100) reduces carbon dioxide emission by 74% compared with petroleum diesel [11].

Other than vegetable oils and biodiesels many organic compounds like alcohols, ethers, nitromethane, nitroethane, dimethylfuran, isoamyl nitrate, ethylene glycol and many others can be blended in diesel as additives to alter its properties. Out of these, oxygenated compounds are more important because of their potential to reduce emissions without affecting engine performance [12]–[14]. Oxygenated additives are renewable fuels and hold up the local agriculture industry [15], [16]. The presence of oxygen in molecular structure, low viscosity and high volatility of alcohols make them the favorite choice for diesel engines.

1.8 Limitations of biofuels

Use of Biofuels can reduce pollution and maintain sustainability towards the future. But at the same time, bio-fuels have certain limitations. To produce crops for biofuels, the land used needs to change. This may cause additional impact on the biological cycle and in turn on the environment. This factor needs to be taken into account during calculation of the net GHG (greenhouse gases). The land-use change can be: (a) direct, as when biofuels feed stocks are produced in the farms by cleaning forests, (b) indirect, when biofuel production displaces the production of other crops which are then produced on converted land in another region. In the present scenario, the cost of major biofuels is more than fossil fuels because of the requirement of large sites, mass production and latest technologies used in the production of fossil fuels. Bio-fuel production costs are expected to go down with scale and technology over time. It is predicted that biofuels will be cost-competitive to fossil fuels by 2030. An important non-economic hurdle in the

development of biofuels is uncertainty regarding their sustainability. The demolition of eco-cycle and competition with food crops has limited the growth of biofuels.

To compete with fossil fuels in cost, biofuel plants can be co-located with existing power plants or other industrial facilities to reduce capital costs. This will further help in exploring the advantages such as more efficient use of by-products and utilization of better technologies already available at site. Still, most of the low-carbon and energy-efficient technologies are more expensive for bio-fuels than their fossil-based counterparts. This factor needs to be taken into account not only for carbon trading, but also for minimizing the cost difference by the intervention of governmental policies.

1.9 Alcohol as alternative fuel

Alcohols are bio-oxygenated compounds. The presence of oxygen; low viscosity and high volatility of alcohols make them suitable fuels for I.C. engines. Ethanol and Methanol have been successfully used in S.I. engines and have proven to be competitive with Gasoline. The use of alcohols in C.I. engines is limited and researchers are now actively exploring new possibilities in this direction. The cost of alcohols in comparison to diesel and poor ignitability are the main barriers that limit the use of alcohols in C.I. engines. Now interest is increasing towards use of lower alcohols viz. ethanol, methanol and butanol in diesel engines to control the exhaust emissions.

Methanol is produced by distillation of wood, the distillation of coal or by natural gas and petroleum gas. Ethanol is a renewable fuel and can be obtained from biomass sources viz., plants and live-stocks and thus plays an important role in energy security and sustainability. Ethanol can also be produced by synthesis from petroleum or mineral coal. In comparison to methanol and ethanol, n-butanol has a higher heating value and lower latent heat of vaporization. Its Cetane number is higher as compared to methanol and ethanol. Methanol and ethanol have limited solubility and stability with diesel and have high hygroscopicity towards water. Methanol absorbs water directly from the atmosphere and thus has a tendency to dilute the blend, and may cause phase separation. These blends have been known to exhibit phase separation at specific compositions and at lower temperatures, thus making the solution more viscous at the bottom. This in turn causes stalling of the engine and obstruction of normal running. N-butanol is completely

miscible in diesel and there is no need of any surface reactant or solvent to mix it with diesel. The stability of butanol-diesel blends remains constant for a wide range of temperature. The boiling temperature and flash point of butanol are higher than that of methanol and ethanol and are nearer to that of diesel. These properties make butanol safer than methanol and ethanol and it can be distributed through existing fuel distribution and storage infrastructure. The calorific value of n-butanol is also higher than methanol and ethanol. This implies that same amount of n-butanol produces higher power from the same engine running on ethanol/methanol-diesel blends. Butanol produces approximately 25% more energy than methanol and ethanol, thus yielding better power/millage. N-butanol can be produced by fossil matter as well as by waste biomass (namely bio-butanol). However, the properties of n-butanol produced from both sources are same.

1.9.1 Advantages of alcohols

Alcohol operated engines show higher flame speed, higher peak temperature, and less emissions. Wider flammability range of alcohols permits smooth engine operation at leaner mixtures. The presence of oxygen in fuel reduces the air required to burn the fuel. This means that for the same amount of air, more fuel can be burned. This, in turn, improves the power output of the engine. Also, availability of oxygen in fuel enhances combustion and reduces smoke. The alcohols mix in all proportions with water and hydrocarbons due to the polar nature of OH group. Alcohols having high latent heat of vaporization cool the air entering the combustion chamber of the engine; thereby increasing the air density and mass flow. This effect increases the volumetric efficiency and reduces gas temperature inside the combustion chamber. However, due to the high heat of vaporization and lower boiling point, cold starting is found to be difficult with neat alcohols. This problem is not as severe as in case of alcohols blended with gasoline, as gasoline has a low boiling point (27-225°C) in comparison to diesel (187-343 °C). On a positive note, alcohols produce lesser GHG emissions and thus mitigate the problem of ozone depletion.

1.9.2 Limitations of alcohol

Large storages are required for alcohols as compared to gasoline and diesel at distribution stations due to lower calorific value of alcohols. In the case of methanol-diesel blends, the distribution system needs special attention because of highly hygroscopic nature of

methanol. To mitigate this problem, either the ratio of methanol is kept very low in the blend, or its mixing with diesel is done at the time of filling only. Lower Cetane number causes poor auto-ignition characteristics of alcohols. They have poor cold starting characteristics due to low boiling temperature. The vapor lock in fuel lining at high altitudes during summer days is a serious problem with ethanol because of lower boiling points and higher vapor pressure. Higher vapor pressure and lower viscosity of ethanol as compared to that of diesel results in the formation of vapor lock in the fuel delivery system. Generally, vapor formation occurs at the locations of lowest static pressure, such as the intake side of the injector. This reduces the quantity of fuel being delivered to the injector and may lead to cavitations inside the injector. Also, due to low vapor pressure, air can leak into storage tanks, and this can result in the formation of combustible mixtures.

The relatively high latent heat of vaporization of alcohols, particularly methanol (1.2 MJ/kg) and ethanol (0.92 MJ/kg) in comparison to diesel (0.23-0.60 MJ/kg), may cause cooling of the mixture at the intake manifold of the engine. This necessitates heating of the intake manifold at the time of cold starting. The heating of intake manifold decreases the density of charge, which in turn reduces the volumetric efficiency of the engine. Further, relatively high latent heat of ethanol can also cause problems in mixing of ethanol with air and its transportation through the intake manifold to the engine.

Methanol and ethanol are hygroscopic in nature and absorb water. This may cause phase separation in mixtures. The propensity to absorb water and inclination towards corrosion are two major problems regarding transport and storage of methanol and ethanol. While selecting the infrastructure for storing and dispensing these alcohols, the issue of material compatibility poses a big challenge. Alcohol is much more corrosive than petroleum fuel on rubber, plastic and metal parts. This puts some restrictions on the design and manufacturing of engines to be used with these fuels. Also, ethanol has low lubricity which increases friction in engines.

1.9.3 Use of alcohols in C.I. engines

There are several techniques of using alcohols in C.I. engines. The most common techniques for the purpose are:

1. Blending: Mixing of alcohols in diesel in various proportions is the easiest way of use in C.I. engines. The alcohols can be blended up to 40% in diesel subjected to their miscibility. N-butanol is completely miscible in diesel and shows no separation up to a long storage time.

2. Fumigation of alcohols: The mixing of alcohols with air in the intake manifold displaces up to 50% of diesel fuel requirement. Fumigation is a process of introducing alcohol into an intake manifold of the diesel engine by an injector, carburetor or vaporizer. At the same time, the diesel pump delivers less quantity of diesel. In this process, diesel fuel is used for generating a pilot flame, and alcohol is used as a fumigated fuel.

3. Dual injection: In this technique, there are separate injection systems for each fuel. In dual injection systems, a small amount of diesel is injected (prior to injection of alcohol) as a pilot fuel for the start of combustion and a large amount of alcohol is injected as the main fuel. Up to 90% of diesel can be replaced by alcohols.

4. Alcohol in diesel fuel emulsions: In this technique, an emulsifier is needed to agitate the fuel to prevent separation. In this method up to 25% diesel fuel can be displaced by alcohol. A hydro-shear emulsification unit can be used to produce emulsions of diesel alcohol. However, the emulsion remains stable for a very short duration. Moreover, this method has the disadvantage of high specific fuel consumption at low speeds, and the cost of the technique is also high. Therefore, other methods have been preferred over emulsification.

Out of all the above mentioned techniques, blending is the simplest. The problem of miscibility of alcohol with diesel can be solved by using additives or surfactants. A water proof fuel system and proper selection of materials can help in eliminating the phase separation and corrosion issues.

1.10 Addition of nitrogenated and oxygenated additives:

Simultaneous reduction in nitric-oxides and smoke emissions is quite difficult due to the smoke/NO_x trade off and is often accompanied by fuel consumption penalties.

The stringent emission norms cannot be met through engine design alone. Several methods like retarding the injection timing, use of high injection pressure, EGR, split injection, modifying the combustion chamber geometry to enhance the swirl & squish etc. are being tried to reduce emissions; but there are still problems in the operation of these techniques. Improvement of fuel properties by utilization of oxygenated compounds such as alcohol, ether, or acetate groups have become essential for elimination of exhaust gas emissions from diesel engines.

One prospective method to solve this problem is to use highly oxygenated additives with high Cetane number along with bio-base fuels. This appears to be a promising approach in serving the above-mentioned objective. Such fuels can also be used as supplementary fuels to the diesel engine [17].

Other than alcohols, many nitrogenated and oxygenated compounds can be mixed in limited amounts in diesel or in alcohol-diesel blends to achieve required performance and reduced emissions. The availability of higher oxygen content in the molecular structure of these compounds makes them suitable for mixing with diesel. Some of these oxygenated additives have the capability of improving Cetane number and can restore the viscosity of alcohol-diesel blends. Different mixing techniques for these additives can be used, but blending is the most popular method for small proportions. The blending of additives in n-butanol-diesel blends is the object of interest in the current research.

1.11 Compatibility with engine operation and material

Vegetable oils have comparable energy density, Cetane number, heat of vaporization, and stoichiometric air/fuel ratio with mineral diesel [18]. Vegetable oils obtained from Jatropha, Mahua, Neem, Thumba, algae, peanut oil, sunflower oil and many others are compatible with diesel engines. These oils have a reasonable Cetane number and hence possess less knocking tendency, have low sulphur content and hence are environment friendly. They also have good lubricity, and therefore no major modifications are required in the engines. Personal safety is also improved (flash point is generally 100°C higher than that of diesel). Moreover, these are usable with the existing petroleum diesel infrastructure (with minor or no modifications in the engines).

Biodiesels and pure vegetable oils have higher oxygen content in their molecular structures, and hence are potential fuels for diesel engines. However, these oils have poor volatility and higher viscosity than diesel, which may result in poor atomization, carbon deposition or clogging of fuel lines, as well as thickening and gelling of the engine lubricating oil. These major drawbacks of biodiesels limit their use in C.I. engines [19].

Superior volatility and lower viscosity of alcohols compensate for these adverse properties of biodiesels. Oxygenated additives have additional advantages of high oxygen content (firmly bonded with carbon atom), high Cetane number and high heat of vaporization. It has been reported that with the increase in the percentage of renewable/oxygenated fuel in the blends, complete fuel combustion is achieved. Other beneficial effects of the blends are improved fuel properties, better engine performance, good combustion characteristics, and reduced exhaust emissions. In view of these technical merits, research on the simultaneous use of diesel, alcohols and oxygenated additives in the form of ternary blends is drawing more attention.

Both alcohol and other oxygenated additives improve smoke emission characteristics as well as the performance of diesel engine because of improved combustion. Most of the studies have reported higher NO_x emission for alcohol-diesel blends and reduction in NO_x with oxygenated additives-diesel blends as compared to diesel. In fact, it is very difficult to reduce smoke and NO_x simultaneously because all the efforts to improve combustion will lead to increase in the peak temperature, resulting in increased NO_x [20].

Generally, Biodiesels soften and degrade certain types of rubber compounds and elastomers over time. Fuel hose pipes and fuel pump seals, which are made by elastomers, could be damaged when used with biodiesels or higher blends of biodiesels. Manufacturers need to be wary about use of natural or butyl rubbers with pure Biodiesel. Biodiesel will lead to deterioration of these materials over time, although this effect is hampered up to a certain limit with biodiesel blends. With pure Biodiesel, replacement of natural rubber parts with compatible elastomers is recommended.

Lower alcohols such as Methanol are hygroscopic and prone to absorb water vapor from the surroundings. Alcohols are much more corrosive than diesel and gasoline on copper, brass, aluminum, rubber and many plastics. This narrows down the design and

manufacturing options of engines and other parts with alcohols. Fuel lines and gaskets, seals and even metal engine parts deteriorate with long-term alcohol use. Specifically, methanol is very corrosive to metals.

Specific types of fiber glass reinforced plastic tanks, gaskets, sealants, adhesives and tank liners may not be compatible with alcohols. Fuel dispensers could be made from suitable elastomers for ethanol. However, use of plain aluminum components is not recommended. Fuel distribution and storage systems must be waterproof. In addition to that, currently available pipelines for transportation and unloading of fuel through rail or roads must be re-evaluated in the light of above factors.

1.12 Outline of the Thesis

The thesis is arranged in five chapters. The Chapter 1 describes introduction to alternative fuels, their advantages and limitations. Chapter 2 covers exhaustive literature review on biofuels, alcohols and nitrogenated and oxygenated additives for C.I. engines. The Research gap has been identified and objectives and methodology are set on the basis of research gap. Chapter 3 outlines experimental set up and procedure used for carrying out the research. It includes preparation of blends and mathematical modeling for predicting optimum blends. Chapter 4 covers results and discussions. The details of performance curves and mathematical modeling are also discussed. Finally chapter 5 discusses conclusions drawn from the current research and future scope of work.

Chapter 2

Literature Review

This chapter presents a detailed review of literature regarding use of vegetable oils, biodiesel, alcohols and different fuel-additives as alternative fuels for compression ignition (C.I.) engines with or without structural modifications and with different fuelling techniques. On the basis of literature review and analysis of properties of these fuels, the research objectives and methodology were decided.

C.I. engines are more robust and fuel efficient than spark ignition (S.I.) engines. Thus, the use of C.I. engines (which are mostly diesel engines) is increased in stationary applications along with application in transportation and automobile. C.I. engines suffer from high emissions of smoke and NO_x . However, HC and CO emissions are lower than S.I. engine. Smoke emission can be controlled by improving fuel, improving the combustion process or by suitable after-treatment. Out of these options, use of improved fuels would be an easy solution as it would be applicable for new as well as old engines without structural modifications [21].

A variety of alternative fuels and additives such as alcohols [22]–[28], biodiesels [29]–[31] and vegetable oils [18], [32]–[34] can be used in C.I. engines with adequate performance and reduced emissions. Improved fuels can also be obtained by adding suitable percentages of these alternatives to diesel. Among these, oxygenated additives have drawn more attention because of their capability to reduce emissions without much affecting engine performance [12], [35], [36]. Oxygenated additives are renewable in nature and support the local agriculture industry as well [15], [16]. Research in the field of alternative fuels for diesel engines showed that fuels having oxygen in their molecular structure are capable of reducing emissions of smoke, NO_x , CO and HC with unaltered or even improved performance (in some cases). The fuel-bound oxygen plays an important role in more efficient and complete combustion by leaning the fuel rich zone. However, emissions are also affected by fuel type, injection techniques, engine design, operating parameters and engine running conditions [12][37][38]. In view of these facts, an extensive literature review related to use of vegetable oils, biodiesels, bio-alcohols and

other oxygenated and nitrogenated additives in C.I. engines was done to find scope for work on reduction of emissions using these bio-fuels and additives.

2.1 Vegetable oil as C.I. engine fuel:

Jatropha oil-diesel blends (2.6%, 20% and 50% by volume) as well as 100% unheated and preheated Jatropha oil were tested in a direct injection (DI) diesel engine. It was found that Jatropha oil-diesel blends (2.6% by volume) exhibited better efficiency and lower BSFC with lesser emissions as compared to diesel [39]. In a study with different vegetable oils and their biodiesels it was stated that higher viscosity, very high flash point, lower ignition quality and high cost are the main hurdles in the use of vegetable oils as C.I. engine fuels. Performance of engines with vegetable oils and biodiesels was not much changed as compared to diesel. However, in many cases BSFC was slightly higher for vegetable oil as compared to diesel. In general, smoke & NO_x were decreased and CO & HC were increased for vegetable oil/biodiesel-diesel blends in comparison to diesel. With pure vegetable oils, smoke was reported higher in many cases and with biodiesel, NO_x was reported higher in a few cases. It was concluded that approximately 20% blend of vegetable oils with diesel can be used in C.I. engines without any structural modifications and 100% vegetable oil can be used in C.I. engines with modification in fuel system. The performance of biodiesels was found to be moderate and in-between that of vegetable oil and diesel [40]. Experimental studies were conducted at constant speed and different loads using neat Jatropha oil by varying injection timing, injection pressure and injection rate. It was reported that optimization of operating parameters of engine for neat Jatropha oil result in improved thermal efficiency, decreased smoke and HC emission as compared to standard settings for diesel. However, NO_x emission was found to have increased for these optimum settings for Jatropha oil. At retarded injection timing, increased injection pressure and at higher rate of injection, the emissions were lower for neat Jatropha oil as compared to diesel. HC, smoke and NO_x were found to be lesser by 33%, 26% and 34% respectively for Jatropha oil as compared to diesel. The maximum cylinder pressure, heat release rate and brake thermal efficiency were also lower for Jatropha oil as compared to diesel [41]. In an experimental work with Jatropha-diesel blends (0%-100%), it was concluded that lower blends of Jatropha have

performance and emissions very near to that of diesel. However, at higher blends the performance of engine was found to deteriorate and the emissions were also more. Higher smoke with Jatropha-diesel blends is mainly because of higher viscosity and poor volatility of Jatropha as compared to diesel. For 20% Jatropha-diesel blend, the emissions were similar to that of diesel without any notable deterioration in performance [34]. A similar type of study was done using blends of linseed oil, mahua oil, rice bran oil and biodiesel of linseed oil with diesel at constant speed and varying loads. It was reported that transesterification of vegetable oils is an effective technique of reducing vegetable oil viscosity; thus eliminating operational and durability problems associated with it. Smoke emission and BSFC of vegetable oils was higher due to poor atomization characteristics and lower calorific value respectively. 20% blend of biodiesel with diesel resulted in improved performance with reduced smoke emission [42]. It is now known that blends up to 20% of Jatropha oil with diesel can be used in C.I. engines without any operational problems and with satisfactory performance and emission characteristics. However, more than 20% blending requires preheating. Jatropha biodiesel-diesel blends exhibit better performance and reduced emissions as compared to Jatropha-diesel blends under similar operating conditions. The availability of oxygen in biodiesels leads to better combustion as compared to diesel and this results in reduced emissions [43]. In an experimental study, Karanja, Jatropha and Putranjiva oil blends with diesel (10-40%) were tested for performance and emissions. It was reported that up to 20% blending of these oils with diesel did not affect performance and emissions significantly. However, Jatropha showed better performance among these oils at advanced ignition timing [44]. Rapeseed oils (RO) (heated up to 90°C), and biodiesel from waste cooking oil were tested on a diesel engine to compare performance and emissions with that of diesel. Pure vegetable oil produced operational problems as compared to biodiesel due to higher viscosity. Both RO and biodiesel produced lesser smoke and NO_x as compared to diesel. RO produced higher HC, while biodiesel produced lower HC as compared to diesel [33]. In another study, Canola oil blended with 10-50% kerosene (to reduce viscosity of Canola oil) was tested on a diesel engine-generator set. It was observed that smoke and HC were higher and NO_x was lower for all the blends respectively as compared to diesel. Mixing of 50% kerosene in Calona oil resulted in reduced emissions and was well-suited

for diesel operation [32]. In yet another study, Thumba oil was blended in diesel (10-100%) and was preheated using waste heat of exhaust gases. It was reported that 20% thumba-diesel blend (BU20) when preheated; emitted 2.6% lesser smoke, 0.02% lesser CO, 5 PPM lesser HC, 0.08% higher CO₂, and 11 PPM higher NO_x in comparison to the scenario where the same blend was used without heating. However, preheated BU20 emits 5.6% lesser smoke, 0.01% lesser CO, 9 PPM lesser HC, 0.22% lesser CO₂, and 16 PPM lesser NO_x as compared to diesel. It was concluded that preheating with blending of thumba oil could be a good technique for use in C.I. engines [18].

2.2 Biodiesel as C.I. engine fuel:

It has been concluded from literature review of vegetable oils that use of vegetable oils in diesel engine results in inferior performance and higher smoke in comparison to diesel because of their higher viscosity and carbon contents. Cold starting and filter choking are common problems with the use of vegetable oils in engines. The calorific value of vegetable oils is generally lower than that of diesel. These demerits of vegetable oils can be compensated by transforming them into methyl or ethyl esters of fatty acids (usually called Biodiesels) by transesterification. Biodiesels can be used purely (100% without blending) or can be blended with diesel for use in C.I. engines. No engine modifications are required to use biodiesels as fuels, as they possess properties similar to mineral diesel.[45], [46]. Biodiesels are in general a class of non-toxic, biodegradable and renewable fuels. Available oxygen in biodiesels leads to complete combustion and reduced emissions. Biodiesels have higher Cetane numbers as compared to diesel. Generally in comparison to diesel, biodiesel emissions are less, which is very promising towards a pollution free environment [46].

It was observed in an experimental study that with biodiesels, both ignition delay and duration of diffusion combustion were increased as compared to diesel. Despite this, the premixed heat release part was shortened. With sesame-biodiesels, BTE was higher and emissions were lower as compared to biodiesels of Honge and Jatropha oils. Emissions of smoke, CO and HC were found higher for all biodiesels as compare to diesel. Smoke was increased in the range of 17% to 32% for biodiesels as compared to diesel. It is due to higher viscosity and poor volatility of biodiesel in comparison to diesel, which leads to

poor atomization and thus results in higher emissions. Heat release rates of biodiesels are lower during premixed combustion phase, which leads to lower peak temperature and thus reduced NO_x as compared to diesel [45]. Contrary to the results of the study reported in [45]; reduction in PM, HC, CO and an increment in NO_x was reported with Canola biodiesel in the experimental results of a study reported in [46].

Suitability of biodiesels for C.I. engines in pure form and in blended form was reviewed. It was reported that biodiesels and its blends were helpful in reducing smoke, CO and HC emissions without affecting performance of engine too much. However, NO_x emission was found to be more due to higher peak temperature as a result of better combustion. It was found that pure biodiesel could be used in C.I. engines with optimization of injection timing and modification in fuel system. However, on the down side, problems of cold starting, lines clogging and storage are also associated with use of pure biodiesel. The use of biodiesel blends up to 20% (particularly Jatropha biodiesel) with advanced ignition timing showed satisfactory performance with reduced smoke, CO and HC emissions. However, NO_x increases slightly and is dependent on Cetane number, maximum flame temperature, oxygen content and injection timing [47]. A literature review on effects of biodiesels on engine emissions reveals a general trend of reduction in NO_x using retarded injection and slight increment of other emissions. The discrepancy in emission results in different studies can be attributed to different engine designs, different operating conditions, different methodologies, different instruments and calibrations and different properties of biodiesels obtained from various feed stocks. It was reported that in most of the cases, BSFC was found higher because of lower heating value of biodiesel as compared to diesel. However, the effect of lower heating value on BTE is not significant [48]. Another study reviewed the cold flow properties of biodiesel and their impact on engine operation and performance. It was stated that inferior cold flow properties of biodiesels are the main reasons for the plugging of fuel lines and filters. Also, because of poor atomization the combustion is incomplete and results in higher smoke emission. Mixing of some solvent or surfactant with biodiesel was reported to have reduced these problem to some extent [49].

A study with rapeseed biodiesel concluded that 100% biodiesel could be used by optimizing injection timing for reduced emissions with reasonable engine performance.

However, with 100% biodiesel, BSFC increased by 10% and BTE remain approximately similar to that of diesel. Smoke, NO_x, CO and HC were reduced by 50%, 25%, 25% and 30% respectively at retarded ignition timing as compared to diesel [50]. Another study with methyl and ethyl esters of Karanja oil reported inferior performance and reduced emissions as compared to diesel. For biodiesels, NO_x emission was increased in the range of 10-25% at part loads but reduced at full load as compared to diesel. It was concluded that methyl esters were better fuels for C.I. engines than ethyl esters in terms of performance and emissions [51]. Effects of biodiesel, CNG (compressed natural gas)-diesel and CNG-biodiesel blends were evaluated on a dual fuel engine's performance and emissions. It was observed that NO_x emission of all fuel combinations were lower than diesel. However, presence of CNG enhances the NO_x value in any blend. CO and HC emissions were found to decrease with increasing amount of biodiesel in blends; but still remain higher as compared to diesel [30]. Experimental studies with waste cooking oil-biodiesels were conducted with different percentages of blends in diesel and with pure biodiesel. It was observed that BSFC of all biodiesel and blends were higher and BTE was lower as compared to diesel. Smoke, CO and HC emissions were lower with biodiesels of waste cooking oils and more and more reduction was seen with increasing percentage of biodiesel in diesel. The emission of NO_x for all biodiesel blends and for pure biodiesel was found to be higher as compared to diesel. The availability of oxygen in biodiesel leads to complete and better combustion. This in turn reduces smoke, CO and HC. However, NO_x increases due to increased peak temperature in the initial phase of combustion [52], [53].

Jatropha biodiesel and its blends with diesel in the range of 20-80% were tested to evaluate the performance and emission characteristics. It was observed that BSFC of all blends was higher and BTE was slightly better as compared to diesel. NO_x emission was higher for biodiesel and biodiesel blends while other emissions were lower as compared to diesel [54]. Experiments were also conducted with rice bran-biodiesel, blends of biodiesel in diesel and ternary blends of (10%) biodiesel and (5-15%) ethanol in diesel with varying load conditions on a DI diesel engine. BSFC and BTE of biodiesel and all blends were reported to be higher as compared to diesel over the entire load range. The emission of NO_x with biodiesel and all the other fuel blends were lower at lower loads

and higher at higher loads as compared to diesel. CO emission was higher and HC emission was lower of all blends as compared to diesel. HC emission of ternary blends increased and smoke decreased with increasing amounts of ethanol in blends [55].

It can be summarized from the literature review that high viscosity, high molecular weight and low volatility, of biodiesels lead to troubles such as engine deposition, injector cooking and fuel line clogging. These problems become obvious at lower working temperatures, which further increase the viscosity of biodiesel beyond acceptable limits. Currently used diesel engines were developed for operation with fossil diesel. For these engines, biodiesels cannot deliver adequate performance without some structural modifications. Therefore, more investigations are required with some other alternative fuels or fuel additives that are able to compensate various engine operational problems associated with biodiesel.

2.3 Alcohols as C.I. engine fuels:

Superior volatility and lower viscosity of alcohols compensate for the lack of these properties in biodiesels. The oxygenated additives having advantage of high oxygen content in their molecular structure. It was reported that as percentage of oxygen increased in the fuel, combustion was completed more effectively. The blending of these additives in diesel resulted in improved fuel properties, better engine performance, good combustion characteristics, and reduced exhaust emissions.

Both alcohol and other oxygenated additives improve smoke emission as well as the performance of diesel engine because of improved combustion. Many studies have reported higher NO_x emission for alcohol-diesel blends and reduction in NO_x with many oxygenated additives-diesel blends as compared to diesel. In fact it is very difficult to reduce smoke and NO_x simultaneously because all the efforts to improve the combustion will lead to increase in the peak temperature, and thus resulting in increased NO_x.

Alcohols such as methanol, ethanol and butanol are potential alternative fuels for I.C. engines because of factors like high oxygen content, high octane number, being liquid at room temperature and their production from renewable sources. Methanol and ethanol have very high octane ratings but very poor Cetane numbers. Thus they are better fuels for S.I. engines. However, nowadays these alcohols are being tested for C.I. engines also.

2.3.1 Methanol and Ethanol

Methanol is the primary alcohol having one carbon atom. Methanol has many advantages as a C.I. engine fuel such as lower ozone formation, low NO_x emission, lack of sulfur compounds, and easy refueling. It is reported that methanol-diesel blends produce lesser air pollution than diesel in C.I. engines. It has been reported that with increasing percentage of methanol in methanol-diesel blends, Smoke, CO and hydrocarbon emissions decrease, but NO_x emission increases. [56]. An experimental study was done with (5-15 %) methanol-diesel blends by varying injection pressure and injection timing. It was observed that with methanol-diesel blends BSFC and BSEC increased while BTE decreased as compared to diesel. This is due to lower calorific value of methanol. It has been found that with methanol blended fuel, smoke, CO and HC emissions decrease while NO_x emission increase. With methanol-diesel blends any deviation from original injection pressure and injection timing resulted in inferior performance. The increased injection pressure and advanced injection timing resulted in decreased smoke, CO and HC emissions but increased NO_x emission [27]. Experimental study was done with 5-10% methanol and ethanol blended in diesel by varying speed at constant load. Engine showed higher BSFC and lower BTE with blends as compared to diesel. However, ethanol depicted better performance than methanol. In order to prevent phase separation, a solvent was used with methanol and ethanol blends. Emission results were found similar to [27]. Additionally, methanol is more effective in controlling smoke as compared to ethanol due to higher content of oxygen (methanol contains 50 % while ethanol contains 34.8 % oxygen by mass) [26].

An experimental study with different ethanol-diesel blends (E2.5%, E5%, E7.5%, and E10%) reported decrement in BSFC and increment in BTE with increasing levels of blending as compared to diesel. Smoke, CO and HC were reported to be lower with ethanol-diesel blends. The E7.5% blend showed best results of performance and emissions among all the tested fuels [24].

Another study with 5-20% ethanol-diesel blends reported that up to 20% blends can be used in diesel engine without any structural modification. However, performance results reported were inconsistent with [24]. No problem was reported during cold starting. NO_x and CO reduction was reported maximum up to 24% and 62% respectively with ethanol-

diesel blends as compared to diesel [57].

A review study on ethanol-diesel blends reported no noticeable change in performance of engine up to 10% blending of ethanol in diesel. Beyond 10% blending, inferior performance of engine was reported. With ethanol blended fuels, long-term durability tests showed no adverse effects on engine wear as compared to diesel fuel. The emissions with ethanol blends were reduced considerably and were also found to vary from engine to engine [58]. It was reported in a study that ethanol is a bio-based and oxygenated fuel and addition of ethanol up to 20% in diesel was not creating any operational and durability problem. Addition of ethanol is also helpful in keeping low lubricant temperature and in controlling emissions of NO_x and CO. Similarly addition of biodiesel up to 20% improved the performance of engine and reduced smoke emission. Vegetable oil methyl esters were found very effective in reduction of emissions of diesel engine as compared to diesel [38]. An experimental study was done with diesel and E85 (85% ethanol and 15% gasoline) under dual fuel mode. E85 was introduced in intake manifold while diesel was injected directly in cylinder. With E85 the combustion duration shortened and ignition delay increased slightly. At partial loads the emission of NO_x was observed lower, while it was higher at full load with increased share of E85. The higher heat of vaporization produces a cooling effect, but on the other hand, the availability of oxygen enhances the combustion temperature. The joint effect of these two factors along with loading conditions decides the increase or decrease of NO_x emission. Smoke was reduced drastically with E85 injection due to increased amount of heat release in premixed phase of combustion. The emissions of CO and HC were increased and BTE was decreased with E85 injection in dual fuel mode [15].

A report on emissions of diesel engine using additive-ethanol-diesel blends with different combinations of speed and load showed that 10% and 15% addition of ethanol were capable of reducing smoke and NO_x simultaneously. The 15% ethanol blended diesel was reported more effective to reduce smoke and NO_x than the 10% blend. The 15% ethanol-diesel blend reduced smoke and NO_x by 22–75% and by 60–84% respectively. The addition of an oxidation catalyst in ethanol-diesel blends resulted in decreased CO and HC along with smoke and NO_x emissions [59]. In a study with 10-15% ethanol blended in diesel, it was reported that to stabilize the blends, especially at lower temperatures,

some emulsifier or co-solvent is desirable. Higher BSFC and slightly higher BTE were reported with ethanol blended fuel as compared to diesel. The reduction in PM for 10% and 15% ethanol blends was 20-27% and 30-41% respectively as compared to diesel. A slight reduction of 4-5% in NO_x along with an increment in HC emission was reported. However, both increase and decrease in CO emission was reported as compared to diesel [60].

Biodiesels (100%) and bioethanol (10-40%)-diesel blends were tested on a turbocharged diesel engine. It was reported that engine ran without any operational problem up to 30% blending of ethanol with a maximum observed reduction of 59% in PM. NO_x was also observed lower as compared to diesel and biodiesels. Biodiesels are more effective in PM reduction (up to 93%) than ethanol-diesel blends but have increased NO_x emission as compared to diesel and ethanol-diesel blends [61].

In an experimental study 3-25% of butanol was blended in equal amount of diesel-biodiesel mixture to see the effect of blending and load variations on performance and emissions of a diesel engine. For all operating conditions and fuels, CO emission increased and of NO_x emission decreased with ethanol-diesel-biodiesel blends as compared to diesel. For lower concentration of ethanol HC decreased and for higher concentrations, it increased. However, above 70% of full load, HC decreased for all ethanol-diesel-biodiesel blends as compared with diesel [62].

The effect of ethanol blending on engine combustion, performance and emissions was evaluated experimentally with varying speed and air-fuel ratio. 5-15% ethanol was mixed with diesel and biodiesel-diesel blend. It was found that effect of fuel oxygen on ignition delay is more significant than that of Cetane number. The ethanol blended diesel showed longer ignition delay as compared to diesel (up to 15.4% longer). Addition of 5-15% ethanol shifts peak of heat release rate and maximum pressure from the T.D.C. due to longer ignition delay (which is the result of high latent heat of vaporization of ethanol). At the same time the addition of 5% biodiesel relocates these peaks towards T.D.C. In this study, slower combustion rate was reported in premixed zone with addition of ethanol, which is contradictory to most of the other studies. BSFC of all the blends was higher as compared to diesel. BTE of all blends was lower except for ethanol-biodiesel-

diesel blend. NO_x and HC emission of ethanol blended fuel were lower as compared to diesel. CO emission was lower at low speed and higher at high speed. At lean mixture all blended fuels emitted lower smoke than diesel, but at richer mixture and moderate speeds, the smoke emission increased for blended fuel. It was concluded that fuel containing 15% ethanol, 5% biodiesel and 80% diesel, would be an efficient fuel for diesel engines [63].

2.3.2 N-butanol:

It was established that addition of bio-alcohols in diesel engines resulted in reduced smoke emission. The structure of alcohols contains more oxygen as compared to biodiesels, thus they are more effective in smoke reduction [38], [64]. A literature review was done to explore benefits of n-butanol as compared to methanol, ethanol and biodiesel as a C.I. engine fuel. The main advantages of n-butanol over lower alcohols are: higher heating value, low volatility, better auto-ignition capability, better miscibility with diesel, less corrosive nature and suitable viscosity (compatible with diesel). It has been established that the volatility of alcohols reduces with increment of carbon atoms in structure. Thus, n-butanol has lower tendency of cavitation and vapor lock in lines when used as a fuel in C.I. engines. N-butanol can be produced by biomass and is usually called bio-butanol. In comparison to biodiesels, n-butanol has higher content of oxygen and is capable of reducing smoke and NO_x simultaneously. In general when n-butanol is blended in diesel, both BSFC and BTE increase slightly. Blending of n-butanol in excess of 40% is not recommended due to irregularities noticed in combustion. Smoke emission for n-butanol blends has been found to decrease as a function of fuel-bound oxygen. Lower combustion temperature because of lower calorific value of n-butanol and higher latent heat of vaporization tends to reduce NO_x . On the other hand, due to lower Cetane number, ignition delay is increased, which tends to create higher peak temperature in premixed combustion and in turn, increases NO_x . The combined effect of these two factors is decisive in the increase or decrease of NO_x . HC emission increases with n-butanol. However, CO emission may increase or decrease and depends on engine design, operating conditions and blending ratio. It was concluded that n-butanol has good potential as a C.I. engine fuel. However, more study and experimental data are needed with different engine designs and operating conditions to reach a definite conclusion about n-butanol [64].

The review study on methanol, ethanol and n-butanol describe various aspects of use of these alcohols in diesel engine. These are the bio-oxygenated fuels and have high oxygen content and low carbon & sulfur in molecular structure. An exhaustive analysis was done to compare these alcohols and their blends in diesel. It was reported that butanol has many properties similar to diesel and is a better fuel for C.I. engines than methanol and ethanol. Butanol has high Cetane number, more volatility and high miscibility with diesel as compared to methanol and ethanol. Butanol has low hygroscopicity (thus less corrosive) than methanol and ethanol. These properties of butanol make it a safer fuel. Further, it is also deemed possible to establish a safe distribution network for butanol using the existing technological infrastructure. On the other hand, blending of methanol and ethanol is recommended just before use due to phase separation tendency in diesel blends. Butanol has a higher flash point than methanol and ethanol and hence is safer to use in I.C. engines. Butanol has better viscosity than methanol and ethanol. However, the main disadvantage of butanol blending in diesel is its lower Cetane number than diesel which weakens the auto-ignition capability of butanol-diesel blends. To overcome these limitations with alcohols in diesel, the need of mixing some suitable additive has been emphasized in this study. The present review concluded that blending of n-butanol in diesel reduces smoke, NO_x and CO emissions while HC emission increases as compared to diesel. NO_x emission also depends on butanol content, use of different analytical techniques, and engine operating conditions. Majority of the studies are in agreement that addition of butanol in engine results in increase of BSFC and reduction of BTE. This is because of lower calorific value of butanol as compared to diesel. Increased injection pressure reduces smoke but increases NO_x . The variation in injection timing also influences engine performance with butanol-diesel blends. It is summarized on the basis of review of literature that there is a need to undertake studies on varying engine operating conditions using butanol-diesel blends and mixing of additives in alcohol-diesel blends; since work in this direction is limited [23].

Many other studies have also reported that the presence of oxygen; low viscosity and high volatility of alcohols make them preferred fuel for diesel engines as compared to vegetable oils and biodiesels. Among alcohols, n-butanol has added advantages of higher heating value, lower latent heat of vaporization, higher Cetane number and better

miscibility with diesel as compared to methanol and ethanol. The calorific value of n-butanol is also higher than methanol and ethanol. This implies that same amount of n-butanol produces higher power from the same engine running on ethanol/methanol-diesel blends [13], [20], [65]–[67].

Blends of ethanol (10%)-diesel and butanol (16%)-diesel were tested for performance and emissions using the New European Driving Cycle (NEDC) with cooled EGR. The fuel consumption using both blends was higher as compared to diesel. Lower heating values of ethanol and butanol are the main factors associated with higher BSFC. Smoke emission with blended fuels is reported considerably less as compared to diesel. Increased content of oxygen in the fuel prevents the production of smoke in fuel rich zones. The emission of NO_x depends on two factors: (i) low Cetane number and high oxygen content lead to higher peak temperature and (ii) high heat of vaporization and lower flame temperature of blends tends to reduce NO_x emission. The cumulative effect of these two factors as well as engine design and operating conditions decide the amount of NO_x emission. However, in the present work, NO_x was found higher with ethanol-diesel and butanol-diesel blends. CO emission with ethanol and butanol blends was reported low as compared to diesel only. The probable reason is the dominant effect of oxygen content than effect of higher heat of vaporization. However emission of HC for blended fuels was more than diesel. The study concluded that emissions for alcohols-diesel blends can be reduced by optimizing the operating parameters [68].

In a study, literature related to effects of ethanol-diesel and n-butanol-diesel blends on performance and emission characteristics of diesel engine operating in transient conditions (i.e. at increased load, acceleration and starting) was reviewed. It was concluded that results in transient operation are very similar to steady state operation. In general, blending of ethanol and butanol in diesel tends to reduce smoke & CO and increase the HC emission. Higher content of oxygen is mainly accountable for reduction in smoke. It was also reported that alcohol-diesel blends are more effective in reduction of smoke as compared to biodiesel-diesel blends. NO_x emission reduction or increment depends on percentage of ethanol/butanol in diesel, engine calibration and operating conditions. It was summarized that trends of NO_x emission with ethanol/butanol-diesel

blends are still not very clear, hence needed more extensive study with varying engine operating parameters [69].

To analyze the effect of vegetable oil and alcohols on engine combustion and emission characteristics under steady state and transient conditions, tests were conducted on a heavy duty automobile diesel engine. Cottonseed oil (10% & 20%), its biodiesel (10% & 20%), ethanol (5% & 10%) and butanol (8% & 16%) were blended with diesel for tests under steady state conditions. Because of higher viscosity of vegetable oil and phase separation tendency of ethanol, the transient tests were conducted with only 30% biodiesel and 25% n-butanol blended fuels. In steady state conditions it was found that ignition delay for alcohol blends increased and injection pressure diagram delayed, while for vegetable oil and biodiesel these remain unaltered. The maximum cylinder pressure and temperature of alcohol blended fuels decreased more than vegetable oil and biodiesel with respect to diesel. The heat release analysis and fuel properties were jointly decisive in the emissions pattern of fuels. For alcohols, smoke and NO_x both decreased, while for vegetable oil and biodiesel, smoke decreased and NO_x increased. Nevertheless, n-butanol blends were found to perform better among all tested fuels. Except vegetable oil blends, for all other blended fuels, CO decreased and HC increased. The availability of fuel-bound oxygen in blended fuel expands the lean spray flame-out region during the delay period. In this region fuel is outside the lean limit of combustion and hence incomplete combustion results in increased HC emission. In transient conditions, smoke emission remains similar to that of steady state condition, but NO_x emission is higher for bio-fuels because of dominant effect of increased temperature in premixed phase [70].

A similar type of study was done under steady state conditions with cottonseed oil and its bio-diesel in ratios of 10/90, 20/80 & 50/50 (by vol.), ethanol 5/95, 10/90 and 15/85 (by vol.), n-butanol and DEE 8/92, 16/84 and 24/76 (by vol.) on a diesel engine. Unlike the results seen in [70], for vegetable oil and biodiesel, it was found that the ignition delay reduced and fuel injection and pressure diagram advanced. The cylinder pressure and temperature were higher in initial phase and lower in expansion stage for vegetable oil and biodiesel. The pressure and temperature were lower for n-butanol & DEE as compared to diesel. Smoke, NO_x and CO emissions were decreased for all blended fuels as compared to diesel. Higher reductions of smoke and NO_x were observed with n-

butanol and DEE respectively. It was also found that BSFC increased and BTE slightly improved for all blended fuels except DEE [12].

In a study with 15% addition of butanol with biodiesel-diesel blends, it was reported that for up to 10% butanol addition, the variation in BSFC was insignificant and an improvement was observed in BTE at moderate and high engine loads. PM, elemental carbon (EC) concentrations, and total number of emission particles were found to have dropped significantly when butanol was added to biodiesel-diesel blend [19]. In another study, butanol was added to microalgae biodiesel-diesel blends up to 20% (by volume) and tested on diesel engine. It was reported that butanol addition caused a slight reduction in torque and brake power. Emissions were also found to have improved [71]. The experiments were conducted using blends of biodiesel-diesel and blends of butanol-diesel. It was reported that both blended fuels effectively reduced smoke and elemental carbon emissions as compared to diesel, but butanol blends were more effective than biodiesel [72].

N-butanol can be produced from fossil matter as well as from biomass feedstock (namely bio-butanol), however, the properties of n-butanol produced from both sources are same [73]–[76]. Experimental studies were conducted on four stroke, DI, diesel engines at steady state conditions with 8%-24% (v/v%) n-butanol-diesel blends. With blended fuels the BSFC was higher and BTE was slightly improved as compared to diesel. The probable reason of this is lower calorific value of n-butanol as compared to diesel. The analysis of cylinder pressure and heat release revealed that with n-butanol-diesel blends, the ignition delay was increased, peak of fuel injection diagram was slightly delayed, peak of heat release diagram was increased in premixed combustion phase and cylinder pressure remained unaffected. High heat release is not reflected in the significant increment of BTE probably because of lower fuel/air equivalence ratio (engine run leaner) in later stages of combustion. The smoke, NO_x and CO emissions were reduced with n-butanol-diesel blends as compared to diesel and this trend of reduction continues with increasing percentage of n-butanol in diesel. However, emission of HC increases with increasing percentage of n-butanol in diesel. It can be summarized that n-butanol is a suitable fuel for diesel engines from the viewpoint of performance and emissions with added advantages of higher Cetane number and better miscibility as compared to other

alcohols [75]–[77]. In a study on high speed DI diesel engine with 8%, 16% and 24% n-butanol-diesel blends, statistical study of the cycle-by-cycle variation of engine combustion and emission parameters was done. It was concluded that n-butanol blending has no significant effects on cyclic pressure variations as well as on performance and emission parameters. Smoke, NO_x and CO decreased and HC emission increased with n-butanol-diesel blends as compared with diesel [78].

A similar type of experimental study was done on a six-cylinder, turbocharged, DI diesel engine on two speeds and three loads under steady state conditions. Data was observed for engine combustion, performance and emissions with (5% & 10%) ethanol-diesel and (8% & 24%) n-butanol-diesel blends. Experimentally obtained heat release values and pressure diagrams were analyzed with energy and state equations and it was concluded that for all the blends, the ignition delay was increased, the fuel injection pressure diagram was delayed and maximum cylinder pressure & temperature were reduced as compared to diesel. The BSFC of blended fuel was higher than diesel and BTE was slightly improved. To achieve same load conditions during tests with alcohols-diesel blends, higher flow rates of fuel mass were required as compared to diesel, and this resulted in increased BSFC. However, the BSFC of n-butanol blends was lesser than that of ethanol blends. The improvement in BTE indicates that lower calorific value is not a dominating factor affecting BTE as opposed to BSFC. Some other factors such as spray property, fuel quality etc. were also found to have counteracting influences on performance [79].

To investigate emission characteristics during transient conditions with biodiesel and n-butanol (bio-butanol), experimental studies were done on an automotive diesel engine. Biodiesel (30%)-diesel and n-butanol (25%)-diesel blends were tested during hot starting and acceleration (with different combination of speeds and loads). It was reported that during hot starting conditions, the performance and emission results of engine are very similar to those at steady state conditions, except that NO_x was reported higher for blends as compared to diesel. However, n-butanol affects combustion and stability behaviour of engine to a lesser extent as compared to biodiesel during hot starting and acceleration tests. During hot starting with biodiesel blends, smoke increased by 40%, while with n-butanol blends, smoke decreased by 69% as compared with diesel. The availability of

oxygen in biodiesel is helpful in reducing smoke but at the same time, higher viscosity of biodiesel plays the most influential role during starting. The spray atomization rate is reduced and mixture heterogeneity in cylinder is increased. This leads to increased smoke emission. On the other hand, with n-butanol blends, engine runs overall leaner and produces less smoke. The NO_x emission was increased by 30% and 51% with biodiesel-diesel and with n-butanol-diesel blends respectively during starting condition. Higher fuel-bound oxygen leads to increased temperature in premixed phase, which in turn increases the NO_x emission. In different acceleration tests it was found that smoke decreased and NO_x increased for biodiesel and n-butanol blends. The maximum values of smoke emission were lesser by 40% and 73% respectively for the biodiesel and n-butanol blends as compared to diesel. In the tests performed, maximum value of NO_x was higher by 52% and 35% respectively for the biodiesel and n-butanol blends as compared to diesel. The leanness due to availability of oxygen and the temperature inside the cylinder plays the decisive role in the production of smoke and NO_x during combustion [80],[81].

In an experimental study, it was reported that smoke and NO_x can be reduced by blending of fuel and management of injection pressure, injection timing & EGR rate without affecting engine performance. It was found that for diesel at higher injection pressure and retarded injection timing, smoke reduced and NO_x increased. Better atomization and high mixing rate were found to be the main factors leading to reduced smoke. Increased ignition delay and high volatility of n-butanol-diesel blends (BU20 and B40) provide sufficient time for better mixing of fuel in air before starting the combustion. The blending of n-butanol at advanced ignition and at low injection pressure creates conditions similar to low-temperature pre-mixed combustion, in which approximately all fuel is injected before the commencement of combustion, and this in turn reduces smoke and NO_x emissions [82]. On the whole, there is strong evidence from past research, that the mixing of n-butanol in diesel, biodiesel, vegetable oil and diesel-biodiesel/vegetable blends results in improved emissions. Some other studies with oxygenated fuels (mainly n-butanol) have been reviewed and summarized in Table 2.1.

Table 2.1 Literature review with various blends of n-butanol, biodiesel and other oxygenated additives in diesel

Author	Engine setup used	Fuel used	Observations and results
Chen et al., 2014[83]	modified, 4-stroke, water-cooled, single cylinder research diesel engine with EGR	n-butanol 40% on volume basis (v/v) in diesel	lower smoke, higher NO _x , butanol with medium EGR has resulted in increased thermal efficiency
Yamamoto et al., 2012[84]	Single cylinder, water cooled, naturally aspirated, Direct Injection(DI), YANMAR Co. Ltd., NFD 170-(E)	ethanol and n-butanol 30%, 40% and 50% (v/v) in diesel	lower smoke, higher NO _x , butanol is better than ethanol
Lopez et al., 2015[85]	4-cylinder, 2.5 L, turbocharged (TC), DI, diesel engine	ethanol and n-butanol 10% (v/v) in diesel	reduced particulate matter and NO _x
Zoeldy et al., 2010[86]	4 Cylinder, 4 stroke, indirect injection PSA XUD 9 A/L, diesel engine	n-butanol 2.5-10% (v/v) in diesel	up to 5% butanol is very effective in reducing NO _x and PM under 50nm size
Sahin and Aksu, 2015 [87]	4 cylinder, 4-stroke, water-cooled, TC, common-rail injection, 1.461 L Renault DI, diesel engine	n-butanol 2-6% (v/v) in diesel	the maximum smoke reduction is 21.75% with B4 and maximum NO _x reduction is 5.03% with B2.
Sahin et al., 2015[88]	4 cylinder, 4-stroke, water-cooled, TC, common-rail injection, 1.461 L Renault DI, diesel engine	n-butanol and fumigated n-butanol 2-6% (v/v))	reduced smoke, reduced NO _x for all combinations except 4% and 6% blends of n-butanol in diesel
Merola et al., 2014 2015[89]	4-cylinder, TC, water cooled, DI, diesel engine	n-butanol 20% (v/v) in diesel	the best trade-off between smoke-NO _x at higher Inj. Pr., BU20 reduced smoke drastically with a slight increment in NO _x and a small increment in BSFC at moderate Inj. Pr.
Siwale et al.,	4-cylinder, 1Z type, 1.9 L-66 kW Turbo-Direct Injection	n-butanol 5-20%	at BU20 max smoke reduction is 85.1%

Author	Engine setup used	Fuel used	Observations and results
2013[90]	(TDI) Volkswagen, diesel engine	(v/v) in diesel	and significant increment of NO _x
Fushimi and Kinoshita, 2013 [91]	single cylinder, 4-stroke, DI diesel engine	1-butanol, 2-butanol and isobutanol (10-50%, by mass)	up to 40% blend BTE unchanged, smoke reduced (up to 85%), up to 30% blend NO _x unchanged and at 40% blend NO _x reduces slightly
Chen et al., 2013[92]	high-speed, TC- inter-cooled, direct injection (DI), diesel engine	n-butanol 20-40% (v/v)in diesel	increased BTE by 2.7%, decreased smoke by 50.3%, increased NO _x by 15.8% at rated power
Zhang et al., 2016[93]	single cylinder, four-stroke, DI, diesel engine (L70AE, Yanmar Corporation), 4.5 kW	butanol and pentanol 10-20% (v/v) in diesel	same BTE, BU20 was showed better result of PM reduction
Ibrahim, 2016[94]	Single cylinder, 4-stroke, DI, air-cooled, TD212, diesel engine	butanol–diesel–biodiesel, Biodiesel	increased brake thermal efficiency (BTE) 6.5%, increased NO _x slightly
Liu et al., 2013[95]	modified single-cylinder, 4-stroke, water-cooled, diesel engine, EGR (0-62%)	n-heptane, iso-octane, n-butanol, 2-butanol and methyl Octynoate 20% (v/v) in diesel	reduced smoke 32.8% for BU20, same BTE and NO _x at different blends, increased EGR resulted in reduced thermal efficiency
Zheng et al., 2015[96]	4-Cylinder, 4-stroke, re-configured to single cylinder, common rail	n-butanol with high pressure direct injection	NO _x and smoke reduced substantially without EGR, advanced Inj.T. cause very high maximum rates of pressure rise while delayed injection timings prone to misfire incidence
Huang et al., 2015[97]	4-cylinder,variable-geometry TC, EGR, DI, high-pressure common rail fuel injection, diesel engine	n-butanol 20-30% (v/v) in diesel	reduced smoke and NO _x with the addition of n-butanol, Reduced smoke and NO _x with advancing

Author	Engine setup used	Fuel used	Observations and results
			the pilot injection
Zhou et al., 2014[98]	A constant volume chamber bore 110 mm, height 65 mm. This chamber can imitate spray and combustion practice of a diesel engine	butanol 12% (v/v) and other compounds 8% (v/v)	better combustion efficiency and emitted approximately zero smoke as compared to diesel
Atmanli et al., 2015, 2014[99], [100]	4-cylinder, 4-stroke, TC, DI, Land Rover 110, diesel engine	vegetable oil 20% (v/v) and n-butanol 10% (v/v) in diesel	increased NO _x , increased BSFC, decreased BTE
Atmanli et al., 2015[101]	4-cylinder, Onan DJC type, indirect injection, diesel engine	n-butanol 20%-60% (v/v) in diesel-vegetable oil	decreased BTE, increased NO _x
Atmanli, 2016[102]	4-cylinder, Onan DJC type, indirect injection, diesel engine	Propanol, n-butanol and 1-pentanol 20% (v/v) in diesel-biodiesel blends	BTE improved by 5.58% for 20% butanol, NO _x reduced for all alcohol blends as compared to diesel-biodiesel blends
Intenan et al., 2015[103]	inline 4-cylinder, water-cooled, TC, diesel engine	Jatropha biodiesel-diesel blend with n-butanol and diethyl ether 5-10% (v/v)	10% n-butanol reduced smoke and NO _x by 27% and 8.8% as compared to biodiesel (20%)-diesel blend, 10% diethyl ether reduces smoke and NO _x by 38.58% and 12% as compared to biodiesel (20%)-diesel blend
Fayad et al., 2017[104]	single-cylinder, 4-stroke water-cooled, common rail fuel injection system, diesel engine	butanol 20% (v/v) in diesel	reduced PM with BU20 and using post injection, increased NO _x slightly, increased BTE slightly

Author	Engine setup used	Fuel used	Observations and results
Isik et al., 2016[105]	4-cylinder, 4-strokes, DI, and water-cooled NWK22 diesel engine generator	n-butanol 10% (v/v) and Biodiesel 10-20% (v/v) in diesel	Increased BTE, reduced NO _x and CO
Vojtisek-Lom et al., 2017[106]	water cooled inline 6-cylinder, TC,5.9-liter, Iveco, Tector, F4a E0681B C109, diesel engine	n-butanol 20% (v/v), isobutanol 20% (v/v)and hydrotreated vegetable oil (HVO)30-100% (v/v)	reduced black smoke, unchanged NO _x and BTE
Nabi et al., 2017[107]	6-cylinder common rail diesel engine	n-butanol 10%, 20% and 30% (v/v) in diesel	reduced power, higher BSFC, PM and UHC reduced, NO _x increased
Saravanan et al., 2017[108]	Constant-speed, single-cylinder, 4-stroke, DI diesel engine (modeling with variation of Inj. T., Inj. Pr. and EGR)	iso-butanol 40% (v/v) in diesel	Isobutanol-diesel blend injected at 240 bar, 23°CA btdc with 30% EGR was predicted to be optimum for engine performance and emissions. The maximum 4% error was found in prediction.
Huang et al., 2017[109]	4-cylinder diesel engine, CR 16.5, 1.99 L and 1600 rpm	butanol 20% v/v (BU20), 10% and 20% PODE ₃₋₄ in BU20	reduced smoke for all blends, increased NO _x slightly, increased CO with BU20, reduced HC and CO with PODE ₃₋₄ in BU20
Nayyar et al. 2017 [110], [111]	Single cylinder 4-stroke, constant speed, VCR diesel engine	n-butanol 10%, 15%, 20% and 25% (v/v) in diesel	20% blending of n-butanol-diesel blend reduced smoke, NO _x and CO, increased CO ₂ and HC as compared to diesel.

From the above literature review it is clear that majority of research agrees that in general, the addition of n-butanol in diesel or biodiesel/vegetable oil-diesel blends reduces smoke significantly and reduces NO_x slightly. However, some of the studies have reported higher NO_x emission for n-butanol-diesel blends. NO_x emission mainly depends

on two factors: (i) peak temperature in the combustion zone and (ii) time duration of sustenance of this peak temperature. The conflicting results pertaining to NO_x may be because of variations in these two factors as well as other factors including n-butanol content, engine operating conditions, engine set-up, the use of different injection techniques, injection pressure etc. [69], [96], [97]. *With the technical merits of n-butanol, several researchers have studied the use of n-butanol in the diesel engine in the past few years. However, the study on the effect of n-butanol-diesel blends on engine operating parameters is limited. This is the main motivation for the current research with n-butanol-diesel blends. Moreover, extensive research on emissions with the use of various blends has shown to have a lot of variations; which makes it difficult to come to a conclusion about an optimal blend. This forms another motivation for using n-butanol-diesel blends to test engine performance and emissions.*

2.4 Other oxygenated additives as C.I. engine fuel:

In C.I. engines, alcohol-diesel blends have improved the emissions up to a certain limit, but at the same time, Cetane number (CN) and viscosity of fuel were observed to be adversely affected. Some Cetane number improvers may need to be blended in alcohol-diesel blends to recover these properties. When a small percentage of oxygenated additives and nitrogenated additives were blended with diesel, Cetane number of the blend and combustion quality inside the combustion chamber were improved. This is because of the participation of molecular oxygen in combustion process, thus leading to complete combustion and eventually resulting in reduced emissions. It was reported that during combustion, ignition delay of blended fuel was reduced due to these additives. The maximum temperature in the combustion chamber was increased and the duration of the maximum temperature was decreased with increased percentage of oxygen due to blending of oxygenated additives in the base fuel [112],[113].

In a study on different oxygenated additives, it was reported that when 30%-40% oxygen is present in the fuel by mass, production of smoke precursors was insignificant. Due to higher levels of O_2 in fuel and the need for more hot air to acquire self ignition temperature because of high heat of vaporization of oxygenated additives, the overall equivalence ratio is reduced in premixed zone. This further reduces the production of

smoke precursors. It was reported that addition of oxygenated additives to fuel reduced CO and HC emissions also. However, this was accompanied by a slight increment in fuel consumption[113].

In another study, diesel, biodiesel-diesel blend and biodiesel-diesel-additive (IRGANOR NPA) blend were tested on diesel engine for performance and emission. It was reported that BU20+1% (20% biodiesel + 1% additive) produced 1.73% and 9% higher brake power as compared to BU20 (20% biodiesel + 80% diesel) and diesel respectively. Specific fuel consumption was found to be 26% and 6% lower for BU20+1% as compared to BU20 and diesel respectively. Fuel BU20+1% produced less CO, NO_x and CO₂ emissions as compared to other fuels [114].

Experiment was done on a marine diesel engine fueled with diesel and ethylene-glycol-monoacetate (5% and 10%)-diesel blends. The experimental results showed that addition of additive caused an increase in BSFC and decrease in excess air, exhaust gas temperature, CO₂, CO and NO_x emissions [115].

Investigation was done on a C.I. engine fuelled with 2, 5-dimethylfuran (DMF)-diesel, butanol-diesel and gasoline-diesel blends. 30% by volume of additives were mixed in these three fuels and the resulting blends were referred to as D30, B30 and G30. It was reported that compared to B30 and G30, D30 has longer ignition delay. This is because of its lower Cetane number, which leads to faster rate of burning and higher rate of pressure rise. D30 showed the lowest smoke emission with higher EGR rates. Long ignition delay and high oxygen content in fuel were two key factors that reduced smoke emission. It was reported that ignition delay has more effect on smoke reduction than fuel oxygen. Moreover, at medium EGR rates (<40%), D30 and B30 both showed improved smoke-NO_x trade-off and expansion of low-emission region without reducing fuel efficiency [116], [117].

A study was done with two ignition promoters, IAN (iso-amyl nitrate) and DTBP (di-tertiary butyl peroxide) blended with 50D:50B (50% diesel and 50% pine oil) on a C.I. engine. It was reported that on addition of ignition promoters, the NO_x emission for 50D:50B-IAN and 50D:50B-DTBP decreased by 12.8% and 19.2%, respectively, as compared to 50D:50B. The reduction of CO and HC emission were 40% and 34%,

respectively as compared to 50D:50B. The additive DTBP was reported to be better among the two ignition promoters, in reducing NO_x emission. The performance of the engine was also reported to have improved for 50D:50B-DTBP [118].

In a review study, the effects of biodiesel and diesel additives were investigated in C.I. engines. It was reported that oxygenated additives were mostly preferred due to their easy availability and low cost. In most of the cases it was reported that addition of these additives results in decreased engine performance (particularly at lower loads) due to cooling effect and low calorific value. However, upon addition of some alcohols and DEE (up to 10% v/v), the engine showed some improvement in performance. In general, addition of alcohols reduces smoke and HC, but increases NO_x and CO emissions. Blending of ethers in diesel has been reported to cause a simultaneous reduction in smoke, NO_x and CO [119].

An experimental study was conducted with diesel (0% oxygen) and five other oxygenated blends containing varying proportions of diesel, biodiesel and an additive (triacetin) (having oxygen in the range of 6.02–14.2%). It was observed that the oxygenated blends have a higher percentage of fuel-bound oxygen, that is helpful in reduction of particulate matter, particle number (PN), unburned hydrocarbon and carbon monoxide emissions significantly with a slight increment in NO emission. As compared to diesel, a maximum reduction of 91% and 76% in PM and PN was observed with the oxygenated fuel blends [120].

A study was done with diesel-oxygenated blends to investigate their effect on size of particulate matter. Acetal (10% v/v)-diesel blend, Soy methyl ester (SME) biodiesel, waste cooking oil biodiesel (WCB) and acetal (10%)-SME (10%)-diesel blend were tested in a diesel engine. Approximately a linear correlation was recognized between the oxygen content and the corresponding total particulate matter and element carbon reduction under 11% fuel oxygen. This can be attributed to higher oxygen content in the fuels, which leads to reduction in total particle mass emissions. It was reported that the smoke produced from oxygenated fuels was oxidized at a faster pace as compared to diesel for each particle size and total number of particles [121].

An experimental study was done with sunflower oil (SF) and karanj oil (KO) with two commercially available additives for diesel, referred to as A1 (composed of long chain carboxylic acids) and A2 (composed of isoparaffins) under similar operating conditions. It was observed that with both vegetable oils i.e. SF and KO, ignition delay increased, leading to increased cylinder pressure, heat release rate (HRR), NO_x and CO emissions. However, BSEC and smoke emission were reduced as compared to diesel. Karanj oil was observed to be more effective in reduction of NO_x and CO as compared to sunflower oil with a slight reduction of BTE. It was reported that both additives were effective in reducing ignition delay, HRR and NO_x emissions with karanj oil whereas these additives were not so effective with sunflower oil. The additive A1 showed a significant reduction in smoke and CO with karanj oil as compared to diesel. It was concluded that karanj oil with additive A1 is very effective to reduce emissions of the diesel engine [122].

2.4.1 Nitromethane

Nitromethane (NM) (CH₃NO₂) having oxygen in its molecular structure (52.4% by weight) reduces the requirement of external oxygen for complete combustion. Nitromethane has been used as a monopropellant and it is non-toxic, non-corrosive, cost economical, and gives high power output. Also, use of NM in I.C. engine results in reduced smoke. Presence of NM in diesel fuel tends to increase chances of pre-ignition, which is desirable up to some extent in diesel engines. Thermal efficiency is decreased because more unburned fuel is lost with exhaust [123], [124]. In an experimental study it has been reported that the peak temperature and peak pressure in combustion chamber were increased with high volume fraction (10%-40%) of gaseous nitromethane in air[125].

Investigations with NM and nitroethane (NE) mixed with diesel and alcohol-diesel blends showed that use of additives reduced viscosity and increased Cetane index. Performance is improved and exhaust smoke is reduced. Nitromethane is thermally sensitive and ignites very quickly after injection in the combustion chamber, which is desirable for C.I. engines. The increase in BTE against increased BSFC is because of low boiling point of NM. This improves atomization and the spray quality of the blended fuel. Another reason for higher BTE could be related to oxygenating quality of nitroparaffins. It was found that smoke reduced up to 16.2% with NM-diesel blend and NO_x increased up to 5.1%

with NM-diesel blend. The two factors (i) higher content of oxygen (52.4% by wt) and (ii) higher latent heat of vaporization jointly affect the smoke formation mechanism in NM-diesel blends. It was reported that the increment of NO_x with blended fuels is mainly because of thermal NO_x , and not because of nitrogen present in the structure of nitrogenated additives [126]. Studies with oxygenated additives (2.5% v/v)-ethanol (5-10% v/v)-diesel blends have reported that use of additives recovered viscosity and Cetane index of ethanol-diesel blends. Three additives, nitroethane (NE), nitromethane (NM) and 2-methoxy ethyl ether/Diglyme (DGM) were added in ethanol-diesel blend to investigate the performance and emission of diesel engine. It was observed that smoke reduced in the range of 50-27% with the application of these additives respectively. The emissions of CO and CO_2 reduced for NM and DGM blends, NO_x increased for NM blend, but decreased for DGM blend and HC increased for all additive-blended fuels as compared to ethanol-diesel blend [127], [128].

In a study the use of oxygenated additives, alteration of injection timing, use of biodiesel emulsion and EGR were reviewed as NO_x reduction technologies. It was stated that in general, oxygenated additives aided in increasing NO_x emission. The effect of oxygenated additives on NO_x emission depends on engine design, its maintenance and operating condition. Along with peak temperature, the temperature distribution in cylinder also affects the rate of NO_x production. Ternary blends with EGR at optimized injection timing were found effective in controlling NO_x emission [14]. In an experimental study, a modeling tool was used to optimize the emission and performance with different oxygenated additives, metal additives and by varying speed and load conditions. Improvement of CN and viscosity was reported when oxygenated and nitrogenated additives were added in ethanol-diesel blend. In general, results showed that the tertiary blends of additive-alcohol-diesel were able to decrease smoke emission and to improve engine performance [129]. A similar kind of study showed that ternary blends of NM (1%)-n butanol (5-10%)-diesel reduced smoke while increased NO_x and CO. However, power of engine was decreased and BSFC was increased. Addition of some nano particles were found helpful in restoring the lost power [130]. It has been stated that the additives which reduce the ignition delay could lead to reduction in NO_x emission as well. Shorter ignition delays allow lesser amounts of fuel before ignition, thus resulting in

lower peak temperatures. Nevertheless, availability of NM in fuel enhances the combustion rate, which in turn leads to increase in NO_x . On the whole, the results for nitromethane did not yield substantially conclusive results and thus need further experimental investigations. It has been stated that production of NO_x depends on engine design, aging of solution and contents of NO and NO_2 [131].

In a homogeneous charged compression assisted ignition engine, Nitromethane shortened the combustion period and increased the indicated mean effective pressure. Nitromethane improved the combustion rate when blended with methanol irrespective of cycle variations [132].

2.4.2 2-Methoxyethyl ether/Diglyme (DGM)

In an experimental study it was reported that higher Cetane number (CN) of fuel is mainly accountable for higher power output and lower smoke & NO_x emissions. It was found that the addition of alcohols in diesel/biodiesel reduced the CN of blends, thus creating the problem of poor self-ignitability. To cope with this, CN-improvers such as ethylhexyl nitrate ($\text{C}_8\text{H}_{17}\text{NO}_3$), cyclohexyl nitrate ($\text{C}_6\text{H}_5\text{NO}_3$) and 2-methoxyethyl ether/Diglyme ($\text{C}_6\text{H}_{14}\text{O}_3$) were mixed in methanol-biodiesel blends. At the initiation of combustion, the intermolecular bonds of these additives break before fuel ignition takes place and produce C, H, N and O radicals which collide with each other and associate to form CO, CO_2 , NO_x and H_2O , and release their binding energy, which in turn leads to reduction in ignition delay. This way, Cetane number improvers reduce the ignition delay period and accelerate the combustion rate of the fuel. When Cetane number improvers were added into alcohol-diesel/biodiesel blends, the nature and concentration of radicals is changed, and this in turn, changes the ignition reaction and combustion products. At rated conditions, the three improvers reduced smoke and NO_x emissions from 11.76% to 38.24% and 3.87% to 12.90% respectively as compared to methanol-biodiesel blend. However, HC and CO emissions were increased. Among these improvers, diglyme showed the best effects on reduction of smoke and NO_x emissions of methanol-biodiesel blends [56]. In other experimental studies with NE, NM, DGM and metal additives, it has been reported that mixing these additives with ethanol-diesel blends improved performance and reduced emissions. The DGM blended fuel showed best performance, while the NM blended fuel showed best results in smoke reduction. In general, smoke

was reduced for all additive-blended fuels while NO_x and CO were found to vary according to the nature of additive and operating conditions [127]–[129].

A study was conducted with diglyme and five other oxygenated additives blended with diesel fuel on a DI diesel engine. It was found that on addition of these additives the total duration of combustion decreased, but at the same time, combustion improved due to availability of oxygen, particularly during the diffusion combustion phase. It was observed that with DGM blended fuel, the initial phase of combustion advanced and the maximum rate of heat release decreased. It was reported that the effect of Cetane number is more pronounced on ignition delay compared to mass fraction of oxygen in fuel. This was reflected in the form of ignition delay being reduced with DGM-diesel blend (DGM having higher Cetane number than diesel), while showing an increase with other oxygenated additives having Cetane number lower than diesel. The trend of increased ignition delay with other oxygenated additives was observed to continue with increasing quantities of these additives in diesel (thus increased oxygen mass fraction in blends). Smoke emission was reduced with all oxygenated additives-diesel blends. Increased oxygen in fuel leads to burning of more fuel in the initial phase and thus reduces the amount of fuel burned in the diffusion phase. Lesser availability of fuel for burning in diffusion phase and oxidation of smoke precursors in diffusion phase, were the main reasons for reduction of smoke with oxygenated additives. It was concluded that smoke reduction is mainly dependent on mass fraction of oxygen in fuel rather than on the type of additive. In general, 10% oxygen mass fraction in fuel reduces smoke by 30-40%. A slight reduction in NO_x was observed with oxygenated additive blended fuels. The emission of CO and HC were also decreased with increased oxygen content in blends [133].

An experimental study was conducted with diglyme-diesel blends under five engine loads and at two engine speeds of 1800 rpm and 2400 rpm. Diglyme-diesel blends containing 5%, 10.1%, 15.2%, 20.4%, 25.7% and 53% of diglyme (v/v) contain 2%, 4%, 6%, 8%, 10% and 20% of oxygen (by mass) respectively. The blending of DGM in diesel resulted in increased BSFC with a maximum increase of 45.1% observed for 53% DGM-diesel blend. BTE was improved slightly for lower blends, but reduced for higher blends. BTE was reduced by 3.6% with 53% DGM blend as compared to diesel. It was observed that

smoke emission reduced with increased oxygen content in fuel. NO_x also reduced slightly with DGM blending in diesel. The increased oxygen content in blended fuel replaced some carbon content and enhanced combustion in the diffusion phase along with a reduction of aromatics compounds in the blended fuel, and this led to reduced smoke emission [134]. Another investigation showed that reduction of HC is more for additives having less percentage of oxygen. The reduction in PM is generally dependent on the oxygen content in fuel, whereas reduction in CO and HC emissions depends on the molecular composition of the oxygenating additives too. Up to 15% blending of diethylene-glycol-dimethyl-ether (Diglyme) with diesel resulted in 60% reduction in smoke. Significant reduction in CO and HC emissions were reported with only a slight increment in NO_x emissions [135].

2.4.3 Diethylether

Dimethylether (DME) and diethylether (DEE) are considered as promising alternative fuels or oxygenated additives for C.I. engines. They have high Cetane number, low auto-ignition temperature and high oxygen content in molecular structure which results in rapid and smokeless combustion along with reduced emissions of NO_x and CO when used purely or in blended form with diesel. DME, having a simple structure and properties similar to LPG, can be used in C.I. engines without any difficulty. DEE is similar to DME except that DEE is liquid in normal atmospheric conditions. Thus it is easy in storage, handling and on-board use in automobiles. This gives DEE an edge of preference as a fuel over DME. DEE can be produced from ethanol using dehydration process; thus it is a renewable fuel. The energy density of DEE is higher and cold starting is better than ethanol [136]–[138].

Experimental study with 5% and 10% diethyl ether (DEE)-diesel blends was done to analyze combustion and emission characteristics of an agricultural C.I. engine. Reduced ignition delay was reported at lower loads as less fuel is injected into the cylinder. Higher Cetane number of DEE also plays a prominent role in this. On the other hand, at higher loads, high amount of fuel is injected into the cylinder and higher latent heat of vaporization becomes the dominant factor that acts towards decreasing the cylinder temperature and thus increases ignition delay as compared to lower loads. The premixed mixture is increased due to increased delay and this further increases peak pressure. The

BSFC of 10% DEE blended fuel decreased and BTE increased considerably at higher loads. The smoke emission reduced with DEE blends but higher smoke was reported at higher blends of DEE because of phase separation. In general, it was found that mixing of DEE with diesel reduces the ignition delay due to high Cetane number. The lower calorific value and smaller ignition delay, both contribute towards lower cylinder temperature, and this leads to reduced NO_x emission with DEE blends. The emission of HC and CO was reported to have increased with DEE blends [37].

In a study, the effects of dimethylether (DME) and diethylether (DEE) on combustion and emission characteristics for a DI diesel engine were simulated using a thermodynamic cycle model. For equal injection rates of DME and DEE (changed equivalence ratio), the performance of engine was reported inferior as compared to diesel. The brake power decreased by 32.1% and 19.4% at 4200 rpm while BSFC increased by 47.1% and 24.7% at 2200 rpm for DME and DEE respectively. Irrespective of increased BSFC and reduced power, BTE improved with DME and DEE due to improved combustion. For the same equivalence ratio, the performance improved, but fuel consumption increased by 64% and 32% for DME and DEE respectively. Brake power increased by 13.6% and 6% at 4200 rpm for DME and DEE respectively as compared to diesel. BSFC increased by 43.5% for and 23.6% for DME and DEE compared to diesel. BTE also showed improvement for DME and DEE as compared to diesel. Lower CO emission were reported for DME and DEE at all conditions; while CO and NO_x were found to be slightly higher for DME and DEE at equal equivalence ratio condition [139].

Blends of DEE with diesel and karanja-biodiesel in a range of proportions varying from 5-20% were tested on a diesel engine. It was found that BTE improved with all DEE blends. Improvements of 5.5% and 9.2% with 15% DEE-biodiesel and DEE-diesel blends were observed respectively. 5-10% blending of DEE in diesel or biodiesel resulted in minimum level of smoke at full load condition. Blending of DEE in diesel or biodiesel reduced NO_x emission more effectively than other emissions. It was seen that 15% and 20% DEE blends have greater effect on reduction of NO_x (average 40% and 51% respectively) than the other DEE blends. Blending of DEE up to 5% in diesel and biodiesel reduced CO and HC emissions. However, more than 5% blending of DEE resulted in increased CO and HC. This increase can be attributed to the expansion of *lean*

flame out region. It was concluded that 5% DEE-Diesel blend and 15% DEE-Biodiesel blend are optimal blends in terms of performance and emissions characteristics [17].

Experiments were conducted with DEE (5%)- biodiesel (25%)-diesel and ethanol (5%)-biodiesel (25%)-diesel blends and results for performance and emissions were compared with biodiesel (30%)-diesel (B30) blend. The BSFC of DEE blend was observed slightly lower than that of B30. DEE and ethanol blended fuel showed lesser smoke emission than B30. However, DEE blend was more effective in smoke reduction than ethanol blend. For DEE blend, variation in NO_x was negligible, but for ethanol blend, NO_x was increased as compared to B30. Unburned HC increased while CO emission decreased for DEE and ethanol blends as compared to D30 [140]. The effects of premixed-DEE on combustion and emissions were studied in a HCCI-DI diesel engine. The premixed fuel ratio of DEE was varied from 0% to 40% and results were compared with neat diesel operation. It was observed that ignition delay and thus, amount of fuel in premixed phase increased, while span of premixed stage decreased. Lower heat release was observed for all premixed DEE fuels as compared to neat diesel operation. It was reported that at higher premixed DEE ratio (40%), the rate of combustion in initial phase of combustion is enormous, thus resulting in high pressure rise and eventually leading to detonation. In HCCI mode, premixed fuel is homogeneously introduced into the cylinder. This minimizes the rich fuel regions in combustion chamber and generation of smoke precursors is barred. The smoke emission was decreased up to 76% with increased premixed fuel ratio of DEE. The homogeneous combustion reduced average temperature in cylinder, thus resulting in reduced NO_x emission with premixed DEE. It was observed that for up to 10% premixed DEE, cycle to cycle variations were not significant. However, beyond 20% premixed DEE, distinct variations were noted. CO and HC emissions were increased by 91.6% and 44% with 30% premixed DEE as compared to neat diesel [141].

An experimental study with 24% DEE-diesel blend was done to analyze combustion and cyclic irregularities at different loads and constant speed. It was reported that the effect of higher latent heat of vaporization was more dominant than high Cetane number when using 24% DEE-diesel blend at higher load. Thus in spite of higher Cetane number of DEE, the ignition delay was increased, peak of heat release and peak pressure were

delayed, dynamic injection timing was decreased and peak pressure & temperature were decreased for DEE blend as compared to diesel. No cycle to cycle variations and unsteady operation of the engine were noted for up to 24% blending of DEE in diesel. BTE remained unaltered with DEE blended fuel. Smoke, NO_x and CO emissions were reduced while HC emission was increased with increased percentage of DEE in DEE-diesel blends [142], [143]. A similar kind of study with 20% n-butanol and DEE blended in cottonseed oil and its biodiesel was done on a high speed engine. It was observed that with these blends, the fuel injection pressure curves were delayed, dynamic injection timings were decreased, ignition delays were increased, and peak cylinder pressures and temperature were decreased as compared to pure cottonseed oil and its biodiesel. BSFC was decreased while BTE was increased with the use of these blended fuels as compared to cottonseed oil and its bio-diesel. Smoke, NO_x and CO emissions were reduced while unburned HC emissions were increased with the use of these blended fuels as compared to cottonseed oil and its bio-diesel. The DEE blends exhibited superior performance and emission characteristics as compared to n-butanol blends. It was concluded that n-butanol and DEE, which can be produced from biomass (bio-butanol and bio-DEE), when blended in the vegetable oil or in biodiesel, resulted in improved performance and reduced emissions without any requirement of co-solvent and without any operational problems of engine [144]. An experimental investigation was done with diesel, cottonseed oil (CSO), biodiesel of cotton seed oil, cottonseed oil (20-100% v/v)-diesel blends, orange oil (5-15%)-CSO blends and DEE (10-30%)-CSO blends on a small diesel engine. The 30% DEE blend exhibited better performance with reduced emissions among the tested blends of DEE. In comparison to neat cottonseed oil at full load condition, the BTE of 30% DEE blend increased from 28% to 29.5%; smoke and CO reduced by 10.25% and 25% respectively; and NO_x increased by 4.8% [145].

In an experimental study, DEE was blended in the range of 10-30% (v/v) in diesel. It was observed that 20% blending of DEE yields very good results of performance and emissions. When 5% EGR was applied with 20% DEE blend, smoke and NO_x were reduced by 54% and 20% respectively [146]. In two different studies, DEE (1-10%)-diesel and DEE (5-25%)-diesel blends were tested in a diesel engine. It was reported that addition of DEE improved the performance and reduced emissions. The 5% blend of

DEE (B5) showed higher BTE and lower BSFC at higher loads as compare to other blends. B5 was found effective in reducing smoke, CO and HC. However, it led to an increase in NO_x emission. Up to 15% blending of DEE was found more effective in smoke reduction, but increased CO and HC emissions as compared to diesel [147], [148].

The effect of blending DEE (10-50%) on diesel engine emissions and performance was experimentally examined. The indicated specific fuel consumption was observed to increase for DEE blended fuel due to its lower calorific value. HC and CO emissions were reduced for DEE blended fuels. Smoke emission was reduced and NO_x emission was increased with DEE blended fuel as compared to diesel [149].

2.5 Motivation and research gap

Many notable developments have taken place in the field of use of alternative fuels and additives in C.I. engines. Still, the use of n-butanol and oxygenated additives in C.I. engines has more or less been limited to some pilot studies or lab experiments only. Much research is required to rank these fuels (obtained through literally a plethora of combinations via blending) with respect to performance and emissions. Research is also lacking as far as quantification of emissions from these fuels is concerned.

On the basis of literature review, the following factors were considered for carrying out research on the proposed topic:

1. Many studies have been done on alcohol-diesel blends and testing of performance of engines. However, the detailed studies with diesel-alcohol blends mixed with multiple additives were limited.
2. Most of the research work has been aimed at reducing smoke from C.I. engines by blending oxygenated additives and towards reduction in NO_x using different rates of EGR. It is observed from literature review that there is scope of work in NO_x reduction by using additives in diesel-alcohol blends.
3. Literature related to the effects of variable compression ratios on smoke and NO_x in engines fuelled with n-butanol-diesel blends is limited.
4. It was also observed from literature review that most of the studies have been done within a narrow range of weight/volume percentage for oxygen containing additives.

5. Modeling of performance and emission parameters using multiple additives is also limited in existing literature.
6. Extensive research on emissions with the use of various blends has shown to have a lot of variations; which makes it difficult to reach a conclusion about an optimal blend. This forms another motivation for current research.
7. The most work in this area has been experimental. Indeed it would be a convenience to be able to predict the results of fuel blending and testing without sophisticated engine setups and measuring equipment. Mathematical prediction models come in handy in such instances. Surprisingly, despite its proved usefulness, there is very little representation in literature from mathematical modeling in the field of fuel blending and its effects. This forms another major research gap which the present research work aims to bridge.

In view of these aspects, research on the simultaneous use of diesel, alcohols and other oxygenated additives to form ternary blends is proposed. Guided by the literature survey, it was decided to select n-butanol as bio-oxygenated fuel and nitromethane (NM), 2-methoxyethyl ether/Diglyme (DGM) and diethylether (DEE) as the experimental additives. Also, in order to make the results of research more impactful, it was decided to use a diesel engine that is mostly used in agricultural applications as well as in small vehicles used for local transportation. By this selection of the engine, it was ensured that an all-inclusive approach was applied to cover the local industry, the transportation sector and the agricultural sector. The current research thus aims to present an experimental investigation using selective combinations of “*additive-n-butanol-diesel*” ternary blends to determine the optimum blend for performance and emissions of a diesel engine having widespread applicability.

2.6 Objectives

Based on the motivation and research gap the major objectives of the proposed research work are formalized as follows:

1. To find out suitable additives for oxygenated biofuel-diesel blend for improved engine performance and reduced emissions and to determine the optimum blend & additive for C.I. engines.
2. To develop a mathematical model to predict engine performance and emissions for different blends of the suggested additive with oxygenated biofuel-diesel blend.

2.7 Research procedure and methodology

In order to achieve the stated research objectives in a structured manner, the following stepwise methodology/research plan was followed:

1. Detailed literature review regarding C.I. engines operated on alternative fuels. Study of possible additives in diesel engines and their effects on engine performance and emissions. Finding out the research gap and identification of most promising additives for proposed research work.
2. Procurement of required VCR engine test rig, gas analyzer and smoke meter.
3. Generation of baseline data using diesel fuel.
4. Engine test run with different percentages of n-butanol in diesel to find out optimum blend for minimum smoke and NO_x emissions without altering performance. Analysis of performance and other emissions were also done.
5. Performance and emission study using Nitromethane (NM) with optimum blend of diesel-n butanol. Analysis of observed data.
6. Mathematical modeling and optimization of NM blending for better performance and reduced emissions.
7. Activities 5 and 6 were repeated for Diglyme and Diethylether.
8. Comparative analysis of results obtained with three ternary blends to identify the best blend.
9. Documentation of the research work – final report writing.

Chapter 3

Experimental Set-Up and Procedure

3.1 Test engine

A small size, modified, single cylinder, four stroke, constant speed, water cooled, direct injection variable compression ratio (VCR) diesel engine was used for the experiments. The technical specifications of the engine are given in Table 3.1. A lifting and lowering cylinder block mechanism was used for changing the compression ratio without interrupting the engine operation and without varying the geometry of combustion chamber.

Table 3.1 Specification of test-engine

Engine –make	Diesel-Kirloskar (TV1) (crank start and self-start)
No. of cylinder	01
Stroke	4 stroke
Cooling	Water cooled
Rated Power	3.75 kW
RPM	Constant Speed of 1500 rpm
Stroke and bore	110 mm and 87.5 mm
Capacity	660 cubic centimetre

3.2 Test installation description

The engine was mounted on a semi-automated test bed and coupled to an eddy current dynamometer. The dynamometer was equipped with a load cell for the measurement of engine torque. The electric sensors for measurement of speed and load (torque) were also incorporated. The sensors fed signals to digital torque indicator and controller. The required load could be set on the dynamometer through a control panel by the operator. Thermocouples were located at appropriate points on the engine test rig. Their indicators were mounted on the control panel. Facilities to observe and control engine variables such as engine speed, load, water and exhaust gas temperature, fuel and air flows, etc., were also installed on the control panel. A computer and a printer were also set up along

with the test rig. To analyze and display results on computer, LABVIEW based software package was incorporated. The description of instrumentation and formulae used to calculate different quantities are given in Table 3.2.

Table 3.2 Specifications of test set-up and formulae used to calculate different quantities

Dynamometer	Make: Power MAG, Torque rating available: 3.75 kW, Speed: 1500 RPM
Torque/Load Measurement: Torque (T) Nm= load (kg) × r (m) (r=0.16 m) x 9.81	Range of torque: 0-6.00 kg-m, Torque resolution: 0.01 kg-m, Transducer: Load cell connectivity: through RS485 port
Fuel Rate Measurement:	Range: 0-5000 g, Weighing resolution: 1g Range of fuel rate: 0-10kg/h, Resolution: 0.06 kg/h, The principle of working of this unit is based on loss of weight. The microcontroller notes the amount of loss of weight for a known interval of time and calculates the rate of fuel and shows it on display screen. A minimum of one minute time is required to stabilize the reading.
Intake air Measurement/Air Flow Indicator: Airflow (m ³ /s): $Q = C_d A \{2gh (\rho_w - \rho_a) / \rho_a\}^{1/2}$, where C_d = Coefficient of discharge = 0.62 A = area of orifice in m ² (orifice dia. =20mm), $g = 9.81 \text{ m/s}^2$ h = Manometer deflection in m ρ_w = density of water, ρ_a = density of air	The intake manifold of the engine is connected to an air box. The atmospheric air is sucked into the engine through an orifice provided in the intake side of the air box. The pressure drop across the orifice is measured using a differential pressure sensor (Piezo resistive type). Range of h (manometer deflection): 0-200mm, Resolution of h: 1mm Transducer: differential pressure, 0-250mm of the water column. Range of air rate: 0-50.0 m ³ /h, resolution: 0.1 m ³ /h, The differential pressure sensor is calibrated for manometer deflection in mm. With this as input, the unit calculates air flow in m ³ /s.
Temperature Measurement (Five Channel Indicator)	Channels : 5 off, Sensor: RTD (Pt100), Range of temperature: 0-400°C Resolution : 0.1°C
High-Temperature Indicator (for Exhaust gas)	Temperature range: 0-800°C, Resolution: 1°C, Type of sensor: Thermocouple, K-type
Water Flow Measurement	Range of flow measurement: 0-99.9 cc/s, Resolution: 0.1 cc/s, Type of Transducer: Turbine flow type
Unit for measurement of diesel injection pressure(DI)	Make: PCB Piezotronics-USA, Range of pressure: 0 – 2000 bar for DI Resolution: 1 bar for DI, Sensor type: Piezoelectric (10000 PSI for DI) Response time: 4 microseconds
Computer Connectivity of Instrument	All the indicators are attached to a RS232 to RS485 converter whose output is attached to Comm1 port of the computer

The Injection pressure could be varied by adjusting the spring tension through a screw given on the injector (make: Bosch) and calibration unit. The adjusted injection pressure could be checked by a Nozzle tester (make Bosch H-S/KDEP 99A) available in the laboratory. The injection timing could be varied by lifting the injection pump body relative to plunger of pump. The schematic layout and actual engine set up of the engine test bed, instrumentation and data logging system are shown in Fig. 3.1(a), 3.1(b) and Fig. 3.2.

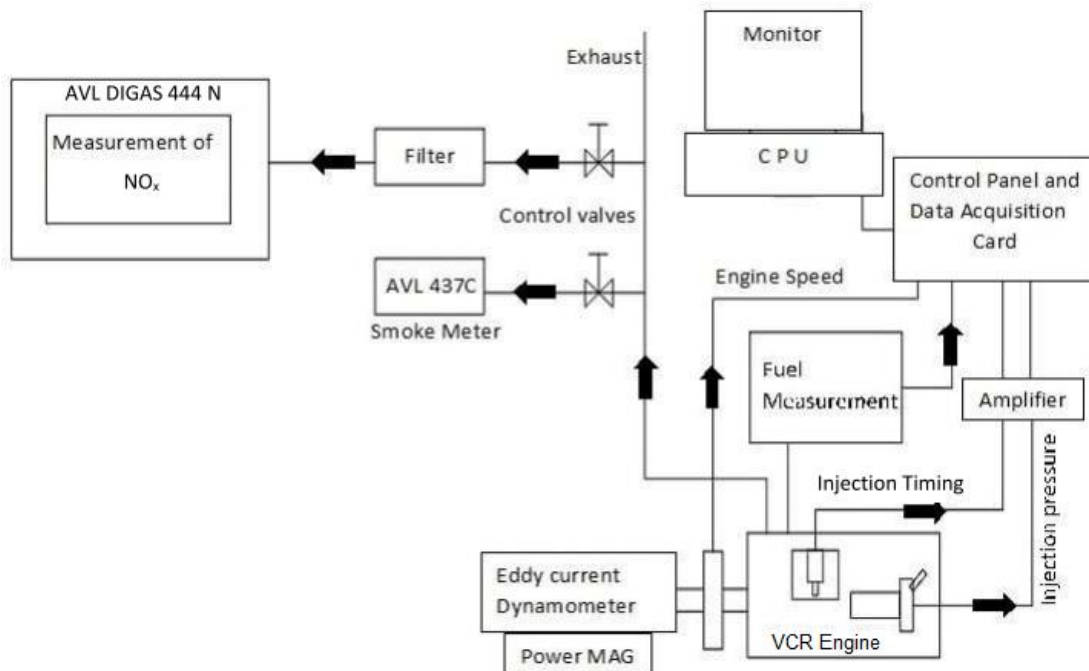
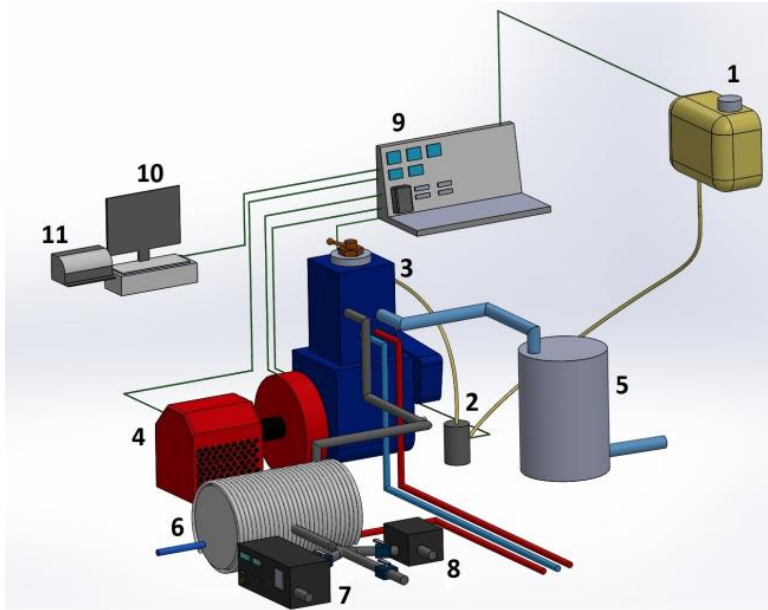


Fig. 3.1 (a) Schematic of engine set-up



- | | |
|----------------------------|--------------------------|
| 1.Fuel Tank | 7.Exhaust gas analyser |
| 2.Fuel Pump | 8.Smoke meter |
| 3.Engine Block | 9.Data aquisition system |
| 4.Eddy current dynamometer | 10.Computer |
| 5.Air Box | 11.Printer |
| 6.Exhaust gas calorimeter | |

Fig. 3.1 (b) Schematic of engine set-up

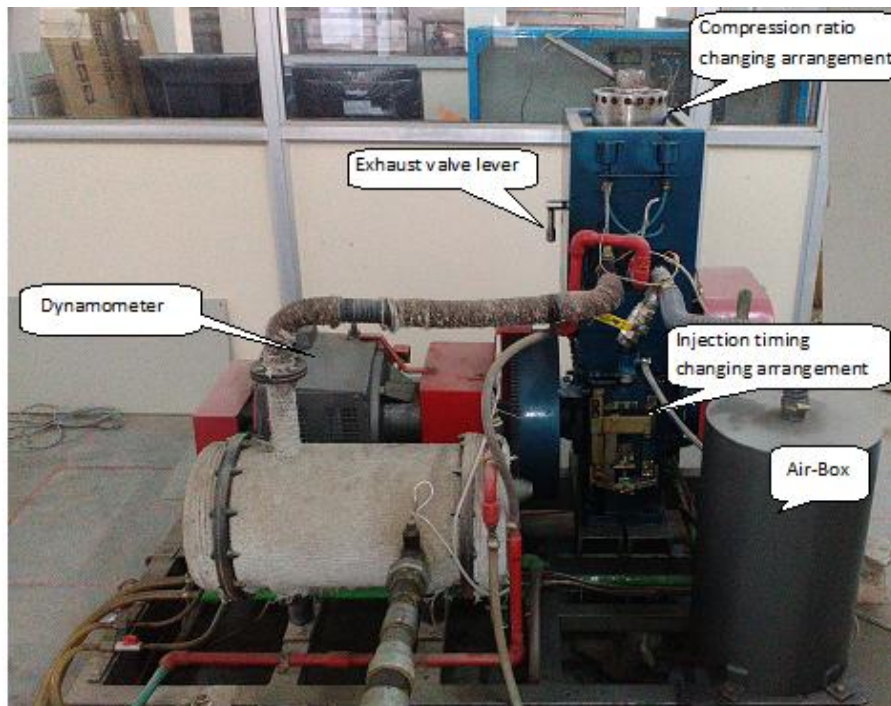


Fig. 3.2 Actual engine set-up

3.3 Emission measurements

3.3.1 AVL Smoke-meter (Austria, Model: 437C)

Smoke meters are used to measure smoke opacity and are generally based on the light absorption coefficient principle. The smoke meter used in the present research work was equipped with advanced microprocessor technology with printer and RS232 serial port for a personal computer interface. Measurement range and resolution of the smoke meter used are given in Table 3.3. The AVL smoke meter used is shown in Fig. 3.3.

Table 3.3 Specifications of AVL 437C smoke meter

Description	Specifications
Make/Modal no.	AVL India pvt. ltd. gurgaon /437C
Application	Opacity, absorption, rpm, oil temp. and free-acceleration test measurements.
Measuring range and resolution	
Opacity	Range 0-100 %, Resolution 0.1%
Absorption	Range 0-99.99 m ⁻¹ , Resolution 0.01 m ⁻¹
RPM	Range 400-6000 1/min , Resolution 1
Oil temp.	Range 0-150°C, Resolution 1°C
Warm-up time	5 Minutes (>70°C)
Light source	Halogen lamp (12V / 5W)
Sensor	Selenium photocell
Span calibration	Digital



Fig. 3.3 AVL smoke-meter

3.3.2 Exhaust gas analyzer (AVL India, Model: 444N)

AVL DIGAS exhaust gas analyzer was used to measure concentrations of exhaust gases. CO and HC measurements are based on non-dispersive infrared (NDIR) principle and NO_x is measured by electrochemical principle in this equipment. The analyzer is based on the principle that the quantity of infrared energy absorbed by a compound in a sample cell is proportional to the concentration of the compound in the cell. The analyzer is equipped with advanced microprocessor technology with printer and RS232 serial port for a personal computer interface. Measurement range and resolution of gas analyzer used are given in table 3.4. The AVL gas analyzer used is shown in Fig. 3.4.

Table 3.4 Specifications of exhaust gas analyzer

Description	Specifications
Make/Modal No.	AVL DIGAS 444N
Application	CO ₂ , CO, O ₂ , NO _x and HC Gas Measurements and λ air fuel ratio
Measuring Method, Measuring Range and Resolution	
CO ₂	NDIR, Range 0-20 %, Resolution .01%
CO	NDIR, Range 0-15 %, Resolution .01 %
HC	NDIR, Range 0-30000 ppm, Resolution 1-10 ppm
O ₂	Electrochemical, Range 0- 25 % , Resolution 0.01%
NO _x	Electrochemical, Range 0-5000 ppm, Resolution 1 ppm
Λ	NDIR, Range 0-9.999 Resolution 0.001
Warm-up Time	2 Minutes (>25°C)
Response Time	15 sec (for sampling probe length of 3m)
Sampling System	Direct Sampling From Tail Pipe
Power	15W
Span Calibration	Digital
Power Supply	19V DC \pm 2V, 230VAC \pm 10%, Single Phase, 50-60 Hz
Weight	4 kg
Dimensions	255 x 292 x 187 mm ³



Fig: 3.4 AVL Exhaust gas analyzer

3.4 Fuel Preparation

The bio-oxygenated fuel used in the present work is n-butanol. Optimum n-butanol-diesel blend (BU20) was taken as base fuel to investigate the effects of nitromethane (NM), 2-Methoxy-ethyl-ether/Diglyme (DGM) and Diethylether (DEE) on performance and emissions of the engine. Different n-butanol-diesel blends, NM-n-butanol-diesel blends, DGM-n-butanol-diesel blends and DEE-n-butanol-diesel blends on volume basis were prepared using a magnetic stirrer and glassware for blending and storage. The miscibility of n-butanol and other three additives was excellent in diesel and absolutely no phase separation was observed for a storage period of 72 hours and during the operation of engine.

N-butanol, Nitromethane (NM), Diglyme (DGM) and Diethylether (DEE) used were of 99.0% purity. Different concentrations of n-butanol-diesel blends were prepared to range from 10%-25% on a volume basis (v/v) and were designated as BU10, BU15, BU20, BU25 (The numeral indicating the percentage of n-butanol in the blend). NM-BU20 blends were prepared to range from 1-3% (v/v) and were designated as NM1BU20, NM2BU20, and NM3BU20. DGM-BU20 blends were prepared to range from 5-20% (v/v) and were designated as DGM5BU20, DGM10BU20, DGM15BU20 and DGM20BU20. DEE-BU20 blends were prepared to range from 5-20% (v/v) and were designated as DEE5BU20, DEE10BU20, DEE15BU20 and DEE 20BU20. A listing of properties of diesel, n-butanol, Nitromethane, Diglyme and Diethylether is given in Table 3.5.

Table 3.5 Properties of diesel, n-butanol and additives [98][126]–[128], [150][151]

	Diesel	Butanol	Nitromethane	2-Methoxy ethyl ether (Diglyme)	Diethyl ether
Molecular Formula	C ₁₀ H ₂₀ – C ₁₅ H ₂₈	C ₄ H ₉ OH	CH ₃ NO ₂	C ₆ H ₁₄ O ₃	C ₄ H ₁₀ O
Molecular Weight	170	74	61.04	134.174	74.12
Density (kg/m ³) (20 °C)	837	810	1138	937	713.4
Boiling Point (°C)	180-360	118	100-103	162	35
Flash Point (°C)	60-80	35	35	67	-45
Auto ignition Temperature (°C)	315	385	418	205	160
Specific gravity	0.837	0.810	1.138	0.937	0.7134
Lower heating value (MJ/kg)	43	33.1	10.52	24.5	33.9
Latent heat of Vaporization (kJ/kg)	250	585	561	322	355
Cetane Number	55.5	25	NA	126	>125
Viscosity (40 °C) cSt	4.8	2.26	4.8	2.13	0.23
Oxygen content (wt%)	0	21.6	52.4	36	21.6
Carbon content (wt%)	85-88	64.82	19.6	53.7	54
Hydrogen content (wt %)	12-15	27	4.9	10.3	10

3.5 Experimental procedure

Experiments were performed at a constant engine speed of 1500 rpm and at different engine loads varying from part load to full load (100% of rated load). For testing each fuel blend, the engine was run for a few minutes before recording each set of readings (to obtain steady-state condition). This ensured that the temperature of the cooling water, exhaust gases and lubricant oil reached a constant value. After completion of the tests with each blend, the remaining blend was purged from the fuel tank and fuel line in order to prevent mixing and alteration of actual ratio of blends.

Investigations were performed in four stages. In the first stage, tests were performed using diesel (B0) to obtain base line data involving the optimal settings of compression ratio, injection timing and injection pressure. In the second stage, tests were performed with n-butanol-diesel blends on the optimum engine settings as obtained in the first stage. From this set of data, optimum blend (which eventually turned out to be BU20) was selected. In the third stage, tests were performed on varying compression ratios, injection timings and injection pressures to optimize these operating parameters for BU20. In the fourth stage, tests were conducted with NM-BU20, DGM-BU20 and DEE-BU20 blends. (See Appendix B)

3.6 Uncertainty in measurement

During the observations there are always possibilities of error/uncertainty because of operating conditions, calibration of equipments, accuracy of measuring equipments, human errors and planning of experiments [152]. The uncertainties of various parameters were calculated, and are shown in Table 3.6.

Table 3.6 Uncertainty of various parameters

Measured quantity	Range of experiments	Resolution	% Uncertainty
BSFC	0.32-1.09 kg/kW-h	-	±0.114
BTE	0.82-27.6%	-	±0.114
Smoke	2-90.7 HSU %	0.1%	±.05
NO _x	20-741 ppm	1 ppm vol.	±3
CO	0.03-0.189 %	0.001%	±3
HC	15-55 ppm	1ppm vol.	±5

Total uncertainty of measurements in experiment [97] = Square root of {(uncertainty of BSEC)² + (uncertainty of BTE)² + (uncertainty of smoke)² + (uncertainty of NO_x)² + (uncertainty of CO)² + (uncertainty of HC)²} = $\sqrt{\{(0.114)^2 + (0.114)^2 + (0.05)^2 + (3)^2 + (3)^2 + (5)^2\}}$ = 6.56%

3.7 Development of prediction models

Analysis and validation of experimental results were done with the help of Design of Experiments (DOE). Minitab-17 and Design Expert (Version 8.0.4.1) were used for regression analysis as well as for generation of prediction models & equations. Initially, the engine operating parameters were optimized using Minitab-17 software with diesel only. The details of 16 experiments using different combinations of compression ratios, injection timings and injection pressures were selected for input in Minitab-17 to optimize engine operating parameters for diesel. Similarly, the experimental data of sets of 16, 36, 12, 16 and 16 were selected for input in Design Expert software in different stages for analysis and optimization of blended fuels. For n-butanol-diesel blends, the analysis and optimization of the input (parameters) and output (response) factors were performed by developing quadratic/cubic prediction models using Full Factorial approach. Factorial design is a fair statistical tool for designing the experiments to find effects of multiple variables and to find optimum conditions for target responses with reduced number of experiments. In the present study, we used modeling to verify our experimental results. Further, diagnosis of data is presented with the help of analysis of variance (ANOVA), normal probability plots, internal residual versus predicted plots and actual values versus predicted values plots. Surface response curves have been generated using software to see the effects of more than one factor simultaneously on responses.

ANOVA was used to perform tests for (i) significance of the regression model and (ii) significance of individual model coefficients. This analysis is based on two assumptions: (a) The variables are normally distributed, and (b) homogeneity of variance. Significant violation of either assumption can increase the probability of errors. Significance of models, individual parameters as well as the responses were checked, and models were developed to identify the most significant blend and operating parameters that improve the performance and emission characteristics of the engine. The developed models for BSFC, BTE, smoke, NO_x, CO and HC have been presented in the form of 3D-Surface

plots and equations. These equations can be used to make predictions about the output (response) for given levels of each input (factor).

In Design-Expert software, to perform regression computations, the experimental variables are represented in coded form. The minimum value of each factor is set to -1 and the maximum is set to +1. The coded equation represents the relative impact of the factors on responses by comparing the factor coefficients. For example, the variable A_{actual} is coded as:

$$A_{\text{coded}} = \frac{2 \times (A_{\text{actual}} - \text{Average of actual values})}{\text{Range between low and high actual values}} \quad (3.1)$$

For a load value of say 12 Nm in the experiments; $A_{\text{actual}}=12$, maximum value=24, minimum value=12, average=18, and range= 12. Hence the coded value for

$$A_{\text{coded}} = \frac{2 \times (12 - 18)}{12} = -1$$

After regression analysis, the coded values of variables are converted into actual values. Design-Expert provides both the coded and actual scale models. The conversion is done by substituting the coded formula for each factor in every term of the model. In the equation of actual factors, the levels are specified in the original units for each factor. This equation can't be used to assess the relative impact of each factor because the coefficients are scaled to accommodate the units of each factor and the graphical intercept is not at the center of the design range. In the models, the responses are presented as functions of variables in the form of multiple polynomial regression equations using least square method for fitting. An example is shown by equation (3.7).

$$\text{Response} = a_0 + a_1A + a_2B + a_3C + a_{12}AB + a_{13}AC + a_{123}ABC \dots \quad (3.2)$$

In Eq. (3.7), a_0 is a general coefficient; a_i (singular suffix coefficients) are coefficients of linearity; a_{ij} (double suffix coefficients) and a_{ijk} (triple suffix coefficients) represent the coefficients of quadratic and cubic effects respectively; A, B and C are the model variables; and AB and ABC represent the interaction between the variables.

All the experiments were performed in four distinct stages. In the first stage, L_{16} orthogonal array based Taguchi methodology was employed to find out the optimum engine parameters with diesel as base fuel.

The second stage involved the following three tasks: (i) Development of prediction models for BSFC, BTE, smoke, NO_x , CO and HC in terms of engine load and blending ratio (n-butanol-diesel blends) at optimum values of CR, injection pressure and injection timing (obtained in first stage) using full factorial design, (ii) Optimization of engine load and blending ratio for the desired values of BSFC, BTE, smoke, NO_x , CO and HC, (iii) Investigation of influence of engine load and blending ratio on BSFC, BSEC, BTE, smoke, NO_x , CO and HC using scatter diagrams and 3D-surface plots.

The third stage involved the following tasks using BU20 (which was the optimal outcome obtained in second stage): (i) Development of prediction models for BSFC, BTE, smoke, NO_x , CO and HC in terms of CR, injection timing and injection pressure at full load condition, (ii) Optimization of CR, injection timing and injection pressure for the desired values of BSFC, BTE, smoke, NO_x , CO and HC, (iii) Investigation of influence of CR, injection timing and injection pressure on BSFC, BTE, smoke, NO_x , CO and HC using column diagrams and 3D surface plots.

The fourth stage involved the following tasks using blends of three additives with BU20 at optimum values of CR, injection pressure and injection timing (obtained in the third stage for BU20): (i) Development of prediction models for BSFC, BTE, smoke, NO_x , CO and HC in terms of engine load and blending ratio (additive-BU20 blends), (ii) Optimization of engine load and blending ratio for the desired values of BSFC, BTE, smoke, NO_x , CO and HC, (iii) Investigation of influence of engine load and blending ratio on BSFC, BTE, smoke, NO_x , CO and HC using scatter diagrams and 3D surface plots.

Chapter 4

Experimental Results and Discussions

4.1 Optimization of engine operating parameters with diesel (B0)

In the first stage, experiments were conducted using diesel only at different loads, compression ratios, injection timings and injection pressures as per the design layout suggested by Minitab software. Taguchi methodology based on L16 orthogonal array was used for the optimization of engine operating parameters for minimization of BSFC and smoke emission and maximization of BTE. Load, compression ratio (CR), injection timing (Inj.T.) and injection pressure (Inj. Pr.) were considered as engine operating parameters while BSFC, BTE and smoke emission were considered as responses. Table 4.1 shows the engine operating parameters and their levels while Table 4.2 shows the complete design layout for experiments and measured values of responses.

Table 4.1 Parameters levels as per L16 orthogonal array based Taguchi design

Parameter	Symbol	Type	Levels			
			1	2	3	4
Load (Nm)	Load	Numeric	12	16	20	24
Compression Ratio	CR	Numeric	16.5	17.5	18.5	19.5
Injection Timing (CA bt/dc)	Inj. T.	Numeric	19	21	23	25
Injection Pressure (bar)	Inj. Pr.	Numeric	180	200	210	220

Table 4.2 Design layout and experimental results for diesel

S.NO.	Load	CR	Inj. T.	Inj. Pr. (bar)	BSFC (kg/kW-h)	BTE (%)	Smoke
1	12	16.5	19	180	0.49	17.09	90.4
2	12	17.5	21	200	0.44	19.03	92.2
3	12	18.5	23	210	0.35	23.9	63.8
4	12	19.5	25	220	0.48	17.44	92.2
5	16	16.5	23	200	0.45	18.6	90.4
6	16	17.5	25	180	0.46	18.1	89
7	16	18.5	19	220	0.48	17.44	77.5
8	16	19.5	21	210	0.42	19.93	91.3
9	20	16.5	25	210	0.37	22.43	90.6
10	20	17.5	23	220	0.45	18.6	95.4
11	20	18.5	21	180	0.41	20.47	69
12	20	19.5	19	200	0.48	17.54	93.8
13	24	16.5	21	220	0.45	18.93	100
14	24	17.5	19	210	0.39	21.93	97.1
15	24	18.5	25	200	0.41	20.27	70.3
16	24	19.5	23	180	0.45	18.81	91.4

The experiments were performed as per the experimental plan and results obtained are shown in Table 4.2. These results were used as input in the Minitab 17 software for further analysis. Table 4.3 shows the Responses for means for BSFC, BTE and Smoke. The mean for a given level of a factor is the average of all the observations for that level of the factor. The Delta value is the difference between the maximum and the minimum values of the means, and rank represents the relative magnitude of the effect of factors on Response. The most effective factor affecting response was obtained by comparing these values. From Table 4.3 it is clear that injection pressure is the most dominating factor that affects BSFC and BTE; followed by compression ratio, injection timing and load. In the same manner, for smoke emission, the compression ratio was found as the most dominating parameter; followed by injection pressure, load and injection timing.

Table 4.3 Response table for means

Level	Load (Nm)	CR	Inj. T. (CA btdc)	Inj. Pr. (bar)
Taguchi Analysis: BSFC (kg/kW-h) versus Load (Nm), CR, Inj. T. (CA btdc), Inj. Pr. (bar)				
1	0.4400	0.4400	0.4600	0.4525
2	0.4525	0.4350	0.4300	0.4450
3	0.4275	0.4125	0.4250	0.3825
4	0.4250	0.4575	0.4300	0.4650
Delta	0.0275	0.0450	0.0350	0.0825
Rank	4	2	3	1
Taguchi Analysis: BTE (%) versus Load (Nm), CR, Inj. T. (CA btdc), Inj. Pr. (bar)				
1	19.37	19.26	18.50	18.62
2	18.52	19.41	19.59	18.86
3	19.76	20.52	19.98	22.05
4	19.98	18.43	19.56	18.10
Delta	1.47	2.09	1.48	3.95
Rank	4	2	3	1
Taguchi Analysis: Smoke (HSU %) versus Load (Nm), CR, Inj. T. (CA btdc), Inj. Pr. (bar)				
1	84.65	92.40	89.45	84.95
2	87.05	93.18	87.67	86.68
3	87.20	70.15	85.25	85.45
4	89.00	92.18	85.52	90.83
Delta	4.35	23.03	4.20	5.88
Rank	3	1	4	2

Figs. 4.1, 4.2 and 4.3 show the main effects plots for means of BSFC, BTE and smoke emission respectively. The main effects plots are very useful when there are several categorical variables to compare. These can give a fair idea about the categorical variables that mainly affect the response. The main effect is significant when the mean of the response shows considerable sensitivity to change in levels of the variable. Minitab generates the main effects plot by plotting the fitted mean for each value of a variable in the model. A line joins the points for each variable. This line determines whether or not a main effect exists for a variable. When the line is horizontal (parallel to the x-axis), then there is no main effect. Each level of the variable influences the response equally, and the response mean is the same across all levels. When the line is not horizontal, then main effect exists. Different levels of the categorical variable influence the response in different ways. The larger the difference in the upright positions of the plotted points, the larger the magnitude of the main effect. By comparing the slopes of the lines, the relative magnitude of the effects can be compared. Minitab also draws a reference line at the overall mean.

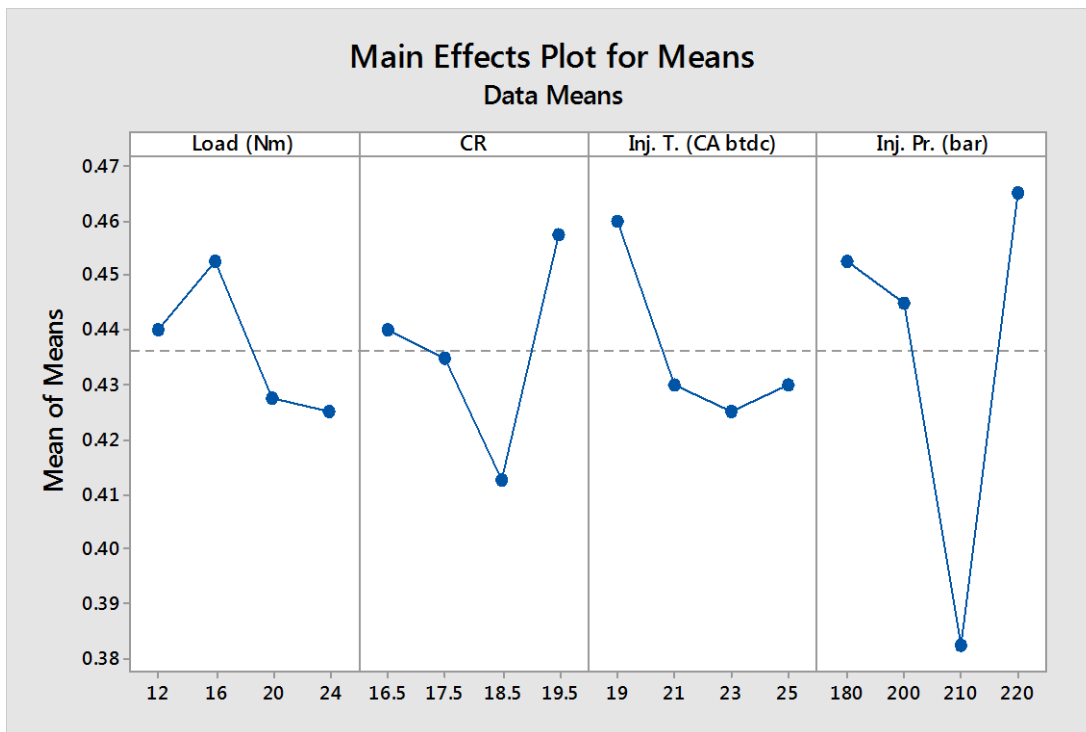


Fig. 4.1 Effect of engine operating parameters on BSFC

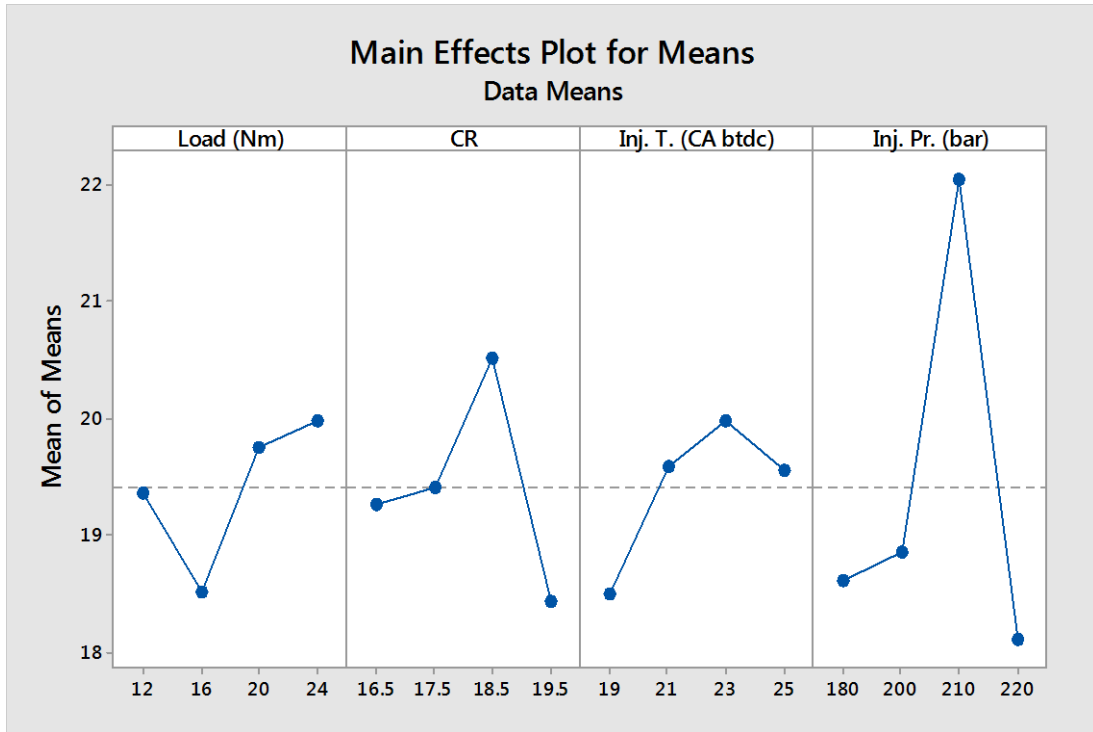


Fig. 4.2 Effect of engine operating parameters on BTE

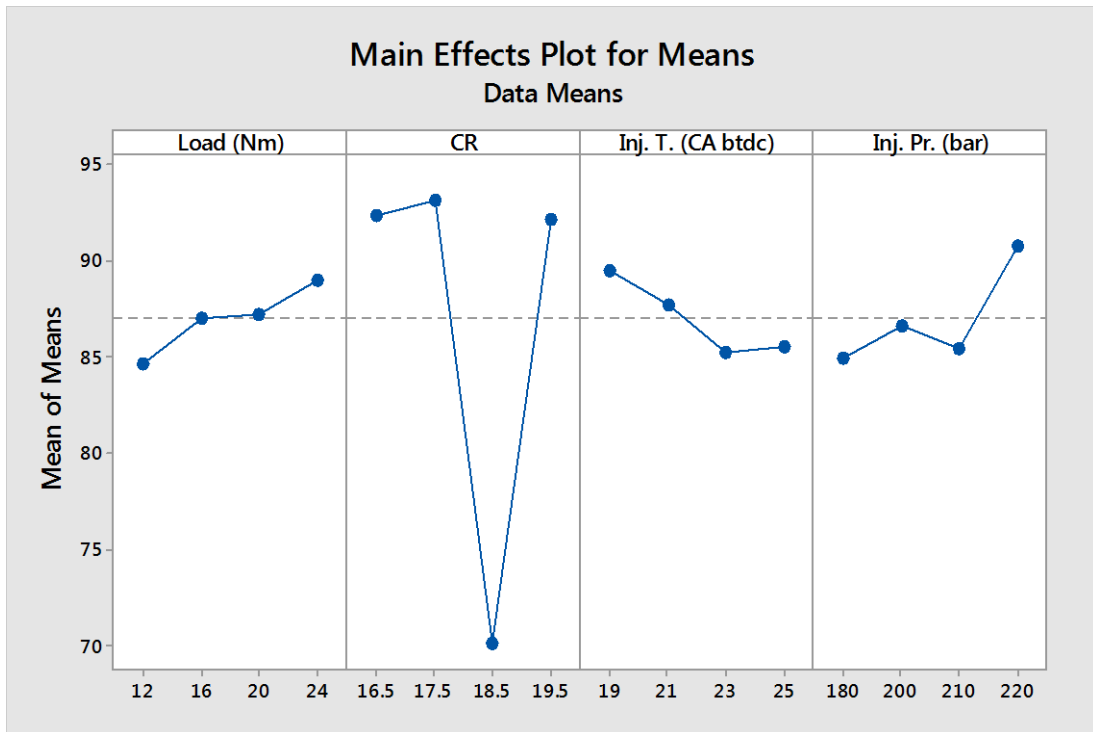


Fig. 4.3 Effect of engine operating parameters on smoke

From Fig. 4.1 to 4.3 it is clear that main effects of factors are present for BSFC, BTE and smoke. The injection pressure can be observed to influence BSFC and BTE mainly. Higher loads show significant effects on BSFC and BTE. BTE initially increases with increase in compression ratio from 16.5 to 18.5; increase in injection timing from 19° CA btdc to 23° CA btdc; and increase in injection pressure from 180 bar to 210 bar. After that it decreases with increase in compression ratio from 18.5 to 19.5; increase in injection timing from 23° CA btdc to 25° CA btdc; and increase in injection pressure from 210 bar to 220 bar. Therefore, maximum BTE was obtained at higher loads, compression ratio of 18.5, injection timing of 23° CA btdc and injection pressure of 210 bar. From Fig. 4.3, it can be observed that smoke emission is minimum at a load of 12 NM, compression ratio of 18.5, injection timing of 23° CA btdc and injection pressure of 180 bar. However the difference in the level of 180 bar and 210 bar is not significant. On the basis of results of this analysis, the engine settings of 18.5 CR, 210 bar Inj. Pr. and 23°CA btdc Inj. T. were selected for further experimentation. Table 4.4 depicts experimental values of BSFC, BTE and smoke emission for B0 (diesel without blending) at full load condition.

Table 4.4 Results for diesel at full load condition.

BSFC (kg/kW-h)	BTE (%)	Smoke (HSU %)
0.33	25.37	91

4.2 Performance and emissions characteristics of the engine using n-butanol-diesel blends:

In the second stage, tests were conducted using n-butanol-diesel blends with the following engine settings: 18.5 compression ratio (CR), 23° CA btdc injection timing and 210 bar injection pressure. The variations in engine performance and emissions for n-butanol-diesel blends were noted at different load conditions (no load to 100% rated power) are shown in Fig. 4.17 to Fig.4.37. Fig. 4.38 gives the comparison of performance and emissions of the engine at maximum load condition for diesel and different n-butanol-diesel blends. The scattered curves drawn by observed data showed that variations are significant at higher loads only. Thus, mathematical analysis was done for loads equal and more than that of 50% of full load.

4.2.1 Analysis of pressure-crank angle diagram for n-butanol-diesel blends

Fig. 4.4 shows the cylinder pressure vs. crank angle diagram for diesel and n-butanol-diesel blends at maximum load condition (100% rated power).

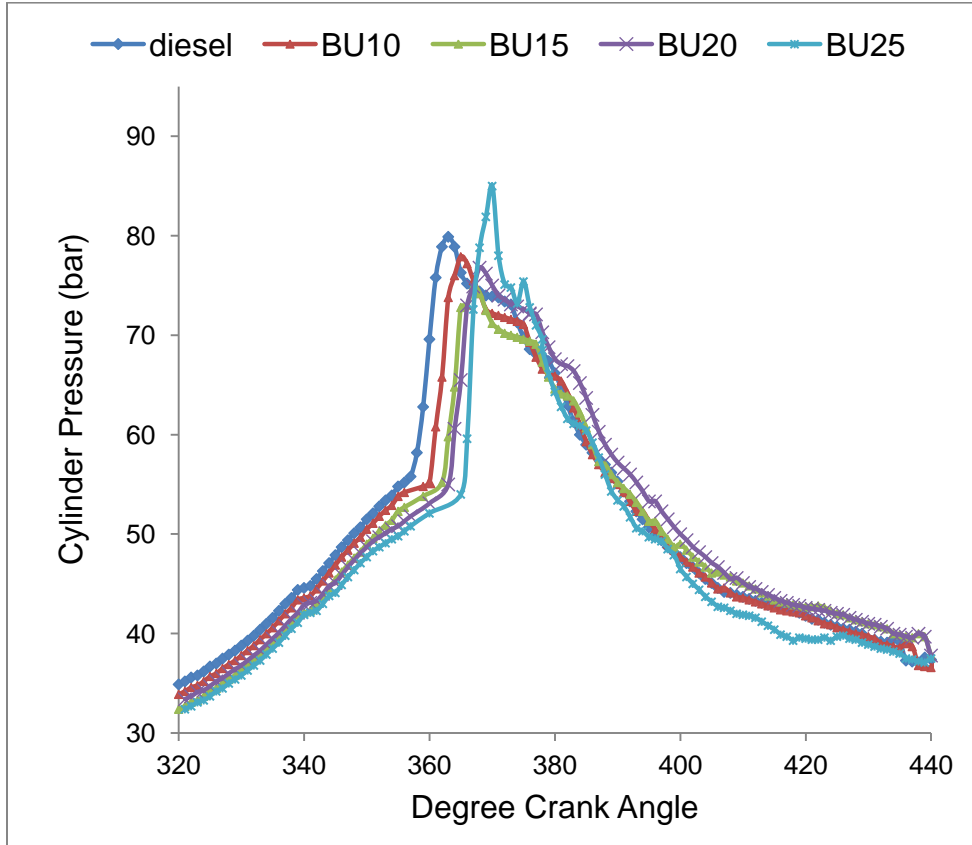


Fig. 4.4 Cylinder pressure vs. crank angle diagram (at 100% rated power)

It can be observed from Fig. 4.4 that for all n-butanol-diesel blends, combustion starts later as compared to diesel. The maximum pressures of blends can be observed to be lower than diesel, and seemingly shift towards the right side in the graph. Rakopoulos et al. [70], [77], [153] reported that n-butanol exhibits longer ignition delay due to low Cetane number. More combustible mixture is available after longer ignition delay. However, at the same time, due to higher heat of vaporization of n-butanol, combustion takes place in a relatively low-temperature environment and thus is delayed. This is the most probable reason of lower peak pressure of n-butanol-diesel blends. Also, Lower heating value of n-butanol releases lower energy during combustion and reduces effective pressure on the piston. Because of lower peak pressure, the maximum temperature in cylinder also decreases. The peak of pressure observed in Fig. 4.4 for BU25 can be

explained along the same lines. The variation in composition of fuel in BU25 (as compared to other blends) in all probability leads to a contradicting combination of ignition delay and availability of oxygen; thus causing an abrupt rise in pressure as observed.

4.2.2 Determination of optimum blend of n-butanol-diesel

To find the optimal n-butanol-diesel blend, the following approach was adopted: (i) Firstly, the selected data of experiments was fed to the DOE software and ANOVA was conducted to check the significance of model and individual terms. (ii) The curves from actual experiments and surface response model were then analyzed to see effect of change of factors on response. (iii) Optimization and verification of predicated model were done by confirmation test.

4.2.3 Modeling for n-butanol-diesel blends

Full Factorial design with the help of Design Expert (Version 8.0.4.1) was employed for the development of prediction models of BSFC, BTE, smoke, NO_x, CO and HC in terms of engine load and blending ratio(n-Butanol diesel blends). An attempt was made to optimize the engine parameters for the desired values of responses (BSFC, BTE, smoke, NO_x, CO and HC). Table 4.5 shows the engine operating parameters and their levels, and Table 4.6 shows the design matrix for experimentation.

Table 4.5 Parameters and their levels according to Factorial design for n-butanol-diesel blends.

Parameter	symbol	Levels			
		1	2	3	4
Load (Nm)	A (Load)	12	16	20	24
n-butanol-diesel	B (Blend)	10	15	20	25

Table 4.6 Design layout and experimental results for n-butanol-diesel blends

Run	Factor 1	Factor 2	Resp. 1	Resp. 2	Resp. 3	Resp. 4	Resp. 5	Resp.6	Resp.7
	A:Load (Nm)	B:blend (v/v %)	BTE (%)	BSFC kg/kW-h	BSEC kJ/kW-h	SMOKE HSU %	NO _x ppm	CO (%)	HC (ppm)
3	12.00	10.00	18.63	0.46	19325	13.5	318	0.089	29
11	16.00	10.00	22.38	0.38	15964	15.2	370	0.069	28
2	20.00	10.00	23.56	0.37	15544	30	482	0.065	27
14	24.00	10.00	24.27	0.35	14704	62.6	555	0.058	25
12	12.00	15.00	18.23	0.47	19512	6.1	284	0.08	41
1	16.00	15.00	21.42	0.40	16606	9.2	354	0.059	39
9	20.00	15.00	22.66	0.39	16191	27.3	470	0.054	37
7	24.00	15.00	23.16	0.37	15361	44.8	537	0.051	33
16	12.00	20.00	20.24	0.45	18459	5.4	280	0.07	23
4	16.00	20.00	23.32	0.37	15177	8.6	352	0.056	22
10	20.00	20.00	24.38	0.36	14767	23.1	468	0.052	20
8	24.00	20.00	25.07	0.35	14357	43	530	0.048	20
6	12.00	25.00	17.25	0.48	19452	7.8	331	0.09	51
15	16.00	25.00	20.06	0.43	17313	13	449	0.077	49
5	20.00	25.00	21.21	0.41	16615	25.4	542	0.068	47
13	24.00	25.00	22.50	0.38	15400	44.5	678	0.064	43

The details of 16 experiments as suggested by DOE from performed experiments are shown in Table 4.6 along with the run order selected at random. These data were used as inputs in the Design Expert 8.0.4.1 software for further analysis.

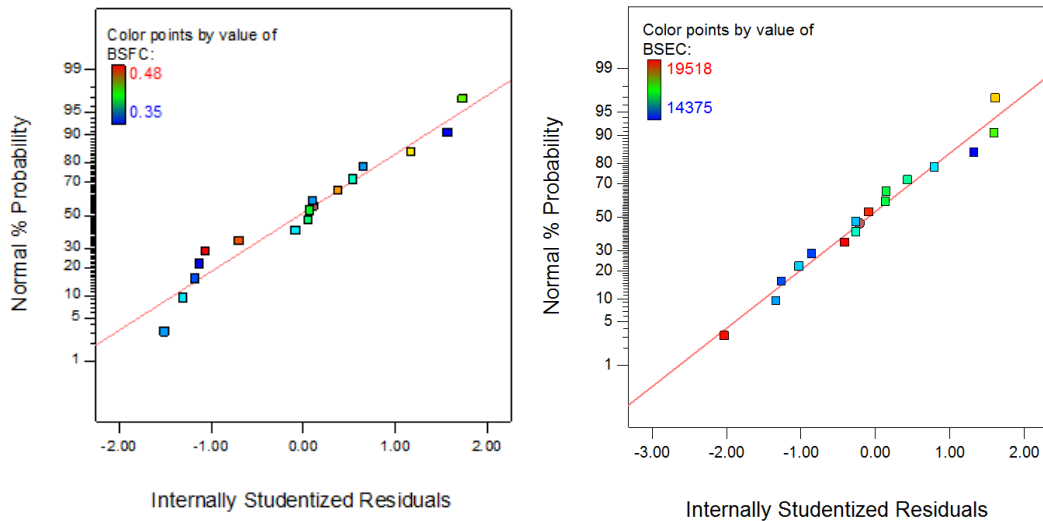
4.2.3.1 Diagnosis of data for analysis of variance n-butanol-diesel blends

Fig. 4.5 to Fig. 4.10 (a) show plots of normal probability vs. internal studentized residuals and internal studentized residuals vs. predicted values for BSFC, BTE, smoke, NO_x, CO and HC emissions respectively when the engine was operated on n-butanol-diesel blends.

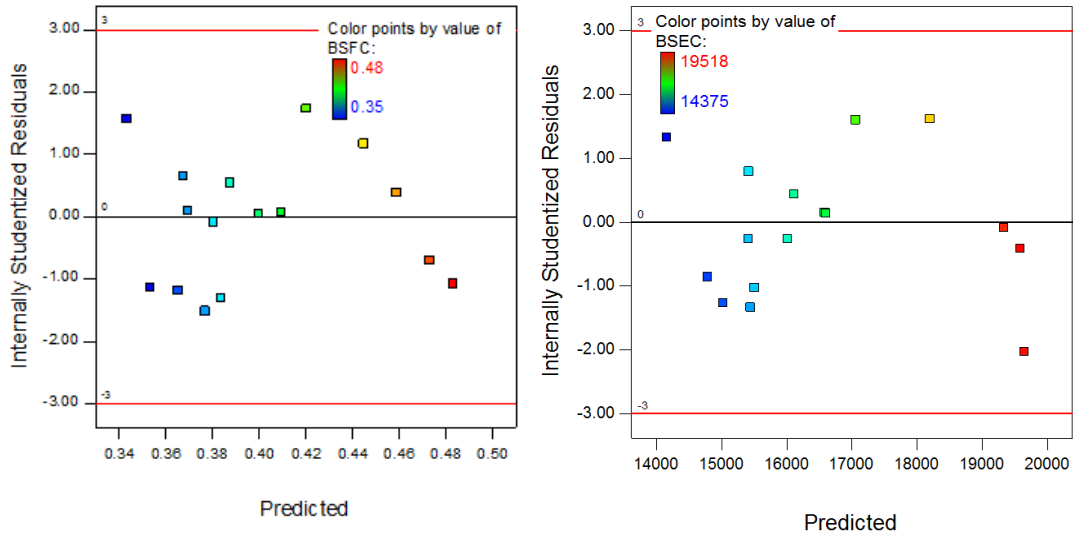
Residual is the difference between the actual and predicted response values. The internally studentized residual is the number of standard deviations that separate the actual and predicted response values. It is the residual divided by the estimated standard deviation of the residual. The normal probability vs. internal residual plot is used to check whether the residuals follow a normal distribution or not. Design-Expert performs the

hypothesis test on the normality of the data on the effects plot. The test is most valid for sample sizes in the range of 10 to 1000. The null hypothesis is that the data come from a normal distribution. When the selection of statistically significant terms is complete, the p-value above 0.10 advocates the rejection of the null hypothesis; indicating that the model terms are not significant. It can be observed from normal probability plots that most of the interaction points are accumulated along a straight line which implies that residuals follow the normal distribution and hence, the fitted model is adequate for a real system.

For the assumption of constant variance to be true in ANOVA, the internal residuals vs. predicted plot should be a random scatter. Fig. 4.5 (b), Fig. 4.6, (b) Fig. 4.7 (b), Fig. 4.8 (b), Fig. 4.9 (b) and Fig. 4.10 (b) reveal no obvious pattern or discernible structure, indicating the validity assumption to be true. It was thus projected that for all the responses, the variance of the observed data is constant and hence is satisfactory. In the plot of internal residuals vs. predicted response expanding variance ("megaphone pattern <") indicates that there is a need for transformation.



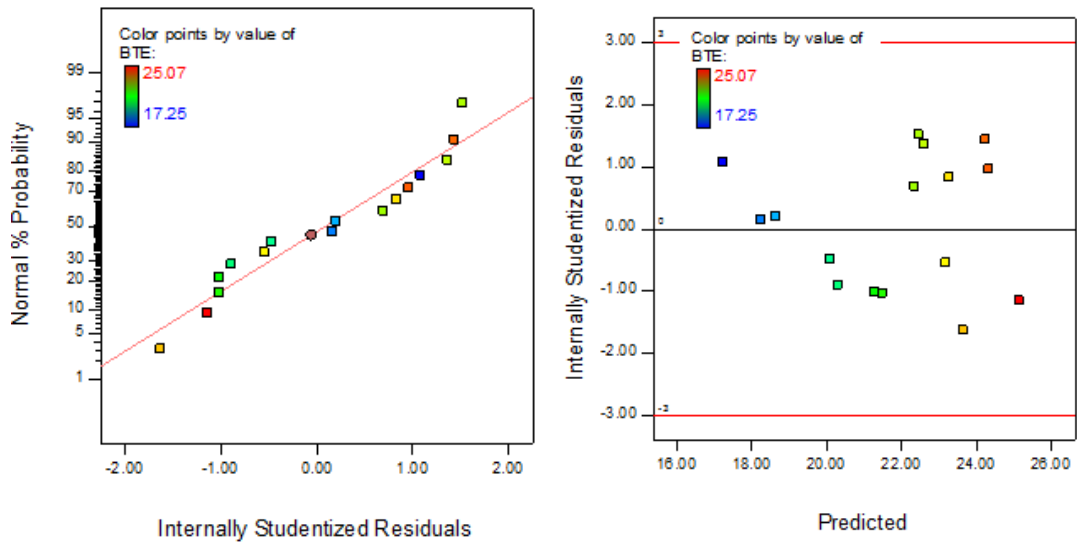
(a)



(b)

Fig. 4.5 (a) Plot of normal % probability vs. internal studentized residuals for BSFC & BSEC

(b) Plot of internal studentized residuals vs. predicted response for BSFC & BSEC

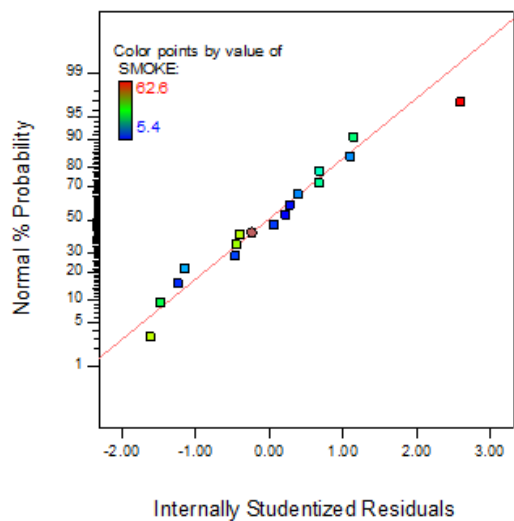


(a)

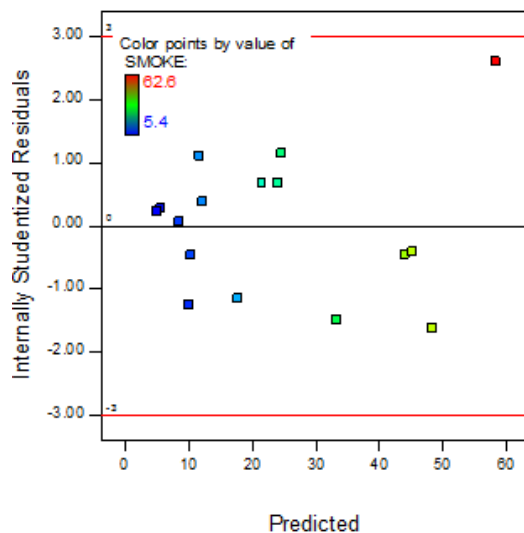
(b)

Fig. 4.6 (a) Plot of normal % probability vs. internal studentized residuals for BTE

(b) Plot of internal studentized residuals vs. predicted response for BTE

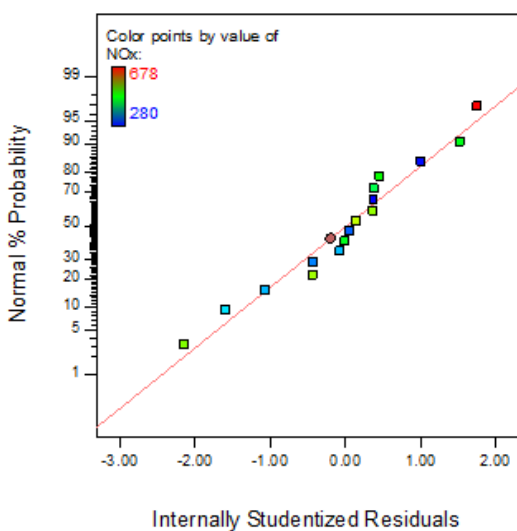


(a)

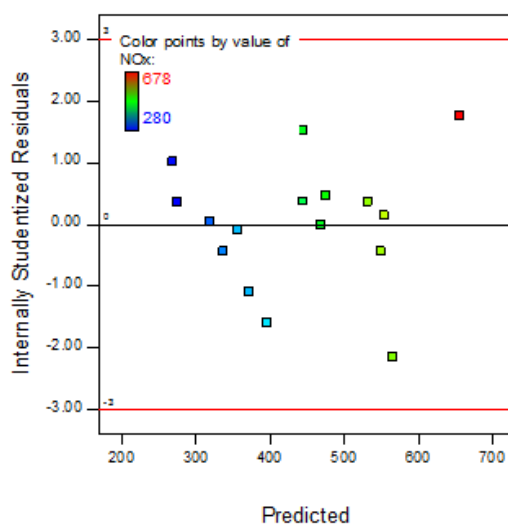


(b)

Fig. 4.7 (a) Plot of normal % probability vs. internal studentized residuals for smoke
(b) Plot of internal studentized residuals vs. predicted response for smoke



(a)



(b)

Fig. 4.8 (a) Plot of normal % probability vs. internal studentized residuals for NO_x
(b) Plot of internal studentized residuals vs. predicted response for NO_x

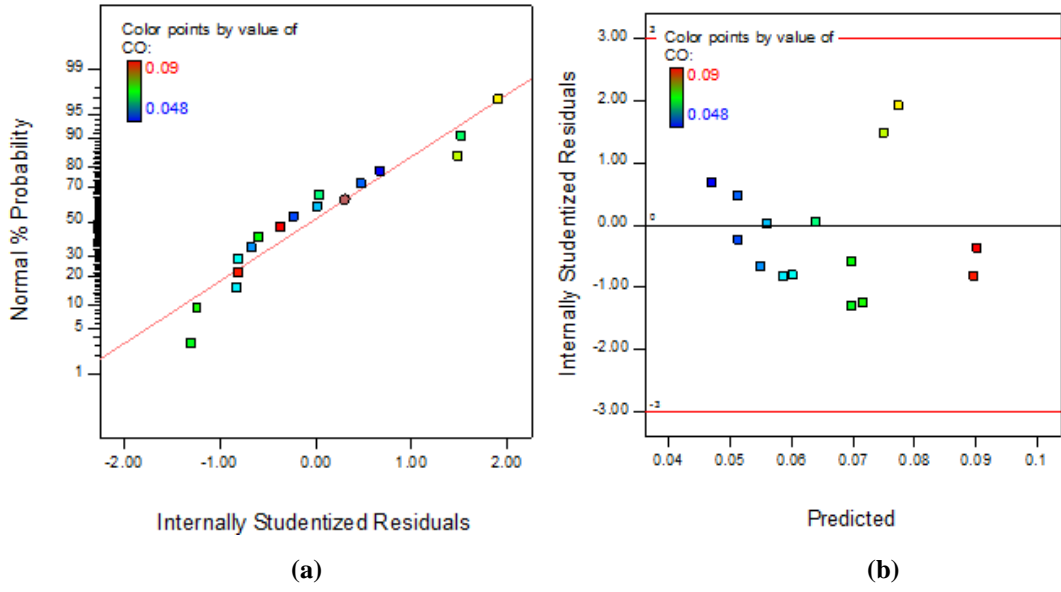


Fig. 4.9 (a) Plot of normal % probability vs. internal studentized residuals for CO
(b) Plot of internal studentized residuals vs. predicted response for CO

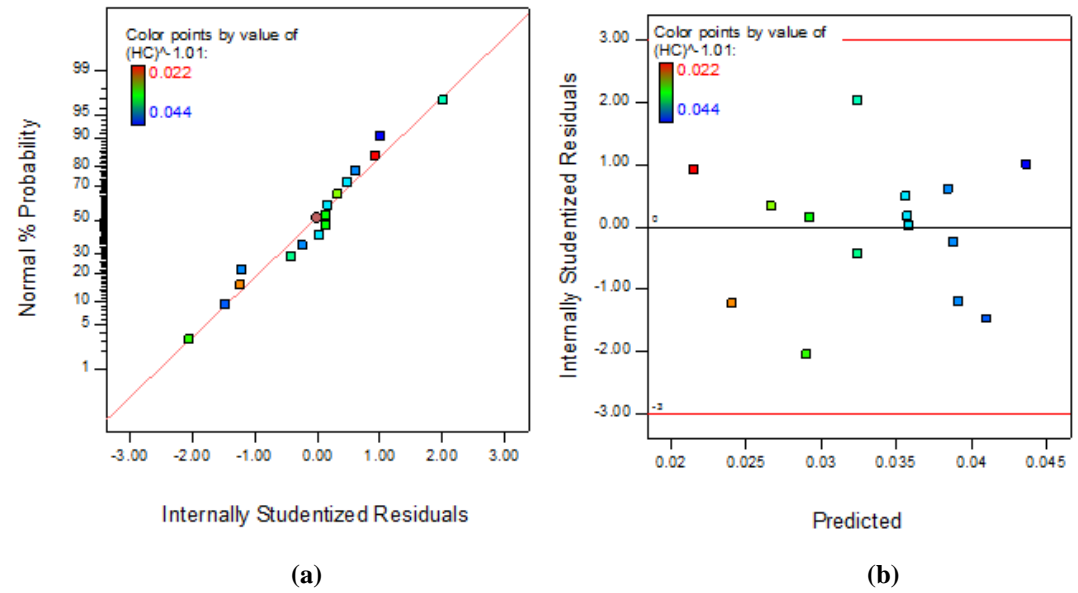


Fig. 4.10 (a) Plot of normal % probability vs. internal studentized residuals for HC
(b) Plot of internal studentized residuals vs. predicted response for HC

4.2.3.2 ANOVA for response surface model for n-butanol-diesel blends

Table 4.7 to Table 4.12 represent the ANOVA tables for the response surface prediction models of BSFC, BTE, smoke, NO_x, CO and HC respectively by selecting the backward elimination procedure to remove the terms that are not significant. In the present work,

ANOVA analysis was carried out for a significance level of $\alpha = 0.05$, i.e. for a confidence level of 95%.

Table 4.7 presents the ANOVA for Response Surface Cubic model for BSFC. In the Table, the value of “Prob. > F” for the model is 0.0001 which is less than 0.05, indicating that the model is significant, i.e. the terms in the model have a significant effect on BSFC. In the same manner, the value of “Prob. > F” for the main effect of blend, second order effect of load and blend and cubic effect of load and blend were also found to be less than 0.05. So these terms are also significant model terms.

Table 4.7 Reduce analysis of variance table and interaction fit for BSFC

Source	Sum of Squares	Degree of freedom	Mean Square	F-Value	p-value Prob > F
Model	0.028	8	3.504E-003	99.65	< 0.0001
A-Load (Nm)	1.281E-004	1	1.281E-004	3.64	0.0980
B-blend (% v/v)	9.838E-004	1	9.838E-004	27.98	0.0011
AB	1.219E-005	1	1.219E-005	0.35	0.5745
A ²	2.557E-003	1	2.557E-003	72.73	< 0.0001
B ²	5.783E-004	1	5.783E-004	16.45	0.0048
A ² B	1.058E-004	1	1.058E-004	3.01	0.1263
A ³	8.964E-004	1	8.964E-004	25.49	0.0015
B ³	2.355E-003	1	2.355E-003	66.96	< 0.0001
Residual	2.461E-004	7	3.516E-005		
Cor Total	0.028	15			
Std. Dev.	5.930E-003		R-Squared		0.9913
Mean	0.40		Adj R-Squared		0.9813
C.V. %	1.48		Pred R-Squared		0.9492
PRESS	1.435E-003		Adeq Precision		31.345

Sum of squares is the differences between the overall average and the amount of variation explained by that row's source. The degree of Freedom is the number of estimated parameters used to compute the source's sum of squares. The sum of squares divided by the degrees of freedom is termed as mean square (also called variance). F-Test has been done for comparing the sources mean square to the residual mean square. Prob > F: (p-value) is checked to find whether the null hypothesis is true or not (there are no factor effects). Small probability values indicate the rejection of the null hypothesis. The probability equals the proportion of the area under the curve of the F-distribution that lies beyond the observed F value. The F distribution itself is evaluated by the degrees of freedom associated with the variances being compared. The standard deviation of the model is 0.00593 and the mean is 0.40. The coefficient of variation (C.V.), also called as relative standard deviation (RSD) for the generated model is 1.48. The C.V. is the ratio of standard ratio to the mean of the data, presented in percent. Predicted Residual Error Sum of Squares (PRESS) is a measure of how the model fits each point in the design. Lower values of PRESS are desirable. In the generated model, PRESS value is 0.001435.

The R-Squared (R^2) value, which is a measure of the proportion of total variability explained by the model; is equal to 0.9913 for the presented case. Its nearness to 1 for the model is indicative of the accuracy and exactness of the model in finding the desired responses. The adjusted R-Squared ($Adj-R^2$) is a measure of variation about the mean described by the model, and is particularly useful when comparing models with different number of terms. Predicted R-squared ($Pred-R^2$) is an indication of how effectively the model predicts a response value. For reliability of model and data, the $Adj-R^2$ and $Pred-R^2$ should be within the range of 0.20 of each other. The Table 4.7 shows that $Pred-R^2$ of 0.9492 is in reasonable agreement with the $Adj-R^2$ of 0.9813; i.e. the difference is less than 0.2. Adequate precision is the gauge of the range of predicted output relative to its allied error, i.e. signal to noise ratio. A value greater than 4 is desirable for significant precision. For the developed BSFC model, the value of Adequate Precision is 31.345, which also shows the significant precision of the model. The final empirical model for BSFC in terms of coded and actual factors is given by Eqs. 4.1 and 4.2 respectively.

$$BSFC = 0.37750 - 0.013513 \times A - 0.0396932 \times B + 0.0015712 \times AB + 0.028446 \times A^2 + 0.0135264 \times B^2 - 0.00776428 \times A^2B - 0.0376575 \times A^3 + 0.0610321 \times B^3 \quad (4.1)$$

$$BSFC = 1.25578 - 0.218884 \times Load + 0.10926 \times blend + 0.00107015 \times Load \times blend + 0.0107078 \times Load^2 - 0.00735464 \times blend^2 - 2.87566e-005 \times Load^2 \times blend - 0.00017434 \times Load^3 + 0.000144669 \times blend^3 \quad (4.2)$$

Table 4.8 presents the ANOVA of Response Surface Cubic model for BTE. In the Table, the value of “Prob. > F” for the model is 0.0001 which is less than 0.05, indicating that the model is significant, i.e. the terms in the model have a significant effect on BTE. In the same manner, the value of “Prob. > F” for main effect of load, blend and interaction effect of load and blend, and second order effect of load and blend, and interaction effect of second order of load and main effect of blend, second order of blend and main effect of load, and cubic effect of load and blend were also found to be less than 0.05. So these terms are also significant model terms.

Table 4.8 Reduce analysis of variance table and interaction fit for BTE

Source	Sum of Squares	Degree of Freedom	Mean Square	F-Value	p-value Prob. > F
Model	81.639	9	9.071	1282.057	0.0001
A-Load	1.349	1	1.349	190.595	0.0001
B-Blend	5.890	1	5.890	832.404	0.0001
AB	0.043	1	0.043	6.069	0.0489
A ²	5.799	1	5.799	819.609	0.0001
B ²	4.648	1	4.648	656.947	0.0001
A ² B	0.297	1	0.297	41.926	0.0006
AB ²	0.149	1	0.149	20.994	0.0038
A ³	0.570	1	0.570	80.565	0.0001
B ³	11.564	1	11.564	1634.443	0.0001
Residual	0.042	6	0.0071		
Cor. Total	81.681	15			
Std. Dev.	0.084		R-Squared		0.999
Mean	21.772		Adj R-Squared		0.998
C.V. %	0.386		Pred R-Squared		0.994
PRESS	0.469		Adeq Precision		118.989

The standard deviation of the model is 0.084 and the mean is 21.7772. The coefficient of variation (C.V.) for the generated model is 0.386. In the generated model, PRESS value

is 0.469. The R-Squared (R^2) value is 0.999. The Pred- R^2 is 0.994, which is in reasonable agreement with the Adj- R^2 of 0.998; i.e. the difference is less than 0.2. For the developed BTE model the value of Adequate Precision is 118.989, which also shows the significant precision of the model. The final empirical model for BTE in terms of coded and actual factors are given by Eqs. 4.3 and 4.4 respectively.

$$BTE = 23.1985 + 1.46961 \times A + 3.07123 \times B - 0.0932492 \times AB - 1.35456 \times A^2 - 1.21272 \times B^2 + 0.41103 \times A^2B + 0.290854 \times AB^2 + 0.949628 \times A^3 - 4.27726 \times B^3 \quad (4.3)$$

$$BTE = 7.4919 + 7.13208 \times Load - 7.07738 \times blend - 0.0870389 \times Load \times blend - 0.301674 \times Load^2 + 0.495209 \times blend^2 + 0.00152233 \times Load^2 \times blend + 0.00086179 \times Load \times blend^2 + 0.00439642 \times Load^3 - 0.0101387 \times blend^3 \quad (4.4)$$

Table 4.9 presents the ANOVA for Response Surface Quadratic model for smoke emission. In the Table, the value of “Prob. > F” for the model, the main effect of load, blend and interaction effect of load and blend, and second order effect of load and blend are less than 0.05. So these terms are significant model terms. The R^2 value is equal to 0.984. Table 4.9 also shows that Pred- R^2 of 0.938 is in reasonable agreement with the Adj- R^2 of 0.976; i.e. the difference is less than 0.2. For the developed smoke model, the value of Adequate Precision is 32.463, which shows significant precision of the model. The final empirical model for smoke emission in terms of coded and actual factors is given by Eqs. 4.5 and 4.6 respectively.

$$SMOKE = 71.88100 - 6.16044 \times Load - 3.25795 \times Blend - 0.062850 \times Load \times Blend + 0.29648 \times Load^2 + 0.11125 \times Blend^2 \quad (4.5)$$

$$SMOKE = 14.3125 + 20.4788 \times A - 3.71625 \times B - 2.82825 \times AB + 10.6734 \times A^2 + 6.25781 \times B^2 \quad (4.6)$$

Table 4.9 Reduce analysis of variance table and interaction fit for Smoke

Source	Sum of Squares	Degree of Freedom	Mean Square	F-Value	p-value Prob. > F
Model	4373.89	5	874.78	121.41	0.0001
A-Load	3727.82	1	3727.82	517.38	0.0001
B-Blend	122.76	1	122.76	17.04	0.0021
AB	39.16	1	39.5	5.48	0.0412
A ²	360.05	1	360.05	49.97	0.0001
B ²	123.77	1	123.77	17.18	0.002
Residual	72.05	10	7.21		
Cor. Total	4445.94	15			
Std. Dev.	2.684		R-Squared		0.984
Mean	23.719		Adj R-Squared		0.976
C.V. %	11.317		Pred R-Squared		0.938
PRESS	276.623		Adeq Precision		32.463

Table 4.10 presents the reduce ANOVA table for Response Surface Quadratic model for NO_x. In the Table, the value of “Prob. > F” for the model, the main effect of load, blend and interaction effect of load and blend, and second order effect of blend are less than 0.05. So these terms are significant model terms. The R² value is equal to 0.980. The table also shows that Pred-R² of 0.956 is in reasonable agreement with the Adj-R² of 0.972; i.e. the difference is less than 0.2. For the developed NO_x model, the value of Adequate Precision is 36.303, which shows significant precision of the model. The final empirical model for NO_x in terms of coded and actual factors is given by Eqs. 4.7 and 4.8 respectively.

$$NO_x = 436.38 + 11.37125 \times \text{Load} - 43.641 \times \text{Blend} + 0.462 \times \text{Load} \times \text{blend} + 0.10156 \times \text{Load}^2 + 1.125 \times \text{Blend}^2 \quad (4.7)$$

$$NO_x = 402.344 + 138.675 \times A + 30.375 \times B + 20.79 \times AB + 63.2813 \times B^2 \quad (4.8)$$

Table 4.10 Reduce analysis of variance table and interaction fit for NO_x

Source	Sum of Squares	Degree of Freedom	Mean Square	F-Value	p-value Prob. > F
Model	193931.99	4	48482.998	132.665	0.0001
A-Load	170940.05	1	170940.050	467.745	0.0001
B-Blend	8201.25	1	8201.250	22.441	0.0006
AB	2134.44	1	2134.440	5.840	0.0342
B ²	12656.25	1	12656.250	34.631	0.0001
Residual	4020.01	11	365.455		
Cor. Total	197952	15			
Std. Dev.	19.1169		R-Squared		0.980
Mean	437.5000		Adj R-Squared		0.972
C.V. %	4.3696		Pred R-Squared		0.956
PRESS	8741.3653		Adeq Precision		36.303

Table 4.11 presents the reduce ANOVA table for Response Surface Cubic model for CO. In the Table, the value of “Prob. > *F*” for the model, the main effect of load, main effect of blend, second order effect of load, second order effect of blend, and third order effect of the blend are less than 0.05. So these terms are significant model terms. The R² value is equal to 0.9899. The table also shows that Pred-R² of 0.9273 is in reasonable agreement with the Adj-R² of 0.9746; i.e. the difference is less than 0.2. For the developed CO model, the value of Adequate Precision is 26.274, which shows significant precision of the model. The final empirical model for CO in terms of coded and actual factors is given by Eqs. 4.9 and 4.10 respectively.

$$CO = 0.053125 - 0.0065625 \times A - 0.0069375 \times B + 0.00117 \times AB + 0.00703125 \times A^2 + 0.0154688 \times B^2 - 0.0016875 \times A^2 B - 0.00185625 \times AB^2 - 0.00590625 \times A^3 + 0.010125 \times B^3 \quad (4.9)$$

$$CO = 0.34129 - 0.04078 \times Load + 0.005542 \times Blend + 0.0004435 \times Load \times Blend + 0.00178125 \times Load^2 - 0.000886 \times Blend^2 - 6.25e-006 \times Load^2 \times Blend - 5.5e-006 \times Load \times Blend^2 - 2.73437e-0005 \times Load^3 + .00002.4e-005 \times Blend^3 \quad (4.10)$$

Table 4.11 Reduce analysis of variance table and interaction fit for CO

Source	Sum of Squares	Degree of Freedom	Mean Square	Value	p-value Prob > F
Model	2.530E-003	9	2.811E-004	65.02	< 0.0001
A-LOAD (Nm)	2.689E-005	1	2.689E-005	6.22	0.0469
B-BLEND (% v/v)	3.005E-005	1	3.005E-005	6.95	0.0387
AB	6.760E-006	1	6.760E-006	1.56	0.2577
A ²	1.563E-004	1	1.563E-004	36.14	0.0010
B ²	7.563E-004	1	7.563E-004	174.92	< 0.0001
A ² B	5.000E-006	1	5.000E-006	1.16	0.3235
AB ²	6.050E-006	1	6.050E-006	1.40	0.2816
A ³	2.205E-005	1	2.205E-005	5.10	0.0647
B ³	6.480E-005	1	6.480E-005	14.99	0.0083
Residual	2.594E-005	6	4.323E-006		
Cor Total	2.556E-003	15			
Std. Dev.	2.079E-003		R-Squared		0.9899
Mean	0.066		Adj R-Squared		0.9746
C.V. %	3.17		Pred R-Squared		0.9273
PRESS	1.857E-004		Adeq Precision		26.274

Table 4.12 presents the reduce ANOVA table for Response Surface Cubic model for HC. In the Table, the value of “Prob. > F ” for the model, the main effect of load, main effect of blend, second order effect of blend, interaction of main effect of load and second order effect of the blend and third order effect of blend are less than 0.05. So these terms are significant model terms. The R^2 value is equal to 0.9954. The Table also shows that Pred- R^2 of 0.9826 is in reasonable agreement with the Adj- R^2 of 0.9923; i.e. the difference is less than 0.2. For the developed HC model, the value of Adequate Precision is 60.285, which shows significant precision of the model. The final empirical model for HC in terms of coded and actual factors is given by Eqs. 4.11 and 4.12 respectively.

$$HC^{(-1.01)} = 0.0323702 + 0.0037535 \times A + 0.024278 \times B + 0.000120498 \times AB + 0.00167383 \times B^2 + 0.00116254 \times AB^2 - 0.0242464 \times B^3 \quad (4.11)$$

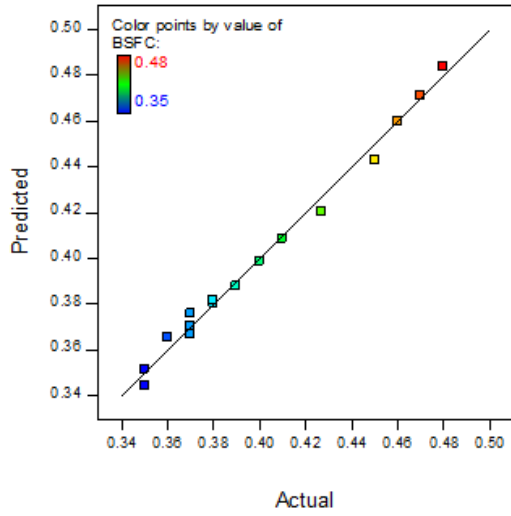
$$HC^{(-1.01)} = 0.263449 + 0.00163362 \times Load - 0.0484858 \times Blend - 0.000117882 \times Load \times Blend + 0.00298509 \times Blend^2 + 3.44455e-006 \times Load \times Blend^2 - 5.7473e-005 \times Blend^3 \quad (4.12)$$

Table 4.12 Reduce analysis of variance table and interaction fit for HC

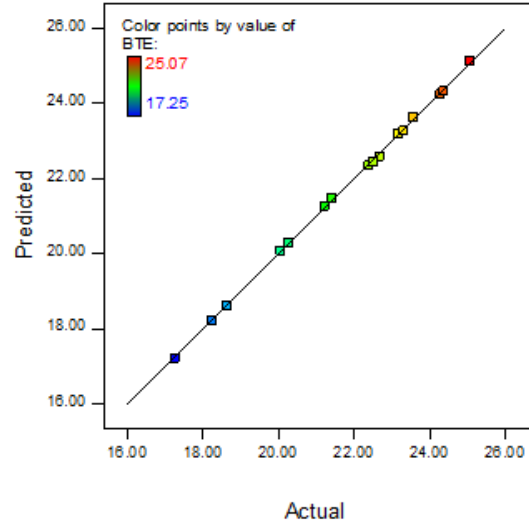
Source	Sum of Squares	degree of freedom	Mean Square	F Value	P value Prob > F
Model	5.975E-004	6	9.958E-005	322.57	< 0.0001
A-LOAD (Nm)	4.887E-005	1	4.887E-005	158.32	< 0.0001
B-BLEND (% v/v)	4.134E-004	1	4.134E-004	1339.19	< 0.0001
AB	7.170E-008	1	7.170E-008	0.23	0.6413
B ²	8.855E-006	1	8.855E-006	28.68	0.0005
AB ²	2.373E-006	1	2.373E-006	7.69	0.0217
B ³	3.716E-004	1	3.716E-004	1203.78	< 0.0001
Residual	2.778E-006	9	3.087E-007		
Cor Total	6.002E-004	15			
Std. Dev.	5.556E-004		R-Squared		0.9954
Mean	0.033		Adj R-Squared		0.9923
C.V. %	1.67		Pred R-Squared		0.9826
PRESS	1.042E-005		Adeq Precision		60.285

4.2.3.3 Comparison of observed and estimated responses

Figs. 4.11 and 4.12 show the plots between the actual and predicted values of BSFC, BTE, smoke, NO_x, CO and HC. These plots clearly show that the values of actual data and predicted data are quite close to each other. This implies that the model is significant. It can be observed from the plots that most of the points are clustered around 45° line. This gives an indication of a fairly good least square fit for the responses.

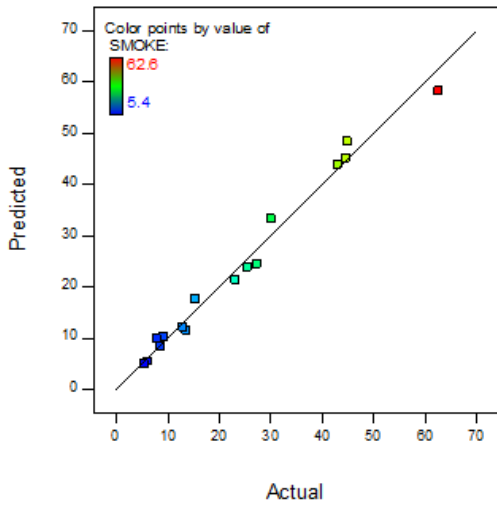


(a)

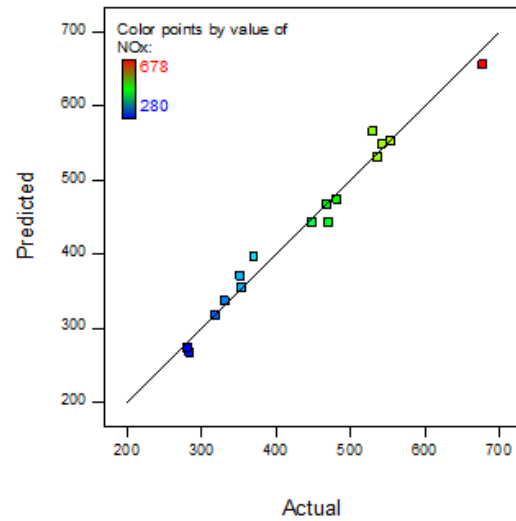


(b)

Fig. 4.11 Plot of actual values vs. predicted values for (a) BSFC (b)BTE



(a)



(b)

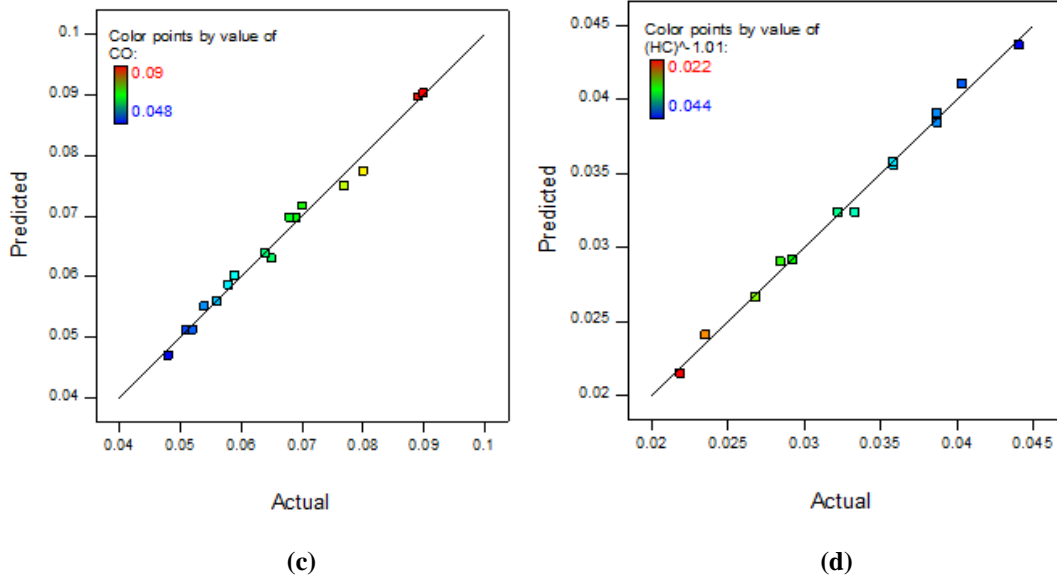


Fig. 4.12 Plot of actual values vs. predicted values for (a) Smoke (b) NO_x (c) CO (d) HC

4.2.4 Performance of engine using n-butanol diesel blends

The results of engine performance tests for BSFC and BTE were recorded and have been presented in this section using scattered diagrams from observed data of experiments and 3D surface plots & interaction plots from mathematical models.

4.2.4.1 Brake specific fuel consumption (BSFC)

It can be seen from Fig.4.13 that the BSFC reduces with increasing load and is lowest at full load. Fig. 4.34 shows that BSEC is higher for all n-butanol-diesel blends in comparison to diesel [23]. The heating value of n-butanol is lesser than that of diesel. This means, for producing the same amount of power, more blended fuel is required. It can be observed (see Appendix C) that with increase in n-butanol percentage in blend, the Cetane number of fuel decreases. Combustion of fuel with lower Cetane number increases ignition delay period [70], [77] which increases accumulated fuel inside the cylinder before combustion starts. The increased delay period increases the time duration of fuel combustion at higher temperature. This, in turn, increases heat transfer to engine parts, and due to this, the effectiveness of energy conversion into brake power decreases. Thus, lower heating value and Cetane number of n-butanol are the main factors that are responsible for increased BSFC of blended fuels [100][64]. At all loads, the BSFC increases for blends BU10 to BU15; but again decreases for BU20. The decrement of BSFC for BU20 can be attributed to better combustion with increased oxygen of n-

butanol in diesel. On the other hand, the increase of BSFC at higher blend is because of longer ignition delay, which leads to lower mean effective pressure. However, BU20 exhibits better performance than other blends. The increment in BSFC and BSEC for BU20 were 6.06% and 8.68% compared to that of diesel at full load condition (100% rated power).

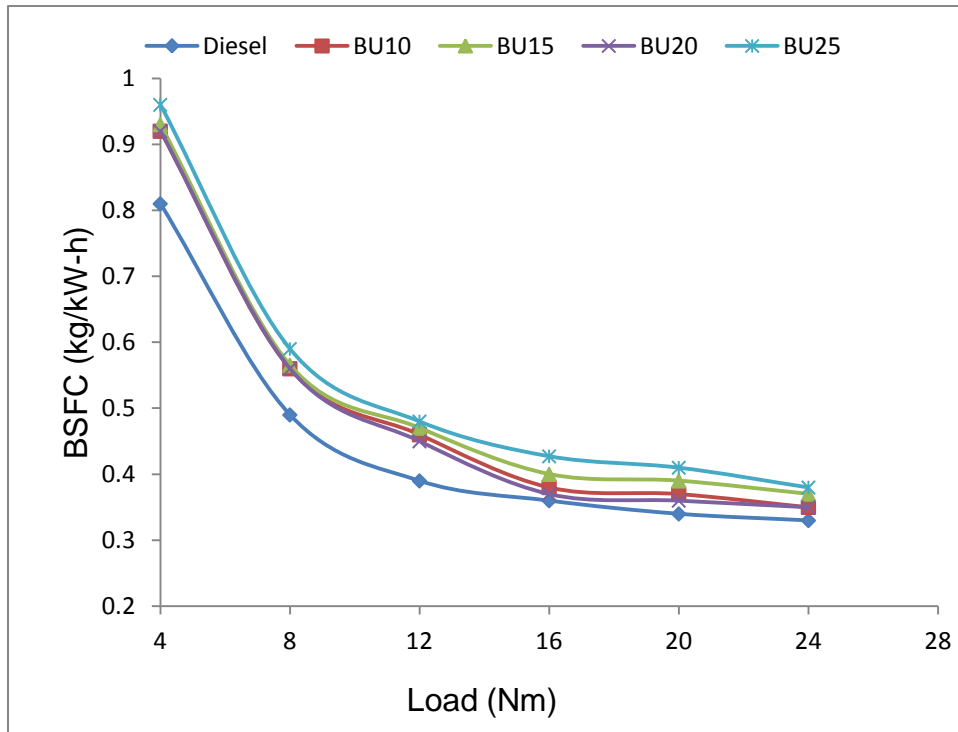


Fig. 4.13 Variation of BSFC with engine load for n-butanol-diesel blends

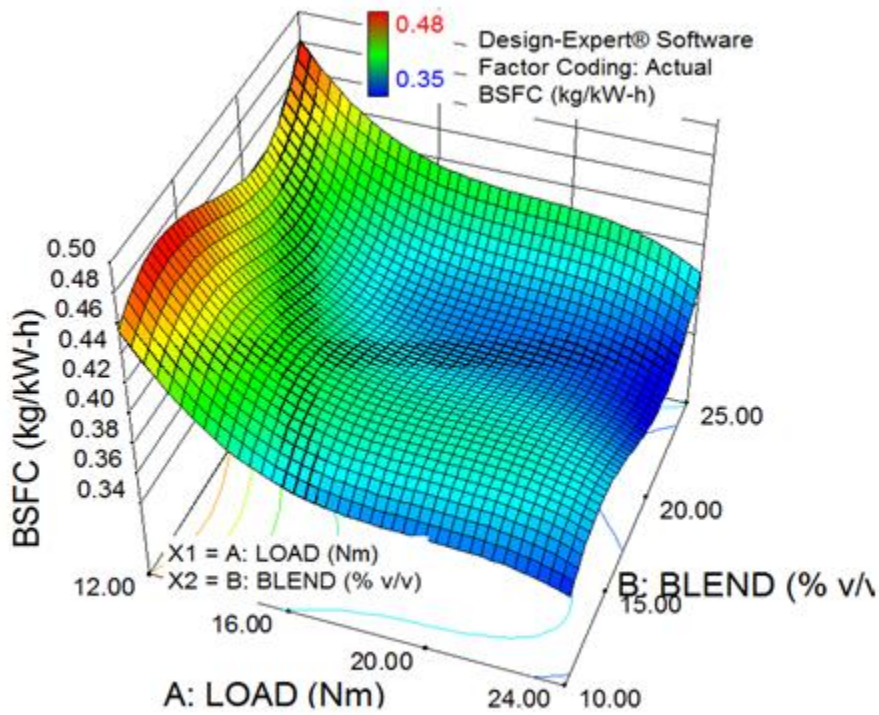


Fig. 4.14 Variation in BSFC due to combined effect of load and n-butanol blending

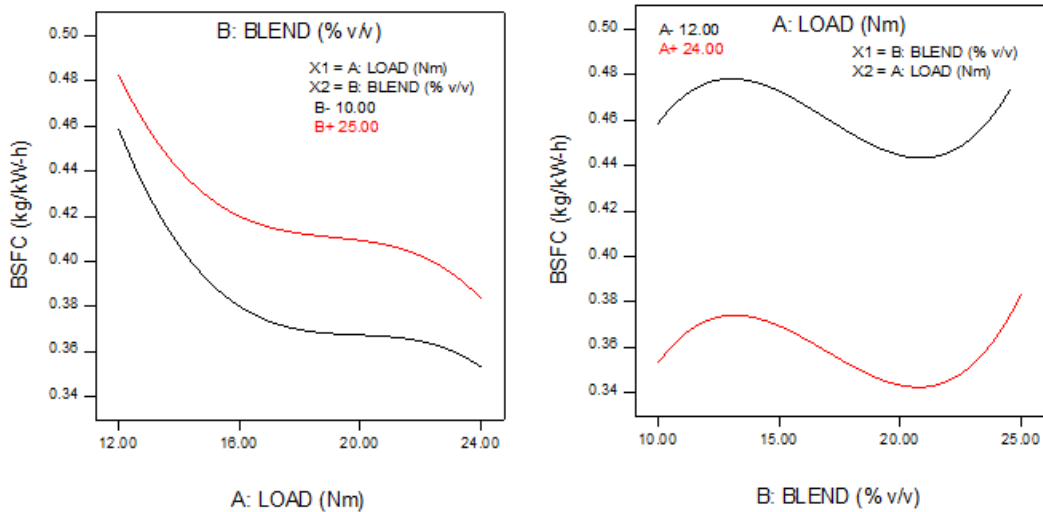


Fig. 4.15 Variation in BSFC with load and n-butanol-diesel blends at minimum and maximum values

It can be observed from Fig. 4.14 and Fig. 4.15 that at higher loads the curves of BSFC for minimum and maximum blends are divergent. The trends of curves for minimum and

maximum loads remain same for blends. The similarity in scattered curves and 3D surface model shows the accuracy of predicted model.

4.2.4.2 Variation of brake specific energy conversion

From the Load vs. BSEC graphs (Fig.4.16), it can be seen that at higher loads, BSEC of BU20 and diesel are very much similar. The increment in BSEC at full load for BU20 compared to that of diesel is only 1.30% against the 6.06% increment of BSFC. Fig. 4.17 compares the variation of BSFC and BSEC for different blends at full load condition. It can be seen that the utilization of energy with BU20 is more effective as compared to other blends.

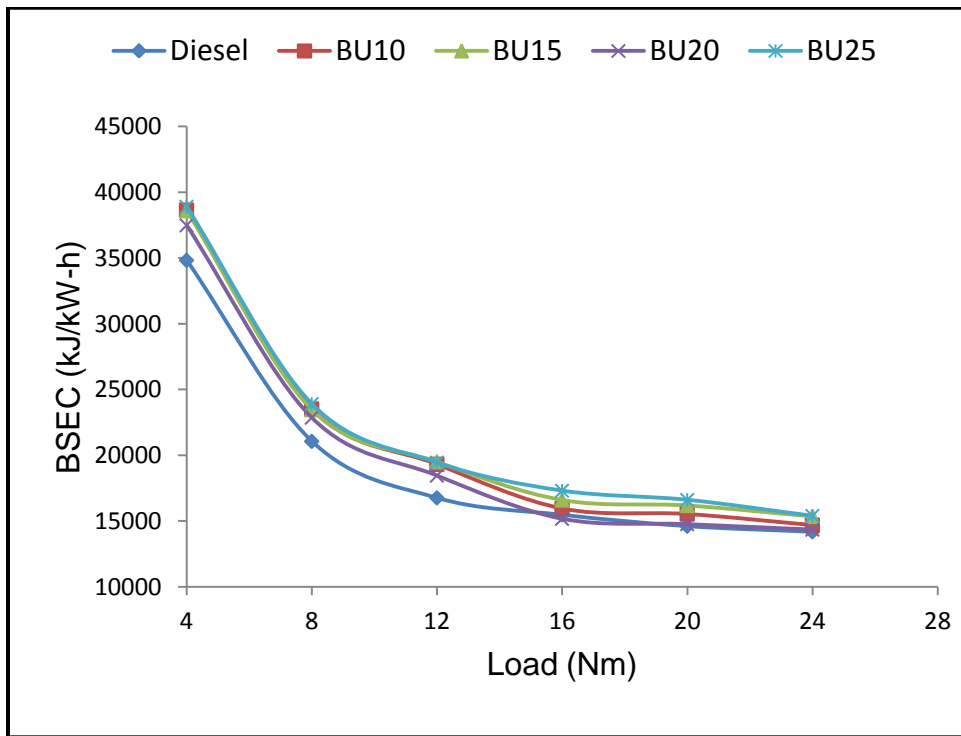


Fig. 4.16 Variation of BSEC with engine load for n-butanol-diesel blends

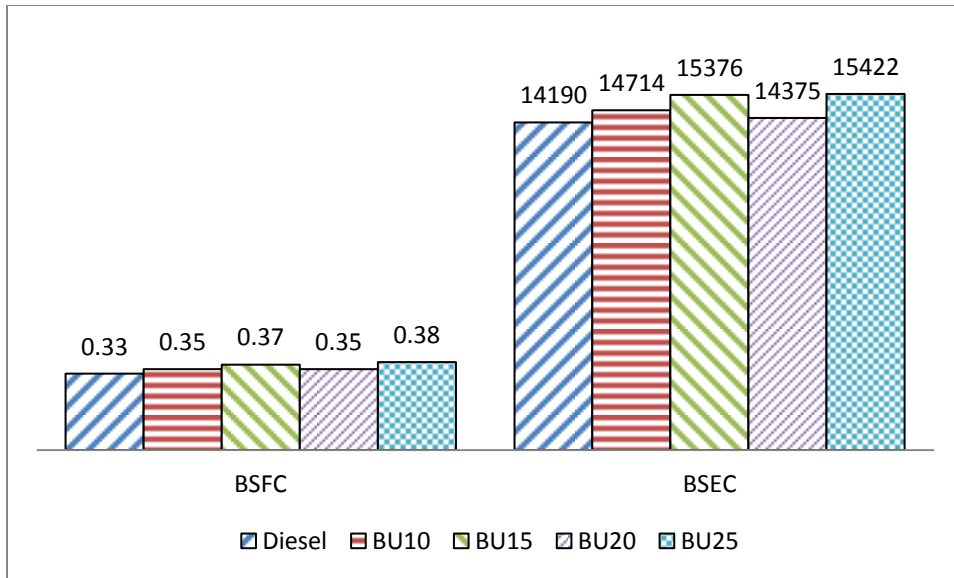


Fig. 4.17 Variation of BSFC and BSEC for different n-butanol-diesel blends at full load condition

4.2.4.3 Brake thermal efficiency

Fig. 4.18 shows the trends of BTE and Fig.4.34 shows the value of BTE at full load condition. It can be observed that BTE for n-butanol-diesel blends is lower as compared to diesel only. The highest BTE is observed for BU20 among tested blended-fuels. It has already been discussed, that the n-butanol-diesel blends exhibit delayed combustion because of low Cetane number and higher heat of vaporization of n-butanol as compared to diesel. This is the most apparent reason of lower peak pressure of n-butanol-diesel blends. The blended fuels release lesser heat because of lower heating value and lower Cetane number of n-butanol, which in turn reduces BTE of engine. It can be observed from Fig 4.34 that for BU20, the decrement in brake thermal efficiency (BTE) is lesser than that of other blends in comparison to diesel only. A loss of about 1.18% in BTE has been observed for BU20 as compared to diesel.

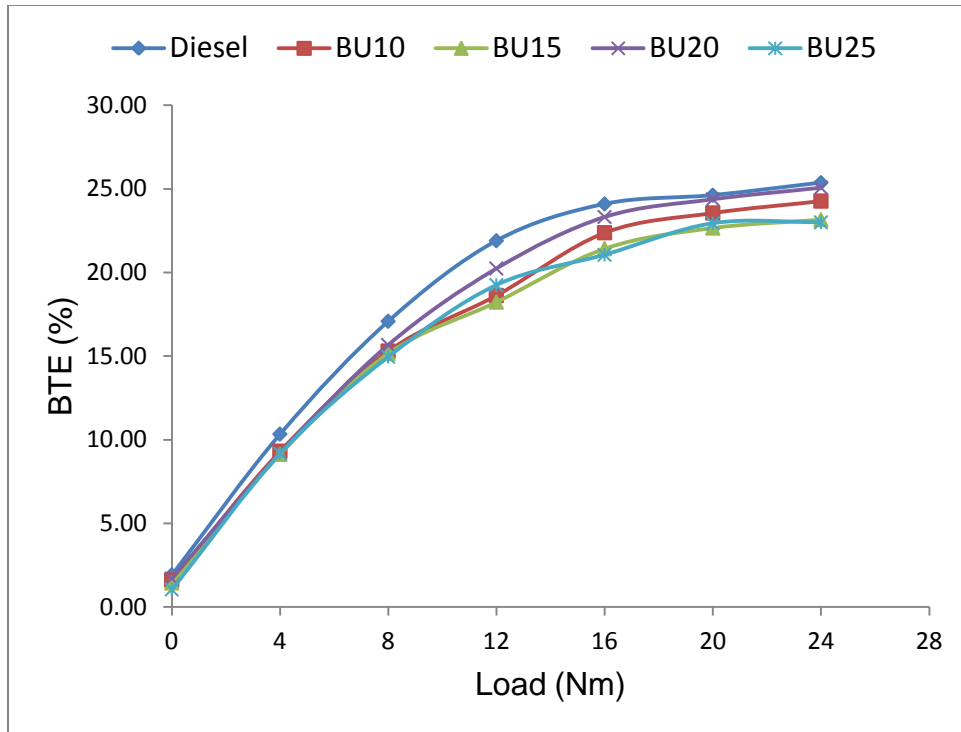


Fig. 4.18 Variation of BTE with engine load for diesel and n-butanol-diesel blends

Fig. 4.19 shows the 3d-surface plot of BTE prediction model for n-butanol-diesel blends. The figure depicts decrement of BTE from blends BU10 to BU15 at full load. From BU15 to BU20, BTE increases and reaches a maximum value near BU20. Increment in BTE for blends from BU15 to BU20 can be attributed to better combustion because of increased oxygen content in fuel and sufficient ignition delay for proper mixing of fuel and oxygen with increasing n-butanol in the blend. On the other hand, the decrement in BTE at BU25 is because of too high ignition delay, which leads to lower mean effective pressure. However, with increasing load, BTE was seen to improve continuously. Fig. 4.20 shows interaction plots for blended fuels. The trends of BTE in fig 4.20 are similar to experimental results (Fig. 4.18) for the whole range of loads and this shows the correctness of predicted models. Fig 4.20 shows that blends give similar performance with respect to each other at minimum and maximum loads.

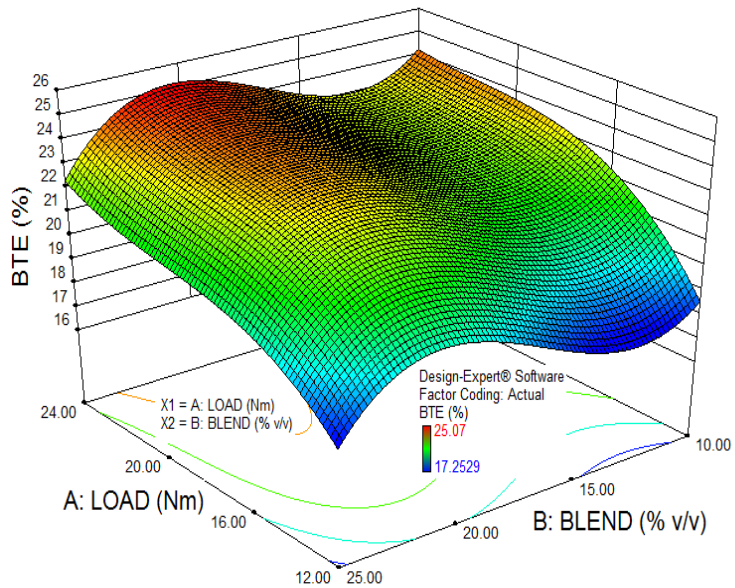


Fig. 4.19 Variation in BTE due to combined effect of load and n-butanol blending

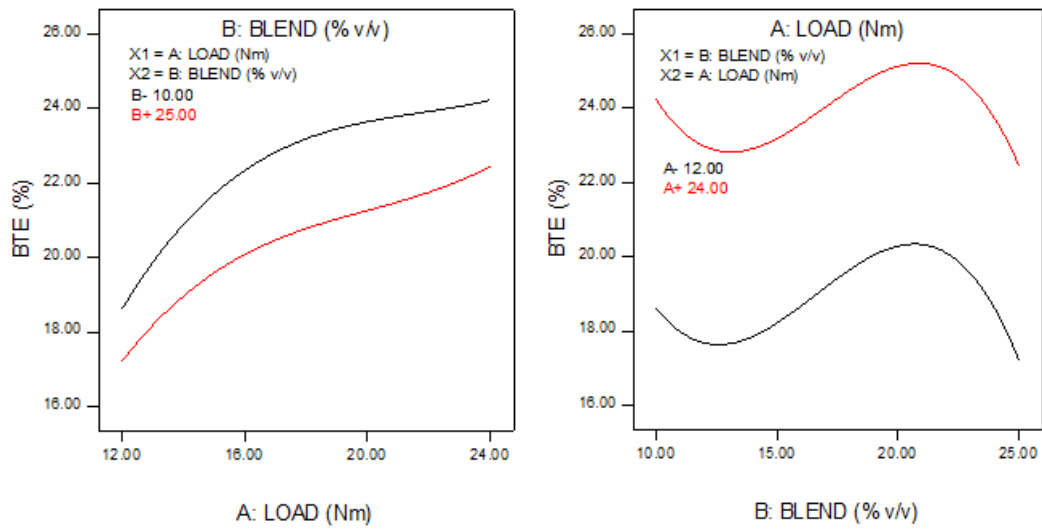


Fig. 4.20 Variation in BTE with load and n-butanol-diesel blends at minimum and maximum values

4.2.5 Emissions of engine using n-butanol blends

4.2.5.1 Variation of Smoke

Figs. 4.21, 4.22 and 4.23 show the variation of smoke emission for n-butanol-diesel blends for experimental results and predicted model.

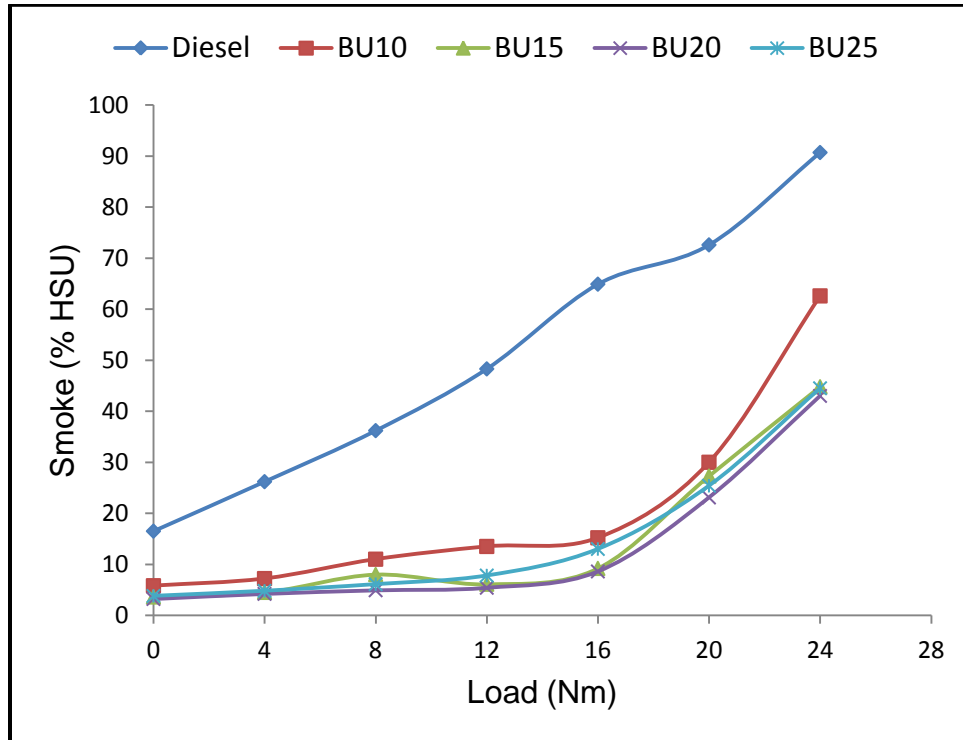


Fig. 4.21 Variation in smoke for n-butanol blends

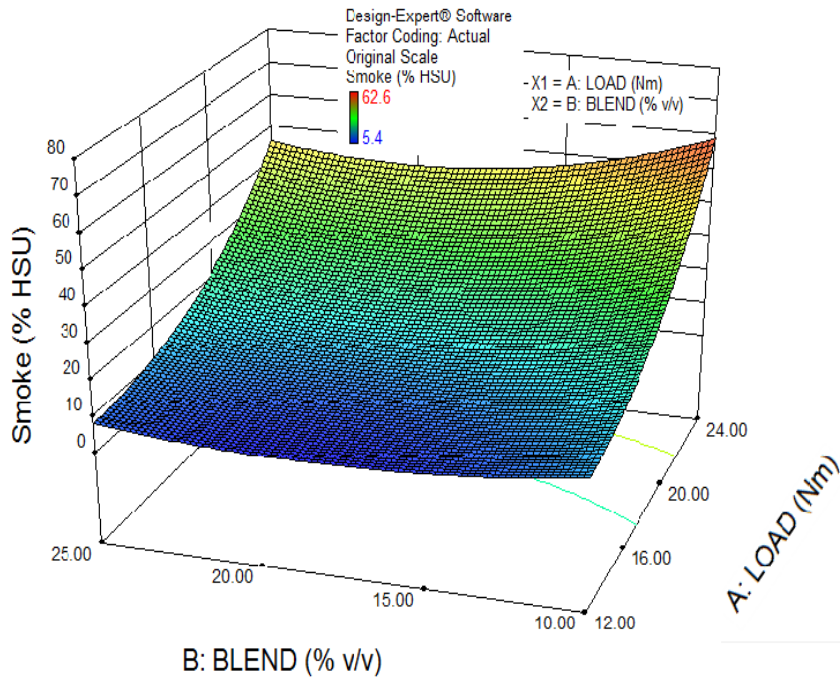


Fig. 4.22 Variation in smoke due to combined effect of load and n-butanol blending

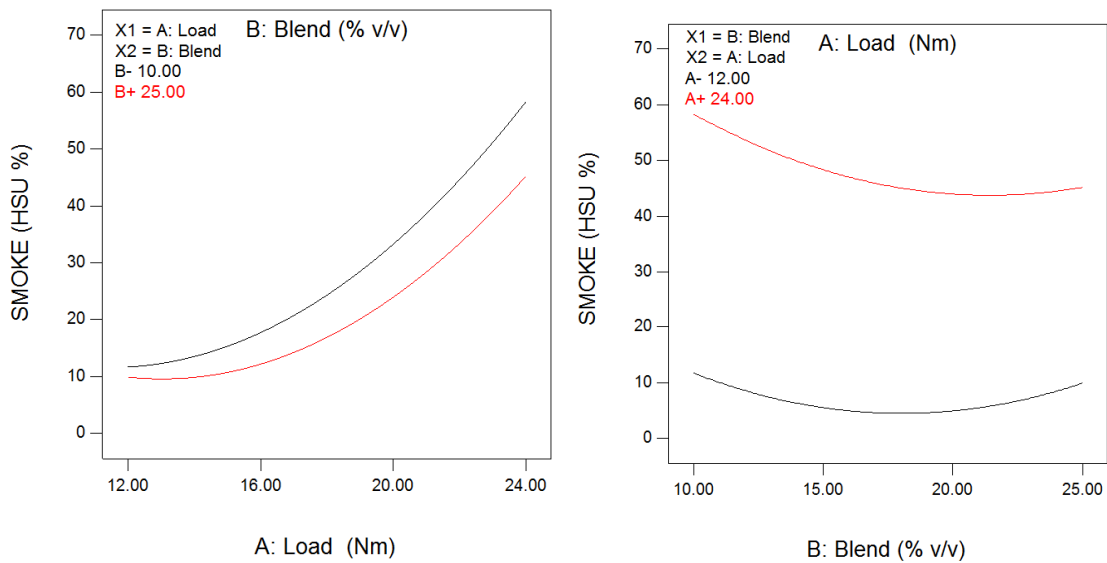


Fig. 4.23 Variation in smoke with load and n-butanol-diesel blends at minimum and maximum values

Significant reduction in smoke was observed from BU10 to BU20 [23][64]. The increased ignition delay which provides sufficient time for fuel-air mixing and better volatility of n-butanol (boiling temp. 118 °C) in comparison to diesel (180-360 °C), enhance the combustion quality. Also, the high content of oxygen in n-butanol provides

enough oxygen in fuel rich zone which is helpful in the oxidation of smoke. While increasing load, smoke increases to the maximum value. At higher loads, temperature is higher, duration of diffusion combustion increased and availability of oxygen is low. All these factors promote thermal decomposition of fuel particles and ultimately resulted in increased smoke [154]. A reduction of 52.59% in smoke emission can be observed from Fig. 4.34 for BU20 compared to that of diesel at full load condition (100% rated power). However, for BU15, the smoke value is quite closer to BU20 at full load condition.

4.2.5.2 Variation of NO_x

Figs. 4.24, 4.25 and 4.26 show the variation of NO_x emission for n-butanol-diesel blends for experimental results and predicted model.

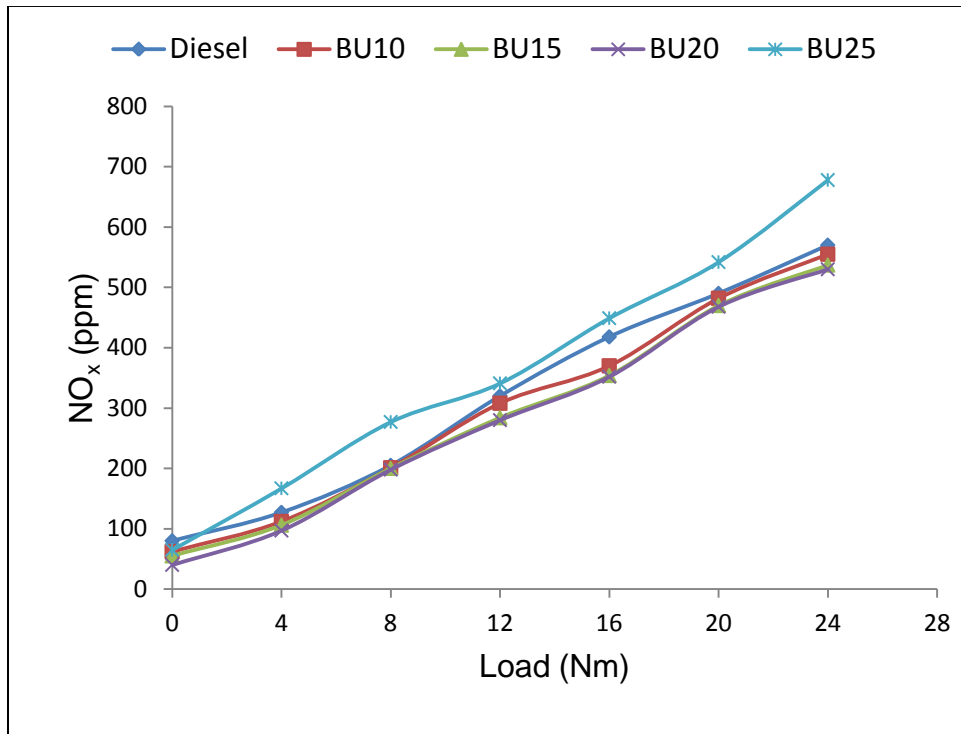


Fig. 4.24 Variation in NO_x for n-butanol blends

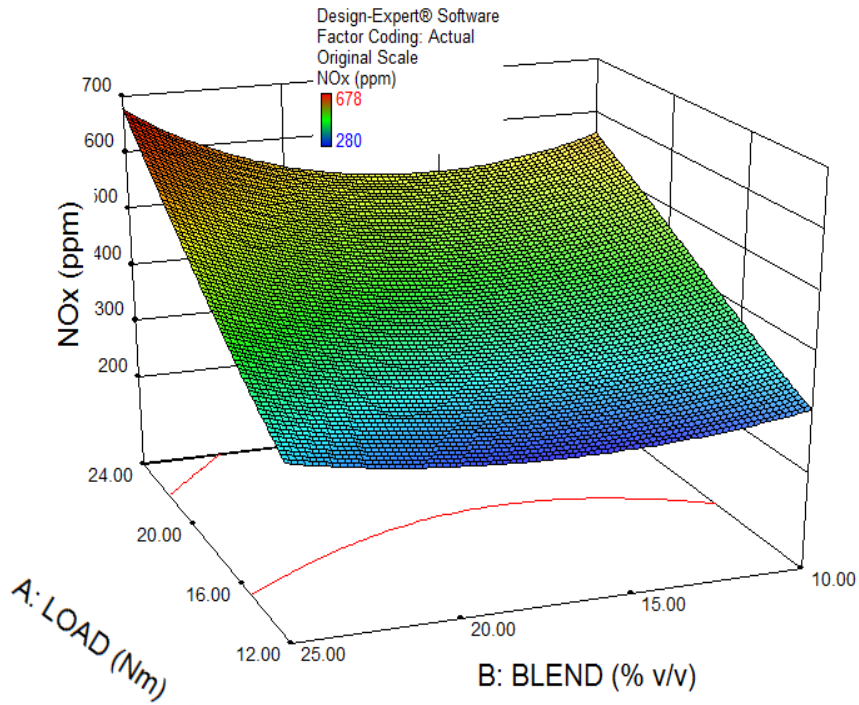


Fig. 4.25 Variation in NO_x due to combined effect of load and n-butanol blending

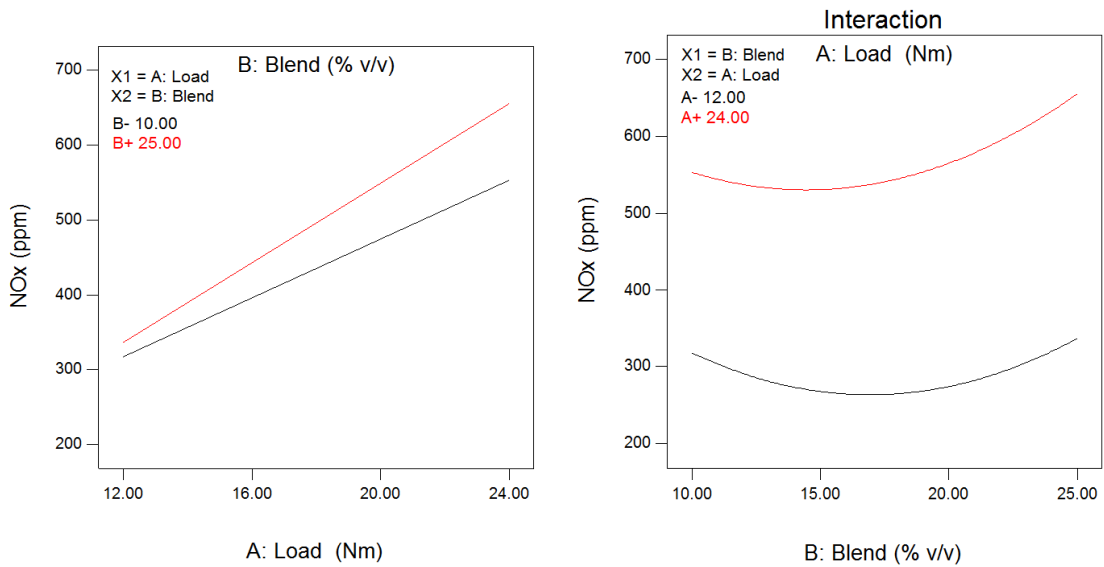


Fig. 4.26 Variation in NO_x with load and n-butanol-diesel blends at minimum and maximum values

Figs. 4.24 and 4.25 show increment in NO_x with load. However, it can also be observed that there is a slightly decreasing trend of NO_x when compared for blends BU10 to BU20 [23]. After BU20, it again increases significantly for BU25. The reduction in NO_x may be justified by two factors. Firstly, the blending of n-butanol in diesel increases the ignition delay period [70], [77] because of low Cetane number and high heat of vaporization of n-butanol. The increased delay allows the fuel to have sufficient time to mix in air and reduces the temperature in the cylinder. The reduction in cylinder temperature results in low NO_x in comparison to diesel. Secondly, better combustion increases the peak temperature, but at the same time, the total span of diffusion combustion and total combustion decreases because of better combustion flame speed. The latter effect seems to be dominant in the case of n-butanol-diesel blends; thus reducing the retention period of peak temperature, which also reduces the NO_x emission [64]. At higher blend (BU25), the ignition delay is too long, making high quantity of fuel available instantly for combustion which results in higher peak temperature and thus an increase in NO_x . It can be observed from Fig. 4.34 that a reduction of 7.01% was achieved in NO_x emission using BU20 as compared to diesel.

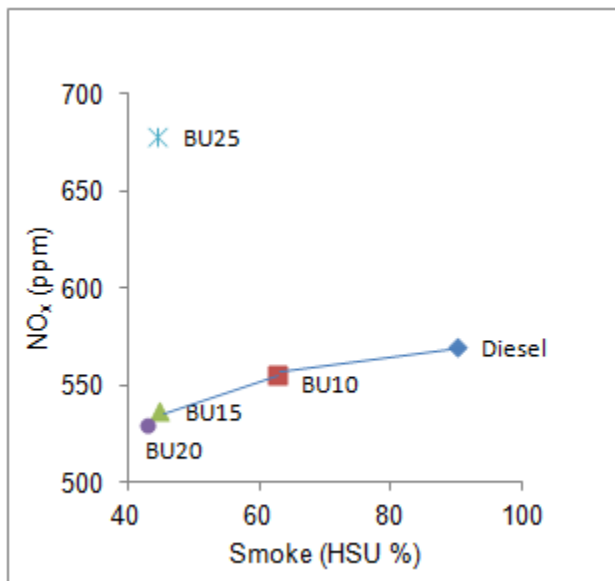


Fig. 4.27 Smoke- NO_x trend for n-butanol diesel blends

Fig. 4.27 shows the Smoke- NO_x relationship with increasing n-butanol percentage in diesel. This trend defeats the general Smoke- NO_x trade-off. However, the rate of

reduction of NO_x is observed to be very low as compared to smoke. As can be observed from the figure, higher blend (BU25) is obviously an outlier in this relationship. There are some previous studies too that support such simultaneous reductions in NO_x and smoke. A few significant studies among these have already been discussed in the introduction (such as [70], [153]).

4.2.5.3 Variation of CO

Figs. 4.28, 4.29 and 4.30 show the variation of CO emission for n-butanol-diesel blends for experimental results and predicted model. Fig. 4.28 shows that emission of CO decreases from BU10 to BU20, but again shows an increase for BU25 [64]. The curves can be seen to retain their respective trends for the whole range of loads.

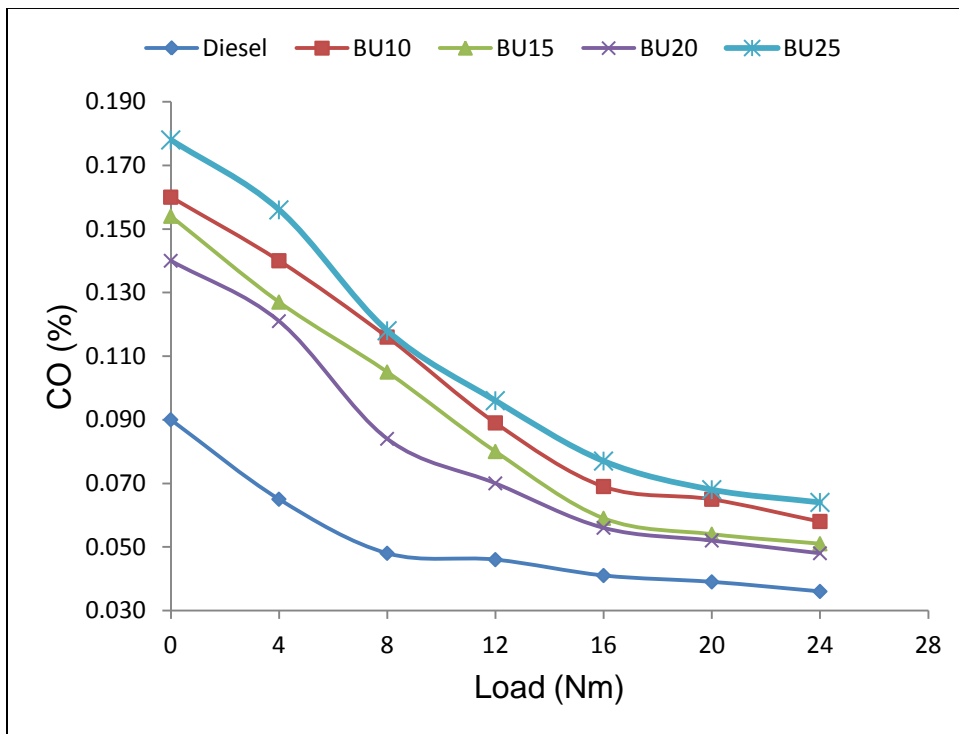


Fig. 4.28 Variation in CO for n-butanol blends

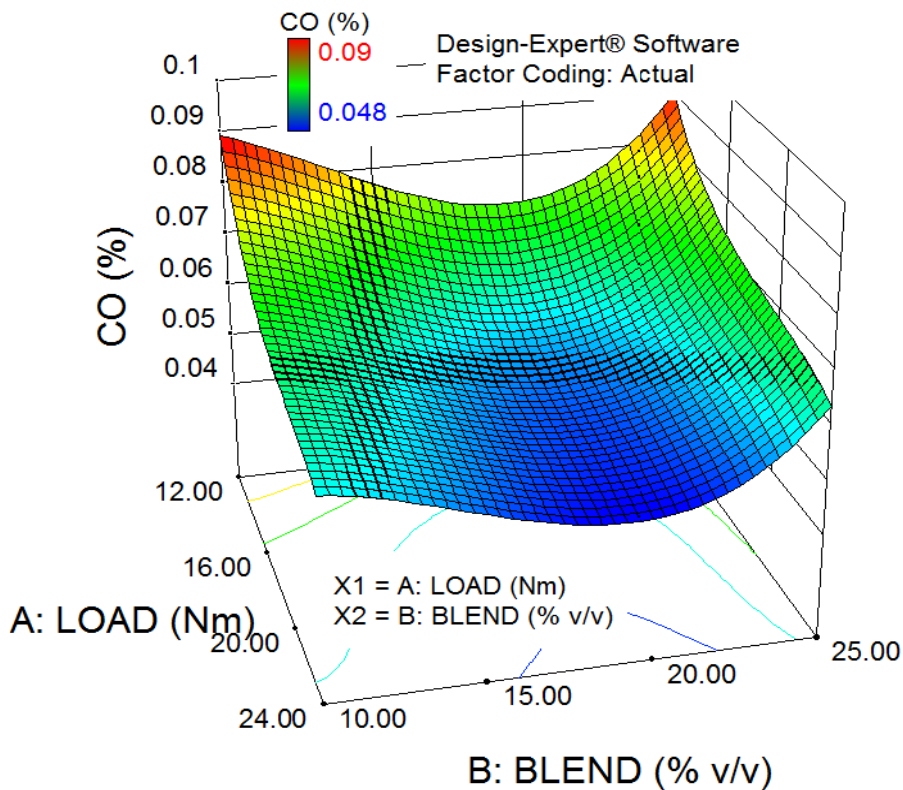


Fig. 4.29 Variation in CO due to combined effect of load and n-butanol blending

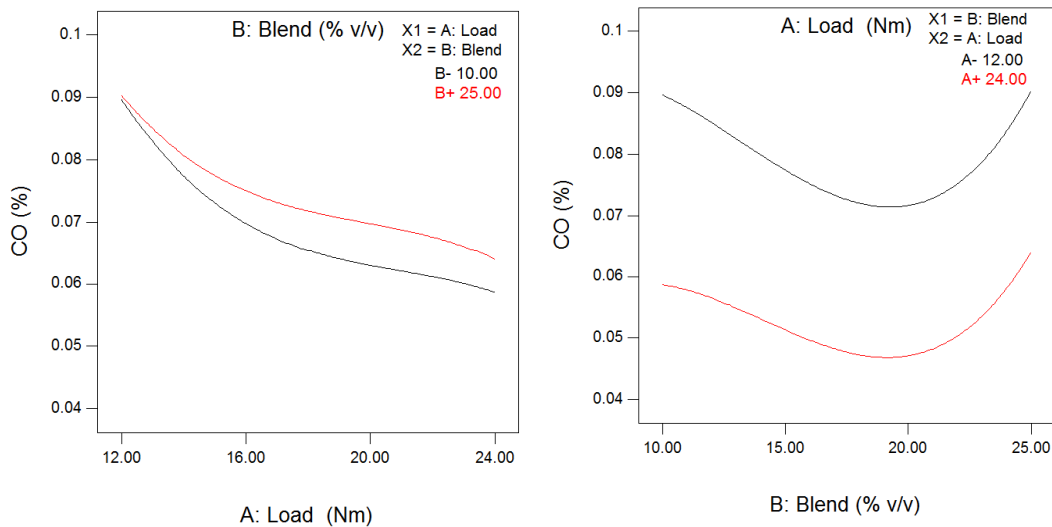


Fig. 4.30 Variation in CO with load and n-butanol-diesel blends at minimum and maximum values

Fig. 4.29 and 4.30 show CO emission using n-butanol-diesel blends for predicted model. It can be observed that with the increasing load, CO decreases and with increased

blending of n-butanol in diesel, CO decreases initially and then increases afterward. The trends of CO are decreasing for BU10 to BU20 and then increasing for BU25. From Fig. 4.34 an increment of 33.33% of CO emission can be noted for BU20 in comparison to diesel at maximum load condition (100% rated power).

4.2.5.4 Variation of HC

Figs. 4.31, 4.32 and 4.33 show the variations of HC emission for n-butanol-diesel blends for experimental results and predicted model.

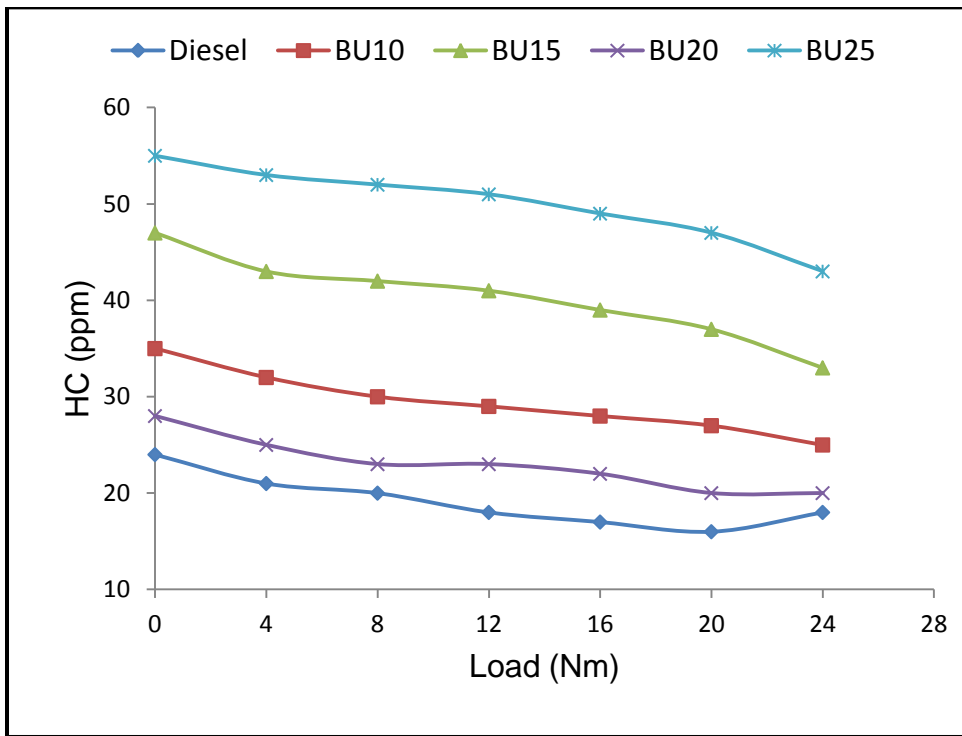


Fig. 4.31 Variation in HC for n-butanol blends

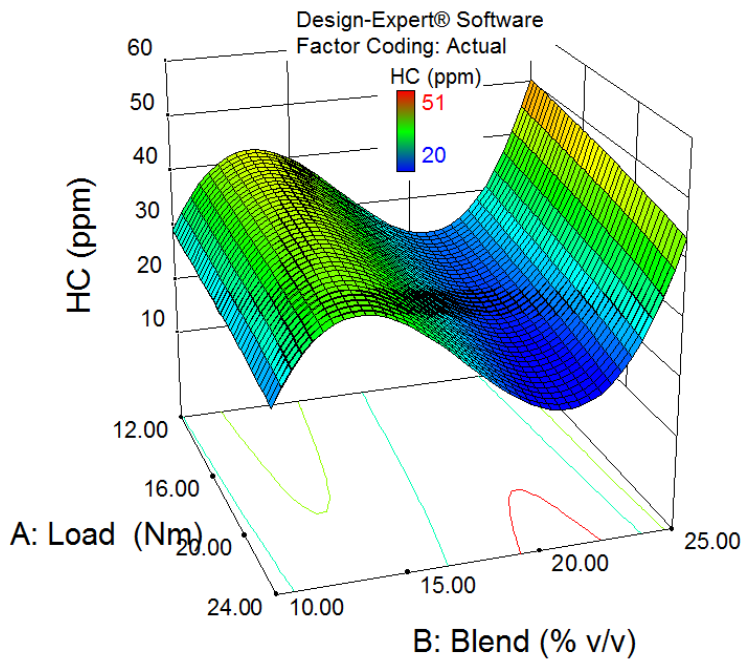


Fig. 4.32 Variation in HC due to combined effect of load and n-butanol blending

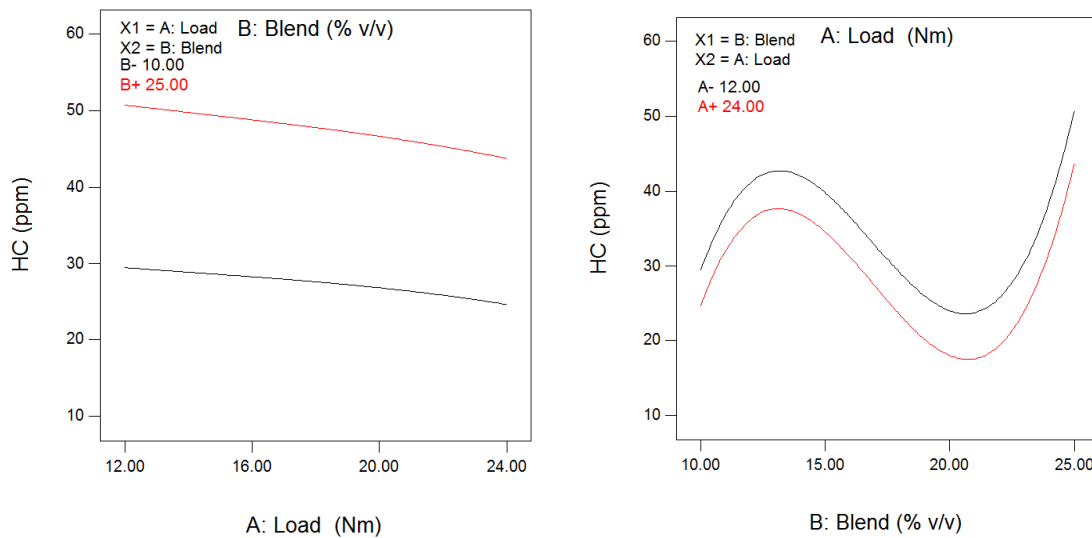


Fig. 4.33 Variation in HC with load and n-butanol-diesel blends at minimum and maximum values

It can be observed from Figs. 4.31 and Fig.4.32 that the emission of HC increases from BU10 to BU15 then reduces at BU20, and again increases to a maximum value for BU25 [23][64]. However, the emission of HC for all blends is higher compared to that of diesel (Fig. 4.34). Late combustion due to longer ignition delay and low boiling point may be

the reasons of higher HC emission. Because of low boiling temperature of n-butanol, the amount of fuel boiling off from the injector during exhaust stroke increases and this in turn increases the unburned HC. Expansion of lean flame-out region due to increased oxygen in fuel is another cause of increased unburned HC[70], [153]. Fayad et al. [104] reported that the butanol content is thermally decomposed into light HC species, and at the exhaust of engine, the concentration of HC species for BU20 are different from diesel. This may be another reason of increase in HC with n-butanol-diesel blends. On the whole, the total HC increment is judged to be the combined effect of unburned HC and HC produced during combustion reactions. An increment of 17.64 % in HC can be observed from Fig. 4.34 for BU20 compared to that of diesel. Most of the studies cited in the introduction are consistent with this result (i.e. increased HC).

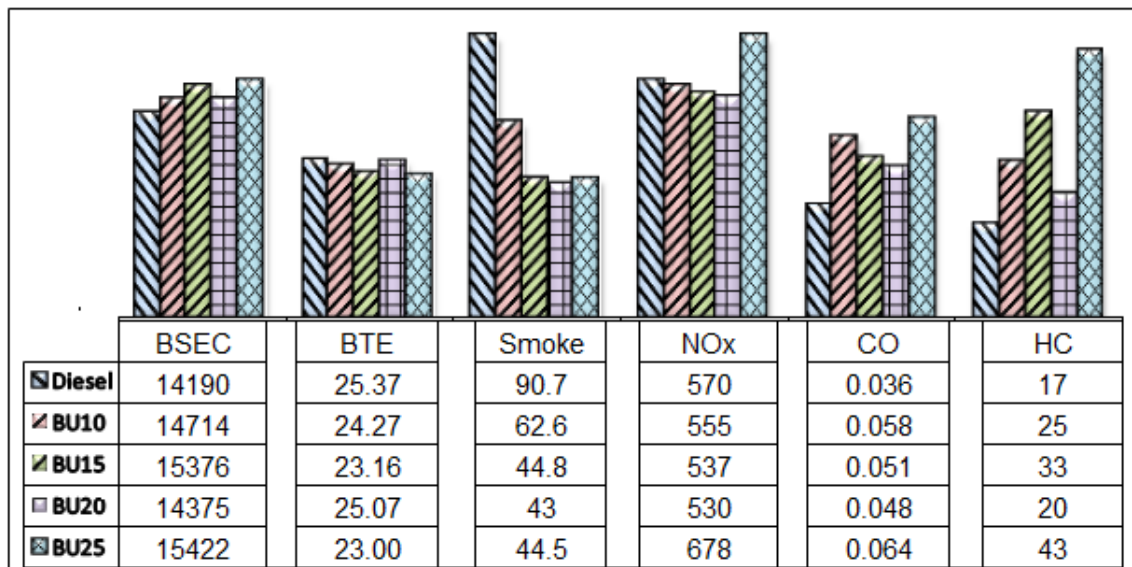


Fig. 4.34 Performance and emission of n-butanol diesel blends (100% rated power)

4.2.6 Validation and optimization of responses

The parameters are optimized for desired values of responses. Table 4.13 summarizes the minimum and maximum values of each response to optimize operating parameters of the engine. On the basis of Table 4.13 and optimization analysis, the optimum blended fuel and their predicted responses were obtained, and are shown in Table 4.14. The test was repeated on full load (24.0 kN) and very near to optimum value of blend (20% n-butanol in diesel) to validate the results predicted by the models. The optimum values of BSFC, BTE, smoke, NO_x, CO and HC were observed to be 0.348, 25.07, 43.28, 530, 0.048 and

20 respectively at full load condition. It can be observed from Table 4.14 that the percentage errors of these results are within tolerance. This shows the exactness of prediction model. On the basis of the validation of experimental results by mathematical modeling, BU20 was selected as the optimum blend of n-butanol with diesel.

Table 4.13 Maximum and minimum limits for each response to optimize performance and emissions

Names	Goal	Lower limit	Upper limit
A: Torque	Is in range	12	24
B: Blend	Is in range	10	25
Response: BSFC	Minimize	0.34982	0.47949
Response: BTE	Maximize	17.2529	25.07
Response: Smoke	Minimize	5.4	62.6
Response: NO _x	Minimize	280	678
Response: CO	Minimize	0.048	0.09
Response: HC	Minimize	20	51

Table 4.14 Optimum conditions of load and blend and their predicted results

Number	Load	Blend	BSFC	BTE	Smoke	NO _x	CO	HC	
1	<u>24.00</u>	<u>19.558</u>	<u>0.346</u>	<u>24.889</u>	<u>44.375</u>	<u>554.383</u>	<u>0.047</u>	<u>20.000</u>	<u>Selected</u>
2	16.367	20.001	0.374	23.419	9.243	379.879	0.055	22.260	
3	17.037	10.000	0.373	22.845	20.821	416.333	0.067	27.891	
4	17.245	10.000	0.372	22.929	21.522	420.412	0.067	27.822	
Confirmation test	24.00	20.00	0.348	25.07	43.28	530	0.048	20	
Error Percentage (× 100)			-0.578	-0.727	2.468	4.398	-2.128	0.00	

4.3 Optimization of engine operating parameters for BU20 (Third Phase):

After selection of BU20 as the fuel for further investigation, in the third stage of experimentations, the engine was optimized for compression ratio, injection timing, and injection pressure. The first set of tests was conducted for compression ratios ranging from 17.5 to 20.5, at constant injection timing of 23°CA btdc and 210 bar injection pressure. From the resulting observations, 19.5 CR was selected as optimum for BU20.

The second set of tests was conducted with retarded injection timing of 21°CA btdc and advanced injection timing of 25°CA btdc at optimized CR of 19.5 and at 210 bar injection pressure. The readings were compared with data of 19.5 CR, 23°CA btdc and 210 bar injection pressure. The 23°CA btdc setting was found optimum for BU20 at 19.5 CR and 210 bar injection pressure.

The third set of tests was conducted with injection pressures of 200 and 220 bar at optimized CR of 19.5 and injection timing of 23°CA btdc. These data were compared with data on 210 bar injection pressure, 19.5 CR and 23°CA btdc. The 210 bar injection pressure setting was found optimum at 19.5 CR and at 23°CA btdc.

The results of these experiments are shown in Figs. 4.41 to 4.50. Figs. 4.41 to 4.43 show engine performance characteristics and Figs. 4.44 to 4.50 show emission characteristics for different CRs, injection timings and injection pressures.

4.3.1 Development of prediction models with BU20

The prediction models were developed for BSFC, BTE, smoke, NO_x, CO and HC in terms of compression ratio (CR), injection timing (Inj. T.) and injection pressure (Inj. Pr.). The selected data from experiments conducted with the optimized blend (BU20) (as obtained in previous stage) was fed to DOE-Design Expert software. Full factorial design was used for the development of prediction model and optimization of engine operating parameters for the desired values of responses. Table 4.15 shows the engine operating parameters and their levels, and Table 4.16 shows the design matrix for the selected experiments according to full factorial design.

Table 4.15 Parameters and their levels according to Factorial design for BU20

Parameter	symbol	Type	Levels			
			1	2	3	4
CR	A (CR)	Numeric	17.5	18.5	19.5	20.5
Injection Pressure (bar)	B (Inj. T.)	Numeric	21	23	25	
Injection Timing (CA btdc)	C (Inj. Pr.)	Numeric	200	210	220	

Table 4.16 Design layout and experimental results for BU20

Blend	Run	Factor	Factor	Factor	Response	Response	Response	Response	Response	Response
		1	2	3	1	2	3	4	5	6
		A: CR	B: Inj.T. (CA btdc)	C:Inj.Pr. (bar)	BSFC (kg/kW-h)	BTE (%)	SMOKE (HSU %)	NOx (ppm)	CO (%)	HC (ppm)
BU20	15	17.5	21	200	0.370	18.4	96.45	534	0.038	45
	14	18.5	21	200	0.360	19.5	77.0	519	0.036	42
	28	19.5	21	200	0.358	19.12	68.7	517	0.033	28
	33	20.5	21	200	0.378	18.6	87.2	545	0.049	36
	24	17.5	23	200	0.365	20.42	79.6	510	0.036	38
	30	18.5	23	200	0.372	21.8	60.1	505	0.035	26
	11	19.5	23	200	0.370	22.26	54.5	501	0.033	24
	2	20.5	23	200	0.380	21.7	78.4	530	0.048	25
	7	17.5	25	200	0.380	18.9	84.3	510	0.040	43
	26	18.5	25	200	0.380	20.98	68.3	518	0.039	32
	17	19.5	25	200	0.375	21.31	59.6	514	0.035	26
	20	20.5	25	200	0.410	20.44	83.5	542	0.051	30
	31	17.5	21	210	0.350	19.12	88.15	529	0.036	40
12	18.5	21	210	0.370	19.75	65.3	516	0.034	38	

6	19.5	21	210	0.380	19.92	61.3	512	0.032	24
18	20.5	21	210	0.390	19.13	83.3	530	0.041	32
8	17.5	23	210	0.360	22.2	71.7	510	0.033	37
13	18.5	23	210	0.350	25.07	43.0	498	0.032	20
23	19.5	23	210	0.340	25.8	42.0	492	0.032	18
34	20.5	23	210	0.380	24.12	65.13	525	0.039	20
25	17.5	25	210	0.370	21.3	72.35	521	0.038	40
36	18.5	25	210	0.392	21.86	49.5	513	0.036	30
32	19.5	25	210	0.390	22.5	47.0	516	0.034	22
5	20.5	25	210	0.420	22.12	75.3	540	0.043	25
19	17.5	21	220	0.360	17.8	92.52	565	0.033	41
3	18.5	21	220	0.382	18.1	73.89	561	0.032	41
9	19.5	21	220	0.380	18.32	75.6	558	0.029	26
35	20.5	21	220	0.424	17.8	87.8	573	0.039	34
10	17.5	23	220	0.390	20.56	75.23	555	0.031	38
21	18.5	23	220	0.385	21.84	58.25	547	0.031	24
4	19.5	23	220	0.380	21.95	54.6	541	0.030	20
1	20.5	23	220	0.430	21.0	70.23	562	0.037	22
29	17.5	25	220	0.430	19.8	77.23	585	0.035	39
27	18.5	25	220	0.420	20.63	62.3	581	0.034	31
22	19.5	25	220	0.400	20.9	58.2	575	0.033	23
16	20.5	25	220	0.430	19.7	75.3	620	0.038	23

4.3.1.1 Diagnosis of data for analysis of variance for BU20

The results obtained from the experiments as per the experimental plan are shown in Table 4.16. These results were used for further analysis. Figs. 4.35 to 4.40 show plots of normal probability vs. Internal studentized residuals and internal studentized residuals vs. predicted values for BSFC, BTE, smoke, NO_x , CO and HC emissions respectively when the engine was operated on n-butanol-diesel blends.

In normal probability plots, it can be observed that points are accumulated along a straight line which implies that residuals follow the normal distribution and hence, the fitted model is adequate for real systems. The internal residuals vs. predicted plots show no obvious patterns thus indicating the validity assumption of ANOVA to be true. It is projected that for all the responses, the variance of the observed data is constant and hence is satisfactory.

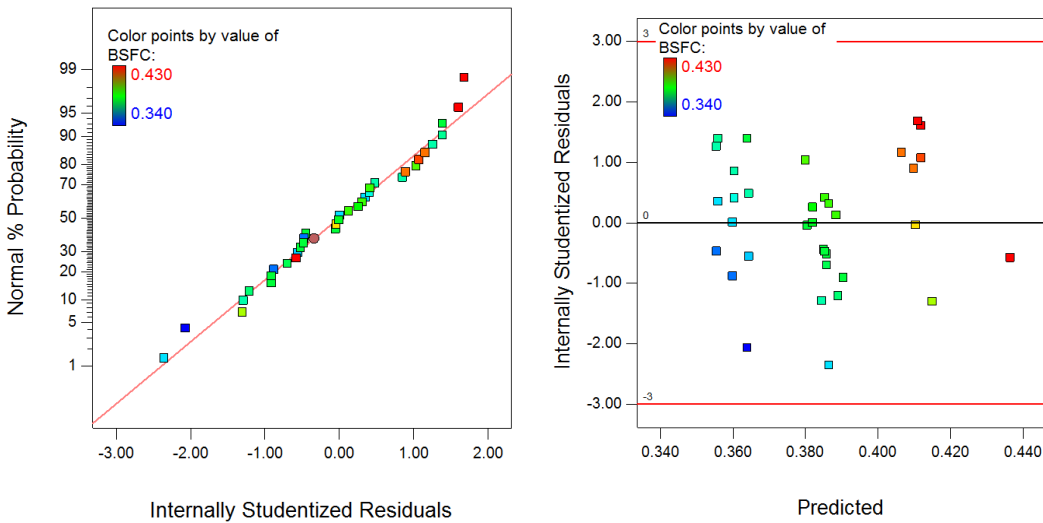


**Fig. 4.35 (a) Plot of normal % probability vs. Internal studentized residuals for BSFC
(b) Plot of internal studentized residuals vs. predicted response for BSFC**

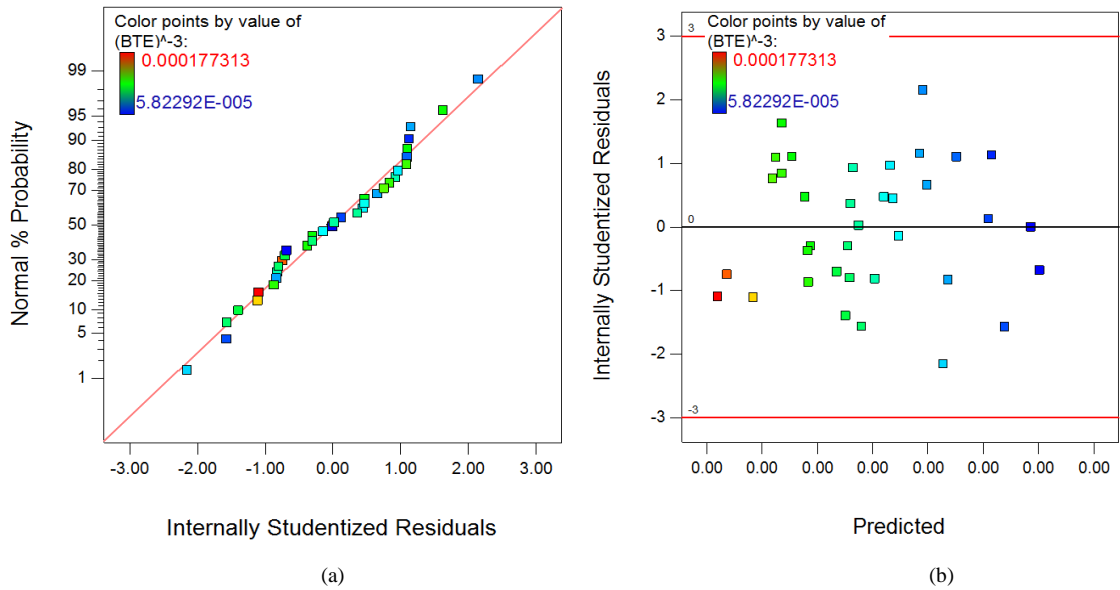


**Fig. 4.36 (a) Plot of normal % probability vs. Internal studentized residuals for BTE
 (b) Plot of internal studentized residuals vs. predicted response for BTE**

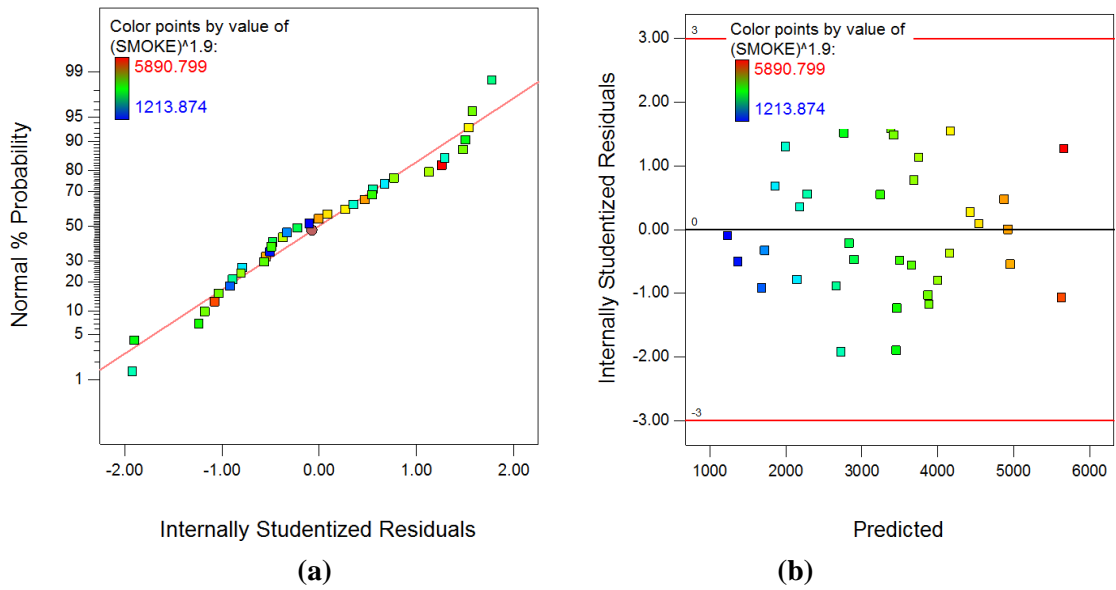
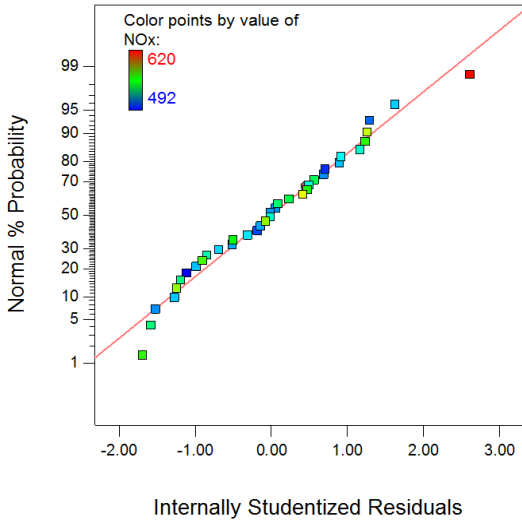
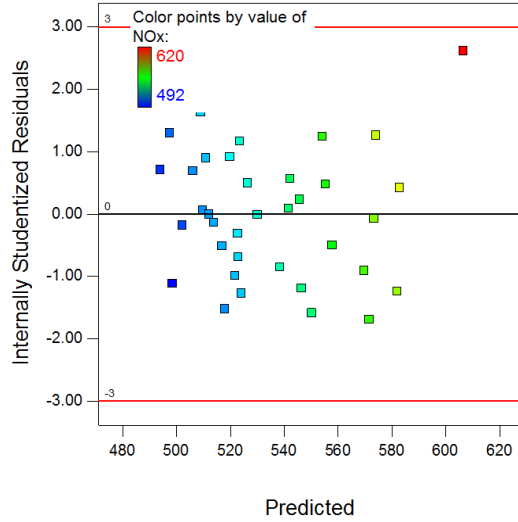


**Fig. 4.37 (a) Plot of normal % probability vs. Internal studentized residuals for smoke
 (b) Plot of internal studentized residuals vs. predicted response for smoke**

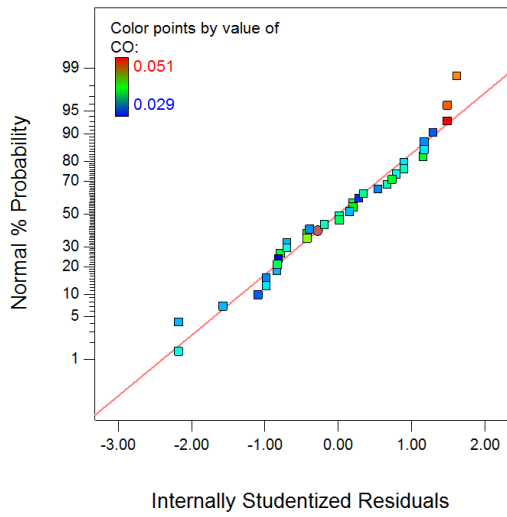


(a)

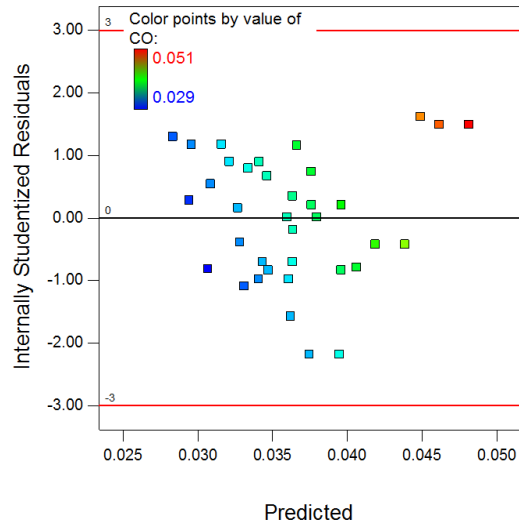


(b)

**Fig. 4.38 (a) Plot of normal % probability vs. Internal studentized residuals for NO_x
 (b) Plot of internal studentized residuals vs. predicted response for NO_x**



(a)



(b)

**Fig. 4.39 (a) Plot of normal % probability vs. Internal studentized residuals for CO
 (b) Plot of internal studentized residuals vs. predicted response for CO**

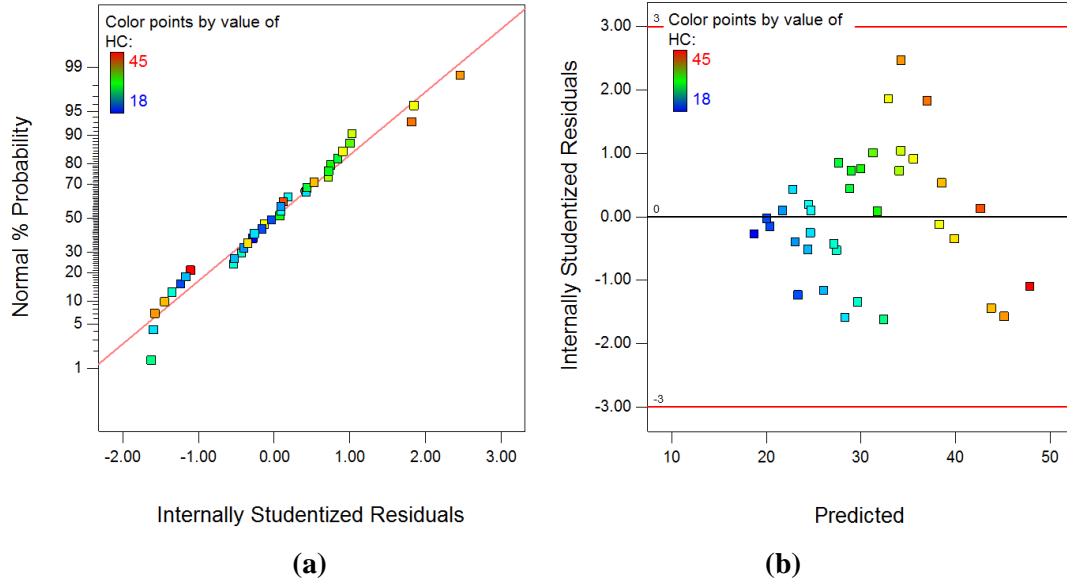


**Fig. 4.40 (a) Plot of normal % probability vs. Internal studentized residuals for HC
(b) Plot of internal studentized residuals vs. predicted response for HC**

4.3.1.2 ANOVA for response surface model for BU20

Tables 4.17 to 4.22 are ANOVA tables for the response surface prediction models of BSFC, BTE, smoke, NO_x , CO and HC respectively by selecting the backward elimination procedure to remove the terms that are not significant. In the present work, ANOVA analysis was carried out for a significance level of $\alpha = 0.05$, i.e. for a confidence level of 95%.

Table 4.17 presents the ANOVA for Response Surface Quadratic model for BSFC. The obtained F-value of 15.63 for the model implies that it is significant. There is only a 0.01% chance that an F-value this large could occur due to noise. In the Table, the value of “Prob. > F” for model is 0.0001, which is less than 0.05, indicating that the model is significant, i.e. the terms in the model have a significant effect on BSFC. In the same manner, the values of “Prob. > F” for main effect of CR, Injection Timing (Inj.T.) and Injection Pressure (Inj. Pr.), second order effect of CR, injection timing and injection pressure were also found to be less than 0.05. So these terms are also significant model terms. The R-Squared (R^2) value is 0.7638. The Pred- R^2 is also 0.6356 which is in reasonable agreement with the Adj- R^2 of 0.7149; i.e. the difference is less than 0.2. For the developed BTE model, the value of Adequate Precision is 12.800, which shows high precision of the model. This model can be used to navigate the design space. The final

empirical model for BTE in terms of coded and actual factors is given by Eqs. 4.13 and 4.14 respectively.

$$BSFC=0.358049 + 0.0127167 \times A + 0.0122917 \times B + 0.0130417 \times C + 0.0145625 \times A^2 + 0.0122917 \times B^2 + 0.0135417 \times C^2 \quad (4.13)$$

$$BSFC = 9.71566 -0.237467 \times CR -0.135208 \times Inj.T.-0.0555708 \times Inj.Pr. + 0.00647222 \times CR^2 + 0.00307292 \times Inj.T.^2 + 0.000135417 \times Inj.Pr.^2 \quad (4.14)$$

Table 4.17 Reduce analysis of variance and interaction fit for BSFC response.

Source	Sum of Squares	degree of freedom	Mean Square	F-Value	p-value Prob > F
Model	0.015	6	2.521E-003	15.63	< 0.0001
A-CR	3.234E-003	1	3.234E-003	20.05	0.0001
B-Inj.T.	3.626E-003	1	3.626E-003	22.48	< 0.0001
C-Inj.Pr.	4.082E-003	1	4.082E-003	25.30	< 0.0001
A ²	1.508E-003	1	1.508E-003	9.35	0.0048
B ²	1.209E-003	1	1.209E-003	7.49	0.0105
C ²	1.467E-003	1	1.467E-003	9.09	0.0053
Residual	4.678E-003	29	1.613E-004		
Cor Total	0.020	35			
Std. Dev.	0.013		R-Squared		0.7638
Mean	0.38		Adj R-Squared		0.7149
C.V. %	3.31		Pred R-Squared		0.6356
PRESS	7.216E-003		Adeq Precision		14.474

Table 4.18 presents the ANOVA for Response Surface Quadratic model for BTE. From the table, it is clear that the values of “Prob. > F” for the model, the main effect of CR, injection timing, injection pressure and interaction effect of CR and injection pressure, injection pressure and injection timing, second order effect of CR, injection timing and injection pressure are all less than 0.05. So these terms are significant model terms. The R² value is equal to 0.9734. Table 4.18 shows that Pred-R² of 0.9514 is in reasonable agreement with the Adj-R² of 0.9656; i.e. the difference is less than 0.2. For the developed BTE model, the value of Adequate Precision is 40.784, which shows high precision of the model. The final empirical model for BTE in terms of coded and actual factors is given by Eqs. 4.15 Eq. 4.16 respectively.

$$BTE = 6.35893e-005 - 5.12868e-006 \times A - 2.01123e-005 \times B + 4.55651e-006 \times C + 3.56644e-006 \times AC - 5.36465e-006 \times BC + 1.84161e-005 \times A^2 + 4.00169e-005 \times B^2 + 2.68245e-005 \times C^2 \quad (4.15)$$

$$BTE = 0.0199939 + -0.000364377 \times CR - 0.000413921 \times Inj.T. - 0.000110556 \times Inj.Pr. + 2.37763e-007 \times CR \times Inj.Pr. - 2.68233e-007 \times Inj.T. \times Inj.Pr. + 8.18494e-006 \times CR^2 + 1.00042e-005 \times Inj.T.^2 + 2.68245e-007 \times Inj.Pr.^2 \quad (4.16)$$

Table 4.18 Reduce analysis of variance and interaction fit for BTE response

Source	Sum of Squares	Degree of Freedom	Mean Square	F-Value	p-value Prob. > F
Model	3.23E-08	8	4.04E-09	123.8264	0.0001
A-CR	5.26E-10	1	5.26E-10	16.11325	0.0004
B-Inj. T.	9.71E-09	1	9.71E-09	297.356	0.0001
C-Inj.Pr.	4.98E-10	1	4.98E-10	15.26225	0.0006
AC	1.7E-10	1	1.7E-10	5.194603	0.0308
BC	4.6E-10	1	4.6E-10	14.10411	0.0008
A ²	2.41E-09	1	2.41E-09	73.8714	0.0001
B ²	1.28E-08	1	1.28E-08	392.3911	0.0001
C ²	5.76E-09	1	5.76E-09	176.3182	0.0001
Residual	8.81E-10	27	3.26E-11		
Cor. Total	3.32E-08	35			
Std. Dev.	5.71E-06		R-Squared		0.9734
Mean	0.000118		Adj R-Squared		0.9656
C.V. %	4.826641		Pred R-Squared		0.9514
PRESS	1.62E-09		Adeq Precision		40.784

Table 4.19 presents the ANOVA for Response Surface Quadratic model for smoke. Table shows that the values of “Prob. > F” for model, main effect of CR, injection timing, injection pressure and interaction effect of CR and injection timing, injection pressure

and injection timing, second order effect of CR, injection timing and injection pressure are all less than 0.05. So these terms are significant model terms. The R^2 value is equal to 0.973. The table also shows that Pred- R^2 of 0.952 is in reasonable agreement with the Adj- R^2 of 0.965; i.e. the difference is less than 0.2. For the developed smoke model, the value of Adequate Precision is 40.168, which shows high precision of the model. The final empirical models for smoke (after transformation) in terms of coded and actual factors are given by Eqs. 4.17 and 4.18 respectively.

$$(Smoke)^{1.9} = 1084.5 - 205.04 \times A - 539.987 \times B - 143.591 \times C + 147.679 \times AB - 127.234 \times BC + 1956.9 \times A^2 + 943.18 \times B^2 + 772.476 \times C^2 \quad (4.17)$$

$$(Smoke)^{1.9} = 783063 - 34318.7 \times CR - 10715.9 \times Inj.T. - 3112.44 \times Inj.Pr. + 49.2264 \times CR \times Inj.T. - 6.3617 \times Inj.T. \times Inj.Pr. + 869.732 \times CR^2 + 235.795 \times Inj.T.^2 + 7.72476 \times Inj.Pr.^2 \quad (4.18)$$

Table 4.19 Reduce analysis of variance and interaction fit for smoke response.

Source	Sum of Squares	Degree of Freedom	Mean Square	F-Value	p-value Prob. > F
Model	48005620	8	6000703	123.200	0.0001
A-CR	840831.2	1	840831.2	17.263	0.0003
B-Inj.T.	6998057	1	6998057	143.677	0.0001
C-Inj.Pr.	494842.3	1	494842.3	10.160	0.0036
AB	290788.2	1	290788.2	5.970	0.0214
BC	259015.5	1	259015.5	5.318	0.0290
A ²	27231630	1	27231630	559.093	0.0001
B ²	7116701	1	7116701	146.113	0.0001
C ²	4773756	1	4773756	98.010	0.0001
Residual	1315084	27	48706.83		
Cor Total	49320705	35			
Std. Dev.	220.6962		R-Squared		0.973
Mean	3315.436		Adj R-Squared		0.965
C.V. %	6.656629		Pred R-Squared		0.952
PRESS	2368948		Adeq Precision		40.168

Table 4.20 presents the ANOVA for Response Surface Quadratic model for NO_x. Table shows that the value of “Prob. > F” for model, main effect of CR, injection timing, injection pressure and interaction effect of CR and injection timing, injection pressure and injection timing, second order effect of CR, injection timing and injection pressure are all less than 0.05. So these terms are significant model terms. The R² value is equal to 0.962. The table also shows that Pred-R² of 0.930 is in reasonable agreement with the Adj-R² of 0.951; i.e. the difference is less than 0.2. For the developed NO_x model, the value of Adequate Precision is 35.305, which shows high precision of the model. The final empirical models for smoke in terms of coded and actual factors are given by Eqs. 4.19 and 4.20 respectively.

$$NO_x = 494.069 + 6.86667 \times A + 3.16667 \times B + 24.0833 \times C + 5 \times AB + 8.4375 \times BC + 18.875 \times A^2 + 18.4167 \times B^2 + 27.6667 \times C^2 \quad (4.19)$$

$$NO_x = 20295.9 - 352.533 \times CR - 330.469 \times Inj.T. - 123.495 \times Inj.Pr. + 1.66667 \times CR \times Inj.T. + 0.421875 \times Inj.T. \times Inj.Pr. + 8.38889 \times CR^2 + 4.60417 \times Inj.T.^2 + 0.276667 \times Inj.Pr.^2 \quad (4.20)$$

Table 4.20 Reduce analysis of variance and interaction fit for NO_x response.

Source	Sum of Squares	Degree of Freedom	Mean Square	F-Value	p-value Prob. > F
Model	27946.64	8	3493.33	85.700	0.0001
A-CR	943.02	1	943.02	23.135	0.0001
B-Inj.T.	240.67	1	240.67	5.904	0.0220
C-Inj.Pr.	13920.17	1	13920.17	341.496	0.0001
AB	333.33	1	333.33	8.177	0.0081
BC	1139.06	1	1139.06	27.944	0.0001
A ²	2533.44	1	2533.44	62.152	0.0001
B ²	2713.39	1	2713.39	66.566	0.0001
C ²	6123.56	1	6123.56	150.226	0.0001
Residual	1100.58	27	40.76		
Cor Total	29047.22	35			
Std. Dev.	6.38		R-Squared		0.962
Mean	535.28		Adj R-Squared		0.951
C.V. %	1.19		Pred R-Squared		0.930
PRESS	2030.81		Adeq Precision		35.305

Table 4.21 presents the ANOVA for Response Surface Quadratic model for CO. Table shows that the value of “Prob. > F” for model, main effect of CR, injection timing, injection pressure and interaction effect of CR and injection pressure, second-order effect of CR and injection timing are all less than 0.05. So these terms are significant model terms. The R² value is equal to 0.8416. The Table also shows that Pred-R² of 0.7549 is in reasonable agreement with the Adj-R² of 0.8088; i.e. the difference is less than 0.2. For the developed NO_x model, the value of Adequate Precision is 19.995, which shows high precision of the model. The final empirical models for smoke in terms of coded and actual factors are given by Eqs. 4.21 and 4.22 respectively.

$$CO = 0.0311042 + 0.00295 * A + 0.001 * B - 0.00295833 * C - 0.001325 * AC + 0.0065625 * A^2 + 0.00225 * B^2 \quad (4.21)$$

$$CO = 1.04239 + -0.0903167 * CR - 0.025375 * Inj.T. + 0.0013825 * Inj.Pr. - 8.83333e-005 * CR * Inj.Pr. + 0.00291667 * CR^2 + 0.0005625 * Inj.T.^2 \quad (4.22)$$

Table 4.21 Reduce analysis of variance and interaction fit for CO response

Source	Sum of Squares	degree of freedom	Mean Square	F Value	p-value Prob > F
Model	7.782E-004	6	1.297E-004	25.68	< 0.0001
A-CR	1.488E-004	1	1.488E-004	29.45	< 0.0001
B-Inj.T.	3.893E-005	1	3.893E-005	7.71	0.0095
C-Inj.Pr.	1.583E-005	1	1.583E-005	3.13	0.0872
AC	2.341E-005	1	2.341E-005	4.63	0.0398
A ²	3.062E-004	1	3.062E-004	60.62	< 0.0001
B ²	4.050E-005	1	4.050E-005	8.02	0.0083
Residual	1.465E-004	29	5.052E-006		
Cor Total	9.247E-004	35			
Std. Dev.	2.248E-003		R-Squared		0.8416
Mean	0.036		Adj R-Squared		0.8088
C.V. %	6.20		Pred R-Squared		0.7549
PRESS	2.267E-004		Adeq Precision		19.995

Table 4.22 presents the ANOVA for Response Surface Quadratic model for HC. Table shows that the value of “Prob. > F” for model, main effect of CR, injection timing, injection pressure and second order effect of CR, injection timing and injection pressure are all less than 0.05. So these terms are significant model terms. The R² value is equal to 0.8833. The table also shows that Pred-R² of 0.8233 is in reasonable agreement with the Adj-R² of 0.8592; i.e. the difference is less than 0.2. For the developed NO_x model, the value of Adequate Precision is 22.089, which shows high precision of the model. The final empirical models for smoke in terms of coded and actual factors are given by Eq. 4.23 and Eq. 4.24 respectively.

$$HC = 20.2708 - 6.91667 * A - 2.625 * B - 1.375 * C + 7.0625 * A^2 + 6.95833 * B^2 + 2.70833 * C^2 \quad (4.23)$$

$$HC = 3414.7 - 123.889 * CR - 81.3333 * Inj.T. - 11.5125 * Inj.Pr. + 3.13889 * CR^2 + 1.73958 * Inj.T.^2 + 0.0270833 * Inj.Pr.^2 \quad (4.24)$$

Table 4.22 Reduce analysis of variance and interaction fit for HC response.

Source	Sum of Squares	degree of freedom	Mean Square	F Value	p-value Prob > F
Model	1968.28	6	328.05	36.59	< 0.0001
A-CR	956.81	1	956.81	106.71	< 0.0001
B-Inj.T.	165.38	1	165.38	18.44	0.0002
C-Inj.Pr.	45.38	1	45.38	5.06	0.0322
A ²	354.69	1	354.69	39.56	< 0.0001
B ²	387.35	1	387.35	43.20	< 0.0001
C ²	58.68	1	58.68	6.54	0.0160
Residual	260.03	29	8.97		
Cor Total	2228.31	35			
Std. Dev.	2.99		R-Squared		0.8833
Mean	30.64		Adj R-Squared		0.8592
C.V. %	9.77		Pred R-Squared		0.8233
PRESS	393.66		Adeq Precision		22.089

4.3.2 Performance of engine using BU20 with varying parameters

The performance and emission results of the engine for diesel and n-butanol-diesel blends were recorded and are presented in the form of scattered and 3D surface plots in Figs. 4.41 to 4.51.

4.3.2.1 Brake specific fuel consumption (BSFC)

It can be observed from Fig. 4.41(a) that BSFC reduces from a CR value of 17.5 to 19.5 and again increases to 20.5. The BSFC is higher at retarded and advanced crank angles compared to that of 23°CA btdc. At 23°CA btdc, BSFC is observed to be lower by 10.46% and 13.37% than that of 21°CA btdc and 25° CA btdc respectively. Similarly, the BSFC is also more at lower and higher injection pressure as compared to that of 210 bar. BSEC at 210 bar injection pressure was found lower by 10.21% and 11.76% respectively when compared to that of 200 bar and 220 bar respectively at full load condition (100% rated load). The Fig. 4.41 (b) shows similar trends of BSEC as of BSFC in Fig. 4.41 (a).

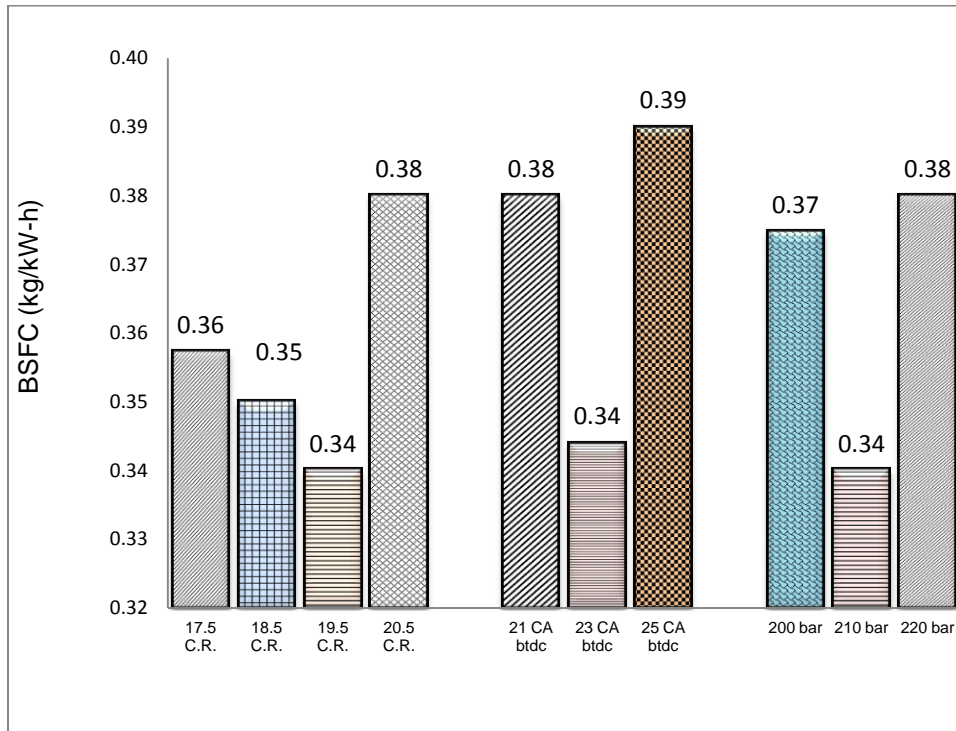


Fig. 4.41(a) BSFC at different CRs, injection timings and injection pressures for BU20

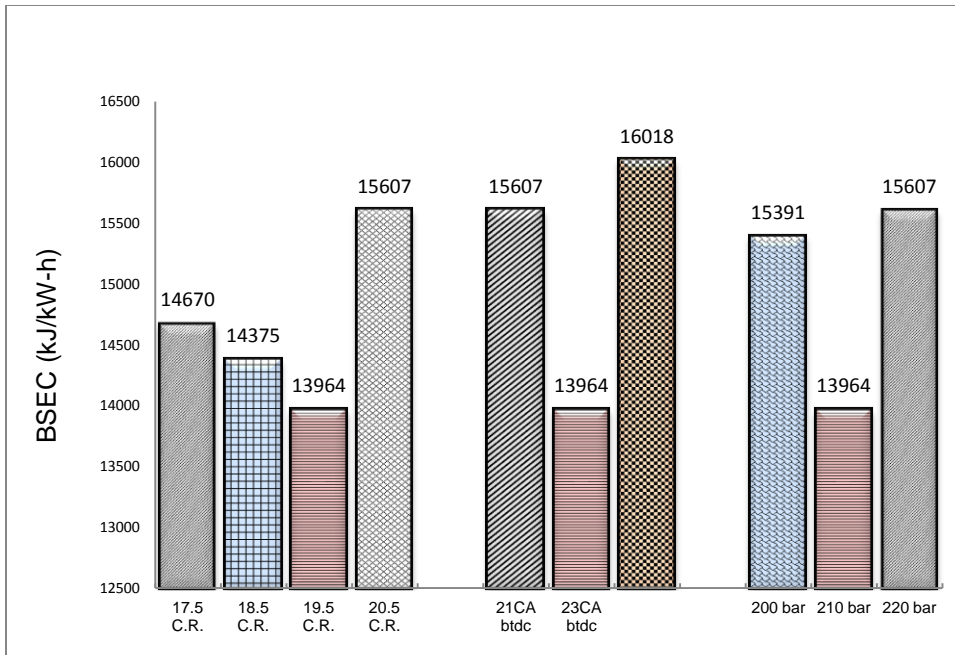


Fig. 4.41 (b) BSEC at different CRs, injection timings and injection pressures for BU20

4.3.2.2 Brake thermal efficiency

Figs.4.42 and 4.43 show the variation of the engine brake thermal efficiency with varying operating parameters.

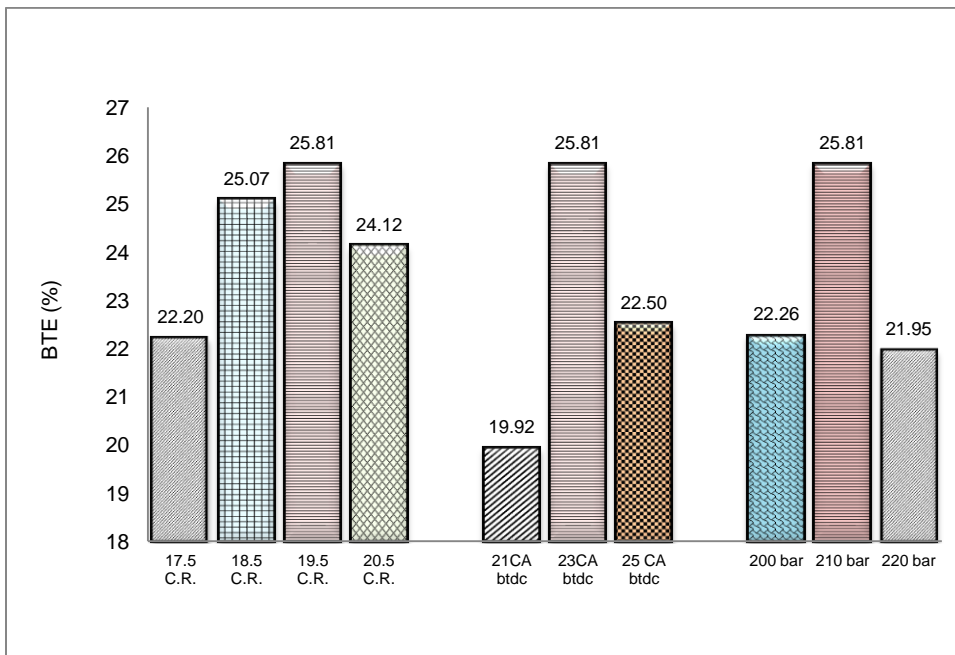


Fig. 4.42 BTE at different CRs, injection timings and injection pressures for BU20

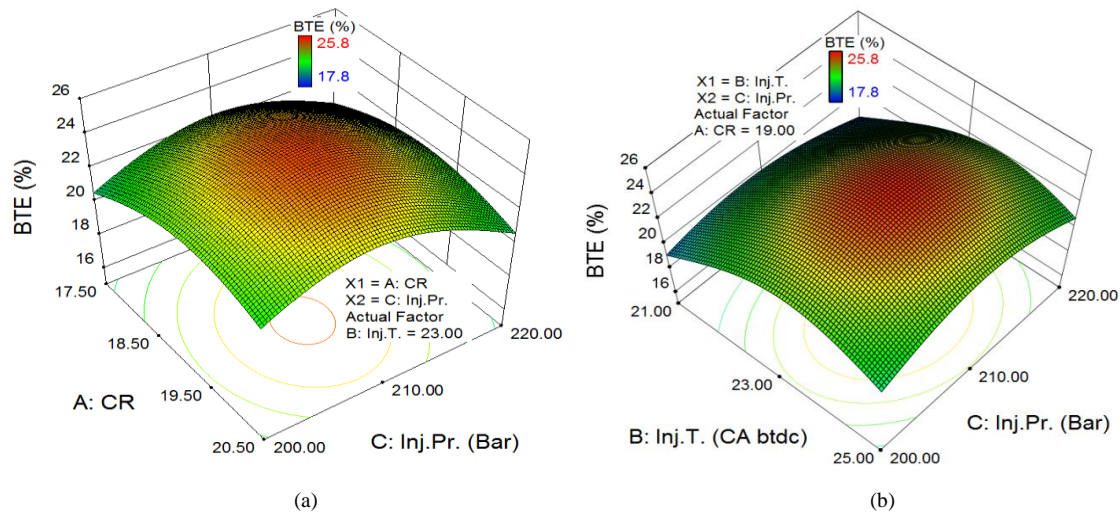


Fig. 4.43 Variation in BTE due to combined effect of (a) CR and injection pressure and (b) injection timing and injection pressure for BU20

It can be observed from Figs.4.42 and 4.43 that the engine brake thermal efficiency increases with CR from 17.5 to 19.5, and after that again decreases at 20.5 CR. The BTE increases from 21°CA btdc to 23°CA btdc injection timing and then decreases towards 25°CA btdc. The BTE increases from 200 bar injection pressure to 210 bar gradually and then decreases as the injection pressure further increases. At higher injection pressure, the fuel consumption increases, and due to this, BTE decreases. It was noted that decrement in BTE is very less in comparison to a corresponding increment in BSFC. This is due to the availability of oxygen in BU20 which improves the combustion efficiency and this is consistent with the conclusions drawn by many researchers cited in the introduction. In the vicinity of 19.5 CR, 210 bar injection pressure and 23°CA btdc injection timing, BTE is optimum among all the settings tested in the designed model at full load condition. At 19.5 CR, the BTE is higher by 3.0% in comparison to that at 18.5 CR; and at 23° CA btdc, BTE is higher by 22% compared to that at 21°CA btdc. The BTE at 210 bar injection pressure is higher as compared to 200 bar and 220 bar by 13.8% and 15.0% respectively.

4.3.3 Emissions of engine using BU20 with varying operating parameters

4.3.3.1 Variation of Smoke

Figs. 4.44 and 4.45 show the variation of smoke emission with different operating parameters and the combined effect of CR & Inj. T. and Inj. Pr. & Inj. T respectively. It can be observed from the figures that smoke emission reduces from 17.5 CR to 19.5 CR and increases from 19.5 CR to 20.5 CR at a fine pace. The smoke reduces from 21°CA bt/dc to 23°CA bt/dc and again increases at 25°CA bt/dc. However, the value of smoke emission at 25°CA bt/dc is less than that of 21°CA bt/dc. The smoke reduces from 200 bar injection pressure to 210 bar and again increases up to 220 bar at a similar rate. The minimum value of smoke is 42 HSU (Hartridge Smoke Units) in the vicinity of 19.5 CR, 210 bar Inj. Pr. and 23° CA bt/dc Inj. T. at full load condition.

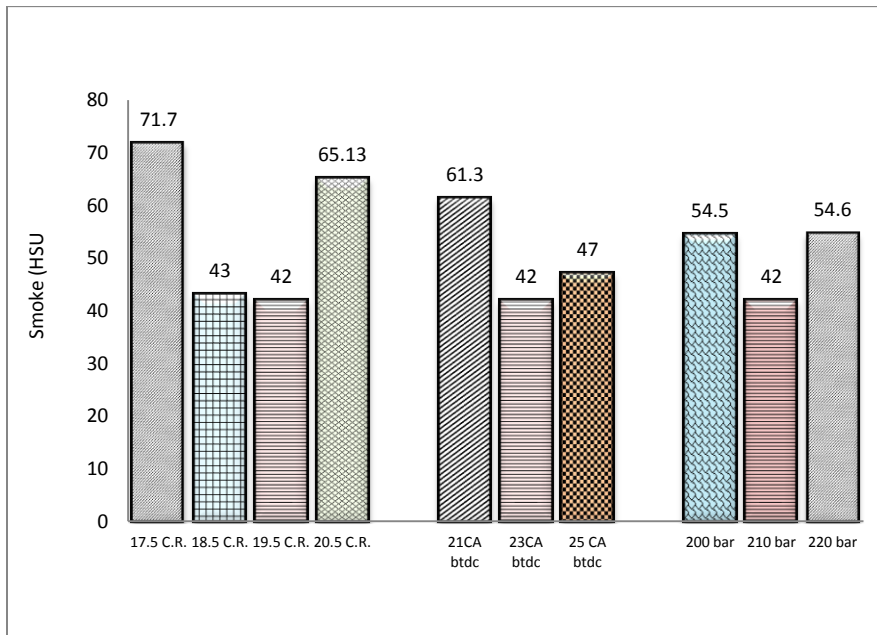


Fig. 4.44 Smoke emission at different CRs, injection timings and injection pressures for BU20

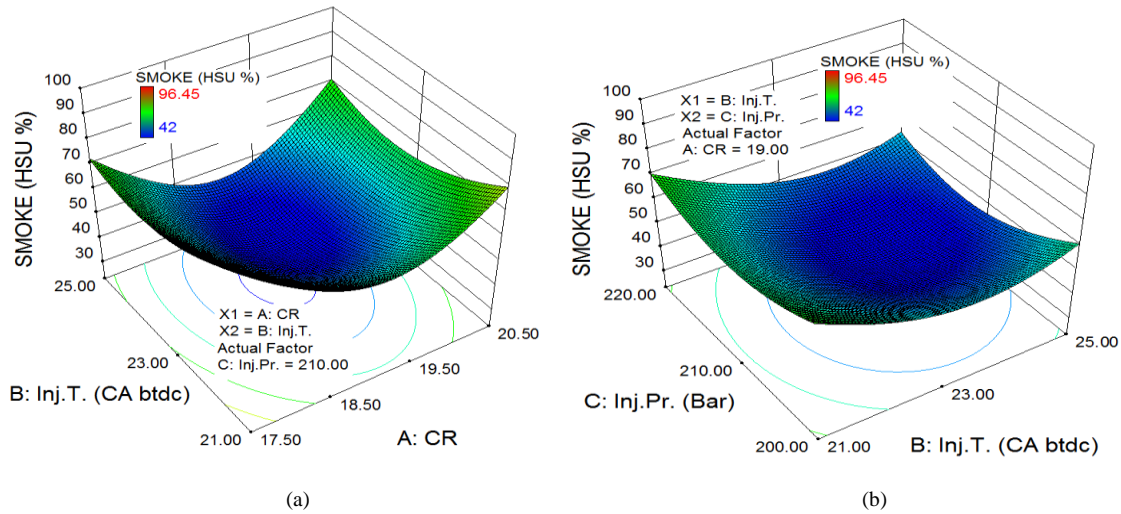


Fig. 4.45 Variation in smoke due to combined effect of (a) CR and injection timing and (b) injection pressure and injection timing for BU20

4.3.3.2 Variation of NO_x

Figs. 4.46 and 4.47 depict the emission of NO_x with different operating parameters and change in CR, injection pressure and injection timing simultaneously. It can be observed from the figures that NO_x is minimum somewhere between 18.5 CR and 19.5 CR. NO_x emission decreases gradually from 17.5 CR to 19.5 CR and increases from 19.5 CR to 20.5 CR. NO_x reduces from 21°CA bt dc to 23° CA bt dc and again increases at 25°CA bt dc. However, the value of NO_x at 21°CA bt dc is lower than that of 25°CA bt dc. Similar trends can be observed for NO_x emission with variation in injection pressure. Near 210 bar injection pressure, the NO_x emission was found to be minimum, and at 220 bar, the level is higher as compared to that of 200 bar.

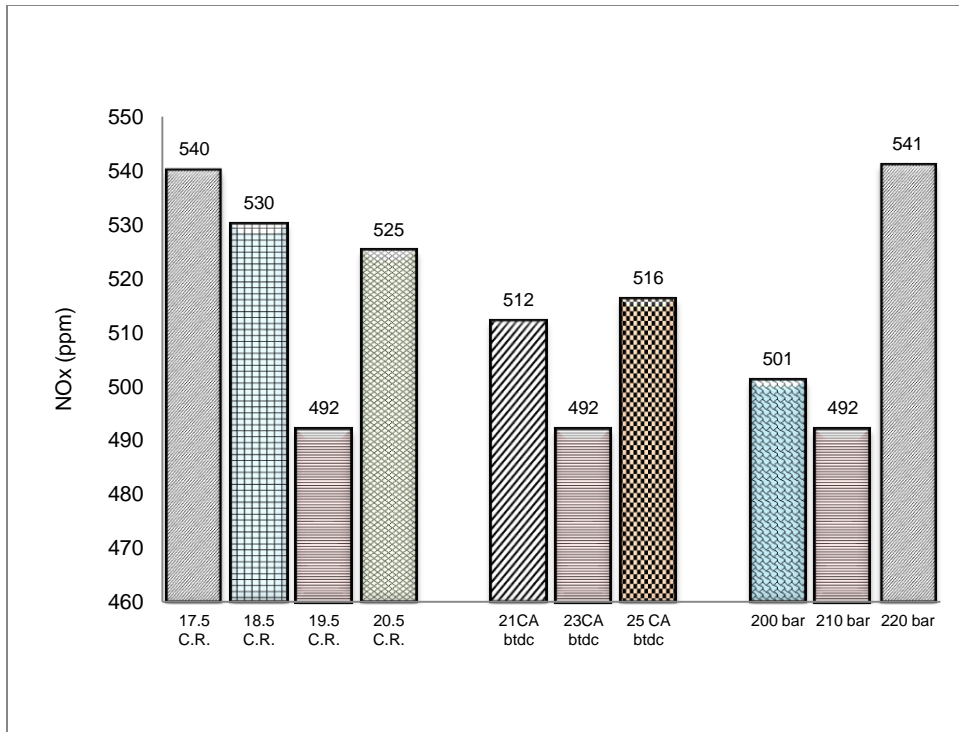


Fig. 4.46 NO_x emission at different CRs, injection timings and injection pressures for BU20

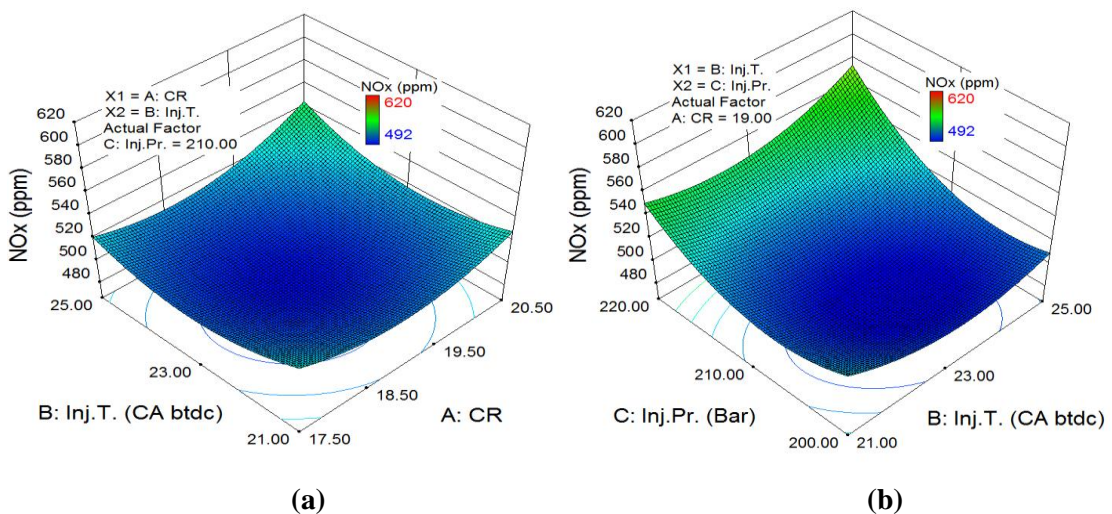


Fig.4.47 Variation in NO_x due to combined effect of (a) CR and Injection Timing and (b) Injection Pressure and Injection Timing for BU20

4.3.3.3 Variation of CO

It can be observed from Fig. 4.48 that emission of CO reduces from CR of 17.5 to 19.5, and again increases to 20.5. CO increases slightly from 21°CA btdc to 23°CA btdc. At 210 bar, CO is lower than 200 bar and higher than 220 bar injection pressure by 6.25% and 12.5% respectively at full load condition (100% rated load). Fig. 4.49 shows

variation in CO with CR and injection pressure simultaneously. The 3D-surface curve verifies the experimental observation as given by fig. 4.48.

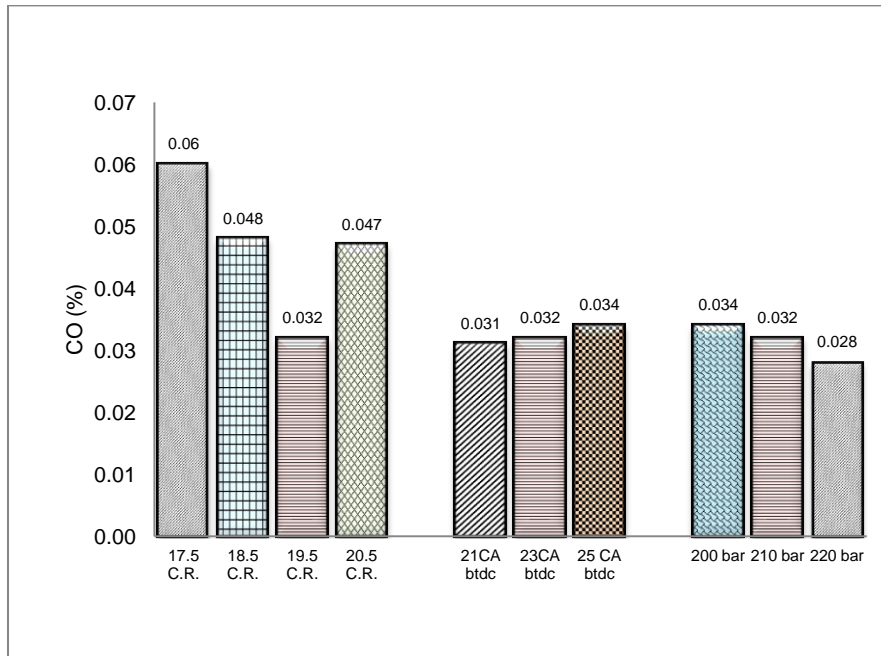


Fig. 4.48 CO emission at different CRs, injection timings and injection pressures for BU20

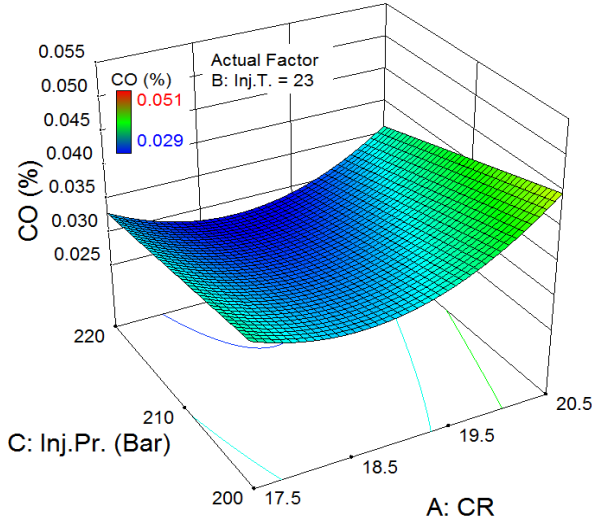


Fig.4.49 Variation in CO due to combined effect of CR and Injection Pressure for BU20

4.3.3.4 Variation of HC

It can be observed from Fig. 4.50 that emission of HC reduces from CR of 17.5 to 19.5 and again increases to 20.5. Similar trends can be observed for injection timing and injection pressure. HC at 23°CA btdc is lower when compared to its values at 21°CA btdc

and 25°CA btdc by 33.3% and 22.2% respectively. At 210 bar, HC levels are lower in comparison to 200 bar and 220 bar injection pressure by 33.3% and 28% respectively at full load condition (100% rated load).

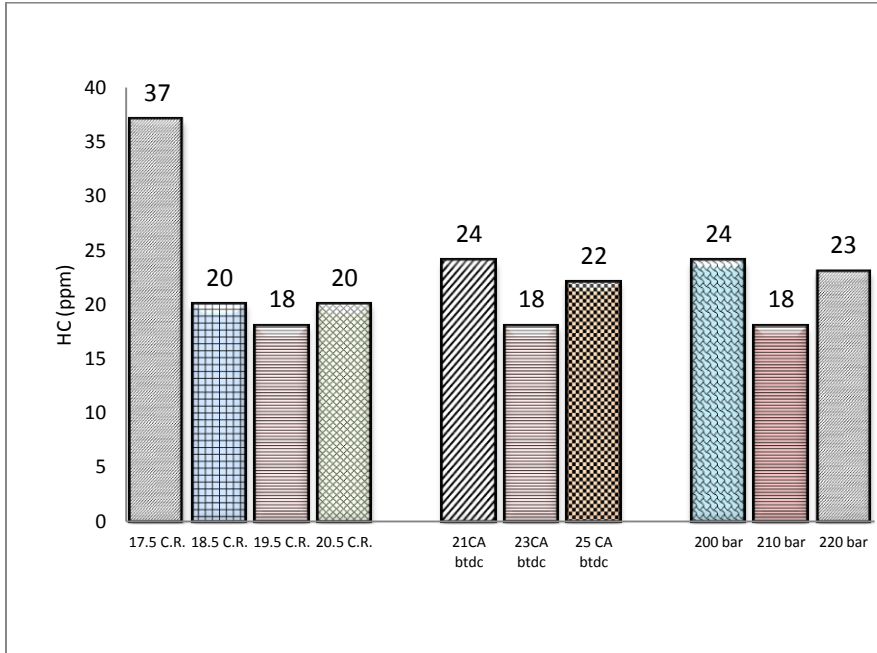


Fig. 4.50 HC emission at different CRs, injection timings and injection pressures for BU20

4.3.4 Validation and optimization of response

All the responses i.e. BSFC, BTE, smoke, NO_x, CO and HC were optimized for input parameters. Table 4.23 shows the optimization analysis of the parameters and their predicted responses. A confirmation test was conducted to verify results predicted by the models. The engine was set as near as possible to the optimum parameters (i.e. CR of 19.483, inj. T. of 23.598°CA btdc and inj. Pr. of 208.54 bar). The optimum values of BSFC, BTE, smoke, NO_x, CO and HC were observed to be 0.345, 25.81, 42, 492, .032 and 18 respectively. Table 4.23 also shows that percentage errors of these results are well within tolerance limits.

Table 4.23 Optimum conditions of blends and their predicted responses for BU20

Number	CR	Inj.T.	Inj.Pr.	BSFC	BTE	SMOKE	NO _x	CO	HC	
1	19.483	23.598	208.546	0.367	25.399	41.595	498.03	0.034	18.870	Selected
2	19.168	23.387	211.173	0.364	25.358	37.920	499.88	0.031	19.213	
3	19.259	24.402	211.877	0.378	24.296	41.461	514.30	0.033	20.705	
4	19.390	23.854	209.831	0.370	25.291	40.155	501.93	0.033	19.122	
5	19.103	23.308	209.608	0.361	25.444	38.260	494.65	0.032	19.649	
6	18.998	23.160	208.876	0.358	25.297	39.184	492.00	0.032	20.301	
Confirmation test	19.5	23	210	0.345	25.81	42	492	0.032	18	
Error Percentage(× 100)				0.060	-0.016	-0.010	0.012	0.059	0.046	

4.4 Comparison of performance and emissions characteristics of diesel and BU20

After optimization of engine parameters for BU20, comparison of engine performance and emissions with diesel and BU20 (at compression ratio of 18.5 and 19.5) was done, and is shown in Fig. 4.51.

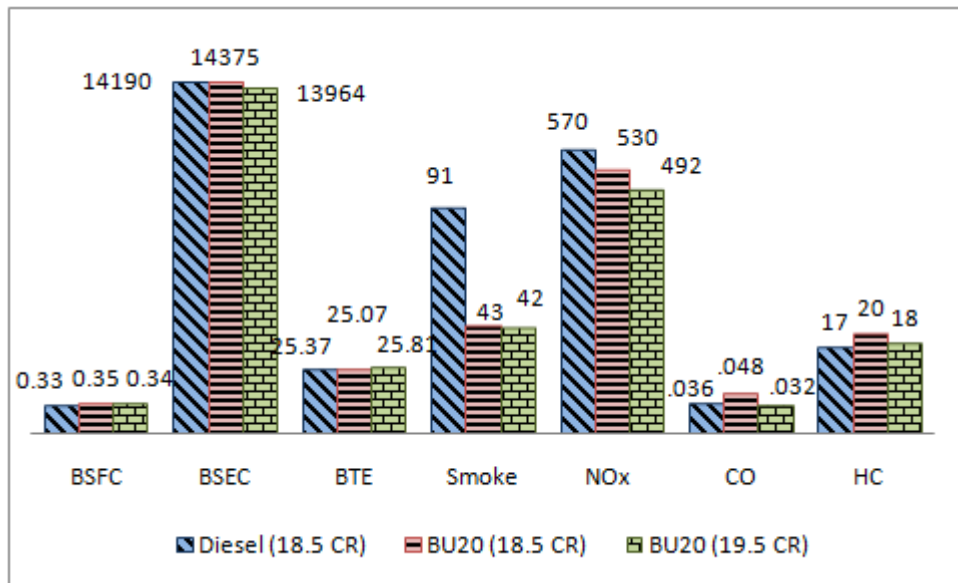


Fig. 4.51 Comparison of diesel and BU20 performance and emissions

Fig. 4.51 shows that for BU20, performance and emission parameters were improved at a compression ratio of 19.5 as compared to 18.5. It can be observed that for BU20, BSFC and BTE increase by 3.03% and 1.73% respectively at 19.5 CR as compared to diesel at

CR of 18.5. The smoke, NO_x, and CO emissions decrease by 53.85%, 13.68% and 11.11% respectively at 19.5 CR as compared to diesel at CR of 18.5 and at same settings of injection timing and injection pressure at full load condition. However, emission of HC increases by 5.88% when using BU20 at 19.5 CR as compared to diesel at CR of 18.5.

From the above observations it was concluded that the existing engine is giving optimum results of performance and emissions for BU20 at 19.5 CR, 23°CA bt dc injection timing and 210 bar injection pressure. For further investigations, these engine operating parameters were fixed and BU20 was taken as the reference fuel.

4.5 Performance and emissions characteristics of the engine using nitromethane-n-butanol-diesel blends:

In the fourth stage, tests were conducted using Nitromethane (NM), Diglyme (DGM) and Diethyl ether (DEE) as additives in BU20 in different proportions with the following engine settings: 19.5 compression ratio (CR), 23° CA bt dc injection timing and 210 bar injection pressure. The variations in engine performance and emissions for these blends were noted at different load conditions (no load to 100% rated power) and are presented in the form of scattered curves in this section. It was observed from these scattered diagrams that the variations in performance and emissions of blends with respect to each other are noticeable at higher loads only. Thus, mathematical modeling has been done for higher load observations only.

4.5.1 Determination of optimum blends of nitromethane-n-butanol (20%)-diesel (NM-BU20):

To find optimal NM-BU20 blend, the following approach was adopted: (i) Firstly, the data for selected experiments was fed to the DOE software and ANOVA was conducted to check the significance of model and individual terms. (ii) The curves from actual experiments and surface response model were then analyzed to see effect of change of factors on response. (iii) Optimization and verification of predicated model were done by confirmation test. 3D surface curves have been drawn for all instances where interaction effect of factors was found to be significant. Otherwise, 2D curves of factors with response have been drawn.

4.5.2 Modeling for NM-BU20 blends

Full Factorial design was employed for the development of prediction models of BSFC, BTE, smoke, NO_x, CO and HC in terms of engine load and blending ratio. An attempt was made to optimize the factors for the desired values of responses (BSFC, BTE, smoke, NO_x, CO and HC). Table 4.24 shows the engine operating parameters and their levels, and Table 4.25 shows the design matrix for modeling.

Table 4.24 Parameters and their levels according to Factorial design for NM-BU20 blends.

Parameter	symbol	Levels			
		1	2	3	4
Load (Nm)	A (Load)	12	16	20	24
NM-BU20 Blend (% v/v)	B (Blend)	1	2	3	

Table 4.25 Design layout and experimental results for NM-BU20 blends

Run	Factor 1 A:Load (Nm)	Factor 2 B:NMBU20 BLEND (v/v%)	Response 1 BSFC (kg/kW-h)	Response 2 BTE (%)	Response 3 Smoke (HSU %)	Response 4 NO _x (ppm)	Response 5 CO (%)	Response 6 HC (ppm)
2	12	1	0.445	21.32	4.4	332	0.065	22
12	16	1	0.400	24.66	6.4	438	0.052	23
5	20	1	0.365	25.89	12.5	483	0.038	23
6	24	1	0.342	26.24	29.9	539	0.03	24
8	12	2	0.460	21.5	5.9	371	0.068	25
3	16	2	0.420	24.85	8.1	508	0.054	26
4	20	2	0.390	26.03	17.50	573	0.042	27
7	24	2	0.360	26.09	37.20	632	0.032	27
10	12	3	0.470	22.76	6.5	375	0.074	31
9	16	3	0.428	25.95	8.5	524	0.056	32
11	20	3	0.400	26.53	18.8	585	0.044	32
1	24	3	0.373	26.9	38.4	680	0.035	33

The details of 12 experiments as suggested by DOE from performed experiments are shown in Table 4.25 along with the run order selected at random. These data were used as inputs in the Design Expert 8.0.4.1 software for further analysis.

4.5.2.1 Diagnosis of data for analysis of variance for NM-BU20 blends

Figs. 4.52 to 4.57 show plots of normal probability vs. internal studentized residuals and internal studentized residuals vs. predicted values for BSFC, BTE, smoke, NO_x, CO and HC emission respectively when the engine was operated on NM-BU20 blends.

It can be observed from normal probability plots that most of the interaction points are accumulated along a straight line, which implies that residuals follow normal distribution and hence, the fitted model is adequate for a real system.

For the assumption of constant variance to be true in ANOVA, the internal residuals vs. predicted plot should be a random scatter. Figs. 4.52 (b), 4.53, (b) 4.54 (b), 4.55 (b), 4.56 (b) and 4.57 (b) reveal no obvious pattern or discernable structure, indicating the validity assumption to be true. It was thus projected that for all the responses, the variance of the observed data is constant and hence is satisfactory.

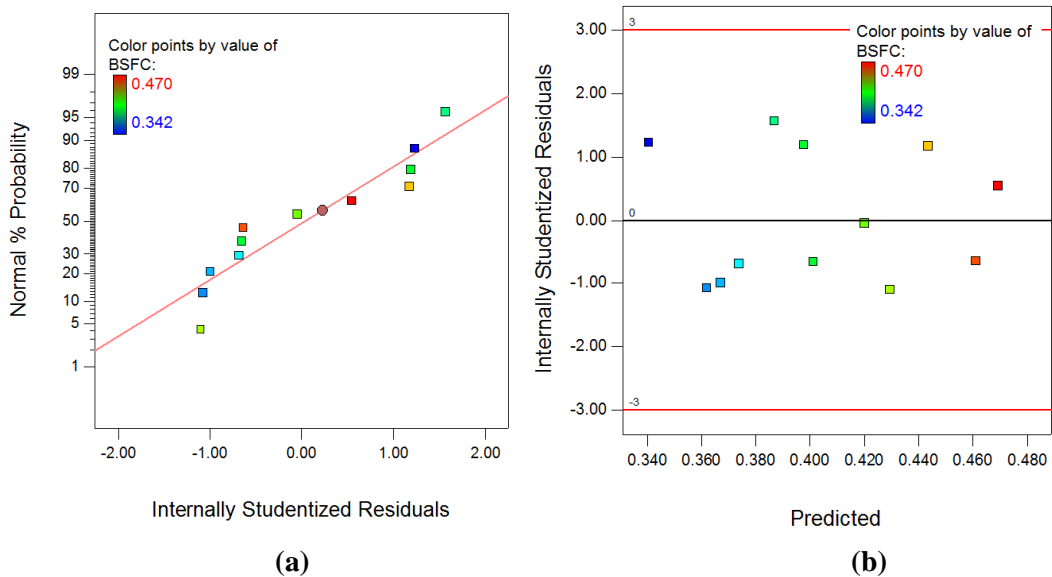
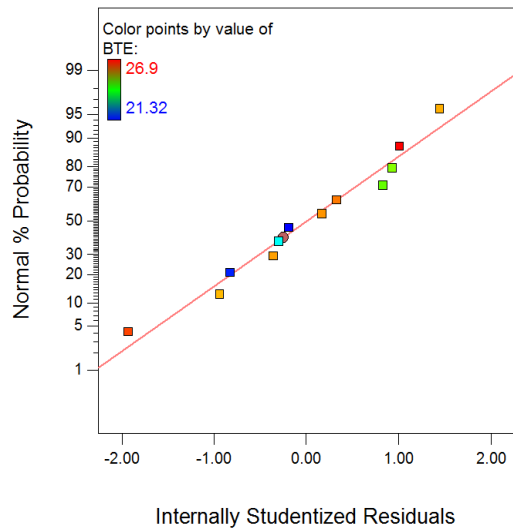
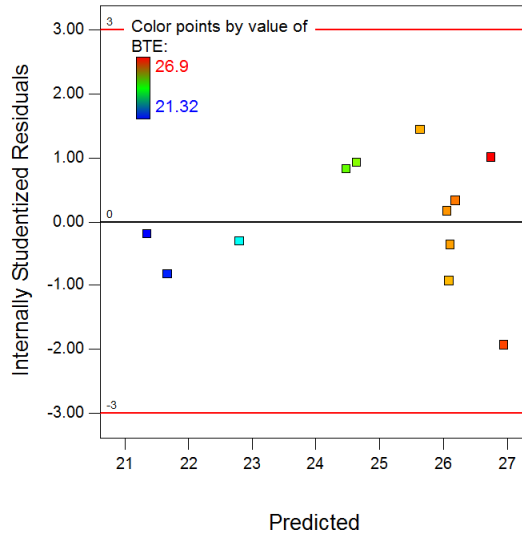


Fig. 4.52 (a) Plot of normal % probability vs. internal studentized residuals for BSFC
(b) Plot of internal studentized residuals vs. predicted response for BSFC

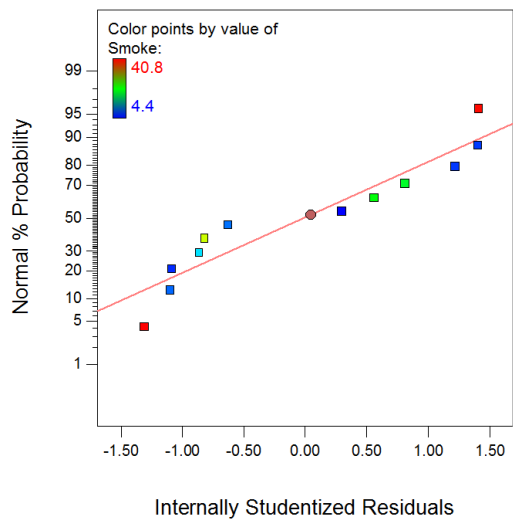


(a)

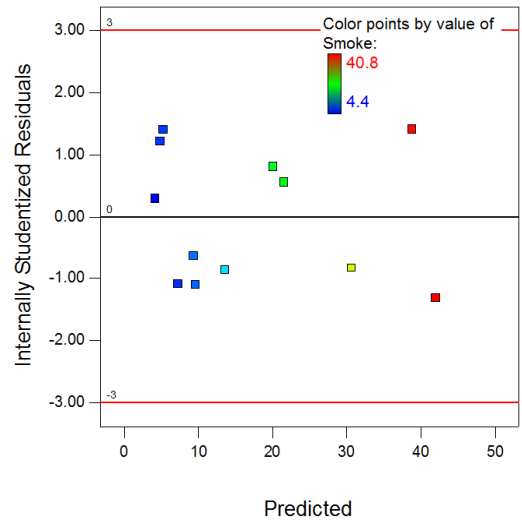


(b)

Fig. 4.53 (a) Plot of normal % probability vs. internal studentized residuals for BTE
(b) Plot of internal studentized residuals vs. predicted response for BTE



(a)



(b)

Fig. 4.54 (a) Plot of normal % probability vs. internal studentized residuals for smoke
(b) Plot of internal studentized residuals vs. predicted response for smoke

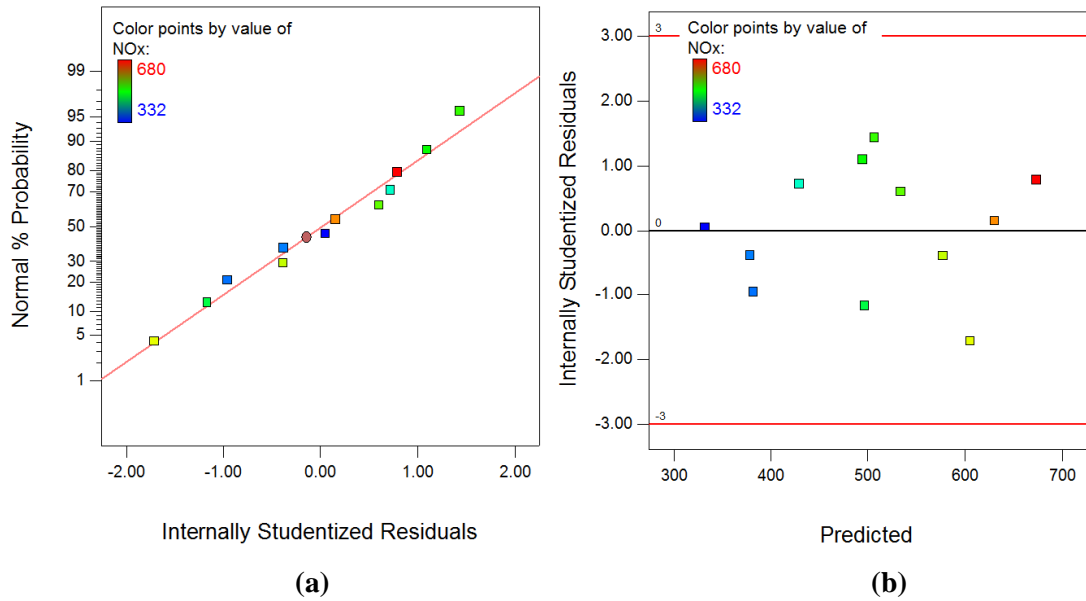


Fig. 4.55 (a) Plot of normal % probability vs. internal studentized residuals for NO_x
(b) Plot of internal studentized residuals vs. predicted response for NO_x

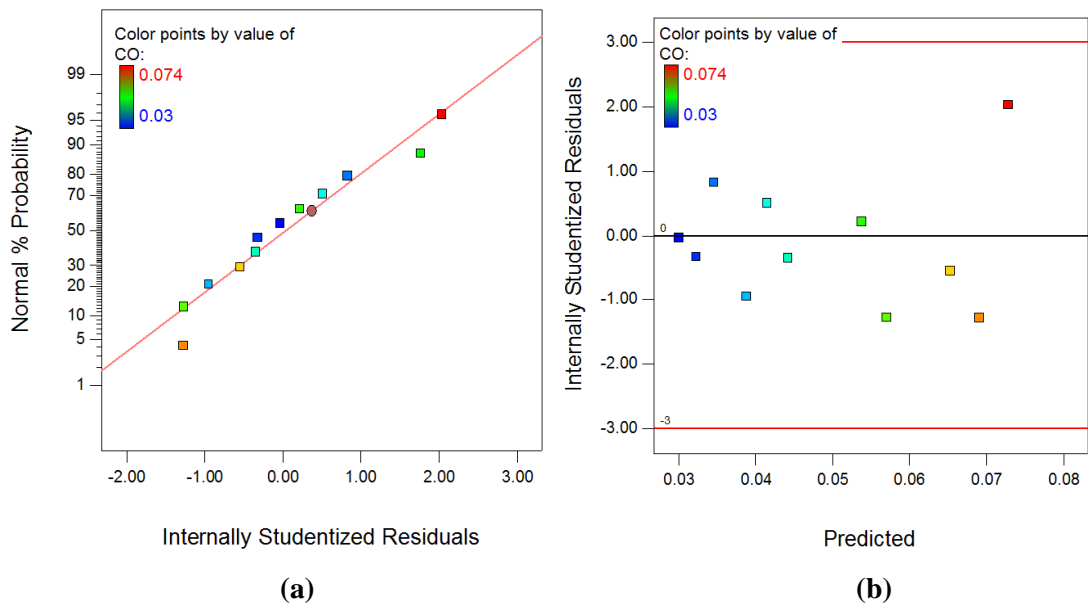


Fig. 4.56 (a) Plot of normal % probability vs. internal studentized residuals for CO
(b) Plot of internal studentized residuals vs. predicted response for CO

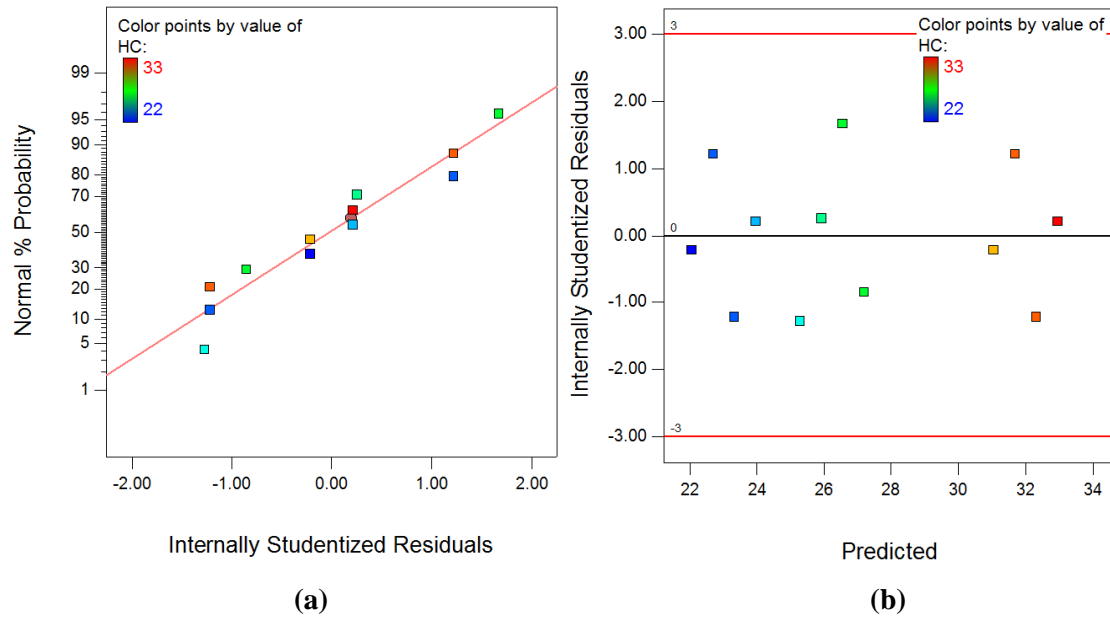


Fig.4.57 (a) Plot of normal % probability vs. internal studentized residuals for HC
(b) Plot of internal studentized residuals vs. predicted response for HC

4.5.2.2 ANOVA for response surface model for NM-BU20 blends

Table 4.26 to Table 4.31 present the ANOVA tables for the response surface prediction models of BSFC, BTE, smoke, NO_x , CO and HC respectively by selecting the backward elimination procedure to remove the terms that are not significant. In the present work, ANOVA analysis was carried out for a significance level of $\alpha = 0.05$, i.e. for a confidence level of 95%.

Table 4.26 presents the ANOVA for Response Surface Quadratic model for BSFC. In the Table, the value of “Prob. > F” for the model is 0.0001 which is less than 0.05, indicating that the model is significant, i.e. the terms in the model have a significant effect on BSFC. In the same manner, the value of “Prob. > F” for the main effect of load, blend, second order effect of load and blend were also found to be less than 0.05. So these terms are also significant model terms.

Table 4.26 Reduce analysis of variance table and interaction fit for BSFC

Source	Sum of Squares	Degree of freedom	Mean Square	F-Value	p-value Prob > F
Model	0.018	5	3.687E-003	654.95	< 0.0001
A-Load	0.016	1	0.016	2916.26	< 0.0001
B-NM-BU20 BLEND	1.755E-003	1	1.755E-003	311.82	< 0.0001
AB	1.625E-005	1	1.625E-005	2.89	0.1403
A ²	1.880E-004	1	1.880E-004	33.39	0.0012
B ²	5.857E-005	1	5.857E-005	10.40	0.0180
Residual	3.378E-005	6	5.630E-006		
Cor Total	0.018	11			
Std. Dev.	2.373E-003		R-Squared		0.9982
Mean	0.40		Adj R-Squared		0.9966
C.V. %	0.59		Pred R-Squared		0.9921
PRESS	1.454E-004		Adeq Precision		76.815

The R-Squared (R^2) value is equal to 0.9982. Its nearness to 1 for the model is indicative of the accuracy and exactness of the model in finding the desired responses. The Pred- R^2 of 0.9921 is in reasonable agreement with the Adj- R^2 of 0.9966; i.e. the difference is less than 0.2. For the developed BSFC model, the value of Adequate Precision is 76.815, which shows high precision of the model. The final empirical model for BSFC in terms of coded and actual factors is given by Eqs. 4.25 and 4.26 respectively.

$$BSFC = 0.402553 - 0.0496253 \times A + 0.0148133 \times B + 0.001912 \times AB + 0.00890499 \times A^2 - 0.00468666 \times B^2 \quad (4.25)$$

$$BSFC = 0.594672 - 0.0178132 \times Load + 0.027824 \times (NMBU20) + 0.000318666 \times Load \times (NMBU20) + 0.000247361 \times Load^2 - 0.00468666 \times (NMBU20)^2 \quad (4.26)$$

Table 4.27 presents the ANOVA for Response Surface Quadratic model for BTE. In the Table, the value of “Prob. > F” for the model is 0.0001 which is less than 0.05, indicating that the model is significant, i.e. the terms in the model have a significant effect on BTE. In the same manner, the value of “Prob. > F” for main effect of load, blend, second order effect of load and blend were also found to be less than 0.05. So these terms are also significant model terms.

Table 4.27 Reduce analysis of variance table and interaction fit for BTE

Source	Sum of Squares	Degree of freedom	Mean Square	F-Value	p-value Prob > F
Model	41.79	5	8.36	110.46	< 0.0001
A-Load	32.18	1	32.18	425.28	< 0.0001
B-NM-BU20 BLEND	2.03	1	2.03	26.83	0.0021
AB	0.22	1	0.22	2.95	0.1365
A ²	6.90	1	6.90	91.20	< 0.0001
B ²	0.46	1	0.46	6.03	0.0494
Residual	0.45	6	0.076		
Cor Total	42.24	11			
Std. Dev.	0.28		R-Squared		0.9893
Mean	24.89		Adj R-Squared		0.9803
C.V. %	1.11		Pred R-Squared		0.9659
PRESS	1.44		Adeq Precision		28.806

The R-Squared (R^2) value is 0.9893 and is indicative of the accuracy and exactness of the model in finding the desired responses. The Pred- R^2 is 0.9659, which is in reasonable agreement with the Adj- R^2 of 0.9803; i.e. the difference is less than 0.2. For the developed BTE model, the value of Adequate Precision is 28.806, which shows high precision of the model. The final empirical model for BTE in terms of coded and actual factors is given by Eqs. 4.27 and 4.28 respectively.

$$BTE = 25.5654 + 2.197 \times A + 0.50375 \times B - 0.22425 \times AB - 1.70625 \times A^2 + 0.41375 \times B^2 \quad (4.27)$$

$$BTE = 2.92017 + 2.14717 \times Load - 0.4785 \times (NMBU20) - 0.037375 \times Load \times (NMBU20) - 0.0473958 \times Load^2 + 0.41375 \times (NMBU20)^2 \quad (4.28)$$

Table 4.28 presents the ANOVA table for Response Surface Quadratic model for smoke emission. In the Table, the value of “Prob. > F” for the model, the main effect of load & blend, interaction effect of load & blend, and second order effect of load & blend are less than 0.05. So these terms are significant model terms.

Table 4.28 Reduce analysis of variance and interaction fit for Smoke

Source	Sum of Squares	Degree of Freedom	Mean Square	F-Value	p-value Prob. > F
Model	1989.86	5	397.97	144.65	< 0.0001
A-Load	1666.37	1	1666.37	605.68	< 0.0001
B-(NM-BU20)	77.50	1	77.50	28.17	0.0018
AB	29.07	1	29.07	10.57	0.0175
A ²	200.08	1	200.08	72.72	0.0001
B ²	16.83	1	16.83	6.12	0.0482
Residual	16.51	6	2.75		
Cor Total	2006.37	11			
Std. Dev.	1.66		R-Squared		0.9918
Mean	17.25		Adj R-Squared		0.9849
C.V. %	9.62		Pred R-Squared		0.9602
PRESS	79.90		Adeq Precision		32.267

The R² value is equal to 0.9918 and is indicative of the accuracy and exactness of the model in finding the desired responses. Table 4.28 shows that Pred-R² of 0.9602 is in reasonable agreement with the Adj-R² of 0.9849; i.e. the difference is less than 0.2. For the developed smoke model, the value of Adequate Precision is 32.267, which shows significant precision of the model. The final empirical model for smoke emission in terms of coded and actual factors is given by Eqs. 4.29 and 4.30 respectively.

$$SMOKE = 13.8208 + 15.81 \times A + 3.1125 \times B + 2.5575 \times AB + 9.1875 \times A^2 - 2.5125 \times B^2 \quad (4.29)$$

$$SMOKE = 48.1483 - 7.405 \times Load + 5.49 \times (NMBU20) + 0.42625 \times Load \times (NMBU20) + 0.255208 \times Load^2 - 2.5125 \times (NMBU20)^2 \quad (4.30)$$

Table 4.29 presents the reduce ANOVA table for Response Surface Quadratic model for NO_x. In the Table, the value of “Prob. > F” for the model, the main effect of load, blend, interaction effect of load & blend, second order effect of load and blend are less than 0.05. So these terms are significant model terms.

Table 4.29 Reduce analysis of variance table and interaction fit for NO_x

Source	Sum of Squares	Degree of Freedom	Mean Square	F-Value	p-value Prob. > F
Model	1.277E+005	5	25533.70	112.63	< 0.0001
A-Load	1.033E+005	1	1.033E+005	455.83	< 0.0001
B-(NM-BU20)	17298.00	1	17298.00	76.31	0.0001
AB	2402.50	1	2402.50	10.60	0.0173
A ²	2760.33	1	2760.33	12.18	0.0130
B ²	1872.67	1	1872.67	8.26	0.0283
Residual	1360.17	6	226.69		
Cor Total	1.290E+005	11			
Std. Dev.	15.06		R-Squared		0.9895
Mean	503.33		Adj R-Squared		0.9807
C.V. %	2.99		Pred R-Squared		0.9670
PRESS	4263.32		Adeq Precision		32.123

The R² value is equal to 0.9895 and is indicative of the accuracy and exactness of the model in finding the desired responses. Table 4.29 shows that Pred-R² of 0.9670 is in reasonable agreement with the Adj-R² of 0.9807; i.e. the difference is less than 0.2. For the developed NO_x model, the value of Adequate Precision is 32.123, which shows significant precision of the model. The final empirical model for NO_x in terms of coded and actual factors is given by Eqs. 4.31 and 4.32 respectively.

$$NO_x = 539.958 + 124.5 \times A + 46.5 \times B + 23.25 \times AB - 34.125 \times A^2 - 26.5 \times B^2 \quad (4.31)$$

$$NO_x = -200.167 + 47.125 \times Load + 82.75 \times (NMBU20) + 3.875 \times Load \times (NMBU20) - 0.947917 \times Load^2 - 26.5 \times (NMBU20)^2 \quad (4.32)$$

Table 4.30 presents the reduce ANOVA table for Response Surface Quadratic model for CO emission. In the Table, the value of “Prob. > F” for the model, the main effect of load, main effect of blend, interaction effect of load & blend and second order effect of load are less than 0.05. So these terms are significant model terms.

Table 4.30 Reduce analysis of variance table and interaction fit for CO

Source	Sum of Squares	Degree of Freedom	Mean Square	F-Value	p-value Prob > F
Model	2.359E-003	4	5.896E-004	581.34	< 0.0001
A-Load	2.257E-003	1	2.257E-003	2225.28	< 0.0001
B-(NM-BU20)	7.200E-005	1	7.200E-005	70.99	< 0.0001
AB	2.500E-006	1	2.500E-006	2.46	0.1604
A ²	2.700E-005	1	2.700E-005	26.62	0.0013
Residual	7.100E-006	7	1.014E-006		
Cor Total	2.366E-003	11			
Std. Dev.	1.007E-003		R-Squared		0.9970
Mean	0.049		Adj R-Squared		0.9953
C.V. %	2.05		Pred R-Squared		0.9884
PRESS	2.736E-005		Adeq Precision		65.837

The R² value is equal to 0.9970 and is indicative of the accuracy and exactness of the model in finding the desired responses. Table 4.30 shows that Pred-R² of 0.9884 is in reasonable agreement with the Adj-R² of 0.9953; i.e. the difference is less than 0.2. For the developed CO model, the value of Adequate Precision is 65.837, which shows significant precision of the model. The final empirical model for CO in terms of coded and actual factors is given by Eqs. 4.33 and 4.34 respectively.

$$CO = 0.0472917 - 0.0184 \times A + 0.003 \times B - 0.00075 \times AB + 0.003375 \times A^2 \quad (4.33)$$

$$CO = 0.122367 - 0.00619167 \times Load + 0.00525 \times (NMBU20) - 0.000125 \times Load \times (NMBU20) + 9.375e-005 \times Load^2 \quad (4.34)$$

Table 4.31 presents the reduce ANOVA table for Response Surface Quadratic model for HC. In the Table, the value of “Prob. > F” for the model, the main effect of load, main effect of blend and second order effect of blend are all less than 0.05. So these terms are significant model terms.

Table 4.31 Reduce analysis of variance table and interaction fit for HC

Source	Sum of Squares	degree of freedom	Mean Square	F-Value	P value Prob > F
Model	172.18	3	57.39	626.12	< 0.0001
A-Load	6.02	1	6.02	65.64	< 0.0001
B-(NM-BU20)	162.00	1	162.00	1767.27	< 0.0001
B ²	4.17	1	4.17	45.45	0.0001
Residual	0.73	8	0.092		
Cor Total	172.92	11			
Std. Dev.	0.30		R-Squared		0.9958
Mean	27.08		Adj R-Squared		0.9942
C.V. %	1.12		Pred R-Squared		0.9914
PRESS	1.49		Adeq Precision		62.356

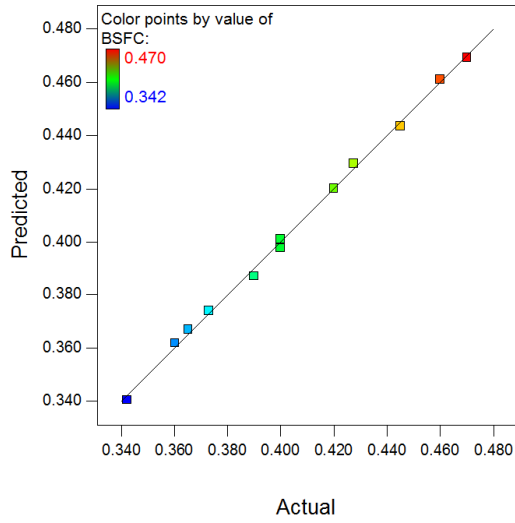
The R² value is equal to 0.9958 and is indicative of the accuracy and exactness of the model in finding the desired responses. Table 4.31 shows that Pred-R² of 0.9914 is in reasonable agreement with the Adj-R² of 0.9942; i.e. the difference is less than 0.2. For the developed HC model, the value of Adequate Precision is 62.356, which shows significant precision of the model. The final empirical model for HC in terms of coded and actual factors is given by Eqs. 4.35 and 4.36 respectively.

$$HC=26.25 + 0.95 \times A + 4.5 \times B + 1.25 \times B^2 \quad (4.35)$$

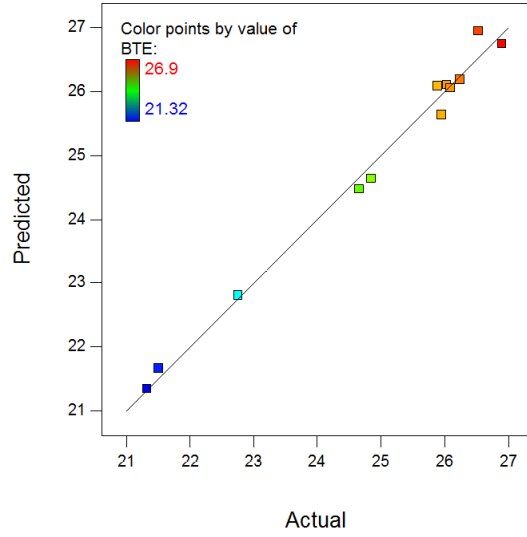
$$HC=19.4 + 0.158333 \times Load - 0.5 \times (NMBU20) + 1.25 \times (NMBU20)^2 \quad (4.36)$$

4.5.2.3 Comparison of observed and estimated responses for NM-BU20 blends

Figs. 4.58 and 4.59 show the plot between the actual and predicted values of BSFC, BTE, smoke, NO_x, CO and HC. These plots clearly show that the values of actual data and predicted data are quite close to each other. This implies that the model is significant. It can also be observed from the plots that most of the points are clustered around 45° line. This gives an indication of a fairly good least square fit for the responses.

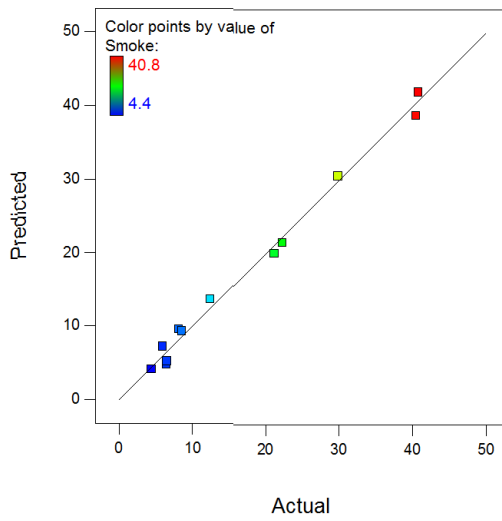


(a)

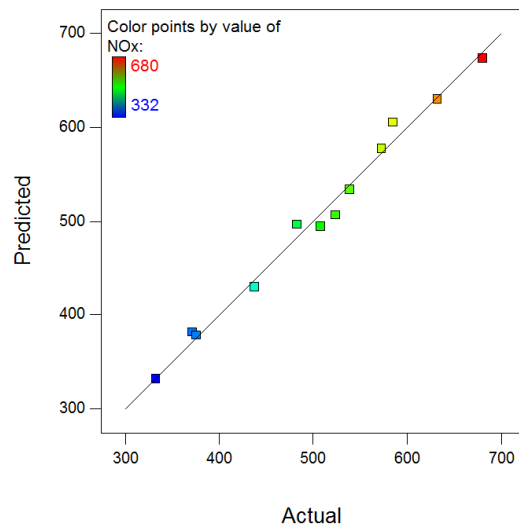


(b)

Fig. 4.58 Plot of actual values vs. predicted values for (a) BSFC and (b) BTE



(a)



(b)

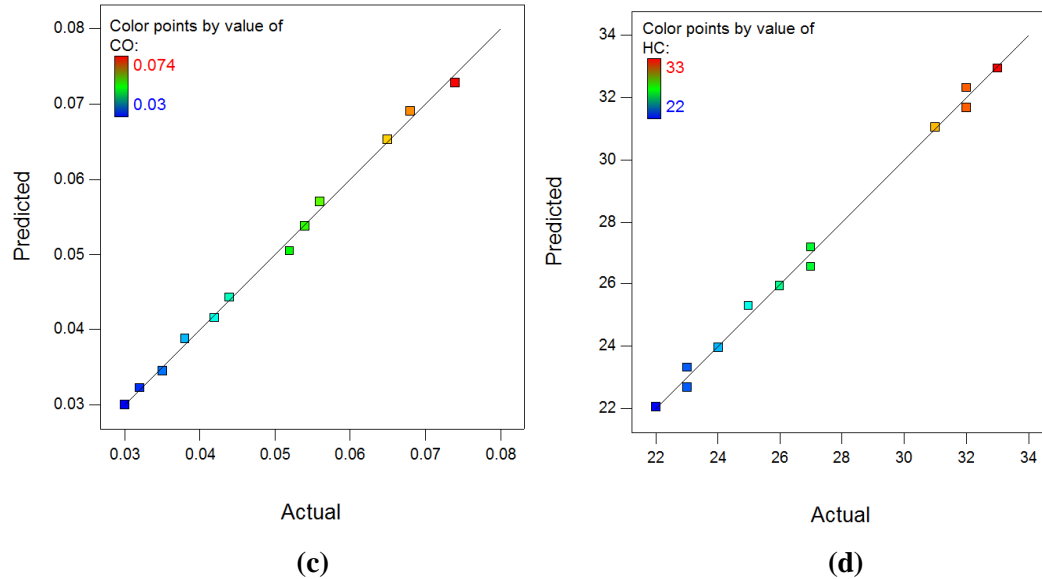


Fig. 4.59 Plot of actual values vs. predicted values for (a) Smoke (b) NO_x (c) CO and (d) HC

4.5.3 Performance of engine using nitromethane-n-butanol-Diesel (NM-BU20) blends

The results of engine performance tests for BSFC and BTE were recorded and have been presented in this section using scattered diagrams from observed data of experiments and 3D surface plots & factor-response graphs from mathematical models.

4.5.3.1 Brake specific fuel consumption (BSFC)

It can be seen from Fig.4.60 (a) that the BSFC reduces with increasing load, and is lowest at full load. Fig. 4.72 shows that BSEC is higher for all NM-BU20 blends in comparison to BU20. Blending of NM results in increased BSFC up to 9 % than that of BU20 at full load condition. The most probable reason for this is the lower energy density of this additive. However, NM1BU20 has marginally lower BSFC than BU20 as compared to NM2BU20 and NM3BU20. The increment of BSFC with nitromethane has been supported by some previous studies too [126][113]. The Fig. 4.60 (b) shows similar trends of BSEC as of BSFC in Fig. 4.60 (a).

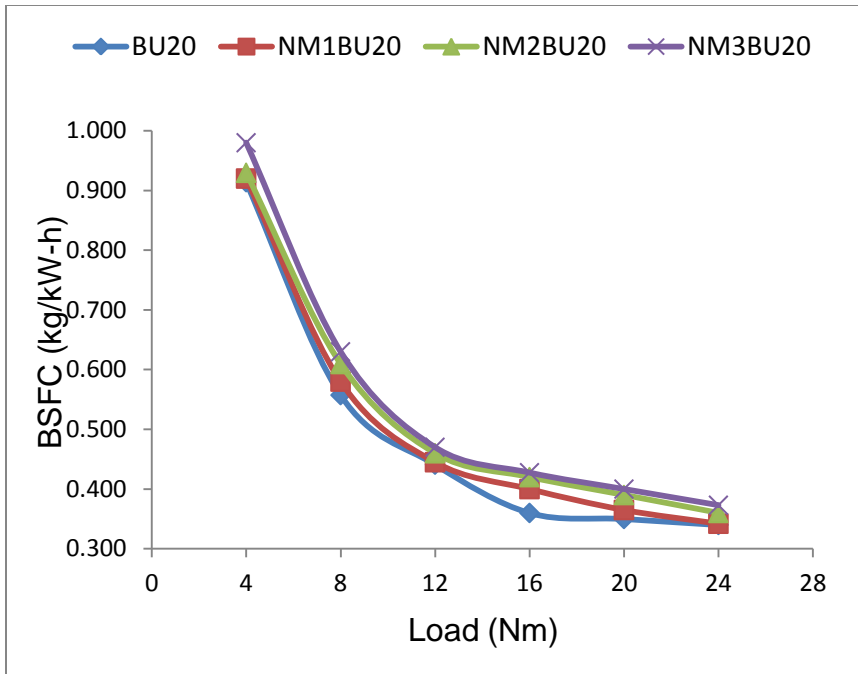


Fig. 4.60 (a) Variation of BSFC with engine load for NM-BU20 blends

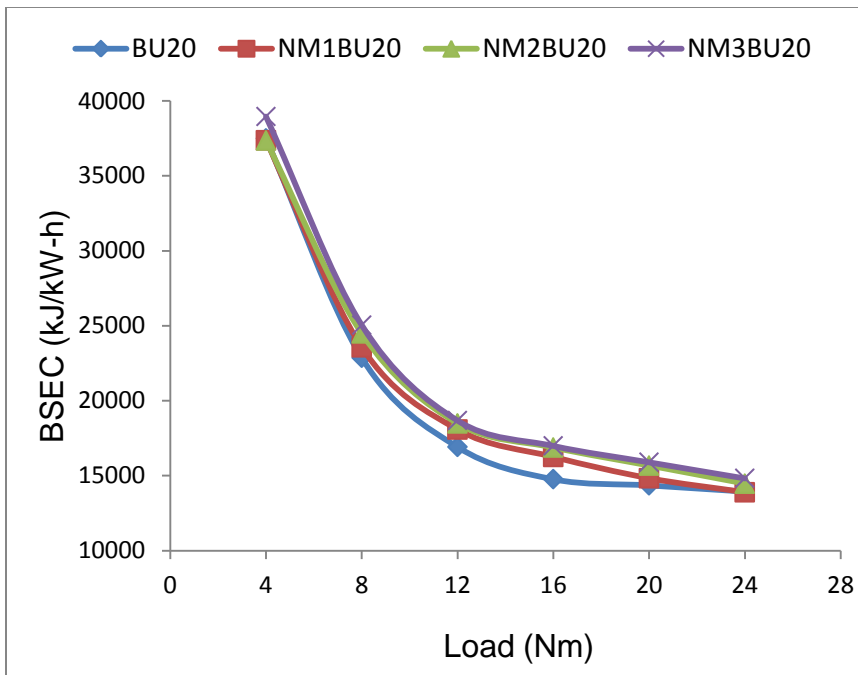


Fig. 4.60 (b) Variation of BSFC with engine load for NM-BU20 blends

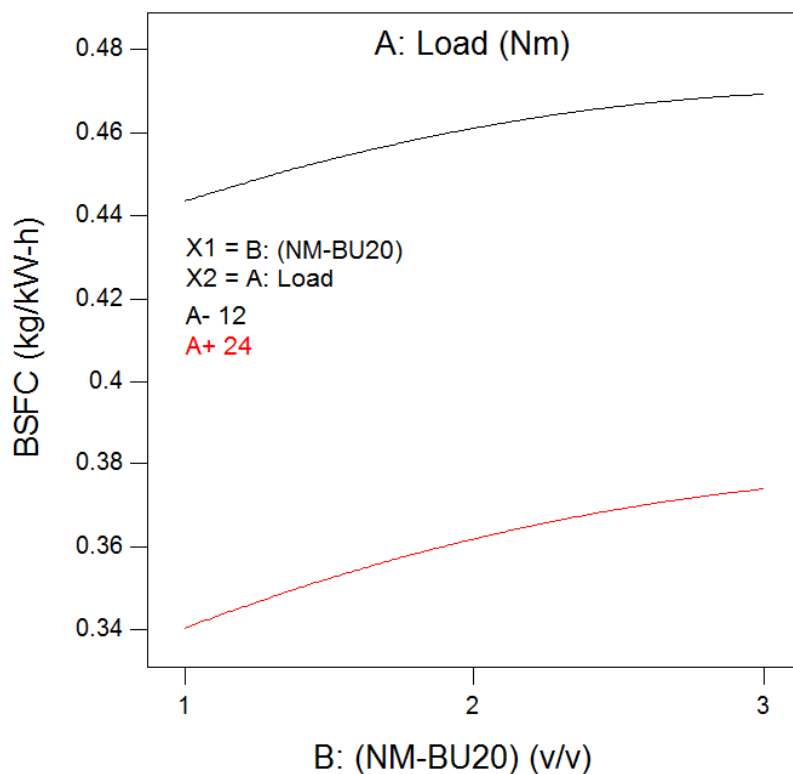


Fig. 4.61 Variation in BSFC with NM-BU20 blends at medium and full load

It can be observed from Fig. 4.61 that trends of BSFC are same at moderate load and maximum load.

4.5.3.2 Brake thermal efficiency

Fig. 4.62 shows the trends of BTE and Fig.4.72 shows the value of BTE at full load condition. It can be observed that BTE for NM-BU20 blends are slightly higher as compared to BU20. The highest BTE is observed for NM3BU20 among tested fuels. The maximum gain is of 4.21% at full load condition. The brake thermal efficiency of NM blended fuel is high because of lower boiling temperature (100°C as compared to 150°C and 118°C of diesel and n-butanol respectively). The atomization and the spray quality of the NM-blended fuel is better due to lower boiling temperature. Besides, higher BTE is also generally associated with availability of higher oxygen in nitroparaffins [155], [156]. These additives are thus found to nudge combustion towards yielding higher energy output.

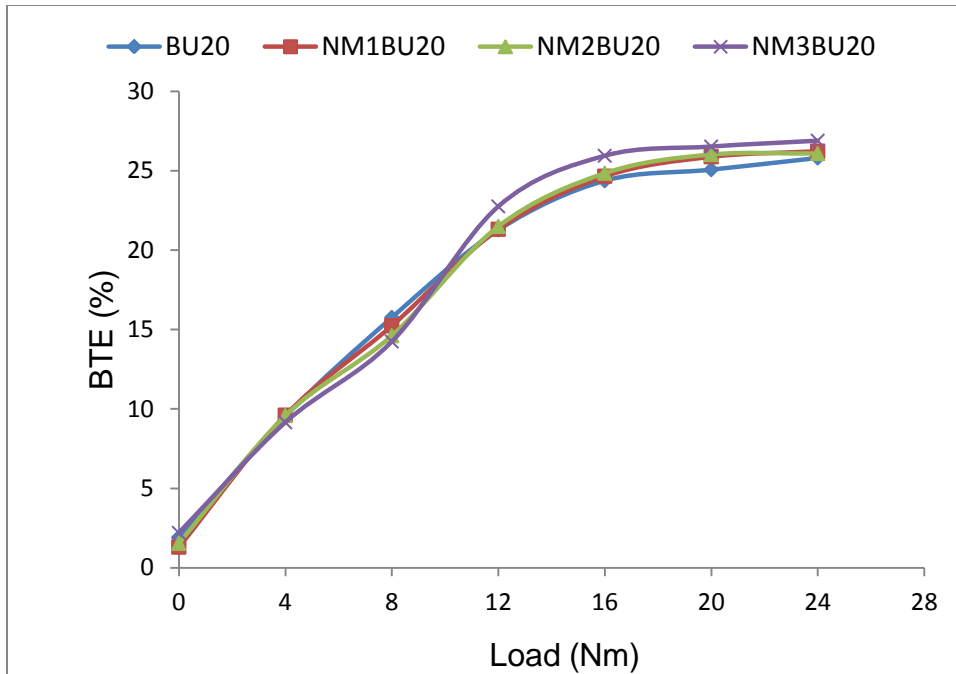


Fig. 4.62 Variation of BTE with engine load for NM-BU20 blends

Fig. 4.63 shows variations of BTE with nitromethane blending at medium and maximum load conditions. It can be observed from the figure that the rate of increment in BTE is higher at moderate loads as compared to higher loads.

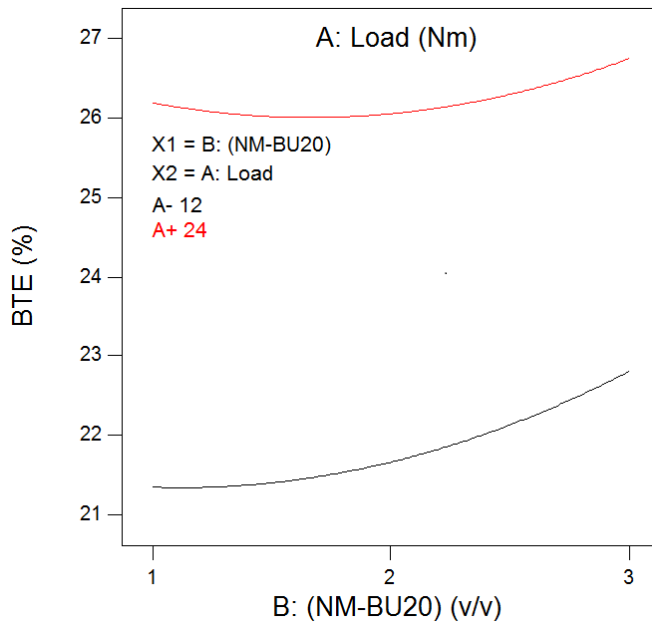


Fig. 4.63 Variation in BSFC with NM-BU20 blends at medium and full load

4.5.4 Emissions of engine using nitromethane-n-butanol-diesel (NM-BU20) blends

4.5.4.1 Variation of Smoke

Figs. 4.64 and 4.65 show the variations of smoke emission for NM-BU20 blends for experimental results and predicted model.

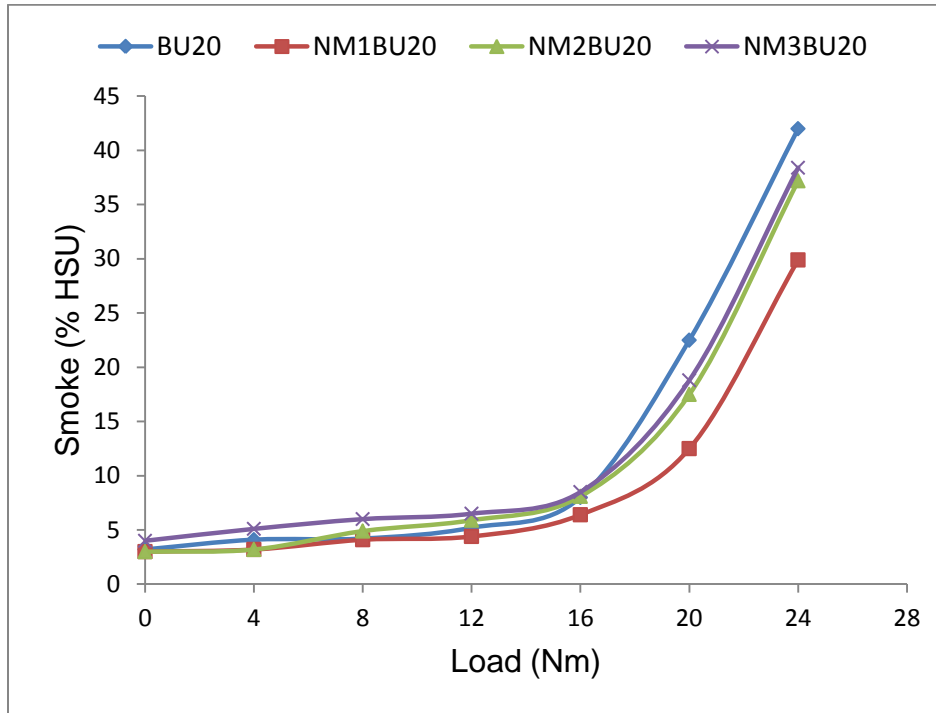


Fig. 4.64 Variation in smoke for NM-BU20 blends

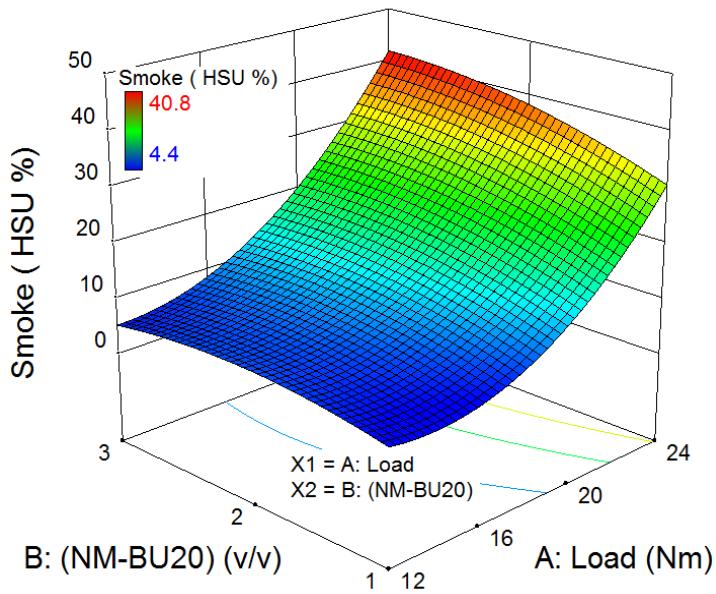


Fig. 4.65 Variation in smoke due to combined effect of load and NM blending

Significant reduction in smoke was observed for NM1BU20. Smoke reduces up to 28.8% for NM1BU20 as compared to BU20 at full load condition. The smoke reduction is associated with two factors: (i) Higher oxygen content of nitromethane (52.4% by weight) enrich the blended fuel with more oxygen. In nitromethane the O₂ is strongly bonded to carbon. In the premixed zone, reactions are not capable of breaking this bond; thus carbon is not available to participate in combustion reactions that lead to production of carboneous compounds (smoke). (ii) The other factor affecting smoke generation is the higher latent heat of vaporization of the blended fuel. Because of high heat of vaporization of NM, more hot air is required to reach auto ignition temperature, and this reduces the overall equivalence ratio (i.e. it leads to a leaner mixture). Both of these factors (oxygen enrichment and latent heat of vaporization) result in decreased smoke in premixed zone, which in turn, reduce the smoke emission for NMBU20 blends [126], [130].

4.5.4.2 Variation of NO_x

Figs. 4.66 and 4.67 show the variations of NO_x emission for n-butanol-diesel blends for experimental results and predicted model.

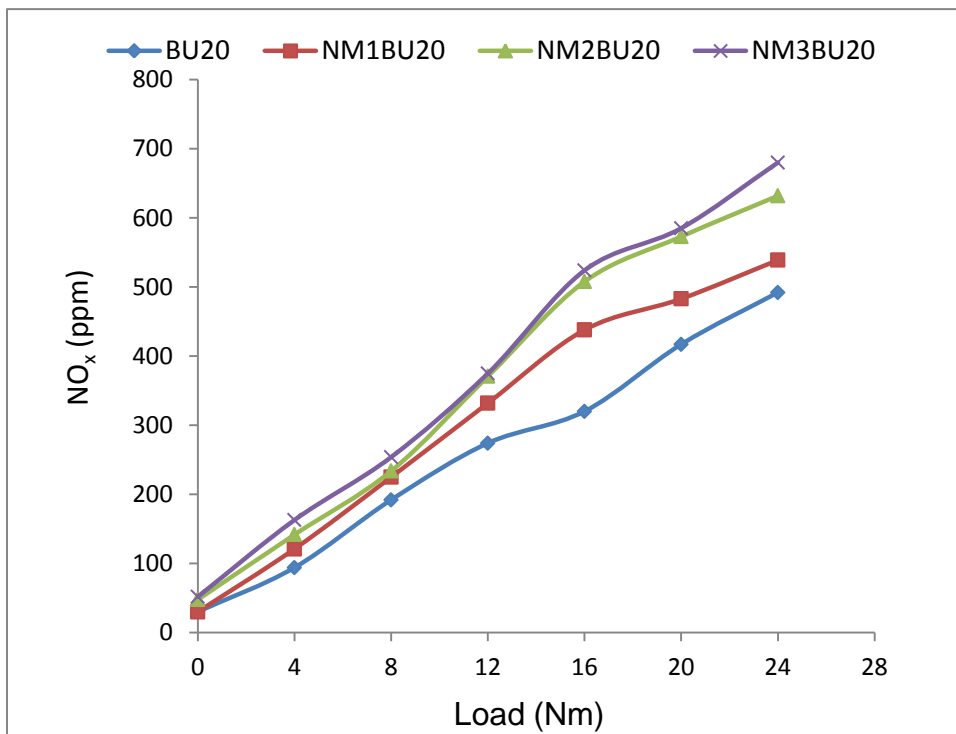


Fig. 4.66 Variation in NO_x for NM-BU20 blends

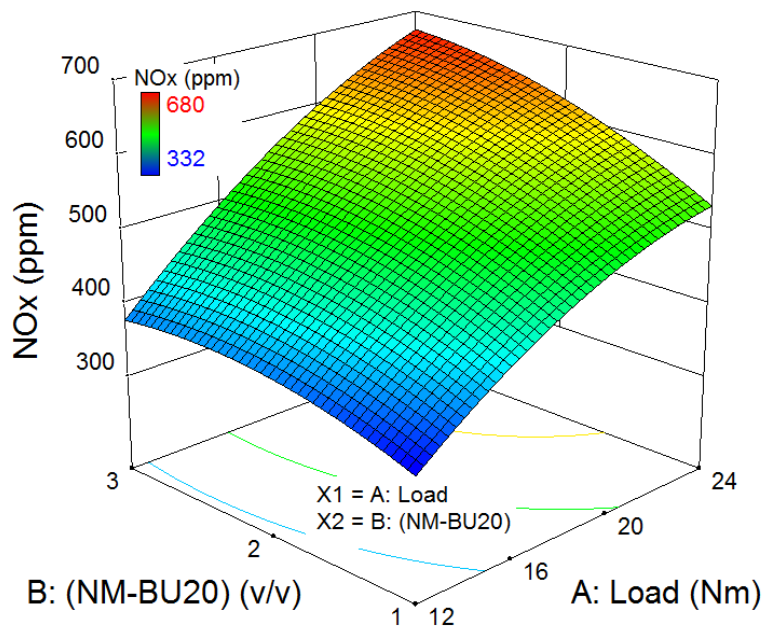


Fig. 4.67 Variation in NO_x due to combined effect of load and NM blending

Figs. 4.66 and 4.67 show increment in NO_x with load and NM-BU20 blends. NO_x increases with load and percentage of NM in blended fuel. A significant increment in NO_x can be observed for 3% NM at full load condition. The increment of maximum temperature in combustion chamber due to better combustion with NM leads to increase in NO_x formation (this is also reflected by increased BTE). The increased NO_x is mainly due to thermal NO_x, and not due to the nitrogen available in NM [126]. Nitromethane is a Cetane number improver that reduces the ignition lag. In general, Cetane improver reduces NO_x because of lesser availability of fuel in a short duration. However, NM behaves differently and increases NO_x when used in fuel due to fast burning rate. Changed distribution of NO and NO₂ is another probable reason of variation of total NO_x in case of NM [14], [131]. The results indicating increasing smoke and NO_x with nitromethane follow the general trends and are supported by previous studies as discussed in the introduction (such as [14], [126], [129], [131]).

4.5.4.3 Variation of CO

Figs. 4.68 and 4.69 show the variations of CO emission for NM-BU20 blends for experimental results and predicted model. It can be observed from Fig. 4.68 and Fig. 4.72

that CO emission is lesser for NM1BU20; same for NM2BU20; and higher for NM3BU20 as compared to BU20 at full load condition.

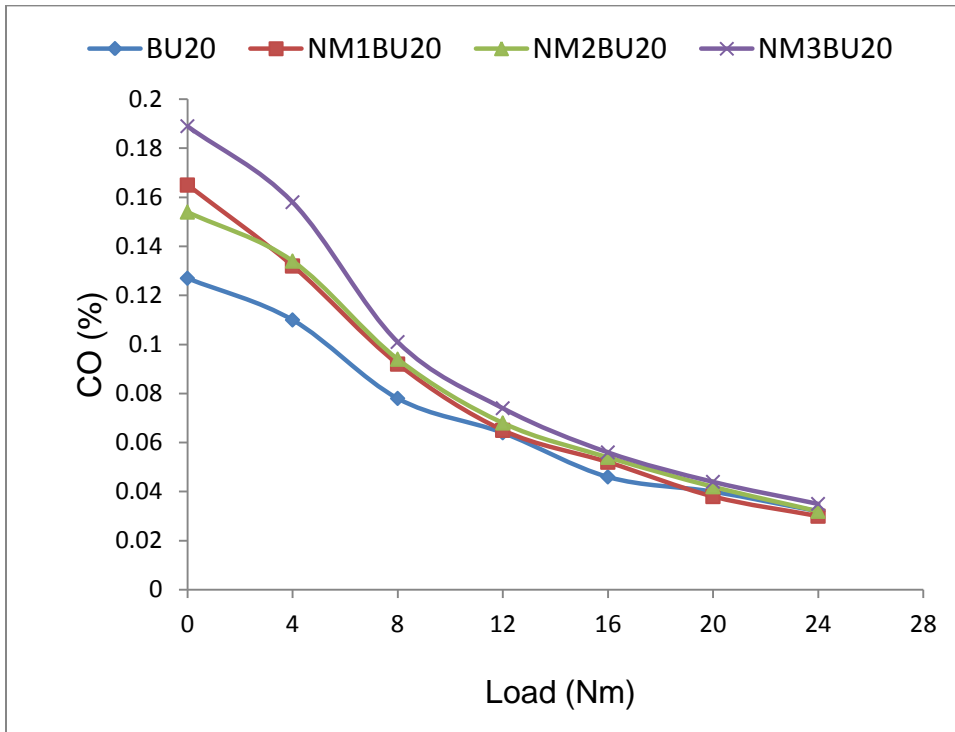


Fig. 4.68 Variation in CO for NM-BU20 blends

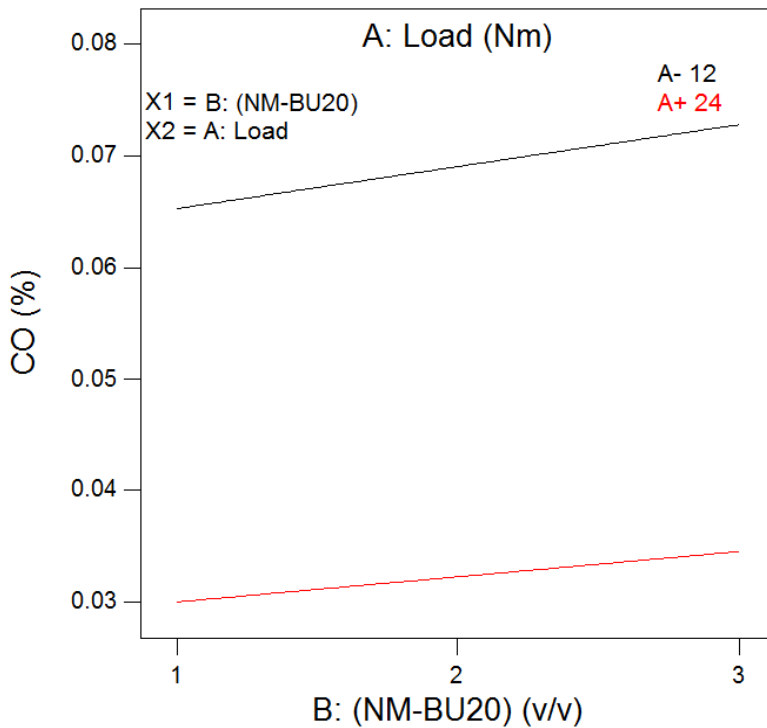


Fig. 4.69 Variation in CO with NM-BU20 blends at medium and full load

Fig. 4.69 shows trends of CO emission using NM-BU20 blends for predicted model. It can be observed that with the increase of NM in blended fuel, CO increases. CO is the intermediate product, which is produced during the combustion process. Low oxygen concentration, low reaction temperature and short reaction time are the probable reasons of the generation of CO. The addition of NM enhances O₂ concentration and combustion reactions and results in low CO emission. On the other hand, at higher percentage of NM, the ignition delay is reduced so much that there is insufficient time for complete combustion. This in turn results in higher emission of CO.

4.5.4.4 Variation of HC

Figs. 4.70 and 4.71 show the variations of HC emission for NM-BU20 blends for experimental results and predicted model.

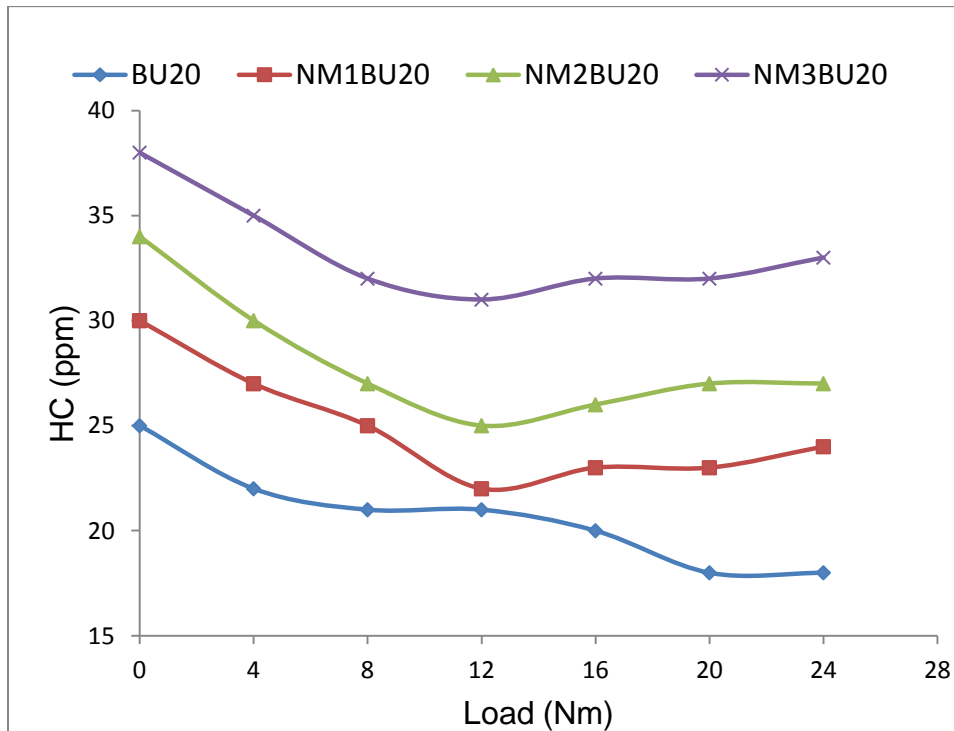


Fig. 4.70 Variation in HC for NM-BU20 blends

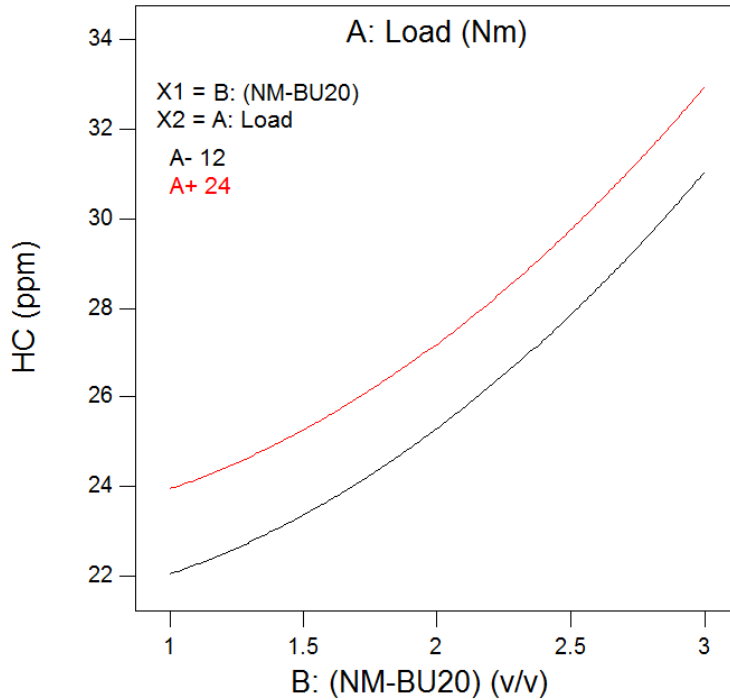


Fig. 4.71 Variation in HC with NM-BU20 blends at medium and full load

When the engine load increases, emission of HC decreases initially up to half of the full-load and then increases up to full load condition for all NM-BU20 blends. However, for BU20, HC slightly increases near to half of full load and then again decreases. As already discussed, the premixed combustion duration shortens and the diffusion combustion duration extends with addition of NM in fuel. Non-homogeneous mixture during the diffusion combustion process generates more HC. It can be observed from Fig. 4.72 that the emission of HC for all blends is higher as compared to that of BU20. Expansion of lean flame-out region due to increased oxygen in the fuel is another cause of increased unburned HC [70], [153]. An increment of 33.33% in HC can be observed from Fig. 4.72 for NM1BU20 compared to that of BU20. Most of the studies cited in the introduction are consistent with this result (i.e. increased HC).

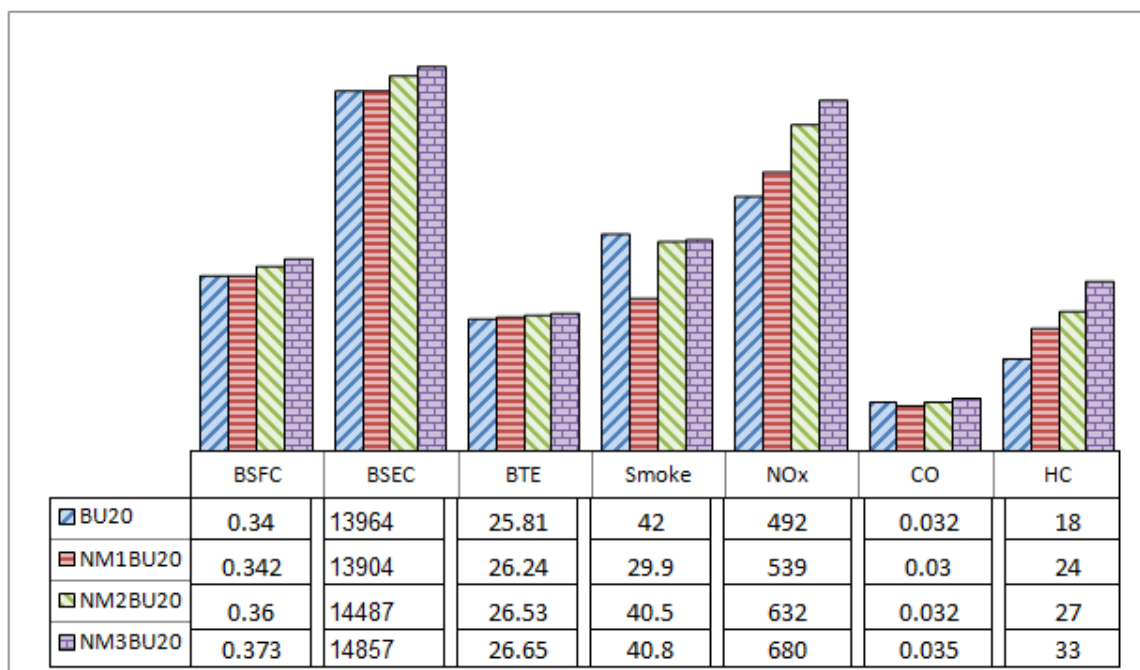


Fig. 4.72 Performance and emission of NM-BU20 blends (100% rated power)¹

4.5.5 Validation and optimization of responses

The parameters were optimized for desired values of responses. Table 4.32 summarizes the minimum and maximum values of each response to optimize operating parameters of the engine. On the basis of Table 4.32 and optimization analysis, the optimum blended fuel and their predicted responses were obtained, and are shown in Table 4.33. The test was repeated at very near to optimum values of load (21.5 Nm) and blend (1% NMBU20) to validate the results predicted by the models. The optimum values of BSFC, BTE, smoke, NO_x, CO and HC were observed to be 0.356, 26.48, 18.6, 518, 0.035 and 23 respectively. It can also be observed from Table 4.33 that the percentage errors of these results are within tolerance. This shows the exactness of predicted model. On the basis of the validation of experimental results by mathematical modeling, NM1BU20 (1% Nitromethane in BU20) was selected as the optimum blend of NM with BU20.

¹Fig. is not on scale.

Table 4.32 Maximum and minimum limits for each response to optimize performance and emissions for NM-BU20 blends

Names	Goal	Lower limit	Upper limit
A: Load	Is in range	12	24
B: Blend (NM-BU20)	Is in range	1	3
Response: BSFC	Minimize	0.342	0.47
Response: BTE	Maximize	21.32	26.9
Response: Smoke	Minimize	4.4	40.8
Response: NO _x	Minimize	332	680
Response: CO	Minimize	0.03	0.074
Response: HC	Minimize	22	33

Table 4.33 Optimum conditions of load and blend and their predicted results for NM-BU20 blends

Number	Load	(NM-BU20)	BSFC	BTE	Smoke	NO _x	CO	HC
1	<u>21.251</u>	<u>1.000</u>	<u>0.358</u>	<u>26.286</u>	<u>18.076</u>	<u>511.806</u>	<u>0.036</u>	<u>23.515</u> Selected
2	21.332	1.000	0.357	26.294	18.388	512.659	0.036	23.528
3	21.644	1.000	0.355	26.317	19.632	515.861	0.035	23.577
4	21.802	1.000	0.354	26.325	20.284	517.417	0.034	23.602
5	22.091	1.000	0.352	26.333	21.502	520.127	0.034	23.648
Confirmation test	21.5	1.0	0.356	26.48	18.6	518	0.035	23
Error Percentage (× 100)			0.56	-0.74	-2.90	-1.21	2.78	2.19

4.6 Performance and emissions characteristics of the engine using diglyme-BU20 blends:

The tests were conducted using 2-Methoxyethyl ether/Diglyme (DGM) as additive in BU20 in different proportions with the following engine settings: 19.5 compression ratio (CR), 23° CA btdc injection timing and 210 bar injection pressure. The variations in engine performance and emissions for the blends were noted at different load conditions (no load to 100% rated power) and are presented in the form of scattered curves in this section. It was observed from these scattered diagrams that the variations in performance

and emissions of blends with respect to each other are noticeable at higher loads only. Thus, mathematical modeling has been done for higher load observations only (50% of full load to 100% of full load).

4.6.1 Determination of optimum blend of diglyme-BU20 (DGM-BU20)

To find out the optimum DGM-BU20 blend, the following approach was adopted: (i) Firstly the selected data of experiments was fed to DOE software and ANOVA was done to check the significance of model and individual terms. (ii) The curves from actual experiments and surface response model were analyzed to see effect of change of factors on response. (iii) Optimization and verification of predicated model was done by confirmation test. 3D surface curves were drawn for all instances where interaction effect of factors was found to be significant. Otherwise, 2D curves of factors with response were drawn.

4.6.2 Modeling for diglyme-n-Butanol (20%)-diesel (DGM-BU20) blends

Full Factorial design was employed for the development of prediction models of BSFC, BTE, smoke, NO_x, CO and HC in terms of engine load and blending ratio. An attempt was made to optimize the factors for the desired value of responses (BSFC, BTE, smoke, NO_x, CO and HC). Table 4.34 shows the engine operating parameters and their levels, and Table 4.35 shows the design matrix for selected experimentation.

Table 4.34 Parameters and their levels according to Factorial design for Diglyme-BU20 blends

Parameter	symbol	Levels			
		1	2	3	4
Load (Nm)	A (Load)	12	16	20	24
DGMBU20 Blend (% v/v)	B (Blend)	5	10	15	20

Table 4.35 Design layout and experimental results for Diglyme-BU20 blends

	Factor 1	Factor 2	Response 1	Response 2	Response 3	Response 4	Response 5	Response 6
Run	A:LOAD (Nm)	B:DGM-BU20 BLEND(v/v)	BSFC (kg/kW-h)	BTE (%)	SMOKE (HSU %)	NOx (ppm)	CO (%)	HC (ppm)
3	12	5	0.463	17.86	9.2	270	0.073	22
11	16	5	0.406	21.18	19.4	308	0.056	22
2	20	5	0.368	23.18	38.1	412	0.048	22
14	24	5	0.356	24.12	56.4	488	0.04	23
12	12	10	0.472	18.93	6.8	266	0.095	26
1	16	10	0.42	22	9.4	300	0.078	25
9	20	10	0.378	23.6	24.1	400	0.068	25
7	24	10	0.367	25.16	44.1	465	0.058	26
16	12	15	0.484	21.98	4.9	248	0.09	25
4	16	15	0.427	24.8	7.1	296	0.068	24
10	20	15	0.386	26.4	13	392	0.058	24
8	24	15	0.369	27.6	30	445	0.047	25
6	12	20	0.497	20.37	6	292	0.102	27
15	16	20	0.436	22.37	7.8	344	0.075	25
5	20	20	0.401	23.83	17	432	0.065	25
13	24	20	0.378	24.96	32	498	0.055	26

The details of 16 experiments suggested by DOE from performed experiments are shown in Table 4.35 along with the run order selected at random. These data were used as inputs in the Design Expert 8.0.4.1 software for further analysis.

4.6.2.1 Diagnosis of data for analysis of variance for DGM-BU20 blends

Figs. 4.73 to 4.78 show plots of normal probability vs. internal studentized residuals and internal studentized residuals vs. predicted values for BSFC, BTE, smoke, NO_x, CO and HC emission respectively when the engine was operated on DGM-BU20 blends.

It can be observed from normal probability plots that most of the interaction points are accumulated along a straight line, which implies that residuals follow normal distribution and hence, the fitted model is adequate for a real system.

For the assumption of constant variance to be true in ANOVA, the internal residuals vs. predicted plot should be a random scatter. Figs. 4.73 (b), 4.74, (b), 4.75 (b), 4.76 (b), 477

(b) and 4.78 (b) reveal no obvious pattern or unusual structure, indicating the validity assumption to be true. It was thus projected that for all the responses, the variance of the observed data is constant and hence is satisfactory.

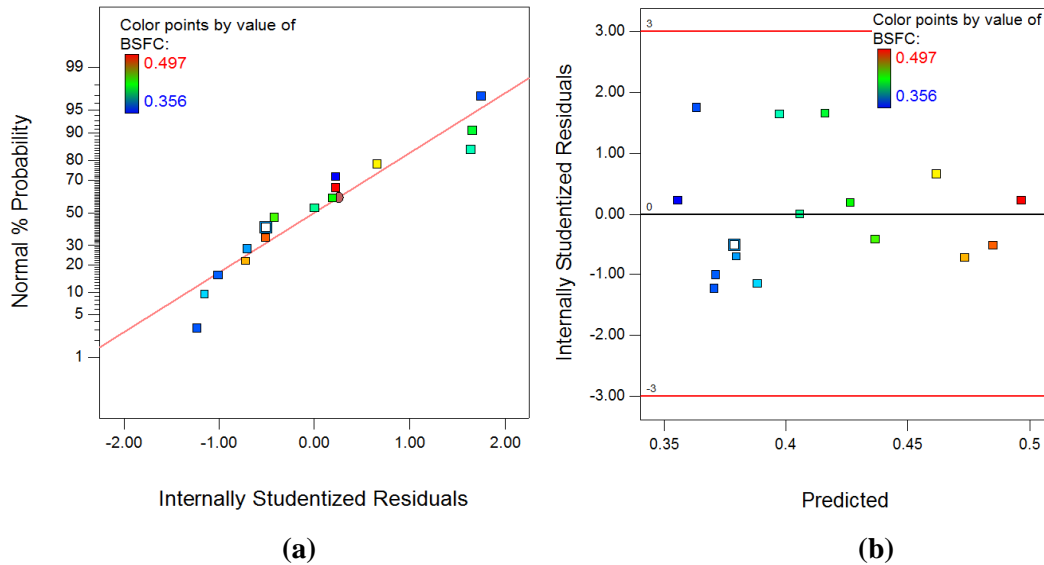


Fig. 4.73 (a) Plot of normal % probability vs. internal studentized residuals for BSFC
(b) Plot of internal studentized residuals vs. predicted response for BSFC

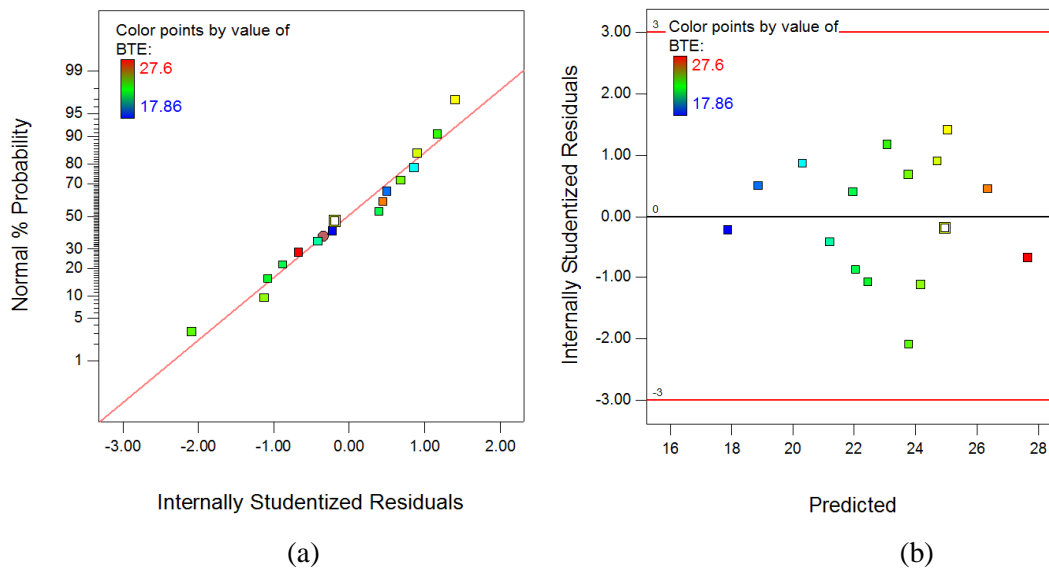


Fig. 4.74 (a) Plot of normal % probability vs. internal studentized residuals for BTE
(b) Plot of studentized internal residuals vs. predicted response for BTE

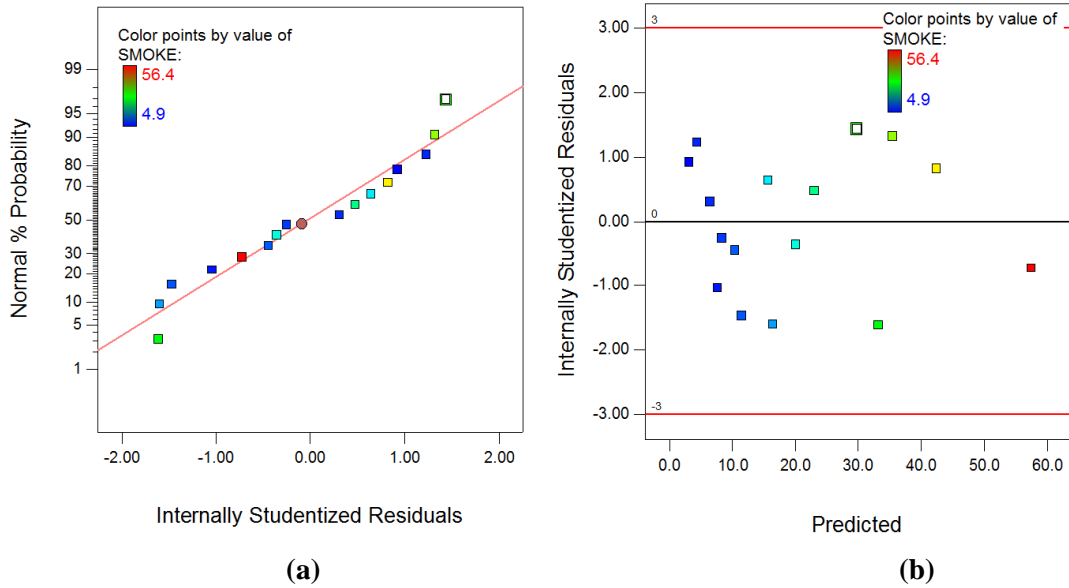


Fig. 4.75 (a) Plot of normal % probability vs. internal studentized residuals for smoke
(b) Plot of internal studentized residuals vs. predicted response for smoke

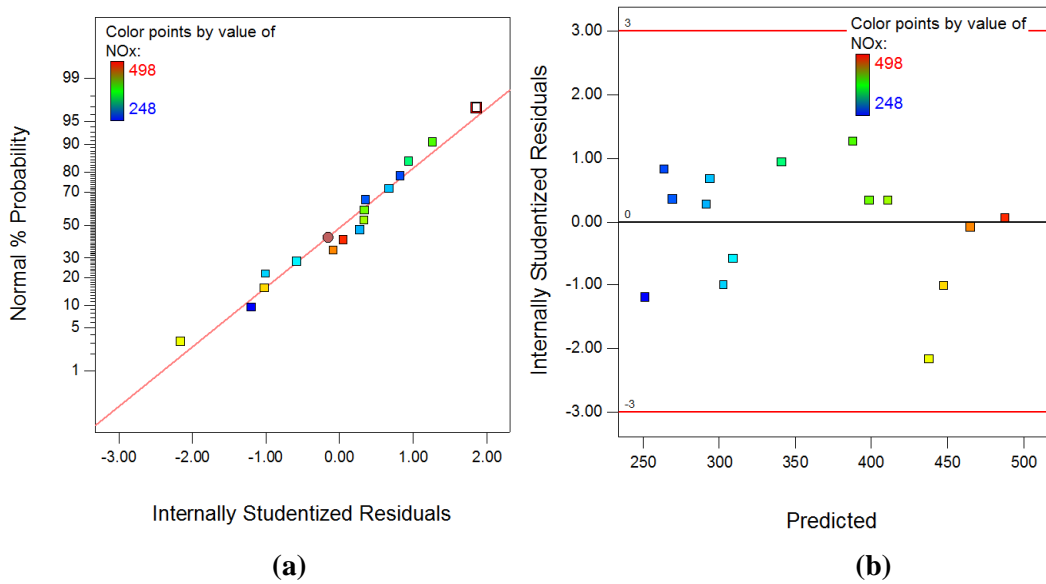


Fig. 4.76 (a) Plot of normal % probability vs. Internal studentized residuals for NO_x
(b) Plot of internal studentized residuals vs. predicted response for NO_x

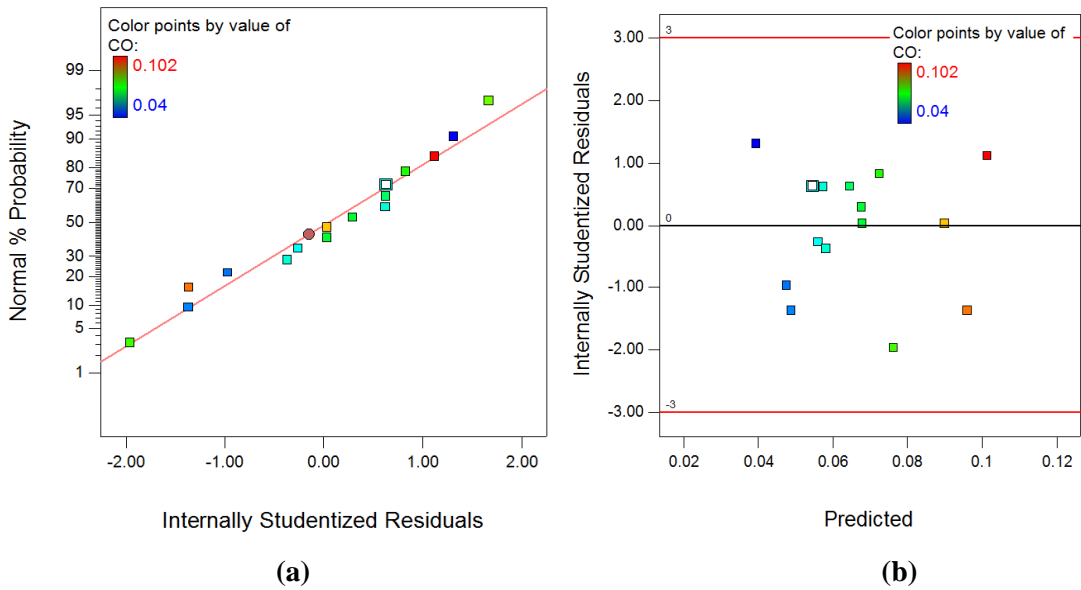


Fig. 4.77 (a) Plot of normal % probability vs. internal studentized residuals for CO
(b) Plot of internal studentized residuals vs. predicted response for CO

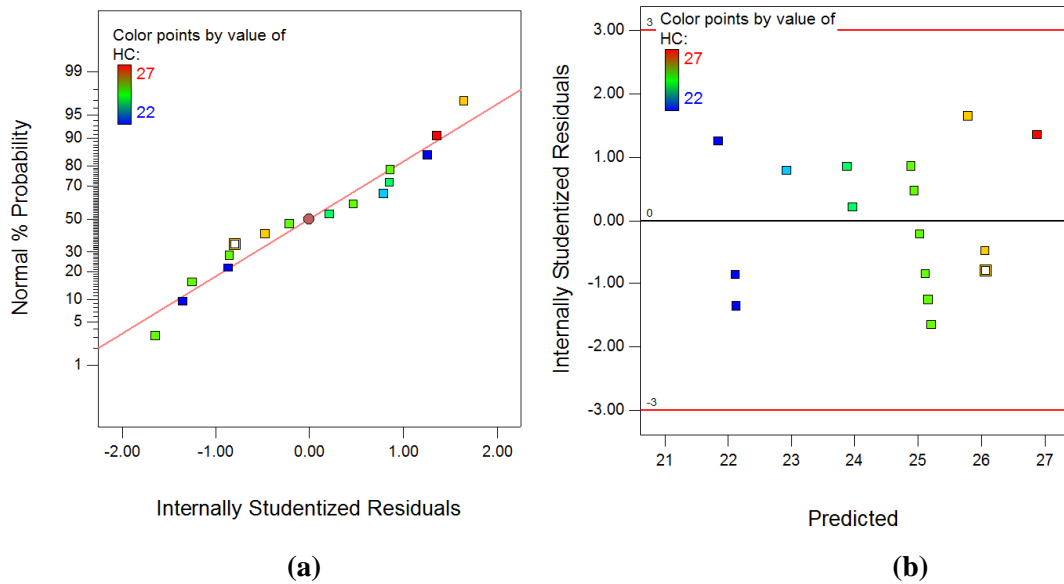


Fig.4.78 (a) Plot of normal % probability vs. internal studentized residuals for HC
(b) Plot of internal studentized residuals vs. predicted response for HC

4.6.2.2 ANOVA for response surface model for DGM-BU20 blends

Tables 4.36 to 4.41 are ANOVA tables for the response surface prediction models of BSFC, BTE, smoke, NO_x, CO and HC respectively. These have been obtained by using the backward elimination procedure for removing insignificant terms. In the present work, ANOVA analysis was carried out for a significance level of $\alpha = 0.05$, i.e. for a

confidence level of 95%.

Table 4.36 presents the ANOVA table for Response Surface Quadratic model for BSFC. In the Table, the value of “Prob. > F” for the model is 0.0001, which is less than 0.05, indicating that the model is significant, i.e. the terms in the model have a significant effect on BSFC. In the same manner, the value of “Prob. > F” for the main effect of load, blend, interaction effect of load and blend and second order effect of load were also found to be less than 0.05. So these terms are also significant model terms.

Table 4.36 Reduce analysis of variance table and interaction fit for BSFC

Source	Sum of Squares	Degree of freedom	Mean Square	F-Value	p-value Prob > F
Model	0.031	4	7.871E-003	1329.19	< 0.0001
A-LOAD	0.017	1	0.017	2799.96	< 0.0001
B-DGMBU20 BLEND	1.862E-003	1	1.862E-003	314.51	< 0.0001
AB	4.096E-005	1	4.096E-005	6.92	0.0234
A ²	1.681E-003	1	1.681E-003	283.87	< 0.0001
Residual	6.514E-005	11	5.922E-006		
Cor Total	0.032	15			
Std. Dev.	2.433E-003		R-Squared		0.9979
Mean	0.41		Adj R-Squared		0.9972
C.V. %	0.59		Pred R-Squared		0.9963
PRESS	1.181E-004		Adeq Precision		103.649

The R-Squared (R²) value is equal to 0.9979. Its nearness to 1 for the model is indicative of the accuracy and exactness of the model in finding the desired responses. The Pred-R² of 0.9963 is in reasonable agreement with the Adj-R² of 0.9972; i.e. the difference is less than 0.2. For the developed BSFC model, the value of Adequate Precision is 103.649, which shows high precision of the model. The final empirical model for BSFC in terms of coded and actual factors is given by Eqs. 4.37 and 4.38 respectively.

$$BSFC = 0.409837 - 0.057945 \times A + 0.014475 \times B - 0.00288 \times AB + 0.0230625 \times A^2 \quad (4.37)$$

$$BSFC = 0.7373 - 0.0316 \times Load + 0.003082 \times DGMBU20 - 6.4e-005 \times Load \times DGMBU20 + 0.000640625 \times Load^2 \quad (4.38)$$

Table 4.37 presents the ANOVA table for Response Surface Cubic model for BTE. In the Table, the value of “Prob. > F” for the model is 0.0001, which is less than 0.05, indicating that the model is significant, i.e. the terms in the model have a significant effect on BTE. In the same manner, the value of “Prob. > F” for main effect of load, blend, interaction effect of load & blend, second order effect of load and blend, second order of load and main effect of blend, second order of blend and main effect of load and cubic effect of load and blend were also found to be less than 0.05. So these terms are also significant model terms.

Table 4.37 Reduce analysis of variance table and interaction fit for BTE

Source	Sum of Squares	Degree of freedom	Mean Square	F-Value	p-value Prob > F
Model	102.35	9	11.37	740.10	< 0.0001
A-LOAD	3.19	1	3.19	207.49	< 0.0001
B-DGMBU20 BLEND	9.25	1	9.25	602.01	< 0.0001
AB	0.43	1	0.43	28.08	0.0018
A ²	0.74	1	0.74	48.06	0.0004
B ²	14.07	1	14.07	915.71	< 0.0001
A ² B	0.24	1	0.24	15.89	0.0072
AB ²	0.094	1	0.094	6.11	0.0484
A ³	0.092	1	0.092	6.02	0.0496
B ³	9.86	1	9.86	641.40	< 0.0001
Residual	0.092	6	0.015		
Cor Total	102.45	15			
Std. Dev.	0.12		R-Squared		0.9991
Mean	23.02		Adj R-Squared		0.9978
C.V. %	0.54		Pred R-Squared		0.9937
PRESS	0.64		Adeq Precision		99.828

The R-Squared (R^2) value is 0.9991 and is thus indicative of the accuracy and exactness of the model in finding the desired responses. The Pred- R^2 is 0.9937, which is in reasonable agreement with the Adj- R^2 of 0.9978; i.e. the difference is less than 0.2. For the developed BTE model, the value of Adequate Precision is 99.828, which shows high precision of the model. The final empirical model for BTE in terms of coded and actual factors is given by Eqs. 4.39 and 4.40 respectively.

$$BTE = 25.4734 + 2.20349 \times A - 3.23719 \times B - 0.72405 \times AB - 0.648562 \times A^2 - 9.66938 \times B^2 + 0.372938 \times A^2B - 0.231187 \times AB^2 + 0.3825 \times A^3 - 3.94875 \times B^3 \quad (4.39)$$

$$BTE = -1.35275 + 3.67904 \times Load - 2.70903 \times DGMBU20 - 0.04184 \times Load \times DGMBU20 - 0.137812 \times Load^2 + 0.33183 \times (DGMBU20)^2 + 0.00138125 \times Load^2 \times DGMBU20 - 0.000685 \times Load \times (DGMBU20)^2 + 0.00177083 \times Load^3 - 0.00936 \times (DGMBU20)^3 \quad (4.40)$$

Table 4.38 presents the ANOVA table for Response Surface Quadratic model for smoke emission. In the Table, the value of “Prob. > F” for the model, the main effect of load and blend, interaction effect of load and blend and second order effect of load and blend are less than 0.05. So these terms are significant model terms.

Table 4.38 Reduce analysis of variance and interaction fit for Smoke

Source	Sum of Squares	Degree of Freedom	Mean Square	F-Value	p-value Prob. > F
Model	3633.25	5	726.65	121.02	< 0.0001
A-LOAD	847.88	1	847.88	141.21	< 0.0001
B-DGMBU20 BLEND	1.03	1	1.03	0.17	0.6880
AB	175.17	1	175.17	29.17	0.0003
A ²	178.89	1	178.89	29.79	0.0003
B ²	135.14	1	135.14	22.51	0.0008
Residual	60.05	10	6.00		
Cor Total	3693.29	15			
Std. Dev.	2.45		R-Squared		0.9837
Mean	20.33		Adj R-Squared		0.9756
C.V. %	12.05		Pred R-Squared		0.9494
PRESS	186.94		Adeq Precision		36.283

The R² value is equal to 0.9837 and is thus indicative of the accuracy and exactness of the model in finding the desired responses. Table 4.38 shows that Pred-R² of 0.9494 is in reasonable agreement with the Adj-R² of 0.9756; i.e. the difference is less than 0.2. For the developed smoke model, the value of Adequate Precision is 36.283, which shows high precision of the model. The final empirical model for smoke emission in terms of coded and actual factors is given by Eqs. 4.41 and 4.42 respectively.

$$SMOKE = 10.1675 + 13.1032 \times A + 0.8325 \times B - 5.95575 \times AB + 7.52344 \times A^2 + 6.53906 \times B^2 \quad (4.41)$$

$$SMOKE = 30.5375 - 3.02344 \times Load - 1.57545 \times DGMBU20 - 0.13235 \times Load \times DGMBU20 + 0.208984 \times Load^2 + 0.11625 \times (DGMBU20)^2 \quad (4.42)$$

Table 4.39 presents the reduce ANOVA table for Response Surface Cubic model for NO_x. In the Table, the value of “Prob. > F” for the model, the main effect of load & blend, interaction effect of load and blend, second order effect of load & blend, second order effect of load and main effect of blend, second order effect of blend and main effect of load and cubic effect of load and blend are less than 0.05. So these terms are significant model terms.

Table 4.39 Reduce analysis of variance table and interaction fit for NO_x

Source	Sum of Squares	Degree of Freedom	Mean Square	F-Value	p-value Prob. > F
Model	1.083E+005	9	12029.49	664.86	< 0.0001
A-LOAD	14313.05	1	14313.05	791.07	< 0.0001
B-DGMBU20 BLEND	4356.47	1	4356.47	240.78	< 0.0001
AB	22.82	1	22.82	1.26	0.3044
A ²	82.69	1	82.69	4.57	0.0764
B ²	1491.86	1	1491.86	82.45	0.0001
A ² B	120.05	1	120.05	6.64	0.0420
AB ²	80.00	1	80.00	4.42	0.0802
A ³	1479.20	1	1479.20	81.75	0.0001
B ³	708.05	1	708.05	39.13	0.0008
Residual	108.56	6	18.09		
Cor Total	1.084E+005	15			
Std. Dev.	4.25		R-Squared		0.9990
Mean	366.00		Adj R-Squared		0.9975
C.V. %	1.16		Pred R-Squared		0.9908
PRESS	999.93		Adeq Precision		72.505

The R² value is equal to 0.9990 and is thus indicative of the accuracy and exactness of the model in finding the desired responses. Table 4.39 shows that Pred-R² of 0.9908 is in reasonable agreement with the Adj-R² of 0.9975; i.e. the difference is less than 0.2. For the developed NO_x model, the value of Adequate Precision is 72.505, which shows high precision of the model. The final empirical model for NO_x in terms of coded and actual factors is given by Eqs. 4.43 and 4.44 respectively.

$$NO_x = 353.5 + 147.635 \times A + 70.25 \times B + 5.265 \times AB + 6.8625 \times A^2 + 99.5625 \times B^2 - 8.26875 \times A^2B + 6.75 \times AB^2 - 48.375 \times A^3 + 33.4688 \times B^3 \quad (4.43)$$

$$NO_x = 1331.7 - 215.16 \times Load + 20.8757 \times DGMBU20 + 0.5195 \times Load \times DGMBU20 + 12.8203 \times Load^2 - 2.755 \times (DGMBU20)^2 - 0.030625 \times Load^2 \times DGMBU20 + 0.02 \times Load \times (DGMBU20)^2 - 0.223958 \times Load^3 + 0.0793333 \times (DGMBU20)^3 \quad (4.44)$$

Table 4.40 presents the reduce ANOVA for Response Surface Cubic model for CO. In the Table, the value of “Prob. > F” for the model, the main effect of load, main effect of blend, interaction effect of load & blend, second order effect of load & blend, second order effect of load and main effect of blend and cubic effect of load and blend are less than 0.05. So these terms are significant model terms.

Table 4.40 Reduce analysis of variance table and interaction fit for CO

Source	Sum of Squares	Degree of Freedom	Mean Square	F-Value	p-value Prob > F
Model	4.674E-003	8	5.842E-004	548.91	< 0.0001
A-LOAD	1.643E-004	1	1.643E-004	154.38	< 0.0001
B-DGMBU20 BLEND	6.378E-005	1	6.378E-005	59.93	0.0001
AB	5.625E-005	1	5.625E-005	52.85	0.0002
A ²	1.058E-004	1	1.058E-004	99.41	< 0.0001
B ²	3.202E-004	1	3.202E-004	300.85	< 0.0001
A ² B	9.800E-006	1	9.800E-006	9.21	0.0190
A ³	2.645E-005	1	2.645E-005	24.85	0.0016
B ³	4.418E-004	1	4.418E-004	415.11	< 0.0001
Residual	7.450E-006	7	1.064E-006		
Cor Total	4.681E-003	15			
Std. Dev.	1.032E-003		R-Squared		0.9984
Mean	0.067		Adj R-Squared		0.9966
C.V. %	1.53		Pred R-Squared		0.9903
PRESS	4.524E-005		Adeq Precision		80.260

The R² value is equal to 0.9984 and is thus indicative of the accuracy and exactness of the model in finding the desired responses. Table 4.40 shows that Pred-R² of 0.9903 is in reasonable agreement with the Adj-R² of 0.9966; i.e. the difference is less than 0.2. For the developed CO model, the value of Adequate Precision is 80.260, which shows high precision of the model. The final empirical model for CO in terms of coded and actual

factors is given by Eqs. 4.45 and 4.46 respectively.

$$CO = 0.0605625 - 0.0157813 \times A + 0.0085 \times B - 0.003375 \times AB + 0.0077625 \times A^2 + 0.046125 \times B^2 + 0.0023625 \times A^2B - 0.00646875 \times A^3 + 0.0264375 \times B^3 \quad (4.45)$$

$$CO = 0.174625 - 0.0326771 \times Load + 0.0341933 \times DGMBU20 - 0.00039 \times Load \times DGMBU20 + 0.00167969 \times Load^2 - 0.00247 \times (DGMBU20)^2 + 8.75e-006 \times Load^2 \times DGMBU20 - 2.99479e-005 \times Load^3 + 6.26667e-005 \times (DGMBU20)^3 \quad (4.46)$$

Table 4.41 presents the reduce ANOVA table for Response Surface Cubic model for HC. In the Table, the value of “Prob. > F” for the model, the main effect of load, main effect of blend, interaction of load and blend, second order effect of load & blend, second order effect of load and main effect of blend and cubic effect of blend are all less than 0.05. So these terms are significant model terms.

Table 4.41 Reduce analysis of variance table and interaction fit for HC

Source	Sum Squares	of Degree of Freedom	Mean Square	F-Value	p-value Prob > F
Model	35.76	7	5.11	170.29	< 0.0001
A-LOAD	0.36	1	0.36	12.00	0.0085
B-DGMBU20 BLEND	1.24	1	1.24	41.49	0.0002
AB	0.81	1	0.81	27.00	0.0008
A ²	3.76	1	3.76	125.19	< 0.0001
B ²	5.76	1	5.76	192.06	< 0.0001
A ² B	0.45	1	0.45	15.00	0.0047
B ³	8.45	1	8.45	281.67	< 0.0001
Residual	0.24	8	0.030		
Cor Total	36.00	15			
Std. Dev.	0.17		R-Squared		0.9933
Mean	24.50		Adj R-Squared		0.9875
C.V. %	0.71		Pred R-Squared		0.9659
PRESS	1.23		Adeq Precision		41.151

The R² value is equal to 0.9933 and is thus indicative of the accuracy and exactness of the model in finding the desired responses. Table 4.41 shows that Pred-R² of 0.9659 is in reasonable agreement with the Adj-R² of 0.9875; i.e. the difference is less than 0.2. For the developed HC model, the value of Adequate Precision is 41.151, which shows high

precision of the model. The final empirical model for HC in terms of coded and actual factors is given by Eqs. 4.47 and 4.48 respectively.

$$HC=23.625 -0.27 \times A + 1.1875 \times B -0.405 \times AB + 1.4625 \times A^2 + 6.1875 \times B^2 + 0.50625 \times A^2B + 3.65625 \times B^3 \quad (4.47)$$

$$HC=8.6 -0.16875 \times Load + 5.04033 \times DGMBU20 -0.0765 \times Load \times DGMBU20 + 0.0078125 \times Load^2 -0.345 \times (DGMBU20)^2 + 0.001875 \times Load^2 \times DGMBU20 + 0.00866667 \times (DGMBU20)^3 \quad (4.48)$$

4.6.2.3 Comparison of observed and estimated responses for DGM-BU20 blends

Figs. 4.79 and 4.80 show plots between the actual and predicted values of BSFC, BTE, smoke, NO_x, CO and HC. From the plots, it can be analyzed that the values of actual data and predicted data are quite close to each other. This implies that the model is significant. It can also be observed from the plots that most of the points are clustered around the 45° line; which indicates a fairly good least square fit for responses.

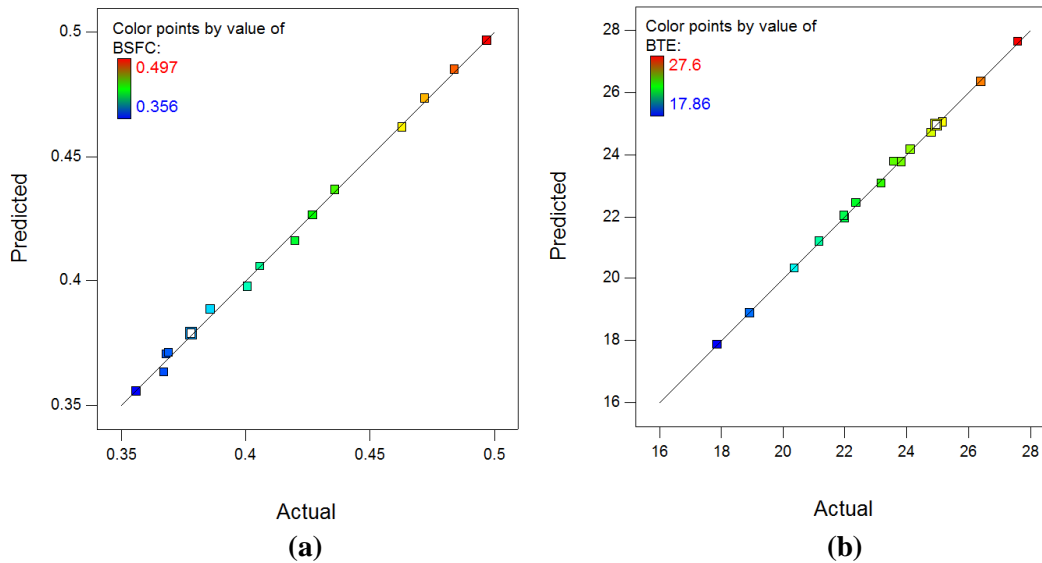
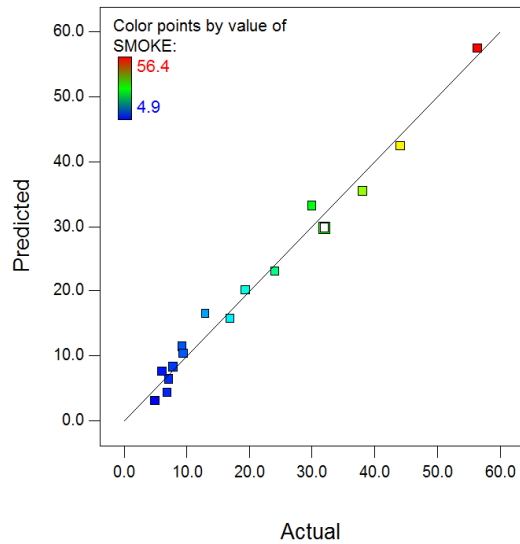
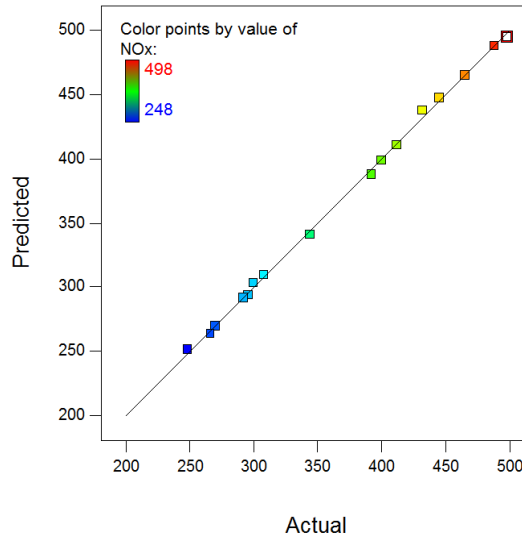


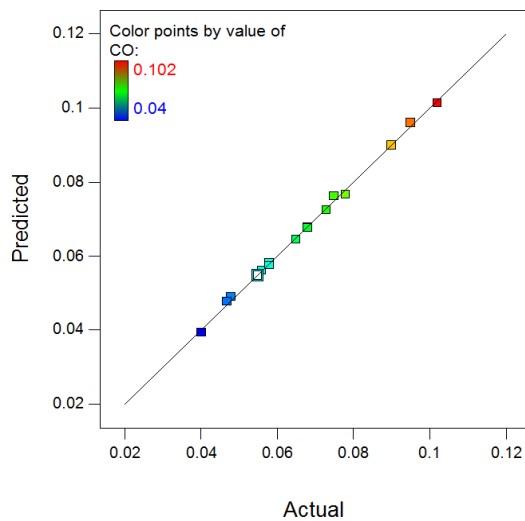
Fig. 4.79 Plot of actual values vs. predicted values for (a) BSFC (b) BTE



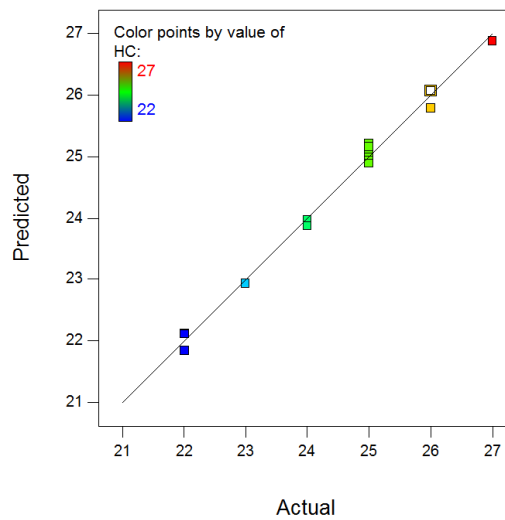
(a)



(b)



(c)



(d)

Fig. 4.80 Plot of actual values vs. predicted values for (a) Smoke (b) NO_x (c) CO (d) HC

4.6.3 Performance of engine using DGM-BU20 blends

The performance results of engine test in the form of BSFC and BTE are presented via scattered diagrams from observed data of experiments and interaction plots from mathematical models.

4.6.3.1 Brake specific fuel consumption (BSFC)

It can be observed from Fig.4.81 (a) that the BSFC reduces with increasing load and is lowest at full load. Fig. 4.81(a) and Fig.4.93 show that BSFC is higher for all DGM-

BU20 blends as compared to BU20. Blending of DGM with the BU20 fuel reduces the lower heating value of the fuels, thus more blended fuel is required to maintain the same power output. Blending of diglyme results in increased BSFC (from 4.70% to 11.17%) as compared to BU20 at full load condition. Fig. 4.82 shows that BSFC increases linearly with percentage of diglyme in BU20. Further, it was also observed that variations of all tested fuels with load are almost similar. The Fig. 4.81 (b) shows similar trends of BSEC as of BSFC in Fig. 4.81 (a). However, at higher loads the difference in BSEC values for different blended fuels were quite closer.

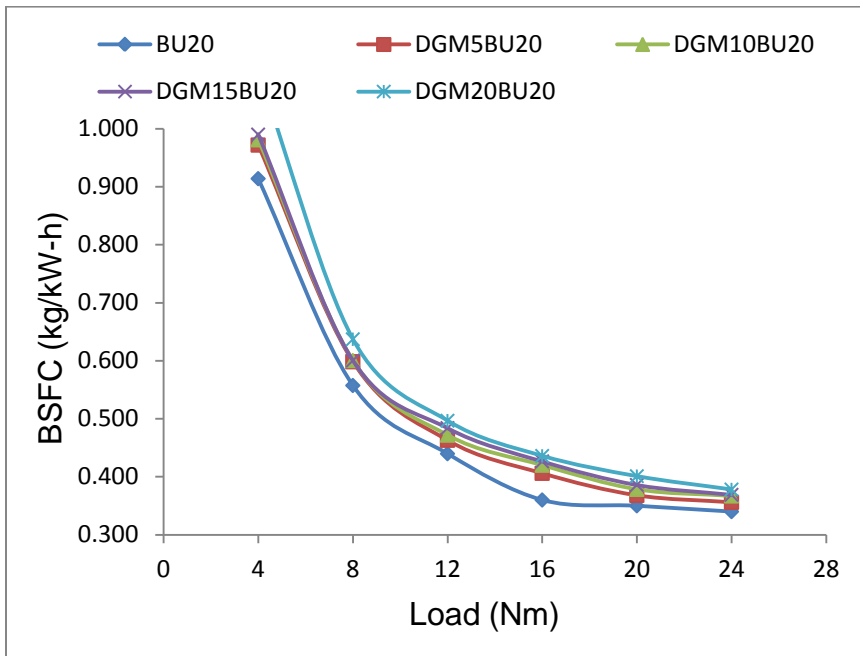


Fig. 4.81(a) Variation of BSFC with engine load for Diglyme-BU20 blends

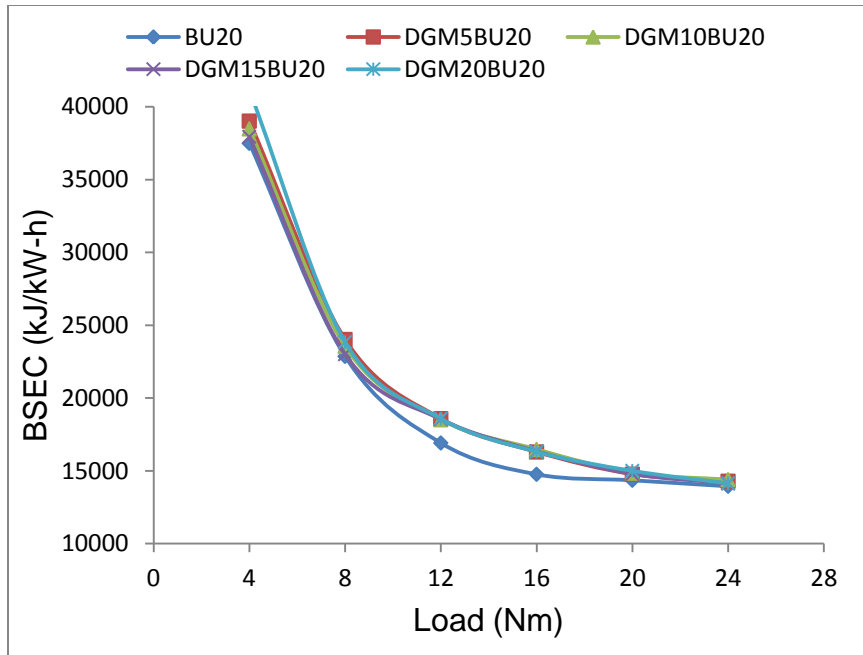


Fig. 4.81(b) Variation of BSEC with engine load for Diglyme-BU20 blends

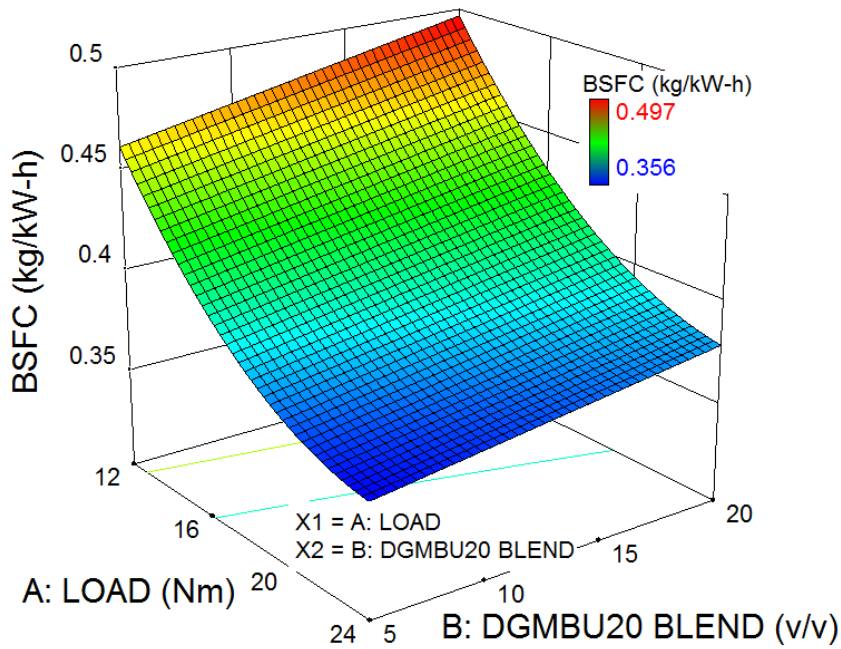


Fig. 4.82 Variation in BSFC due to combined effect of load and Diglyme blending

4.6.3.2 Brake thermal efficiency

Fig. 4.83 shows the trends of BTE and Fig.4.93 shows the values of BTE at full load condition for different diglyme-BU20 blends. It can be observed that BTE increase from DGM5BU20 to DGM15BU20 blend and then reduces for DGM20BU20 [134].

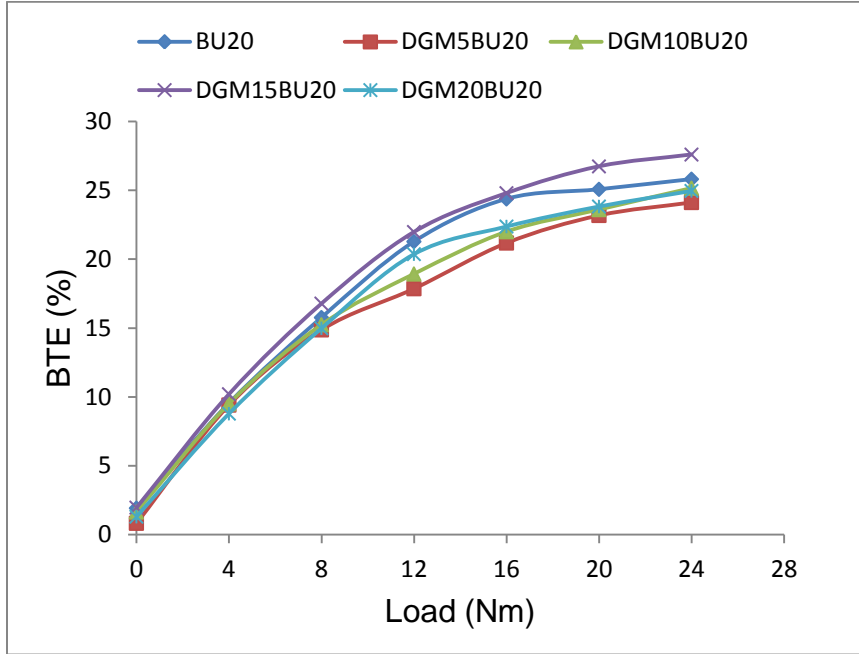


Fig. 4.83 Variation of BTE with engine load for Diglyme-BU20 blends

The blending of diglyme reduces the ignition delay period and improves Cetane number of DGM-BU20 blend. The availability of oxygen in fuel accelerates the combustion rate, especially in diffusion phase. Fig 4.84 shows simultaneous effect of load and blending on variation of BTE. It can be noted that at full load the BTE for DGM15BU20 is higher as compared to other tested fuels. The increment in BTE for DGM15 is 6.9 % as compared to BU20 at full load condition.

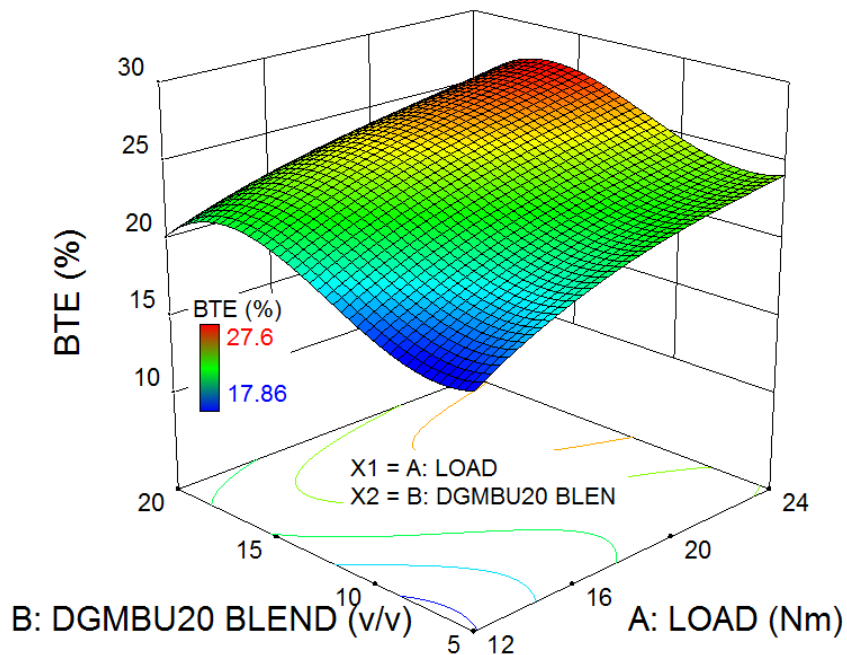


Fig. 4.84 Variation in BTE due to combined effect of load and Diglyme blending

4.6.4 Emissions of engine using DGMBU20 blends

4.6.4.1 Variation of Smoke

Figs. 4.85 and 4.86 show the variations of smoke emission for diglyme-BU20 blends for experimental results and predicted model.

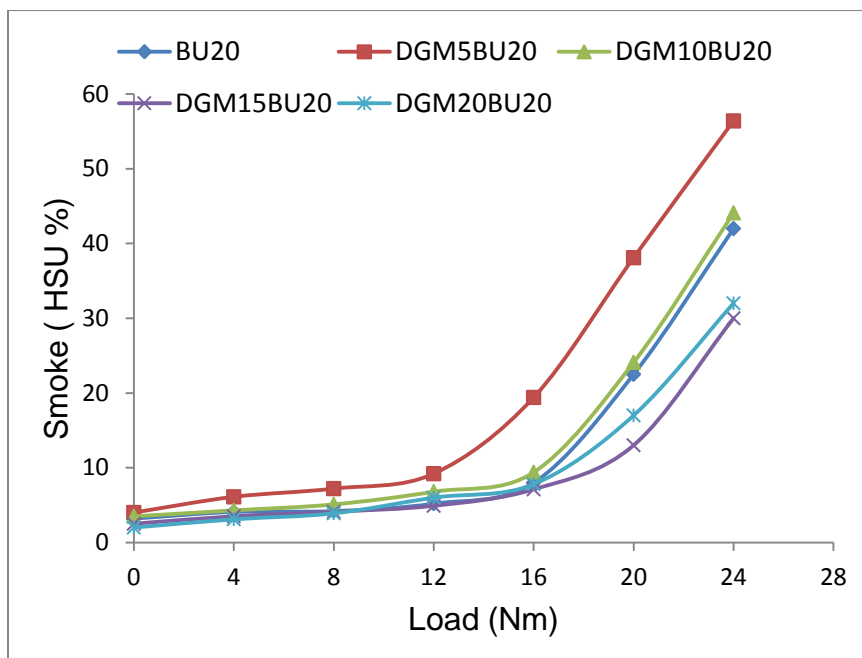


Fig. 4.85 Variation in smoke for Diglyme-BU20 blends

It can be observed from the figures that smoke emission increases with increase in engine load. This is due to increase of the amount of fuel burned in the diffusion phase. Figs. 4.85 and 4.86 show that smoke is comparatively low at low loads, and increases slowly at moderate loads, then increases considerably at higher loads [56].

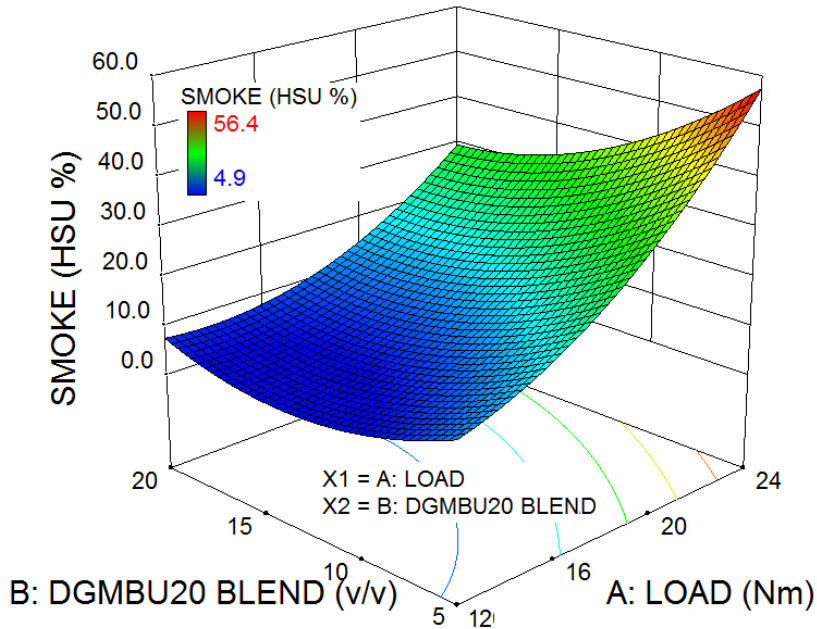


Fig. 4.86 Variation in smoke due to combined effect of load and Diglyme blending

Significant reduction in smoke was observed for DGM15BU20. Smoke reduced up to 28.57% for DGM15BU20 as compared to BU20 at full load condition. The Fig. 4.86 shows that smoke concentration decreases with increase of DGM percentage in the blends, and this trend is more noticeable at high engine loads. This can be attributed to the fact that smoke is mainly generated during the diffusion combustion phase. Blending of diglyme in BU20 results in reduced smoke due to improvement of diffusion combustion and enhancement of post-flame oxidation of smoke precursors towards the end of the expansion stroke. At the same time, reduced amount of fuel burned in the diffusion combustion phase is also helpful in reducing smoke. Several factors may contribute to reduction of smoke with diglyme blended fuels. Primarily, higher oxygen content in the blended fuels promotes fast combustion in the diffusion phase. Secondly, the reduced amount of carbon owing to the increased oxygen content in DGM-BU20 blends directly results in lower smoke generation as there is lesser carbon available for

combustion. Further, the decrease of aromatic compounds in the blended fuel (because of lower bonding energy of oxygenated hydrocarbons) [56] contributes to the reduction of smoke precursors in premixed zone [25], [157]. Lastly, the increased temperature in diffusion combustion phase with the addition of DGM, enhances oxidation of smoke[134],[150], [158].

4.6.4.2 Variation of NO_x

Figs. 487 and 4.88 show the variation of NO_x emission for diglyme-BU20 blends for experimental results and predicted model.

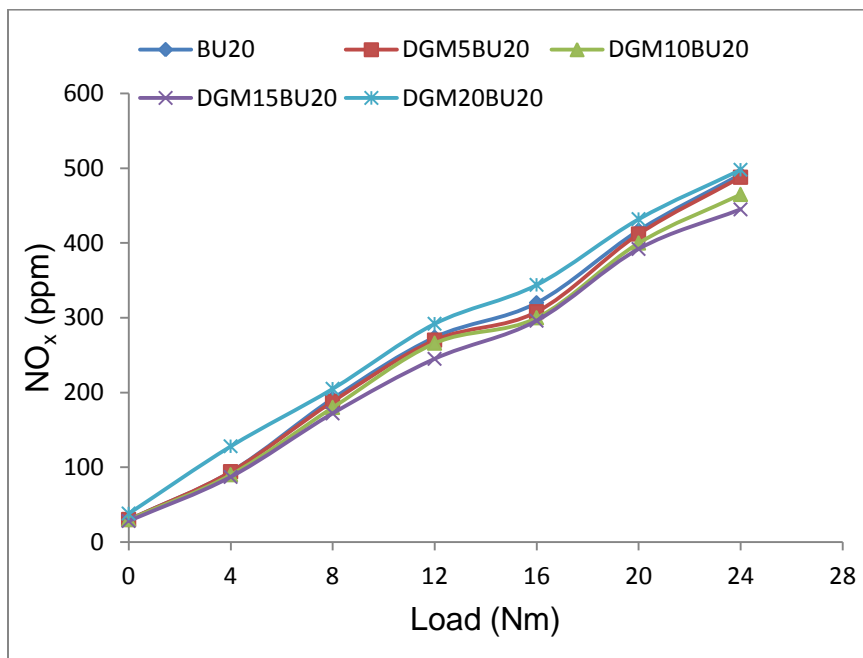


Fig. 4.87 Variation in NO_x for Diglyme-BU20 blends

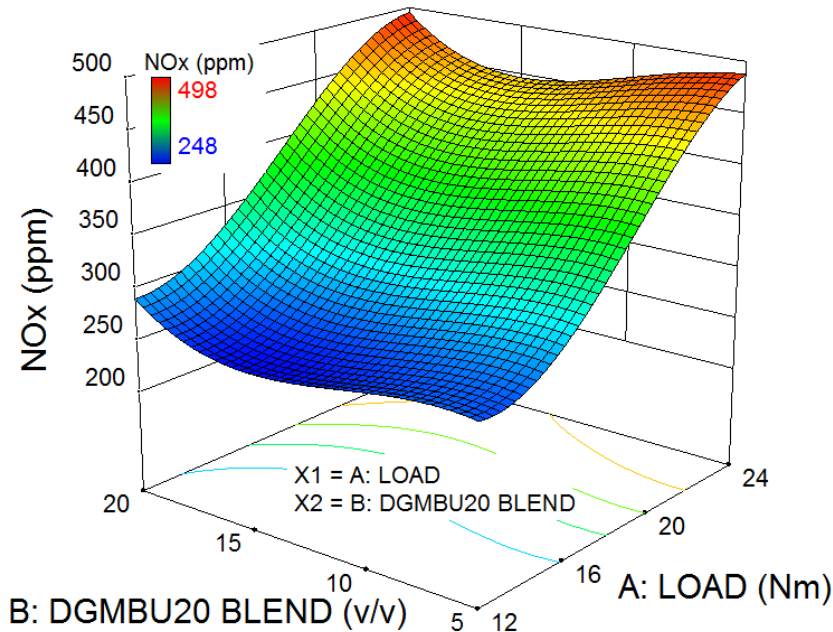


Fig. 4.88 Variation in NO_x due to combined effect of load and Diglyme blending

Fig. 4.87 and Fig 4.88 show variation of NO_x with load and diglyme blends. NO_x increases with load and decreases with increase percentage of diglyme in BU20 (up to 15% on volume basis). Diglyme has a very high Cetane number of 126 that shortens the ignition delay period and thus reduces NO_x also. The formation of NO_x mainly depends on two factors; (i) high temperature of combustion and (ii) duration of retention of high temperature. The availability of oxygen in diglyme improves combustion and leads to an increase of maximum temperature in the combustion chamber. At the same time, owing to high latent heat of evaporation, the temperature of gases is reduced inside the cylinder. The blending of diglyme reduces ignition delay period, thus reducing the premixed combustion duration (retention time) [56], [133]. Also, addition of diglyme in BU20 changes the combustion product type as well as concentration. This in turn changes the ignition reaction and combustion process [56]. As a matter of fact, the amount of NO_x formation from the DGM-BU20 blends is a complex combinatorial result of all the above mentioned factors. . Increase of NO_x for higher blends of diglyme (DGM20) is because of availability of very high temperature in cylinder due to higher concentration of O₂ in fuel. Nevertheless, in comparison with BU20, NO_x formation for DGM15BU20 was found to be 9.5% lesser. The decreasing trend of NO_x with diglyme was found to follow expected

trends and is even supported by some previous studies as discussed in the introduction (such as[56],[134],[150])

4.6.4.3 Variation of CO

Figs. 4.89 and 4.90 show the variation of CO emission for DGM-BU20 blends for experimental results and predicted model. It can be observed from Figs. 4.89 and 4.90 that CO emission decreases with load and increases with DGM blending. At low loads the curves for different blends are parallel, but further at higher loads the CO emission for DGM10BU20 increases at a higher rate; even higher than that of DGM15BU20. CO is an intermediate product during the combustion of any fuel. Less availability of oxygen, low reaction temperature and short reaction period may cause the generation of CO. In the present case, short reaction time may be the probable cause of increased CO emission. In comparison to BU20, the CO emission for DGM15BU20 blend was found to be higher by 38.23%.

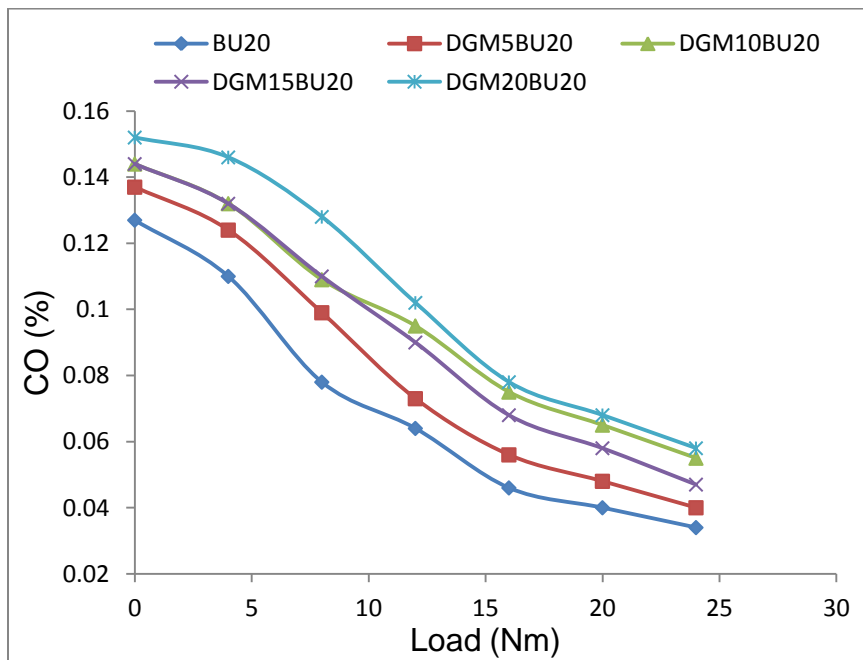


Fig. 4.89 Variation in CO for Diglyme-BU20 blends

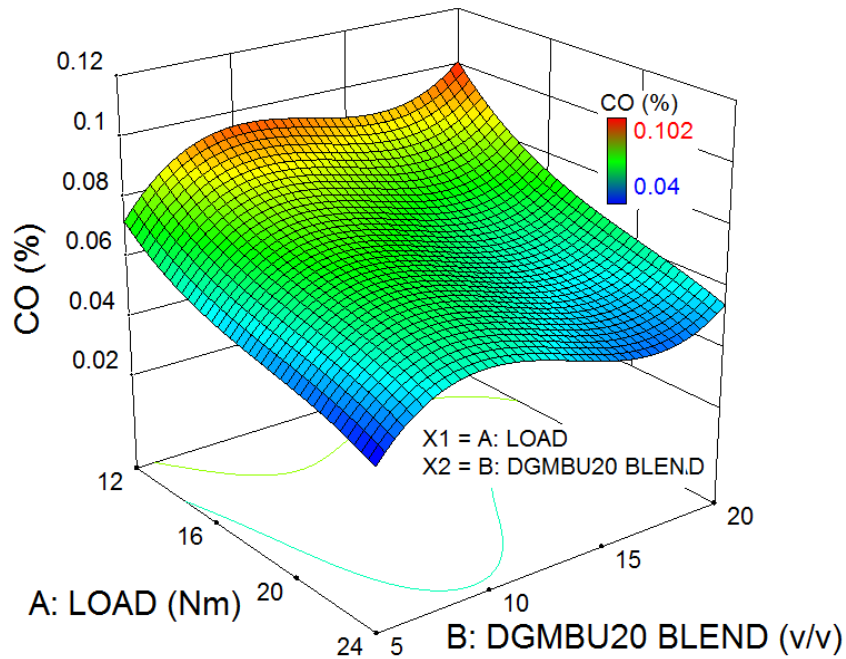


Fig. 4.90 Variation in CO due to combined effect of load and Diglyme blending

4.6.4.4 Variation of HC

Figs. 4.91 and 4.92 show the variation of HC emission for DGMBU20 blends for experimental results and predicted model.

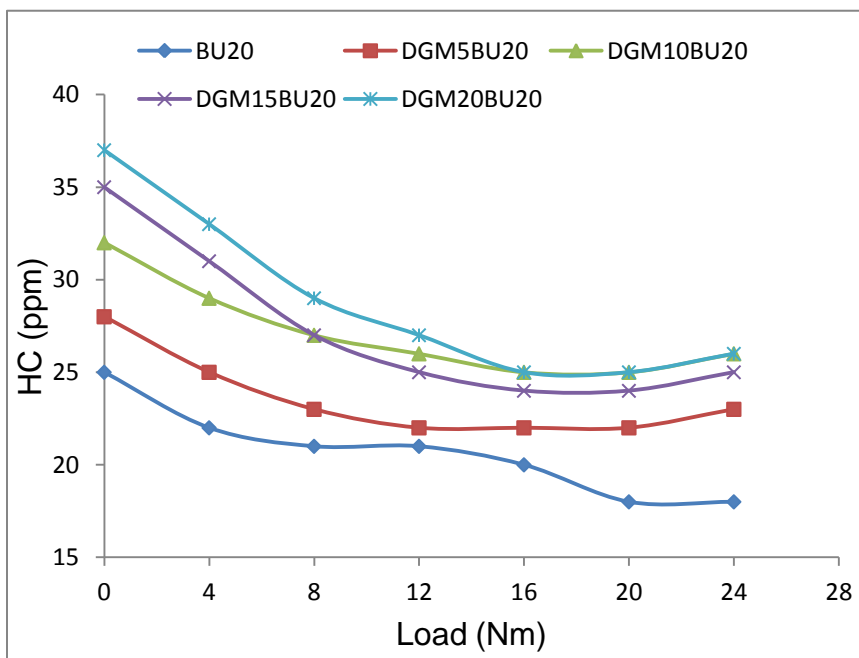


Fig. 4.91 Variation in HC for Diglyme-BU20 blends

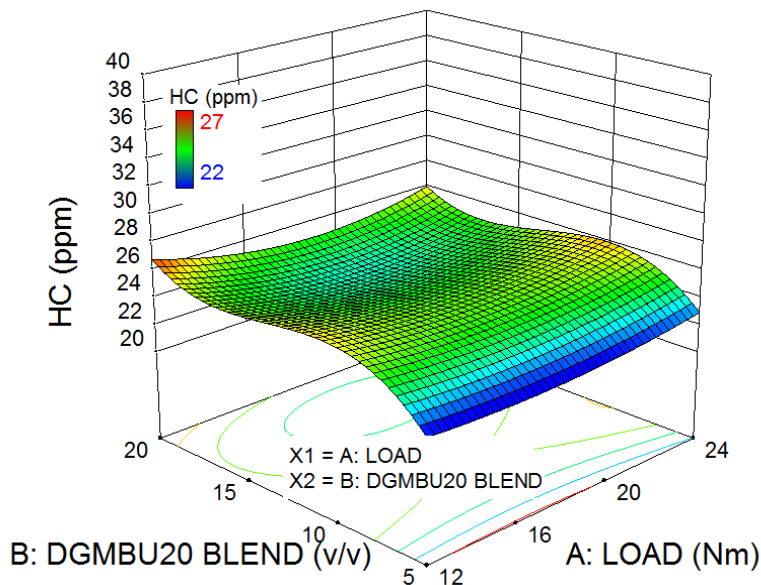


Fig. 4.92 Variation in HC due to combined effect of load and Diglyme blending

When the engine load increases, HC concentration decreases initially up to 50% of the full load and then increases up to full load condition for DGM-BU20 blends. As already discussed, the premixed combustion duration shortens and the diffusion combustion duration extends with addition of diglyme in fuel. Non-homogeneous mixture during the diffusion combustion process generates more HC. It can be observed from Fig. 4.93 that the emission of HC for all blends is higher as compared to that of BU20. Expansion of lean flame-out region due to increased oxygen in the fuel is another cause of increased unburned HC [70], [153]. An increment of 38.88% in HC can be observed for DGM15BU20 as compared to BU20 from Fig. 4.93. Most of the studies cited in the introduction are consistent with this result (i.e. increased HC).

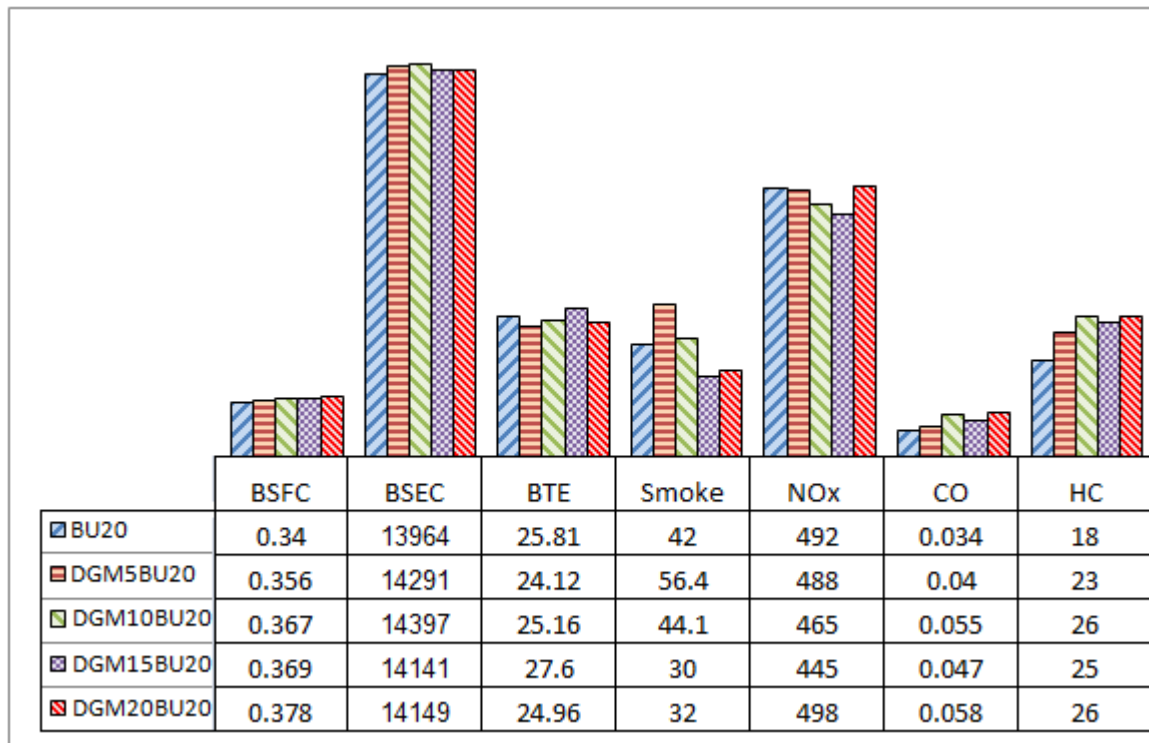


Fig. 4.93 Performance and emission of Diglyme-BU20 blends (100% rated power)²

4.6.5 Validation and optimization of responses

The parameters were optimized for desired values of responses. Table 4.42 summarizes the minimum and maximum values of each response to optimize operating parameters of the engine. On the basis of Table 4.42 and optimization analysis, the optimum blended fuel and their predicted responses were obtained, and are shown in Table 4.43. The test was repeated at near to optimum values of load (18.1 Nm) and blend (16% DGM in BU20) to validate the results predicted by the models. The optimum values of BSFC, BTE, smoke, NO_x, CO and HC were observed to be 0.400, 25.48, 10.6, 350, 0.062 and 23 respectively. It can also be observed from Table 4.43 that the percentage errors of these results are within tolerance. This shows the exactness of predicted models. On the basis of the validation of experimental results by mathematical modeling, DGM15BU20 (15% diglyme in BU20) was selected as the optimum blend of diglyme with BU20.

²Fig is not on Scale

Table 4.42 Maximum and minimum limits for each response to optimize performance and emissions

Names	Goal	Lower limit	Upper limit
A: Load	Is in range	12	24
B: Blend (DGMBU20)	Is in range	5	20
Response: BSFC	Minimize	0.356	0.497
Response: BTE	Maximize	17.86	27.6
Response: Smoke	Minimize	4.9	56.4
Response: NO _x	Minimize	248	498
Response: CO	Minimize	0.04	0.102
Response: HC	Minimize	22	27

Table 4.43 Optimum conditions of load and blend and their predicted results

Number	Load	(DGM-BU20)	BSFC	BTE	Smoke	NO _x	CO	HC	
1	18.148	16.092	0.406	25.823	10.596	347.214	0.060	23.592	Selected
2	18.737	16.043	0.400	26.043	12.117	361.441	0.059	23.598	
3	16.095	0.394	26.308	14.248	379.961	0.057	23.632	0.690	
4	24.000	16.000	0.373	27.764	32.080	450.158	0.046	24.778	
Confirmation test	18.1	16	0.400	25.48	10.6	350	0.062	23	
Error Percentage (× 100)			1.478	1.328	-0.038	-0.802	-3.333	2.509	

4.7 Performance and emissions characteristics of the engine using diethylether-BU20 blends

Tests were conducted using Diethylether (DEE) as additive in BU20 in different proportions with the following engine settings: 19.5 compression ratio (CR), 23° CA btdc injection timing and 210 bar injection pressure. The variations in engine performance and emissions for the blends were noted at different load conditions (no load to 100% rated

power), and are presented in the form of scattered curves and column charts in this section. It was observed from these scattered diagrams that the variations in performance and emissions of blends with respect to each other are significant at higher loads only. Thus, mathematical modeling has been done for higher load observations only (50% of full load to 100% of full load).

4.7.1 Determination of optimum blend of diethylether-BU20

To find the optimum diethylether-n-butanol-diesel blend, the following approach was adopted: (i) Firstly, the selected data of experiments was fed to DOE software and ANOVA was done to check the significance of model and individual terms. (ii) The curves from actual experiments and surface response model were then analyzed to see the effect of change of factors on response. (iii) Optimization and verification of predicated model was done by confirmation test. 3D surface curves were drawn for all instances where interaction effect of factors was found to be significant. Otherwise, 2D curves of factors with response were drawn.

4.7.2 Modeling for diethylether-n-butanol-diesel (DEE-BU20) blends

Full Factorial design was employed for the development of prediction models of BSFC, BTE, smoke, NO_x, CO and HC in terms of engine load and blending ratio. An attempt was made to optimize the factors for the desired values of responses (BSFC, BTE, smoke, NO_x, CO and HC). Table 4.44 shows the engine operating parameters and their levels, and Table 4.45 shows the design matrix for selected experimentation.

Table 4.44 Parameters and their levels according to factorial design for DEE-BU20 blends

Parameter	symbol	Levels			
		1	2	3	4
Load (Nm)	A (Load)	12	16	20	24
DEE-BU20 Blend (% v/v)	B (Blend)	5	10	15	20

Table 4.45 Design layout and experimental results for DEE-BU20 blends

Run	Factor 1	Factor 2	Response 1	Response 2	Response 3	Response 4	Response 5	Response 6
	A:LOAD (Nm)	B:DEE-BU20 BLEND(v/v)	BSFC (kg/kW-h)	BTE (%)	SMOKE (HSU %)	NO _x (ppm)	CO (%)	HC (ppm)
5	12	5	0.432	22.04	5	239	0.078	23
12	16	5	0.375	24.96	8	308	0.058	23
16	20	5	0.348	25.5	21	372	0.045	25
15	24	5	0.338	26.4	41	395	0.04	27
7	12	10	0.420	23.2	5	209	0.082	23
14	16	10	0.360	25.8	7.7	310	0.061	23
11	20	10	0.349	26.8	18	395	0.047	26
9	24	10	0.340	27.4	38	450	0.039	28
4	12	15	0.445	23.14	4.8	346	0.075	25
8	16	15	0.379	25.74	7.6	465	0.058	26
3	20	15	0.354	26.3	17	560	0.049	26
10	24	15	0.346	27.2	36	640	0.043	30
13	12	20	0.450	23.5	4.5	383	0.098	29
1	16	20	0.410	25.7	7.5	498	0.072	31
2	20	20	0.364	26.67	16	624	0.053	31
6	24	20	0.349	27.25	35	741	0.047	33

The details of 16 experiments suggested by DOE from performed experiments are shown in Table 4.45 along with the run order selected at random. These data were used as inputs in the Design Expert 8.0.4.1 software for further analysis.

4.7.2.1 Diagnosis of data for analysis of variance for DEE-BU20 blends

Figs. 4.94 (a), 4.95 (a), 4.96 (a), 4.97 (a), 4.98 (a) and 4.99 (a) show plots of normal probability vs. Internal studentized residuals and internal studentized residuals vs. predicted values for BSFC, BTE, smoke, NO_x, CO and HC emission respectively for the engine operated on DEE-BU20 blends.

It can be observed from normal probability plots that most of the interaction points are accumulated along a straight line, which implies that residuals follow normal distribution and hence, the fitted model is adequate for a real system.

For the assumption of constant variance to be true in ANOVA, the internal residuals vs. predicted plot should be a random scatter. Figs. 4.94 (b), 4.95 (b), 4.96 (b), 4.97 (b), 4.98 (b) and 4.99 (b) reveal no obvious pattern or unusual structure, indicating the validity

assumption to be true. It was thus projected that for all the responses, the variance of the observed data is constant and hence is satisfactory.

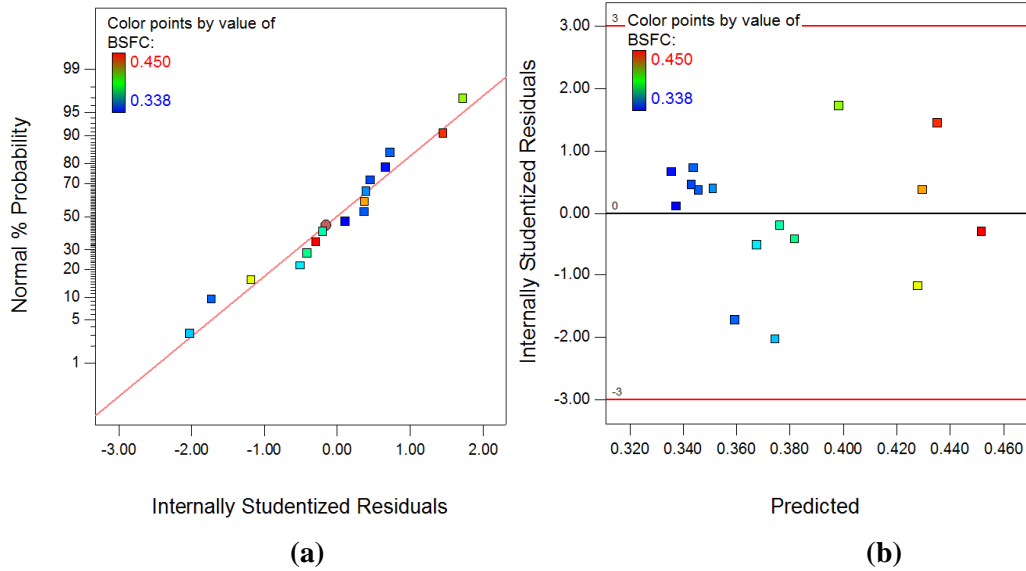


**Fig. 4.94 (a) Plot of normal % probability vs. internal studentized residuals for BSFC
(b) Plot of internal studentized residuals vs. predicted response for BSFC**

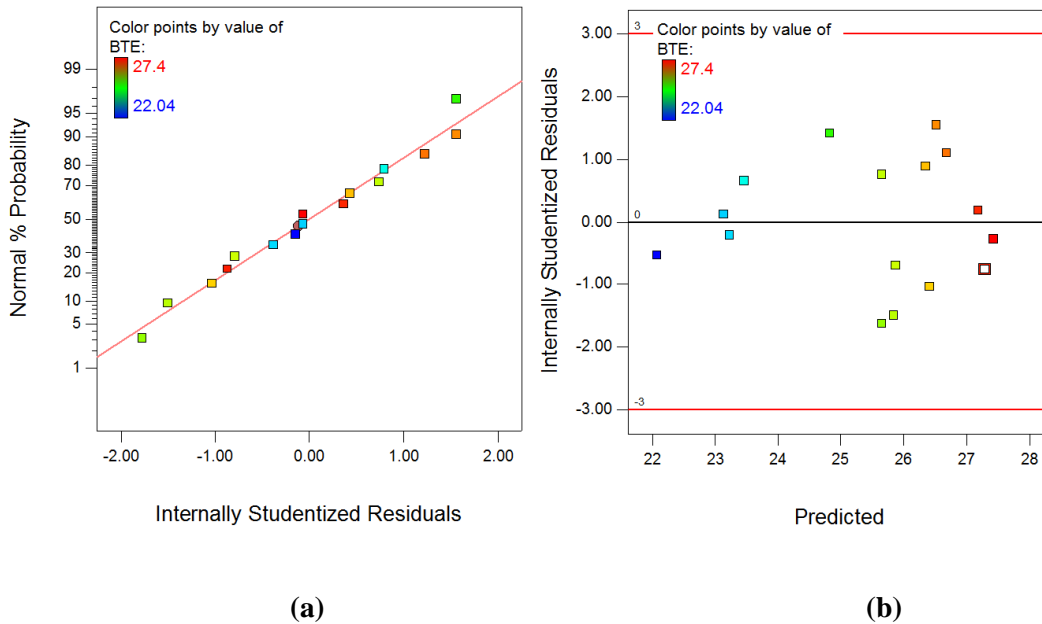


**Fig. 4.95 (a) Plot of normal % probability vs. internal studentized residuals for BTE
(b) Plot of internal studentized residuals vs. predicted response for BTE**

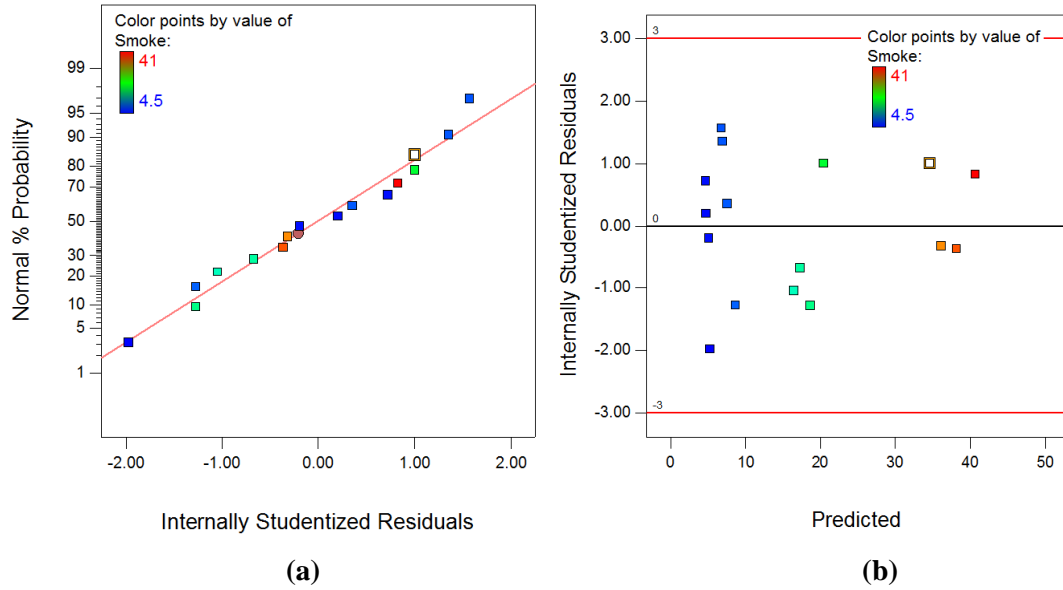


Fig. 4.96 (a) Plot of normal % probability vs. internal studentized residuals for smoke
(b) Plot of internal studentized residuals vs. predicted response for smoke

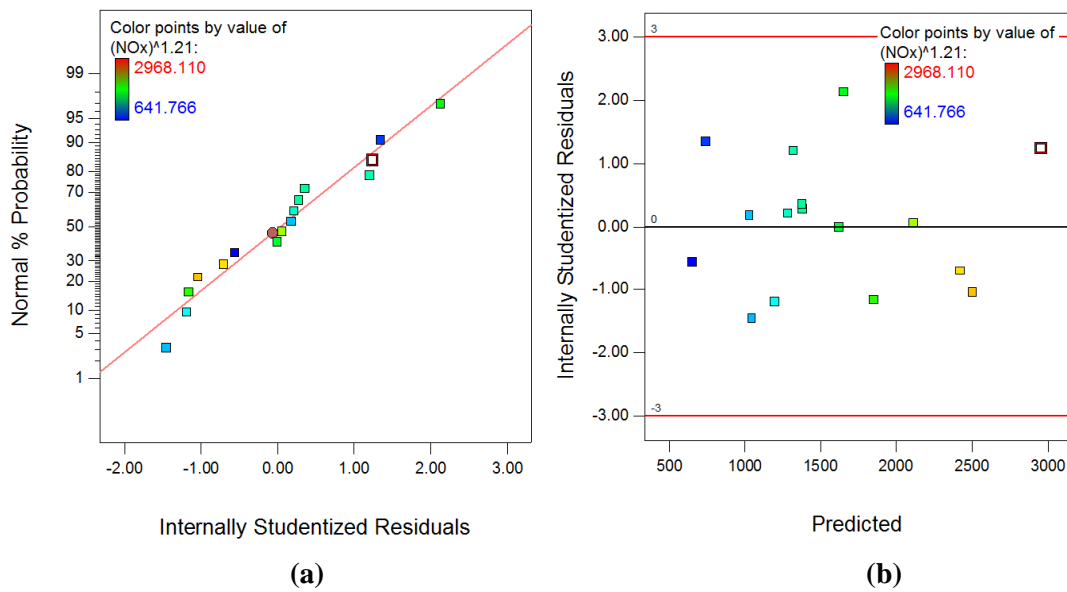


Fig. 4.97 (a) Plot of normal % probability vs. internal studentized residuals for NO_x
(b) Plot of internal studentized residuals vs. predicted response for NO_x

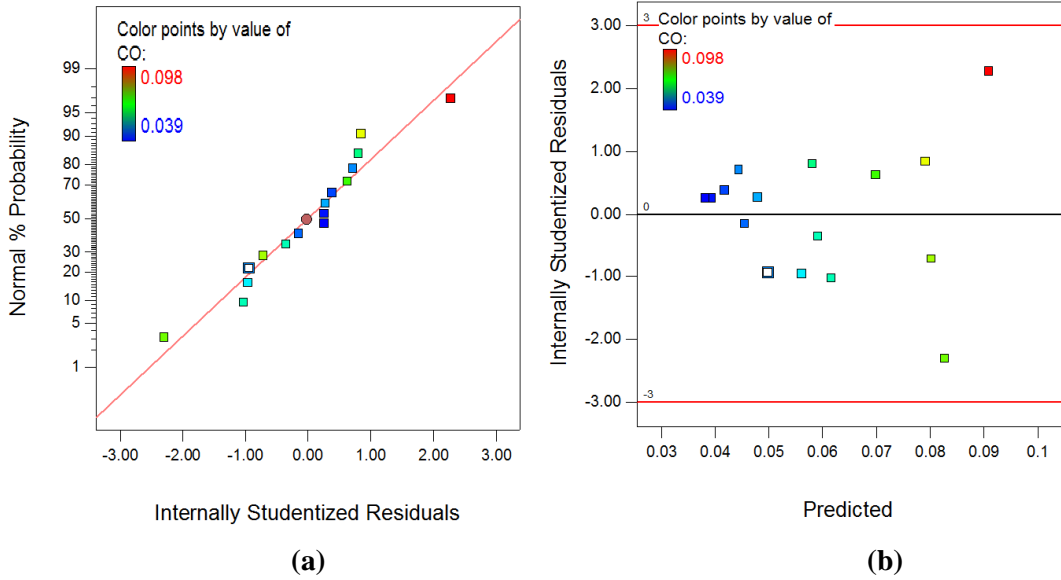


Fig. 4.98 (a) Plot of normal % probability vs. internal studentized residuals for CO
(b) Plot of internal studentized residuals vs. predicted response for CO

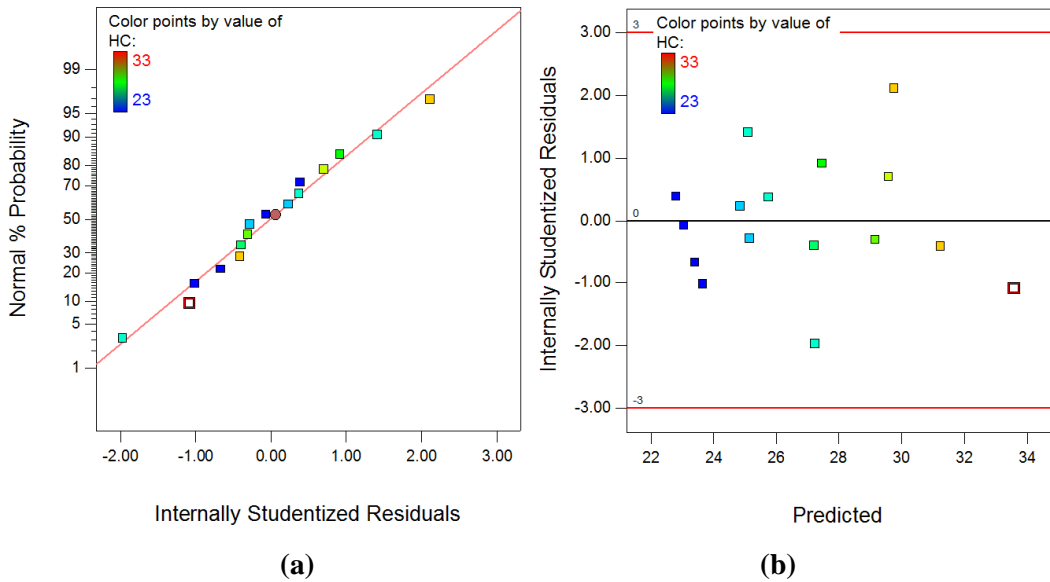


Fig. 4.99 (a) Plot of normal % probability vs. internal studentized residuals for HC
(b) Plot of internal studentized residuals vs. predicted response for HC

4.7.2.2 ANOVA for response surface model for DEE-BU20 blends

Tables 4.46 to 4.51 present the ANOVA tables for the response surface prediction models of BSFC, BTE, smoke, NO_x, CO and HC respectively. These have been obtained using the backward elimination procedure for removing insignificant terms. In the present work, ANOVA analysis was carried out for a significance level of $\alpha = 0.05$, i.e. for a

confidence level of 95%.

Table 4.46 presents the ANOVA for Response Surface Quadratic model for BSFC. In the Table, the value of “Prob. > F” for the model is 0.0001 which is less than 0.05, indicating that the model is significant, i.e. the terms in the model have a significant effect on BSFC. In the same manner, the value of “Prob. > F” for the main effect of load, blend and second order effect of load & blend were also found to be less than 0.05. So these terms are also significant model terms.

Table 4.46 Reduce analysis of variance table and interaction fit for BSFC

Source	Sum of Squares	Degree of freedom	Mean Square	F-Value	p-value Prob > F
Model	0.022	4	5.603E-003	85.96	< 0.0001
A-Load	0.019	1	0.019	290.75	< 0.0001
B-DEE-BU20 Blend	1.090E-003	1	1.090E-003	16.72	0.0018
A ²	2.037E-003	1	2.037E-003	31.25	0.0002
B ²	3.339E-004	1	3.339E-004	5.12	0.0448
Residual	7.170E-004	11	6.518E-005		
Cor Total	0.023	15			
Std. Dev.	8.073E-003		R-Squared		0.9690
Mean	0.38		Adj R-Squared		0.9577
C.V. %	2.13		Pred R-Squared		0.9358
PRESS	1.484E-003		Adeq Precision		25.758

The R-Squared (R²) value is equal to 0.9690. Its nearness to 1 for the model is indicative of the accuracy and exactness of the model in finding the desired responses. The Pred-R² of 0.9358 is in reasonable agreement with the Adj-R² of 0.9577; i.e. the difference is less than 0.2. For the developed BSFC model, the value of Adequate Precision is 25.758, which shows high precision of the model. The final empirical model for BSFC in terms of coded and actual factors is given by Eqs. 4.49 and 4.50 respectively.

$$BSFC = 0.358879 - 0.0461729 \times A + 0.011073 \times B + 0.0253878 \times A^2 + 0.0102788 \times B^2 \quad (4.49)$$

$$BSFC = 0.735985 - 0.0330833 \times Load - 0.00309194 \times DEEBU20 + 0.000705216 \times Load^2 + 0.000182734 \times (DEEBU20)^2 \quad (4.50)$$

Table 4.47 presents the ANOVA table for Response Surface Cubic model for BTE. In the Table, the value of “Prob. > F” for the model is 0.0001 which is less than 0.05, indicating that the model is significant, i.e. the terms in the model have a significant effect on BTE. In the same manner, the value of “Prob. > F” for main effect of load, blend, second order effect of load and blend, second order effect of load and main effect of blend and cubic effect of load and blend were also found to be less than 0.05. So these terms are also significant model terms.

Table 4.47 Reduce analysis of variance table and interaction fit for BTE

Source	Sum of Squares	Degree of freedom	Mean Square	F-Value	p-value Prob > F
Model	41.24	8	5.15	267.24	< 0.0001
A-Load	0.76	1	0.76	39.28	0.0004
B-DEE-BU20 Blend	0.15	1	0.15	7.53	0.0288
AB	0.064	1	0.064	3.32	0.1113
A ²	3.37	1	3.37	174.58	< 0.0001
B ²	0.79	1	0.79	41.07	0.0004
A ² B	0.028	1	0.028	1.46	0.2664
A ³	0.64	1	0.64	33.22	0.0007
B ³	0.56	1	0.56	28.92	0.0010
Residual	0.14	7	0.019		
Cor Total	41.37	15			
Std. Dev.	0.14		R-Squared		0.9967
Mean	25.48		Adj R-Squared		0.9930
C.V. %	0.55		Pred R-Squared		0.9823
PRESS	0.73		Adeq Precision		51.428

The R-Squared (R²) value is 0.9967 and is indicative of the accuracy and exactness of the model in finding the desired responses. The Pred-R² is 0.9823 which is in reasonable agreement with the Adj-R² of 0.9930; i.e. the difference is less than 0.2. For the developed BTE model, the value of Adequate Precision is 51.428, which shows high precision of the model. The final empirical model for BTE in terms of coded and actual factors is given by Eqs. 4.51 and 4.52 respectively.

$$BTE = 26.3266 + 1.03938 \times A - 0.482188 \times B - 0.11385 \times AB - 1.03219 \times A^2 - 0.500625 \times B^2 + 0.126562 \times A^2B + 1.00687 \times A^3 + 0.939375 \times B^3 \quad (4.51)$$

$$BTE = -20.6705 + 5.97892 \times Load + 1.39937 \times DEE-BU20 + -0.019405 \times Load \times DEEBU20 - 0.28625 \times Load^2 - 0.0924 \times (DEEBU20)^2 + 0.00046875 \times Load^2 \times DEEBU20 + 0.00466146 \times Load^3 + 0.00222667 \times (DEEBU20)^3 \quad (4.52)$$

Table 4.48 presents the ANOVA table for Response Surface Quadratic model for smoke emission. In the Table, the value of “Prob. > F” for the model, the main effect of load and blend, interaction effect of load and blend and second order effect of load and blend are less than 0.05. So these terms are significant model terms.

Table 4.48 Reduce analysis of variance and interaction fit for Smoke

Source	Sum of Squares	Degree of Freedom	Mean Square	F-Value	p-value Prob. > F
Model	2655.51	5	531.10	1445.32	< 0.0001
A-Load	2346.86	1	2346.86	6386.62	< 0.0001
B-DEE-BU20 Blend	19.31	1	19.31	52.54	< 0.0001
AB	12.01	1	12.01	32.67	0.0002
A ²	276.39	1	276.39	752.15	< 0.0001
B ²	0.95	1	0.95	2.59	0.1388
Residual	3.67	10	0.37		
Cor Total	2659.19	15			
Std. Dev.	0.61		R-Squared		0.9986
Mean	17.01		Adj R-Squared		0.9979
C.V. %	3.56		Pred R-Squared		0.9958
PRESS	11.14		Adeq Precision		97.105

The R² value is equal to 0.9986 and is indicative of the accuracy and exactness of the model in finding the desired responses. Table 4.48 shows that Pred-R² of 0.9958 is in reasonable agreement with the Adj-R² of 0.9979; i.e. the difference is less than 0.2. For the developed smoke model, the value of Adequate Precision is 97.105, which shows high precision of the model. The final empirical model for smoke emission in terms of coded and actual factors is given by Eqs. 4.53 and 4.54 respectively.

$$SMOKE = 11.5063 + 16.2488 \times A - 1.47375 \times B - 1.55925 \times AB + 9.35156 \times A^2 + 0.548437 \times B^2 \quad (4.53)$$

$$SMOKE = 43.1075 + -6.21031 \times Load + 0.18345 \times DEE-BU20 Blend - 0.03465 \times Load \times DEEBU20 Blend + 0.259766 \times Load^2 + 0.00975 \times (DEEBU20)^2 \quad (4.54)$$

Table 4.49 presents the reduce ANOVA table for Response Surface Cubic model for

NO_x. In the Table, the value of “Prob. > F” for the model, the main effect of load & blend, interaction effect of load and blend, second order effect of load & blend, second order effect of load and main effect of blend and cubic effect of load and blend are less than 0.05. So these terms are significant model terms.

Table 4.49 Reduce analysis of variance table and interaction fit for NO_x

Source	Sum of Squares	Degree of Freedom	Mean Square	F-Value	p-value Prob. > F
Model	6.343E+006	8	7.929E+005	1682.67	< 0.0001
A-Load	2.621E+005	1	2.621E+005	556.17	< 0.0001
B-DEE-BU20 Blend	7.252E+005	1	7.252E+005	1538.95	< 0.0001
AB	3.020E+005	1	3.020E+005	640.81	< 0.0001
A ²	10440.12	1	10440.12	22.16	0.0022
B ²	45133.26	1	45133.26	95.78	< 0.0001
A ² B	6372.22	1	6372.22	13.52	0.0079
A ³	1140.85	1	1140.85	2.42	0.1637
B ³	2.272E+005	1	2.272E+005	482.14	< 0.0001
Residual	3298.45	7	471.21		
Cor Total	6.346E+006	15			
Std. Dev.	21.71		R-Squared		0.9995
Mean	1572.66		Adj R-Squared		0.9989
C.V. %	1.38		Pred R-Squared		0.9968
PRESS	20319.26		Adeq Precision		141.529

The R² value is equal to 0.9995 and is indicative of the accuracy and exactness of the model in finding the desired responses. Table 4.49 shows that Pred-R² of 0.9968 is in reasonable agreement with the Adj-R² of 0.9989; i.e. the difference is less than 0.2. For the developed NO_x model, the value of Adequate Precision is 141.529, which shows high precision of the model. The final empirical model for NO_x in terms of coded and actual factors is given by Eqs. 4.55 and 4.56 respectively.

$$NO_x = 1538.2 + 611.275 \times A + 1077.68 \times B + 247.277 \times AB - 57.4745 \times A^2 + 119.501 \times B^2 + 60.2427 \times A^2B - 42.4837 \times A^3 - 599.514 \times B^3 \quad (4.55)$$

$$NO_x = 1978.25 - 0.106745 \times Load - 602.167 \times DEEBU20 - 2.53731 \times Load \times DEEBU20 + 6.2354 \times Load^2 + 55.4146 \times (DEEBU20)^2 + 0.223121 \times Load^2 \times DEEBU20 - 0.196684 \times Load^3 - 1.42107 \times (DEEBU20)^3 \quad (4.56)$$

Table 4.50 presents the reduce ANOVA table for Response Surface Quadratic model for CO. In the Table, the value of “Prob. > F” for the model, the main effect of load, main effect of blend and second order effect of load & blend are less than 0.05. So these terms are significant model terms.

Table 4.50 Reduce analysis of variance table and interaction fit for CO

Source	Sum of Squares	Degree of Freedom	Mean Square	F-Value	p-value Prob. > F
Model	4.299E-003	4	1.075E-003	65.64	< 0.0001
A-Load	3.740E-003	1	3.740E-003	228.45	< 0.0001
B-DEE-BU20 Blend	2.556E-004	1	2.556E-004	15.61	0.0023
A ²	2.176E-004	1	2.176E-004	13.29	0.0039
B ²	8.556E-005	1	8.556E-005	5.23	0.0431
Residual	1.801E-004	11	1.637E-005		
Cor Total	4.479E-003	15			
Std. Dev.	4.046E-003		R-Squared		0.9598
Mean	0.059		Adj R-Squared		0.9452
C.V. %	6.85		Pred R-Squared		0.9071
PRESS	4.161E-004		Adeq Precision		23.343

The R² value is equal to 0.9598 and is indicative of the accuracy and exactness of the model in finding the desired responses. Table 4.40 shows that Pred-R² of 0.9071 is in reasonable agreement with the Adj-R² of 0.9452; i.e. the difference is less than 0.2. For the developed CO model, the value of Adequate Precision is 23.343, which shows high precision of the model. The final empirical model for CO in terms of coded and actual factors is given by Eqs. 4.57 and 4.58 respectively.

$$CO = 0.0515625 - 0.0205125 \times A + 0.0053625 \times B + 0.00829688 \times A^2 + 0.00520313 \times B^2 \quad (4.57)$$

$$CO = 0.193287 - 0.0117156 \times Load - 0.0015975 \times DEEBU20 + 0.000230469 \times Load^2 + 9.25e-005 \times (DEEBU20)^2 \quad (4.58)$$

Table 4.51 presents the reduce ANOVA table for Response Surface Quadratic model for HC. In the Table, the value of “Prob. > F” for the model, the main effect of load, main effect of blend and second order effect of load & blend are less than 0.05. So these terms are significant model terms.

Table 4.51 Reduce analysis of variance table and interaction fit for HC

Source	Sum of Squares	Degree of Freedom	Mean Square	F-Value	p-value Prob. > F
Model	150.95	4	37.74	75.65	< 0.0001
A-Load	43.51	1	43.51	87.22	< 0.0001
B-DEE-BU20 Blend	90.31	1	90.31	181.04	< 0.0001
A ²	3.06	1	3.06	6.14	0.0307
B ²	14.06	1	14.06	28.19	0.0002
Residual	5.49	11	0.50		
Cor Total	156.44	15			
Std. Dev.	0.71		R-Squared		0.9649
Mean	26.81		Adj R-Squared		0.9522
C.V. %	2.63		Pred R-Squared		0.9324
PRESS	10.57		Adeq Precision		27.353

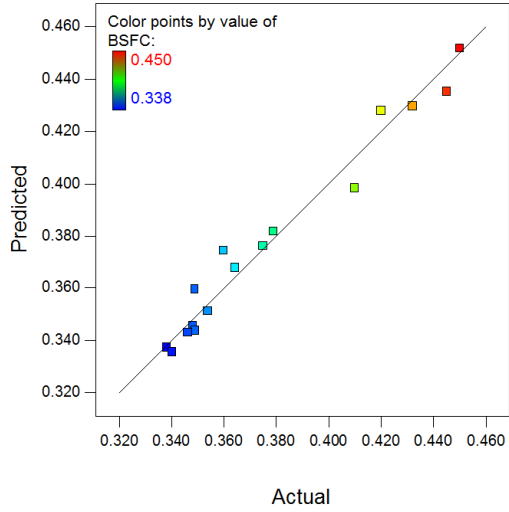
The R² value is equal to 0.9649 and is indicative of the accuracy and exactness of the model in finding the desired responses. Table 4.41 shows that Pred-R² of 0.9324 is in reasonable agreement with the Adj-R² of 0.9522; i.e. the difference is less than 0.2. For the developed HC model, the value of Adequate Precision is 27.353, which shows high precision of the model. The final empirical model for HC in terms of coded and actual factors is given by Eqs. 4.59 and 4.60 respectively.

$$HC=25.0938 + 2.2125 \times A + 3.1875 \times B + 0.984375 \times A^2 + 2.10937 \times B^2 \quad (4.59)$$

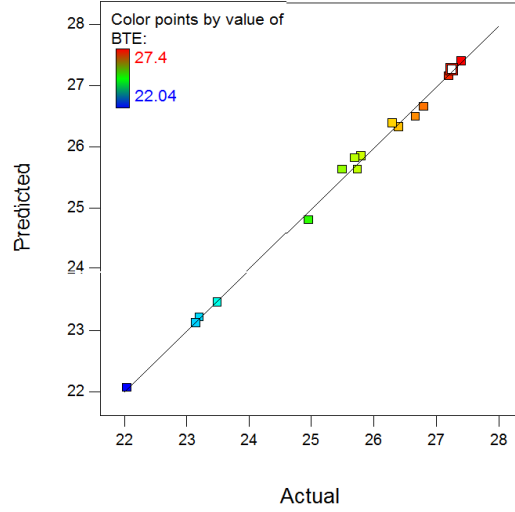
$$HC=27.8625-0.615625 \times Load -0.5125 \times DEEBU20 + 0.0273437 \times Load^2 + 0.0375 \times (DEEBU20)^2 \quad (4.60)$$

4.7.2.3 Comparison of observed and estimated responses for DEE-BU20 blends

Figs. 4.100 and 4.101 show the plots between actual and predicted values of BSFC, BTE, smoke, NO_x, CO and HC. From the plots, it can be analyzed that the values of actual data and predicted data are quite close to each other. This implies that the model is significant. It can also be observed from the plots that most of the points are clustered around the 45° line; which indicates a fairly good least square fit for responses.

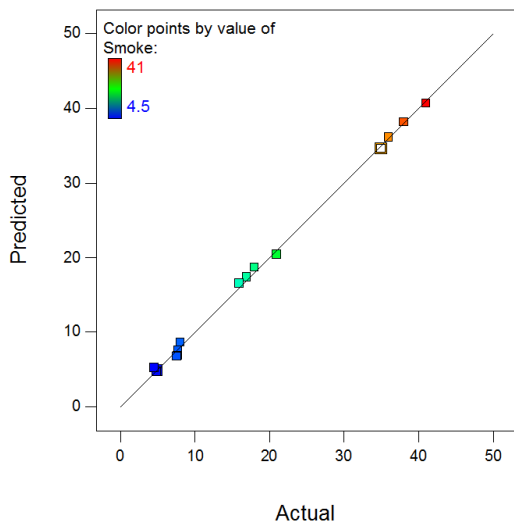


(a)

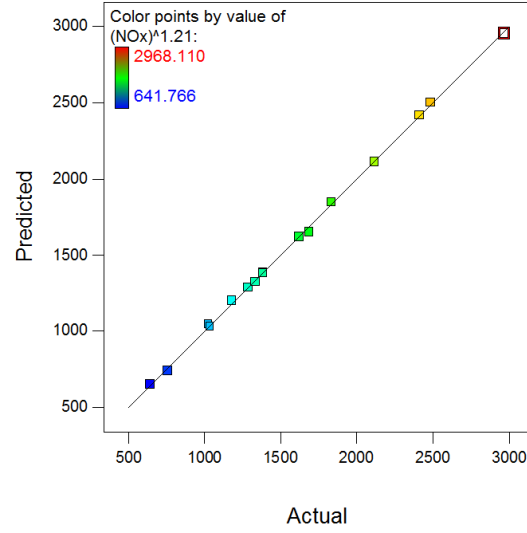


(b)

Fig. 4.100 Plot of actual values vs. predicted values for (a) BSFC (b)BTE



(a)



(b)

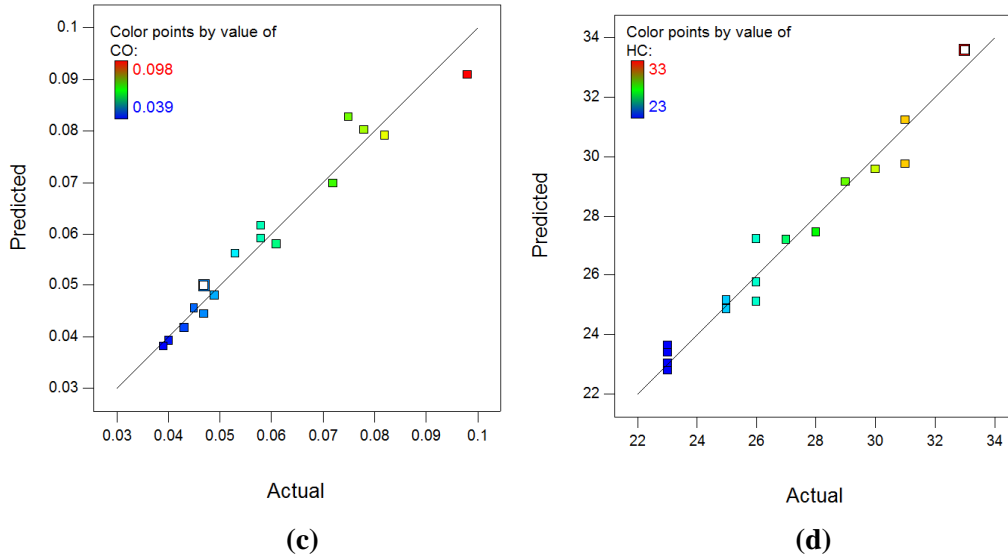


Fig. 4.101 Plot of actual values vs. predicted values for (a) Smoke (b) NO_x (c) CO (d) HC

4.7.3 Performance of engine using diethylether-n-butanol-diesel (DEE-BU20) Blends

The performance results of engine test in the form of BSFC and BTE are presented via scattered diagrams from observed data of experiments and interaction plots from mathematical models.

4.7.3.1 Brake specific fuel consumption (BSFC)

It can be observed from Figs. 4.102 (a) and 4.103 that the BSFC reduces with increasing load and increases slightly with increasing DEE percentage in BU20 fuel. Figs. 4.102 and 4.114 show that for DEE5BU20, BSFC is lesser than BU20; for DEE10BU20 it is similar to BU20 and for DEE15BU20 and DEE20BU20 it is higher than BU20. At lower blends, lower BSFC can be attributed to better combustion of fuel which gives higher heat release. At higher blends, the heating values of blended fuel are reduced significantly, resulting in higher BSFC. At the same time, because of higher volatility of DEE (Boiling point 35°C), the rate of fuel vaporization and mixing with air is increased. This further increases fuel consumption at higher blends of DEE. This also increases the thermal efficiency of engine. At Lower loads, higher Cetane number of DEE is the dominant factor in controlling ignition delay. Due to high Cetane number, the ignition delay decreases with increasing percentage of DEE in BU20 [37]. At higher loads, higher latent heat of vaporization of DEE (thus DEEBU20) is the dominant factor in controlling ignition delay. At higher loads, with increased percentage of DEE, the ignition delay

increases and thus premixed duration increases. This in turn increases the BSFC at higher loads for higher blends [37], [139]–[141], [144]. On the whole, blending of 10% diethylether resulted in an increase of 3.03% in BSFC as compared to BU20 at full load condition. The Fig. 4.102 (b) shows similar trends of BSEC as of BSFC in Fig. 4.102 (a).

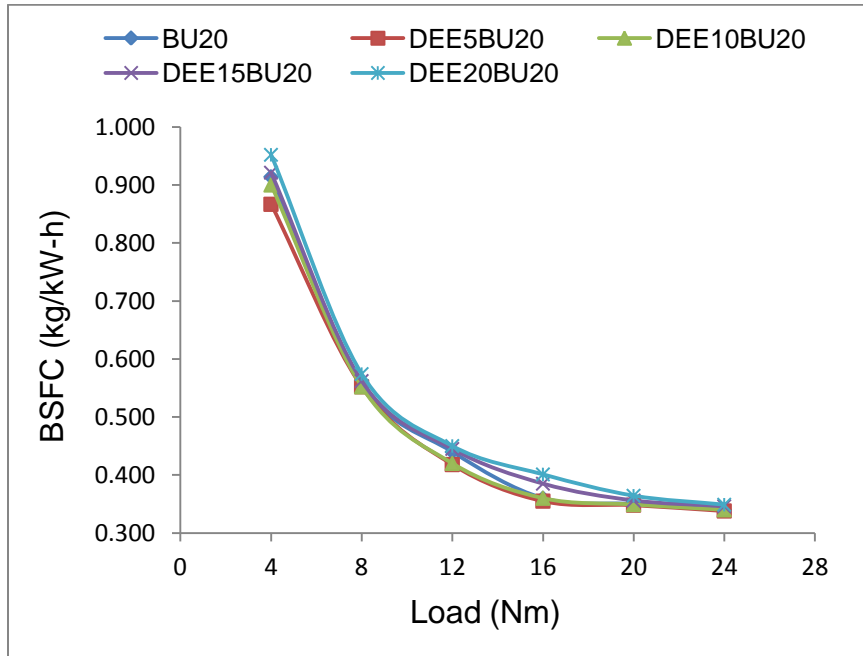


Fig. 4.102 (a) Variation of BSFC with engine load for Diethylether-BU20 blends

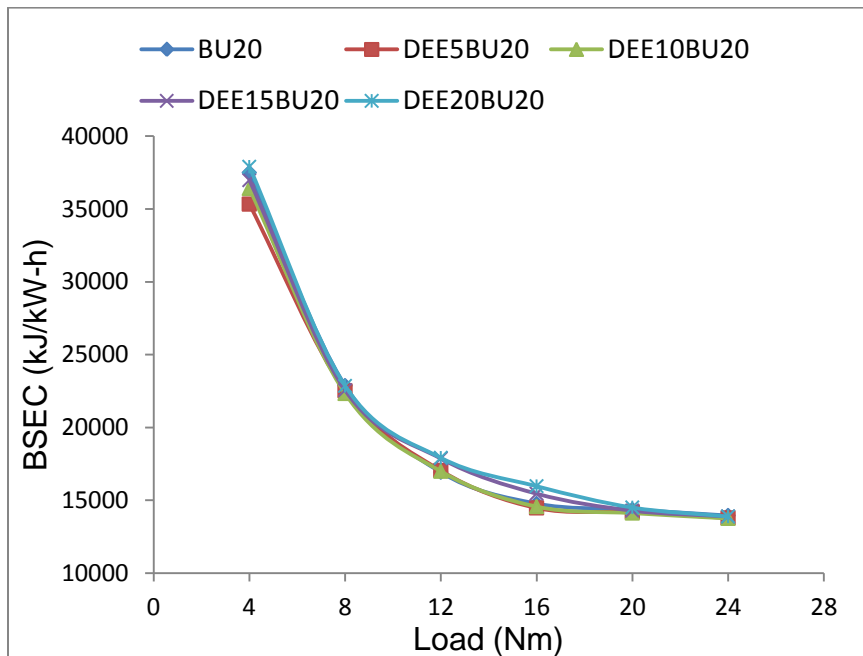


Fig. 4.102 (b) Variation of BSEC with engine load for Diethylether-BU20 blends

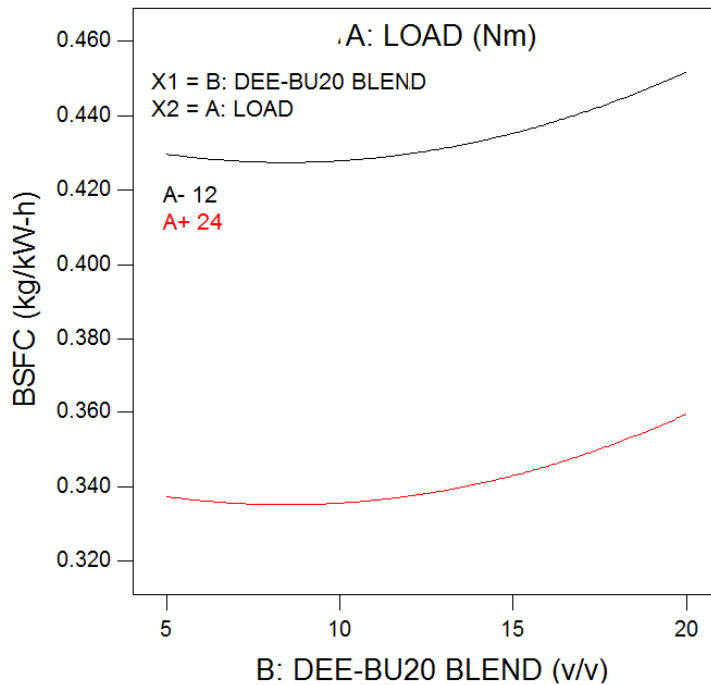


Fig. 4.103 Variation in BSFC with diethylether blending at medium and full load

4.7.3.2 Brake thermal efficiency

Fig. 4.104 shows the trends of BTE and Fig.4.114 shows the value of BTE at full load condition for different diethylether-BU20 blends. It can be observed that BTE increases from DEE5BU20 to DEE10BU20, and then reduces slightly from DEE10BU20 to DEE20BU20. BTE for all DEE-BU20 blends remains higher as compared to BU20.

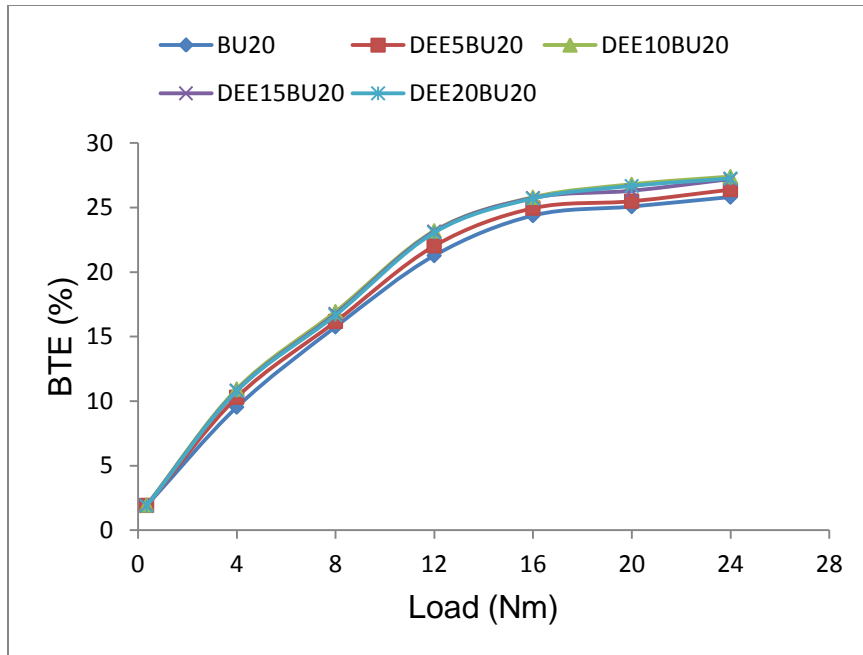


Fig. 4.104 Variation of BTE with engine load for Diethylether-BU20 blends

It has already been stated that for DEE-BU20 blends and at the higher loads, BTE increases due to longer ignition delay. This further leads to a rapid increase in premixed combustion. The oxygen content is slightly high in DEE-BU20 fuel as compared to BU20, which again accelerates the combustion rate. The increase in BTE can be attributed to the capability of DEE to decrease the surface tension or interfacial tension between blended fuels and enhance the atomization of fuel, which ultimately results in improved combustion [37]. For DEE10BU20, the increment in BTE was found to be 6.15% as compared to BU20 at full load condition. Fig. 4.105 shows that the variation of BTE for moderate load and full load following the similar trends.

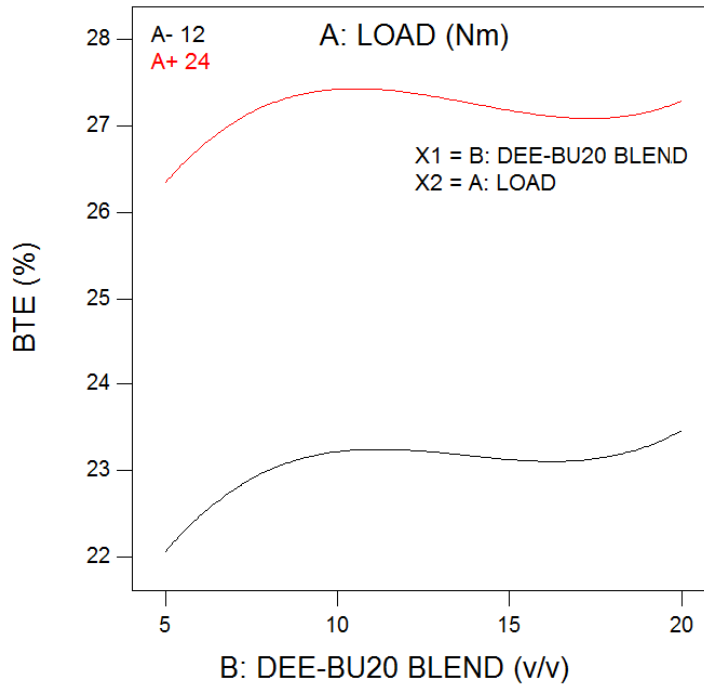


Fig. 4.105 Variation in BTE with diethylether blending at medium and full load

4.7.4 Emissions of engine using diethylether-n-butanol-diesel (DEE-BU20) blends

4.7.4.1 Variation of Smoke

Figs. 4.106 and 4.107 show the variation of smoke emission for diethylether-BU20 blends for experimental results and predicted model. It can be observed from figures that the smoke emission increases with increase in engine load. This is due to increase in the amount of fuel burned in the diffusion mode. Fig 4.107 shows that smoke is comparatively low at low loads, and increases slowly at moderate load, then increases considerably at higher load [56].

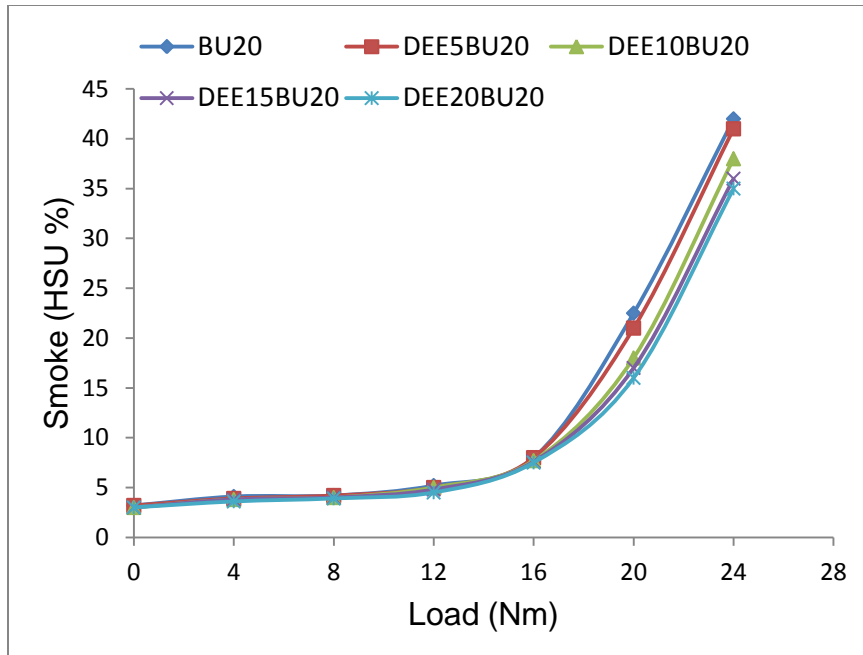


Fig. 4.106 Variation in smoke for Diethylether-BU20 blends

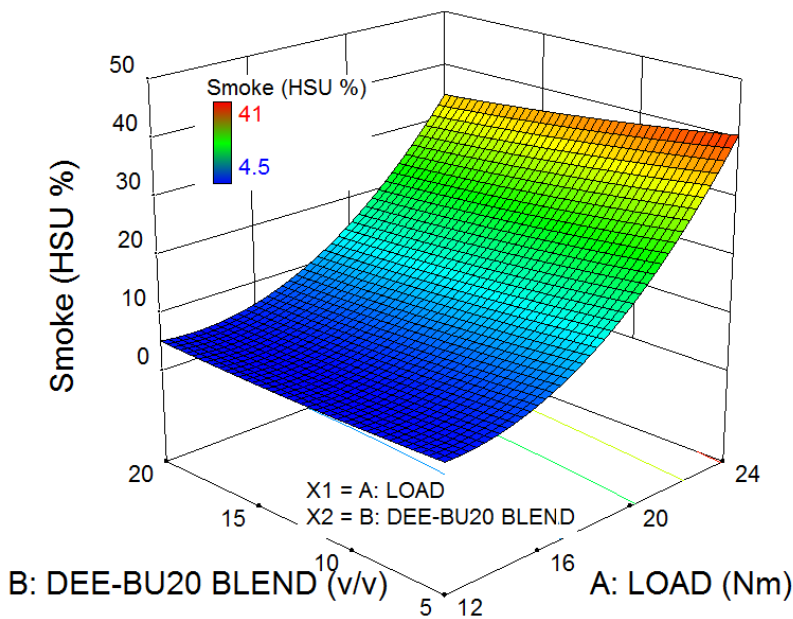


Fig. 4.107 Variation in smoke due to combined effect of load and Diethylether blending

Smoke decreases from DEE5BU20 to DEE20BU20 as compared to BU20 at full load condition. Fig. 4.114 shows that smoke emission decreases with increase of DEE percentage in the blends, and this trend is more noticeable at high engine loads. As this can be attributed to the fact that smoke is mainly generated during the diffusion

combustion phase. Ignition delay increases with addition of DEE in BU20 despite its high Cetane number and the diffusion combustion phase decline [141], [142]. With DEE blended fuel, the engine seemed to operated in an overall ‘leaner’ fashion. Moreover, the combustion was also improved due to more available oxygen (bonded with fuel) in diethylether in fuel rich zones. This also reduces formation of smoke precursors in diffusion combustion. DEE10BU20 and DEE20BU20 showed reduced smoke by 9.52% and 16.67% respectively as compared to BU20 at full load condition.

4.7.4.2 Variation of NO_x

Figs. 4.108 and 4.109 show the variation of NO_x emission for diethylether-BU20 blends for experimental results and predicted model.

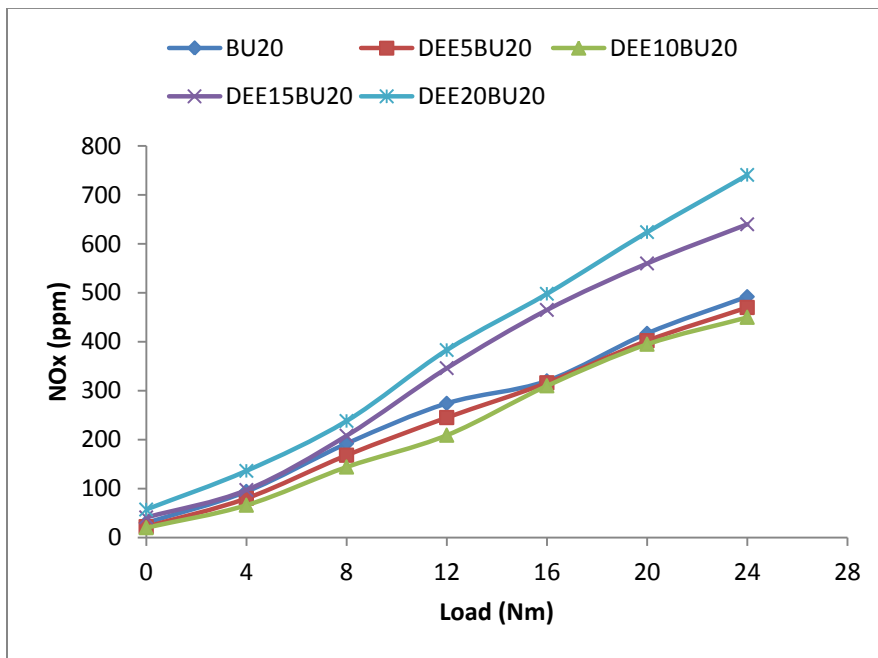


Fig. 4.108 Variation in NO_x for Diethylether-BU20 blends

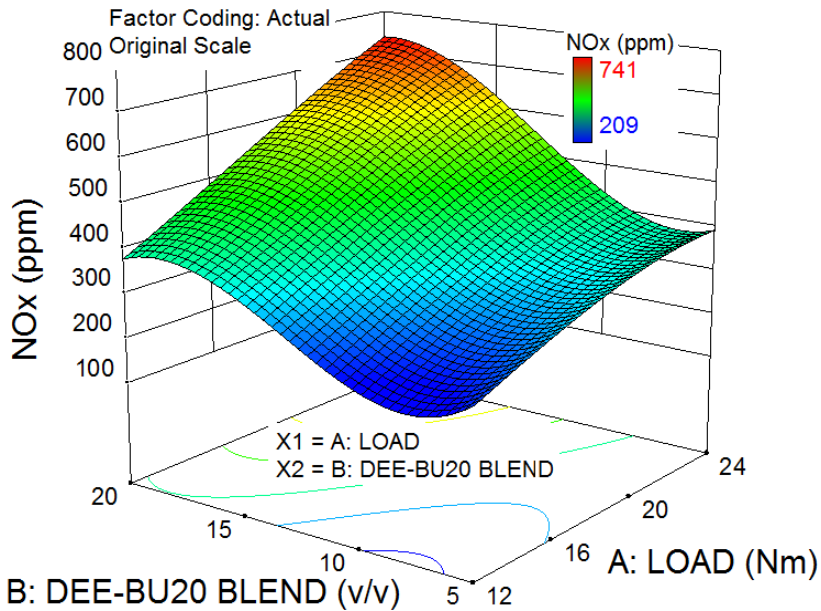


Fig. 4.109 Variation in NO_x due to combined effect of load and Diethylether blending

It can be observed from the figures that NO_x increased with load for all tested fuels. NO_x emission decreases initially from DEE5BU20 to DEE10BU20, and then again increases from DEE10BU20 to DEE20BU20. The results reveal that at lower blend and at higher blend, the formation of NO_x is influenced by different factors. The low calorific value, high Cetane number and high heat of vaporization are the factors that may dominate lower blends. On the other hand, availability of fuel oxygen is the factor that dominates higher blends. Also, at higher loads the variation in NO_x formation among low and high blends is more significant as shown by divergent shape of curves in Figs 4.108 and 4.109.

Low calorific value results in lower temperature in combustion chamber. High Cetane no. of DEE leads to reduction in the ignition delay period, and due to this, less mass of fuel is accumulated in the premixed phase of combustion. This limits the rate of combustion and peak temperature in combustion chamber, and is thus helpful in reducing NO_x emission. Due to high heat of vaporization, the temperature in combustion chamber decreases. All these factors lead to reduction in NO_x formation [37], [139], [141]. The increment in NO_x at higher blends is the result of more complete combustion due to higher percentage of oxygen available in fuel [140].

4.7.4.3 Variation of CO

Figs. 4.110 and 4.111 show the variation of CO emission for DEE-BU20 blends for experimental results and predicted model. It can be observed from these figures that CO emission decreases with load and increases with DEE blending. At all loads, the curves for different blends of DEE exhibit similar trends. However for BU20, at higher loads, the rate of reduction in CO is lower as compared to DEE-BU20 blends. The increment in CO with DEE-BU20 blends at all engine loads is the result of incomplete combustion of the fuel due to excess leaning of the air-fuel mixture [37]. Also, the higher latent heat of vaporization of diethylether tends to slow the vaporization of fuel. Moreover, air-fuel mixing along with insufficient availability of oxygen at full load condition leads to incomplete combustion and hence reduction of BTE as observed in Fig.4.114. As a result, CO emission increases with DEE-BU20 blending [17]. For DEE10BU20, CO emission was found to have increased by 12.82% as compared to BU20 at full load condition.

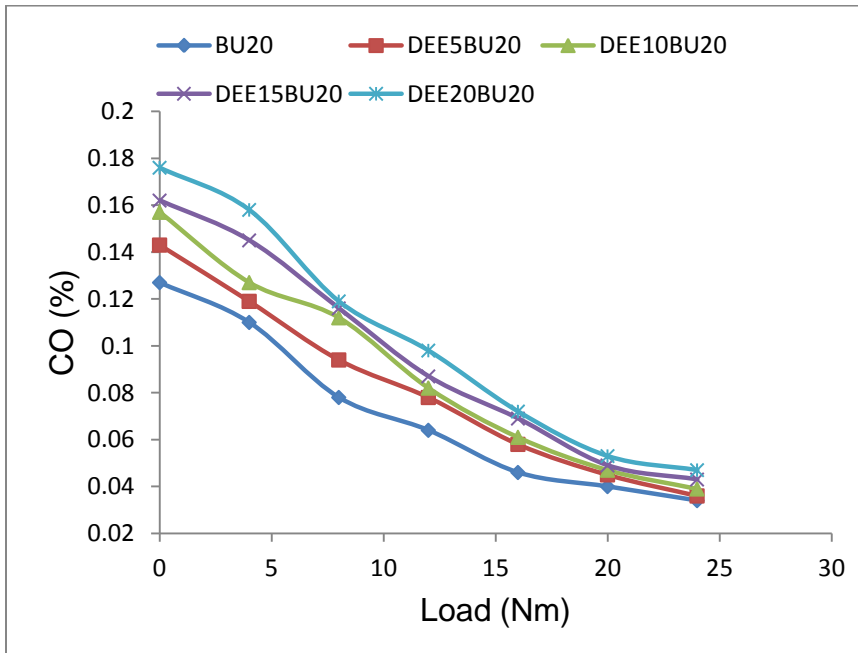


Fig. 4.110 Variation in CO for Diethylether-BU20 blends

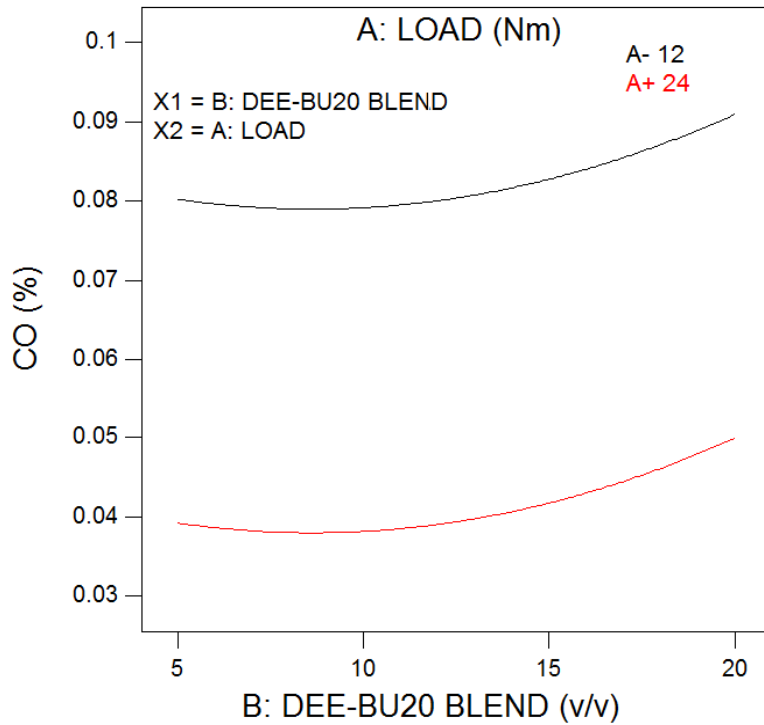


Fig. 4.111 Variation in CO with diethylether blending at medium and full load

4.7.4.4 Variation of HC

Figs. 4.112 and 4.113 show the variation of HC emission for DEE-BU20 blends for experimental results and predicted model.

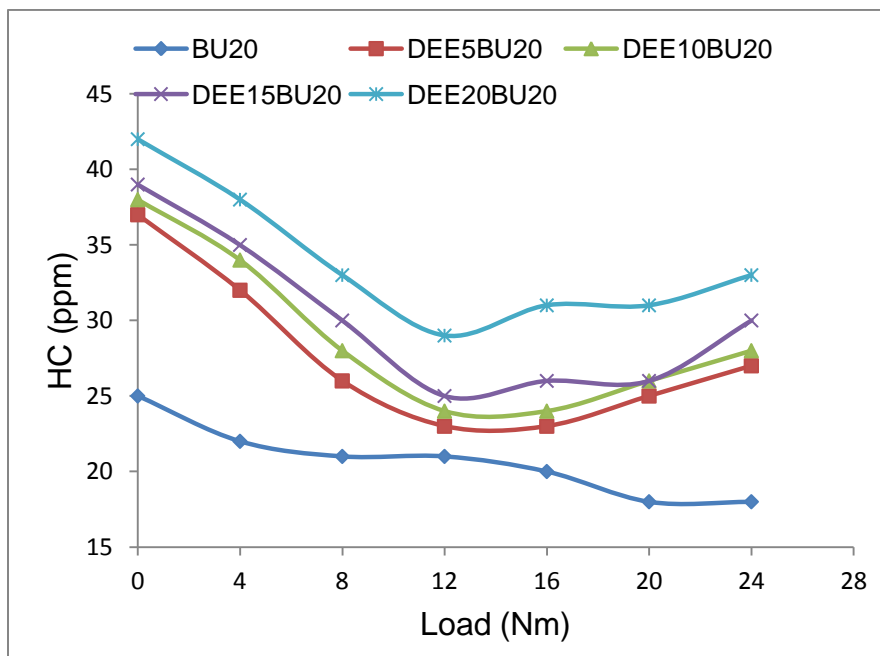


Fig. 4.112 Variation in HC for Diethylether-BU20 blends

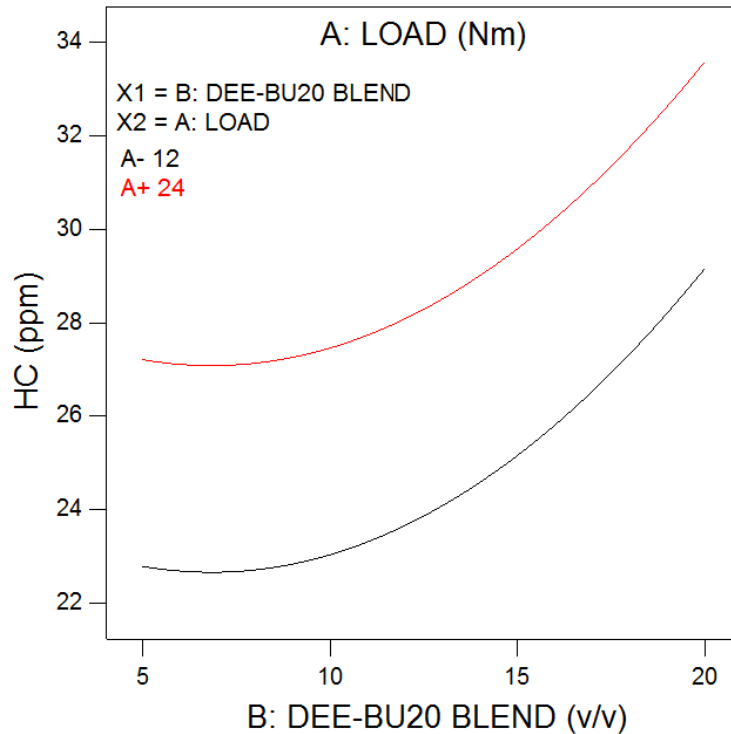


Fig. 4.113 Variation in HC with diethylether blending at medium and full load

The trends of HC emission are similar to DGM-BU20 blends. However, the levels of emission values are different. When the engine load increases, HC concentration decreases initially up to half of the full load and then increases up to full load condition for DEE-BU20 blends. For DEE-BU20 blends, HC emission were found higher compared to BU20. The higher latent heat of evaporation of DEE counteracts the benefit of higher Cetane number and thus results in increased HC emission. HC increases as a result of incomplete combustion of the blended fuel due to excess leaning of the fuel-air mixture at all engine loads. Reduced temperatures and pressures extend the lean flame-out region and increase unburned hydrocarbons [17], [37], [141], [144]. For DEE10BU20 fuel, HC was found to have increased by 35.71 % as compared to BU20 at full load condition.

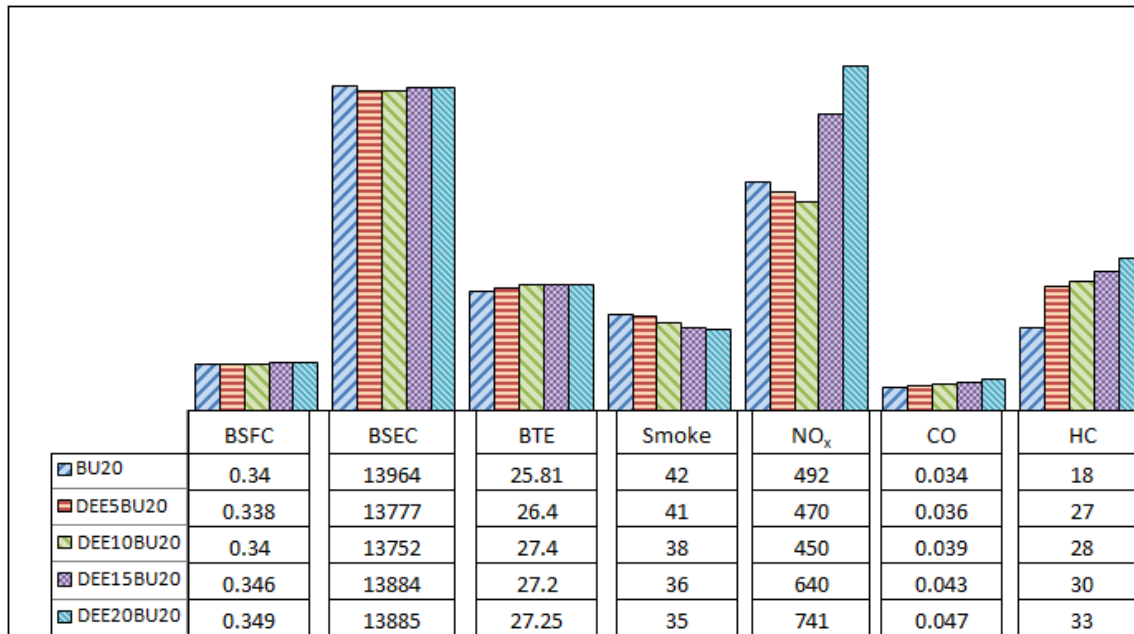


Fig. 4.114 Performance and emission of Diethylether-BU20 blends (100% rated power)³

4.7.5 Validation and optimization of responses

The parameters were optimized for desired values of responses. Table 4.52 summarizes the minimum and maximum values of each response to optimize operating parameters of the engine. On the basis of Table 4.52 and optimization analysis, the optimum blended fuel and their predicted responses were obtained, and are shown in Table 4.53. The test was repeated at very near to optimum values of load and blending (19.7 Nm and 8.5% DEE blended in BU20) to validate the results predicted by the models. The optimum values of BSFC, BTE, smoke, NO_x, CO and HC were observed to be 0.345, 26.7, 18, 378, 0.044 and 24.5 respectively. It can also be observed from Table 4.53 that the percentage errors of these results are within tolerance. This shows the exactness of predicted models. On the basis of this validation of experimental results by mathematical modeling, DEE10BU20 (10% diethylether in BU20) was selected as the optimum blend of diethylether with BU20.

³Fig is not on scale

Table 4.52 Maximum and minimum limits for each response to optimize performance and emissions

Names	Goal	Lower limit	Upper limit
A: Load	Is in range	12	24
B: Blend (DEEBU20)	Is in range	5	20
Response: BSFC	Minimize	0.338	0.45
Response: BTE	Maximize	22.04	27.4
Response: Smoke	Minimize	4.5	41
Response: NO _x	Minimize	209	741
Response: CO	Minimize	0.039	0.098
Response: HC	Minimize	23	33

Table 4.53 Optimum conditions of load and blend and their predicted results

Number	Load	(DEE-BU20)	BSFC	BTE	Smoke	NO _x	CO	HC	
1	<u>19.659</u>	<u>8.395</u>	<u>0.345</u>	<u>26.503</u>	<u>17.987</u>	<u>349.160</u>	<u>0.045</u>	<u>24.646</u>	Selected
2	20.949	10.713	0.340	26.787	22.317	432.102	0.043	25.780	
3	24.000	10.021	0.336	27.407	38.169	450.697	0.038	27.467	
Confirmation test	19.7	8.5	0.345	26.7	18	378	0.044	24.5	
Error Percentage (× 100)			0	-0.74	-0.07	-8.26	2.22	0.59	

4.8 Comparison of performance and emissions of BU20, NM1BU20, DGM15BU20 and DEE10BU20 blends

4.8.1 Heat release rate for BU20, NM1BU20, DGM15BU20 and DEE10BU20 blends

Fig. 4.115 shows heat release rate (HRR) diagram for BU20, NM1BU20, DGM15BU20 and DEE10BU20 blends. It can be observed that peak of heat release of NM1BU20 is very slightly higher than BU20. It may be because of fast burning rate of NM due to higher content of oxygen. The peak of HRR of DGM15BU20 and DEE10BU20 is lower than BU20 [159] and slightly advanced. The probable reason of this is reduced ignition delay due to higher Cetane number of DGM and DEE [56], [133], [139], [141].

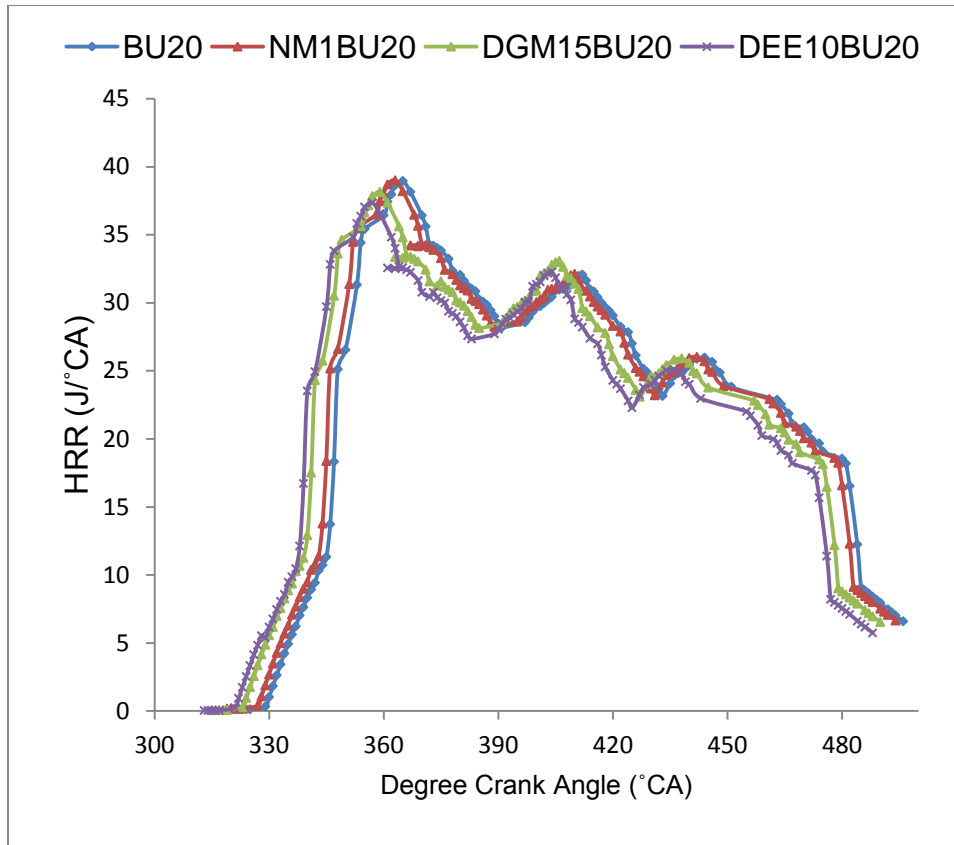


Fig. 4.115 Comparison of heat release rate of different blended fuels

To find out optimum blend for performance and reduced emissions, comparison of optimum blends of NM-BU20, DGM-BU20 and DEE-BU20 was done as shown in figures 4.116 to 4.124 respectively.

4.8.2 Comparison of performance of BU20, NM1BU20, DGM15BU20 and DEE15BU20 blends

Figs. 4.116 and 4.117 show engine performance using different blended fuels (as obtained in previous stages) in terms of BSFC and BTE. Fig. 4.121 depicts the values of performance and emission parameters at full load condition.

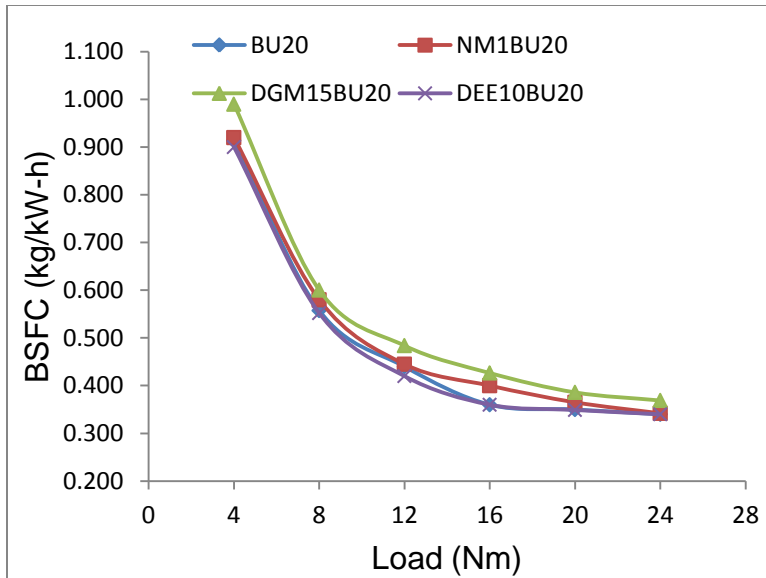


Fig. 4.116 (a) Variation of BSFC with engine load for different blended fuels

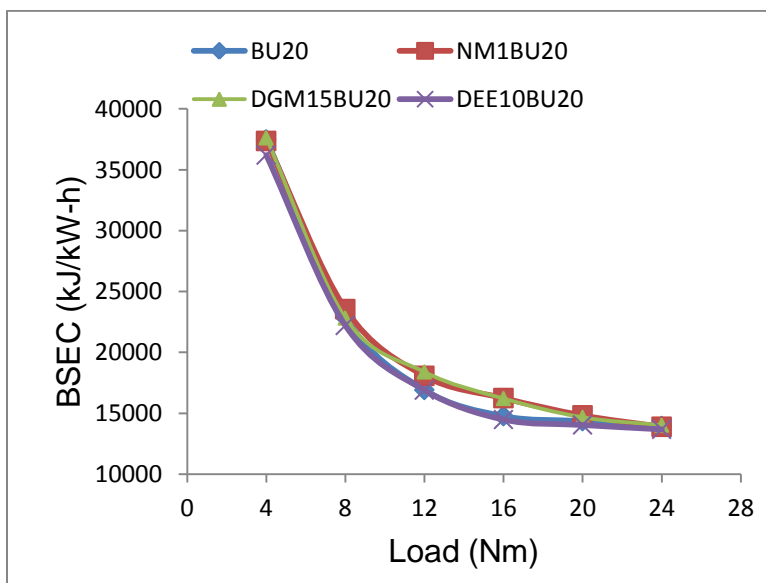


Fig. 4.116 (b) Variation of BSEC with engine load for different blended fuels

It can be observed from figures 4.116 (a) and 4.122 that DGM15BU20 shows highest BSFC in the tested group and DEE10BU10 shows the same value of BSFC as that of BU20. DGM15BU20 shows 8.5%, 7.9% and 8.5% higher BSFC as compare to BU20, NM1BU20 and DEEBU20 respectively. The Fig. 4.116 (b) shows similar trends of BSEC as of BSFC in Fig. 4.116 (a).

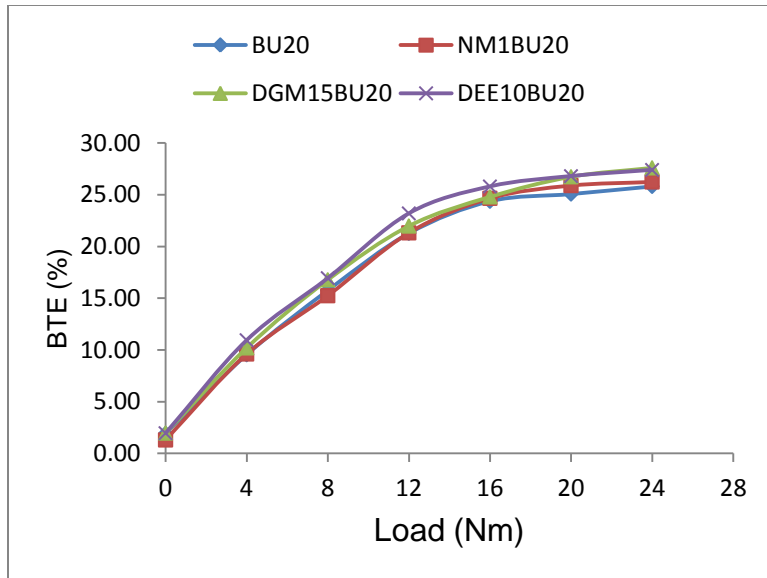


Fig. 4.117 Variation of BTE with engine load for different blended fuels

Fig 4.117 presents the variation of brake thermal efficiency with engine load for different blended fuels (Optimized in previous sections). It can be observed from figures that for the whole range of loads, NM1BU20 shows lower BTE as compared to DGM15BU20 and DEE10BU20. At lower loads, BTE of DEE10BU20 is higher as compared to DGM15BU20, but at higher loads, the BTE of DGM15BU20 is improved and is slightly higher than that of DEE10BU20. The BTE of DGM15BU20 is higher as compared to BU20, NM1BU20 and DEE10BU20 by 6.9%, 5.2% and 0.70% respectively.

4.8.3 Comparison of emissions of BU20, NM1BU20, DGM15BU20 and DEE10BU20 blends

Fig 4.118 shows the variation of smoke for BU20, NM1BU20, DGM15BU20 and DEE10BU20. At lower loads, the emission of smoke is approximately same for all blends, but at higher loads, smoke for NM1BU20 and DGM15BU20 is found to have decreased. It can be observed from Fig. 4.123 that smoke for DGM15BU20 is approximately same as that of NM1BU20, and lesser than BU20 and DEE10BU20 by 28.6% and 21.1% respectively at full load condition.

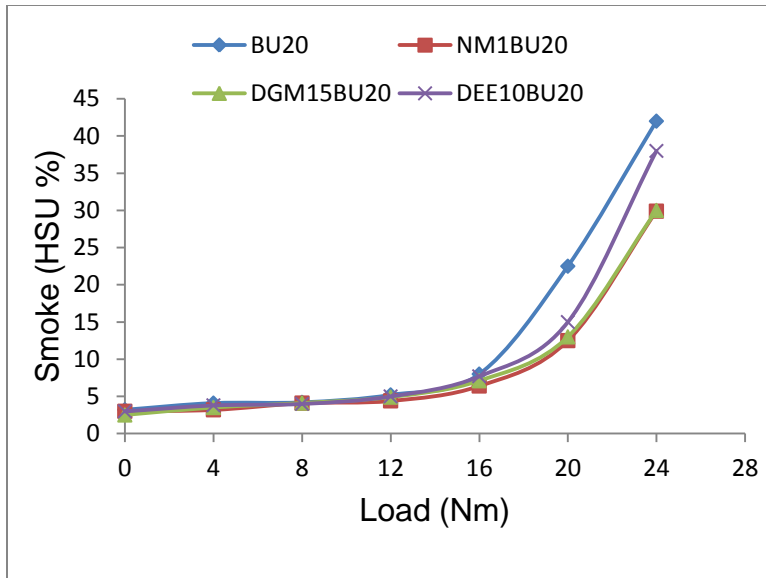


Fig. 4.118 Variation of smoke with engine load for different blended fuel

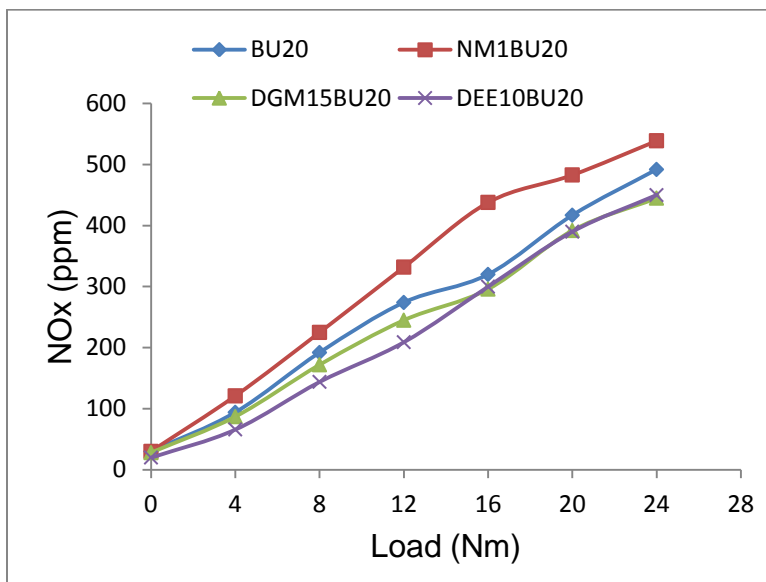


Fig. 4.119 Variation of NO_x with engine load for different blended fuels

Fig. 4.119 shows the variation of NO_x with engine load for different blended fuels. NO_x emission of DGM15BU20 and DEE10BU20 are lower compared to BU20 and NM1BU20 for the whole range of loads. From figure 4.123 it can be observed that DGM15BU20 shows reduced NO_x as compared to BU20, NM1BU20 and DEE10BU20 by 9.6%, 17.4 % and 1.1% respectively at full load condition.

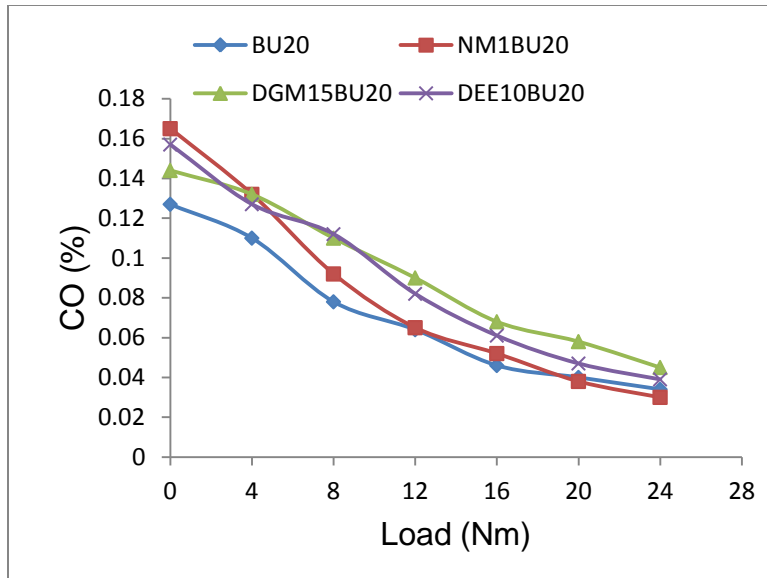


Fig. 4.120 Variation of CO with engine load for different blended fuels

It can be observed from figure 4.120 that with NM1BU20 fuel, CO emission is lowest among all compared blends. With DGM15BU20 the CO emission is higher as compared to BU20, NM1BU20 and DEE10BU20 by 32.4%, 50% and 15.4 respectively at full load condition.

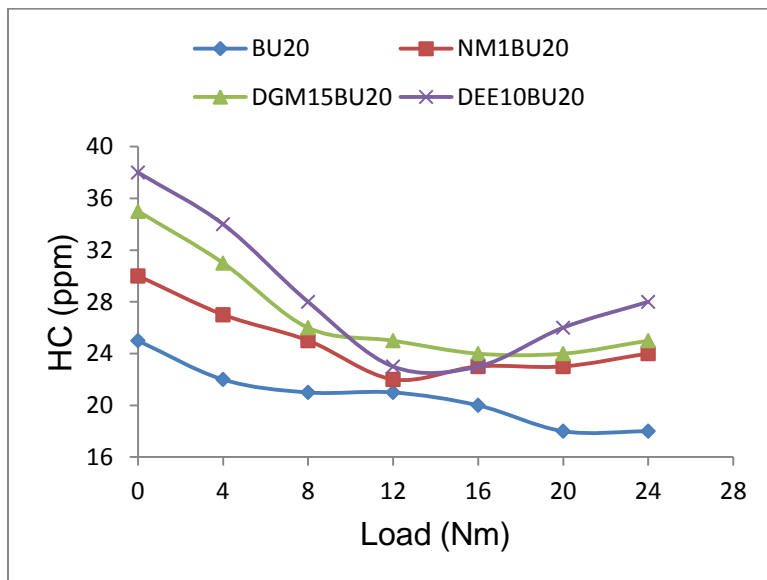


Fig. 4.121 Variation of HC with engine load for different blended fuels

Fig. 4.121 shows that HC emission is higher for all ternary blends as compared to BU20. However, among the three ternary blends, NM1BU20 shows lowest HC emission. HC

emission for DGM15BU20 is higher than BU20 and NM1BU20 by 38.9% and 4.2% and lower than DEE10BU20 by 10.7% respectively.

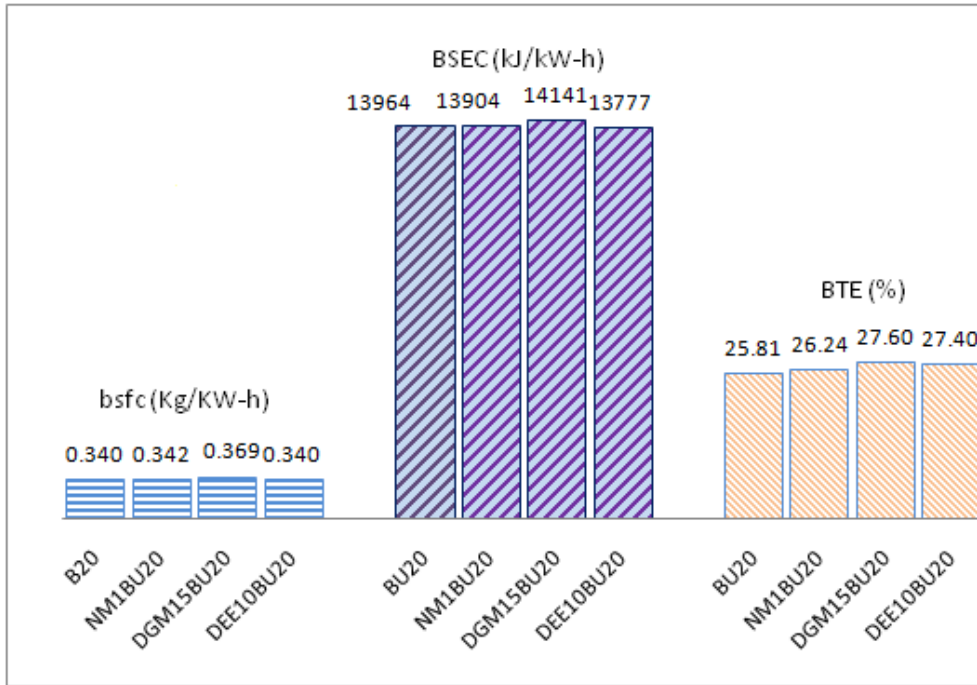


Fig. 4.122 Comparison of BSFC, BSEC and BTE at full load for different blended fuels⁴

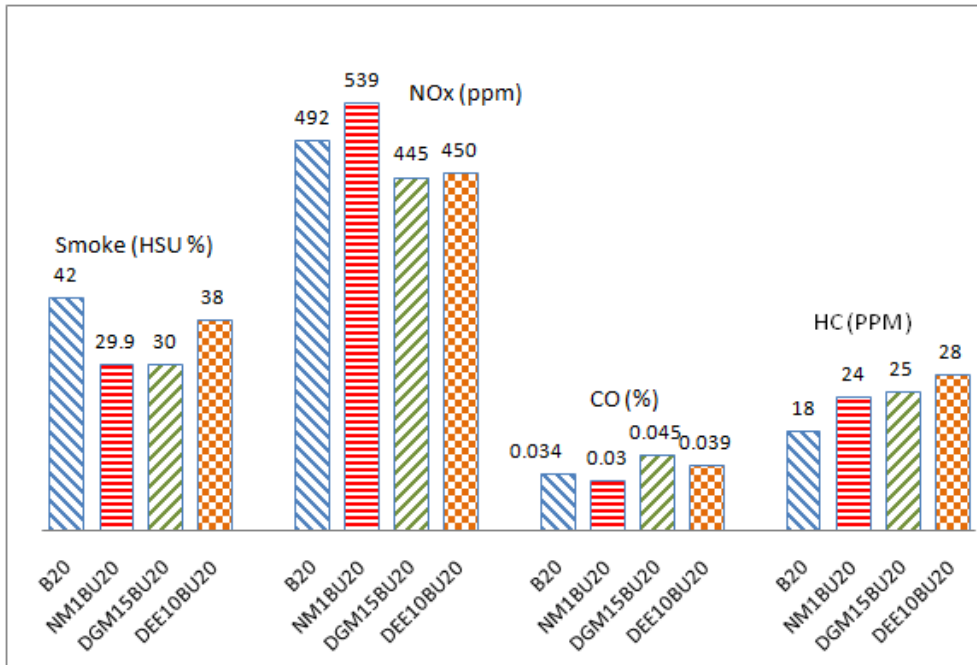


Fig. 4.123 Comparison of smoke, NO_x, HC and CO at full load for different blended fuels⁴

⁴Fig is not on scale.

Comparison of NM1BU20, DGM15BU20 and DEE10BU20 shows that DGM15BU20 is the best choice among all tested ternary blends for reducing smoke and NO_x emissions significantly without much affecting the performance of engine. However, DGM15BU20 has the disadvantage of having higher CO emission compared to other blends.

4.8.4 Smoke-NO_x trade-off for BU20, NM-BU20, DGM-BU20 and DEE-BU20 blends

Fig. 4.124 presents smoke-NO_x trade-off for BU20, NM1BU20, DGM15BU20 and DEE10BU20 blends. It can be observed that DGM15BU20 presents the best smoke-NO_x trade off among the compared blends.

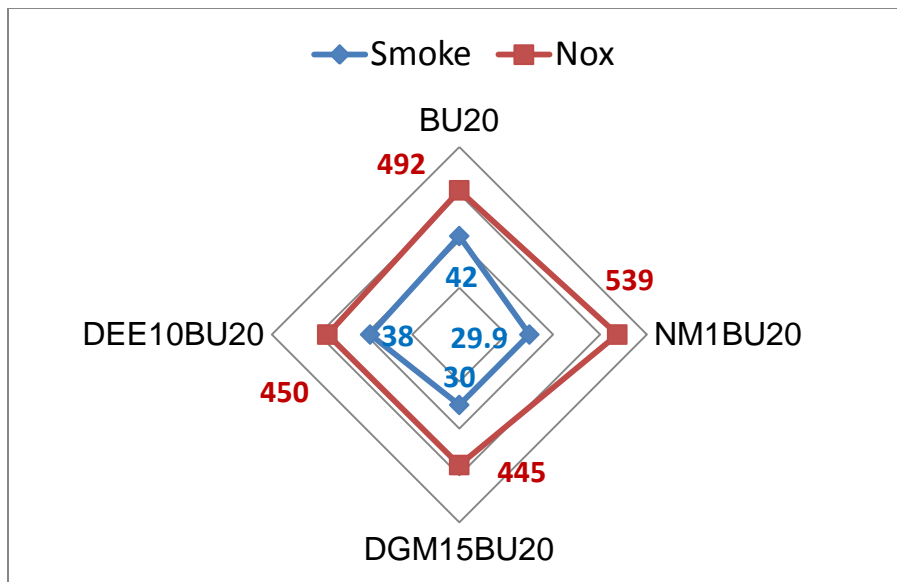


Fig. 4.124 Smoke-NO_x Trade-off for different blended fuels

4.9 Comparison of performance and emissions of DGM15BU20 with diesel

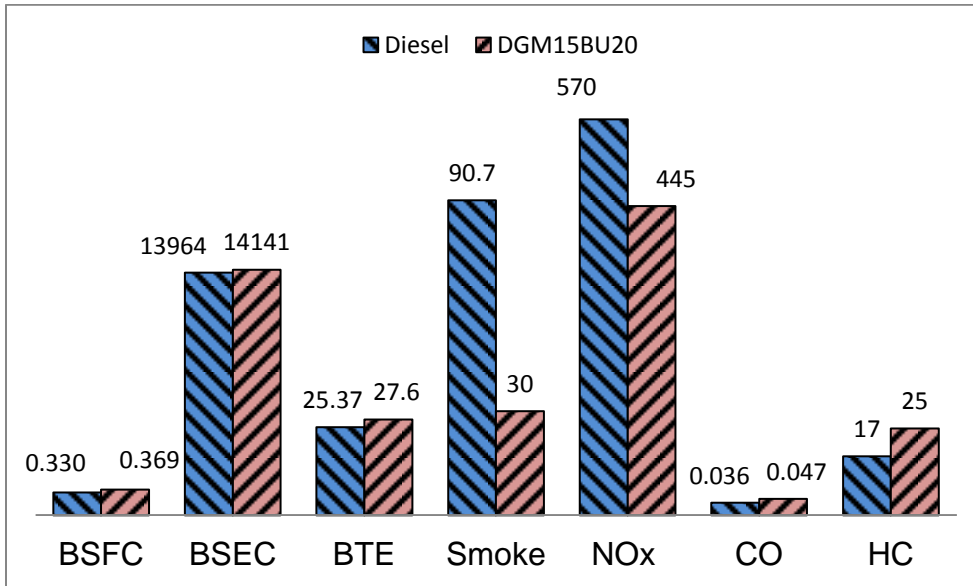


Fig. 4.125 Comparison of performance and emissions for diesel and DGM15BU20

From the previous sections it can be observed that DGM15 BU20 blend is the optimum blend for existing engine in terms of performance and emissions. In Fig. 4.125, the final comparison of performance and emissions parameters is presented between diesel and DGM15BU20. Figure shows that BSFC and BTE of DGM15BU20 are higher as compared to diesel by 11.8% and 8.8% respectively at full load condition. For DGM15BU20, smoke and NO_x are lesser by 66.9% and 21.9% respectively as compared to diesel at full load condition. However, CO and HC are more by 30.6% and 47.1% respectively for DGMBU20 as compared to diesel.

4.10 Economic analysis of blended fuel

Literature gives evidence of economical production of n-butanol by different methods and with different feedstock [160], [161]. The minimum cost of butanol production by ABE (Acetone-Butanol-Ethanol) process was reported to be \$3/gallon (INR 53.55/lit.)⁵ [162]. The average price of n-butanol production (projected from the base year 2007 to 2027) from corn or switch grass through ABE fermentation is estimated to be \$0.77/kg (INR51.95/kg)¹ [163]. The cost of bio-butanol production by wheat straw is estimated to

⁵The conversion rate is \$1= INR67.4 and the cost is ex-factory cost

be \$1.00- 1.41/kg (INR67.48-95.14/kg)⁵. However, this depends on raw material cost and membrane recovery process [164]. The estimated cost of bio-butanol production from corn is \$0.34 -1.07/kg (INR 22.94-72.20/kg)⁵ and depends on the cost of corn, credits for by-products and cost of establishment of plant [165].

N-butanol is available in the Indian local markets at a cost of INR 80/kg (INR 64.78/lit., specific gravity of n-butanol being 0.8098). The diglyme was also procured from Indian local market at a cost of INR 126/kg (INR 118.06/lit., specific gravity of diglyme being 0.937). The cost of BU20 and DGM15BU20 are INR 59.86/lit. and INR 68.59/lit. (diesel cost is INR 58.63/lit.). Diglyme is a colourless, clear liquid having smelling like ether and is lower toxic. Diglyme can be produced by different methods and readily available in market. Table 4.54 shows cost calculation of diesel, BU20 and DGM15BU20 on per kW-h basis. It can be clearly seen that when engine is running on BU20 and DGM15BU20, the increased cost of fuel is INR 4.14/ kW-h and INR 7.52/ kW-h.

Table 4.54 Cost analysis of diesel, BU20 and DGM15BU20 [110]

Fuel	cost/litre	cost/kg	Average BSFC	Cost (INR/kW-h)
Diesel	58.63	70.72	0.37	26.17
BU20	59.86	73.92	0.41	30.31
DGM15BU20	68.59	80.98	0.416	33.69

Chapter 5

Conclusions and Future Scope

5.1 Conclusions

The present research work undertook a detailed experimental study under which different bio-oxygenated blended fuels were tested on a stationary, agriculture based diesel engine for analysis of engine performance and emissions. Different n-butanol-diesel blends were prepared in varying concentrations to find out the optimum percentage of n-butanol that can be mixed in diesel for reduced emissions and optimum performance. With optimum n-butanol-diesel blend (BU20), the engine operating parameters were optimized for performance and emissions. Nitromethane (NM), Diglyme (DGM) and Diethylether (DEE) were blended as additives in BU20 in different proportions and experiments were conducted to observe engine performance and emission characteristics. An overall comparison of all tested fuels was done to find the most suitable ternary bio-oxygenated fuel for optimum engine performance and emissions. Modeling and optimization of engine performance and emissions were done with different blended fuels. Reduced quadratic and cubic models were obtained and were used to predict the optimum values of engine operating parameters with BU20 and blending ratios of different additives for desired values of outputs.

The results obtained in the present research are consistent with past studies presented in literature. The mathematical analysis of responses showed that experimental observations and predicted results from the mathematical models are quite close. This is indicative of the fact that the models developed are quite reliable and can be used for predicting results of experiments without actually having to perform them. Following conclusions were drawn on the basis of experimental results:

1. With diesel, the optimum performance and emissions of the engine was observed at a compression ratio of 18.5, injection timing of 23°CA bt dc and injection pressure of 210 bar.
2. With n-butanol-diesel blends, the optimum performance and emissions of the engine was observed at 20% blending of n-butanol in diesel (BU20) by volume (v/v).

3. From modeling, the predicted optimal values of n-butanol-diesel blends were 19.558% (v/v) at full load and 20.001% (v/v) at part load, which are quite close to the experimental value of 20% (v/v).
4. When the engine operating parameters were optimized for BU20, the optimum performance and emissions results were observed at a higher compression ratio of 19.5 under similar operating conditions.
5. The optimal values of compression ratio (CR), injection timing and injection pressure as predicted by the models were 19.483, 23.598 and 208.546 respectively, which are quite close to experimental results (19.5, 23 and 210 respectively). This data clearly shows that results obtained from the models are reliable in predicting the outcome of such experiments without much error margin. Blending of 20% of n-butanol in diesel at a higher CR of 19.5, improved the thermal efficiency by 5.54% while reducing smoke and NO_x by 59.56% and 15.96% respectively at full load as compared to diesel.
6. When engine was fuelled with BU20; BSFC and BTE increased by 3.03% and 1.73% respectively at 19.5 CR as compared to diesel at CR of 18.5 and at same settings of injection timing and injection pressure at full load condition. The smoke, NO_x, and CO emissions decreased by 53.85%, 13.68% and 11.11% respectively at 19.5 CR as compared to diesel at CR of 18.5. However, emission of HC increased by 5.88% when using BU20 at 19.5 CR as compared to diesel at CR of 18.5.
7. It was concluded that BU20 can be used safely in engines similar to the one used in the experiments. Further, it can now be stated with confidence that the overall effect of using n-butanol-diesel blend is a significant reduction in emissions with a slight improvement in engine efficiency.
8. For all NM-BU20 blends, BSFC was higher and BTE improved slightly in comparison to BU20. Smoke was reduced while other emissions were increased with NM-BU20 blends in comparison to BU20. However, 1% NM blend in BU20 (NM1BU20) showed better results than other NM-BU20 blends. Blending of NM1BU20 increased BSFC marginally and increased BTE by 1.66% at full load condition. Smoke and CO were reduced by 28.8% and 6.3% for NM1BU20 as compared to BU20 at full load condition. NO_x and HC emissions were increased by

- 9.55% and 33.33% for NM1BU20 as compared to BU20 at full load condition. CO and HC showed continued increments with increasing percentage of NM in NM-BU20 blends.
9. For all DGM-BU20 blends, BSFC was higher as compared to BU20. For increasing percentages of DGM in the blends, BTE showed a continual rise within the range of blends from DGM5BU20 to DGM15BU20; but then decreased for DGM20BU20. Significant reduction in smoke was observed for DGM15BU20. Smoke and NO_x were reduced by 28.57% and 9.55% for DGM15BU20 as compared to BU20 at full load condition. CO and HC emissions were increased by 38.23% and 38.88% respectively with DGM15BU20 blend as compared to BU20 at full load condition.
 10. The change in BSFC was negligible with blending of DEE in BU20. DEE10BU20 exhibited better results among DEE-BU20 blends. BTE increased from DEE5BU20 to DEE10BU20, and then reduced slightly from DEE10BU20 to DEE20BU20. For DEE10BU20, the increment in BTE was found to be 6.15% as compared to BU20 at full load condition. Smoke decreased with increased percentage of DEE in BU20. NO_x emission was found lesser for lower blends and higher for higher blends. Smoke & NO_x reduced by 9.52% & 8.53%; while CO & HC increased by 14.7% and 55.55% for DEE10BU20 as compared to BU20 at full load condition.
 11. An overall comparison of BU20, NM1BU20, DGM15BU20 and DEE10BU20 revealed that DGM15BU20 showed better results of performance and emissions. DGM15BU20 presented the best smoke-NO_x trade-off among all the tested fuel blends. BSFC and BTE of DGM15BU20 were higher as compared to diesel by 11.8% and 8.8% respectively at full load condition. For DGM15BU20, smoke and NO_x were lesser by 66.9% and 21.9% respectively as compared to diesel at full load condition. However, CO and HC were more by 30.6% and 47.1% respectively for DGMBU20 as compared to diesel. Although the percentage increments in CO and HC were considerable, the absolute values of CO and HC were within tolerable limits.
 12. The predicted results of responses obtained through mathematical modeling were found to closely follow the experimental results. Thus it was concluded that the developed models for performance and emissions are suitable to be used for

estimating the performance and emission responses of same type of engines (as used in the present experimental work) under similar operating conditions.

13. The ternary blend of Diglyme-n-butanol-diesel (DGM15BU20) was concluded to be the best blended fuel amongst all the tested blends for the experimental C.I. engine. It can also be quite confidently stated that this fuel could contribute well towards a clean environment in near future.

5.2 Future Scope

1. Other than the additives used in the present study, more additives can be blended in diesel to check performance and emission characteristics.
2. With the use of programmable electronic control units (ECUs), operating parameters could be controlled more precisely.
3. Comparison of performance and emissions of oxygenated ternary blends could be done with and without using exhaust gas recirculation, diesel particulate filters and modified injection techniques.
4. The selected additives could be tested on mobile engines under transient conditions and results could be compared with steady state condition.
5. The additives of widely different Cetane number can be used with Reactivity controlled compression ignition (RCC) mode.
6. Means of limiting HC emission could be further explored.

References

- [1] International Energy Agency (IEA), “World Energy Outlook 2016,” France, 2016.
- [2] A. S. World Energy Council and P. S. Institute, “World Energy Scenarios,” London, 2016.
- [3] International Energy Agency (IEA), “India Energy Outlook,” France, 2015.
- [4] The Energy and Resources Institute (TERI), *Energy Security Outlook: Defining a secure and sustainable energy future for India*. New Delhi: The Energy and Resources Institute (TERI), TERI press, 2015.
- [5] H. E. Kebin, Z. Qiang, and H. U. O. Hong, “Types and amounts of vehicular emissions,” *Point sources of pollution: local effects and it’s control*, vol. I. UNESCO-Encyclopedia of life support systems (EOLSS), China, pp. 27–63.
- [6] UCSUSA Report, “Cars, trucks, and air pollution,” 2014. [Online]. Available: <http://www.ucsusa.org/clean-vehicles/vehicles-air-pollution-and-human-health/cars-trucks-air-pollution>. [Accessed: 09-Sep-2017].
- [7] “Domestics sales trends,” *Society of Indian Automobile Manufacturers (SIAM)*. [Online]. Available: <http://www.siamindia.com/statistics.aspx?mpgid=8&pgidtrail=14>. [Accessed: 26-Sep-2017].
- [8] Nielsen, “All India study on sectoral demand of diesel & petrol,” *Pet. Plan. Anal. Cell Rep.*, p. 104, 2013.
- [9] “India overtook China in number of deaths due to pollution: Report,” *THE HINDU*, 16-Nov-2016. [Online]. Available: <http://www.thehindu.com/sci-tech/energy-and-environment/India-overtook-China-in-number-of-deaths-due-to-pollution-Report/article16643789.ece>. [Accessed: 02-Sep-2017].
- [10] Vishwa Mohan, “Nearly 1.59 million premature deaths per year in India linked to air pollution: IEA,” *The Times of India*, 27-Jun-2016. [Online]. Available: <http://timesofindia.indiatimes.com/home/environment/pollution/Nearly-1-59-million-premature-deaths-per-year-in-India-linked-to-air-pollution-IEA/articleshow/52945655.cms>. [Accessed: 02-Sep-2017].
- [11] “Fuels and vehicles,” *Energy Efficiency and Renewable Energy, US Department of Energy*. [Online]. Available:

- https://www.afdc.energy.gov/fuels/biodiesel_benefits.html. [Accessed: 02-Sep-2017].
- [12] D. C. Rakopoulos, C. D. Rakopoulos, E. G. Giakoumis, R. G. Papagiannakis, and D. C. Kyritsis, "Influence of properties of various common bio-fuels on the combustion and emission characteristics of high-speed DI (direct injection) diesel engine: vegetable oil, bio-diesel, ethanol, n-butanol, diethyl ether," *Energy*, vol. 73, pp. 354–366, 2014.
- [13] B. Choi and X. Jiang, "Individual hydrocarbons and particulate matter emission from a turbocharged CRDI diesel engine fueled with n-butanol/diesel blends," *Fuel*, vol. 154, pp. 188–195, 2015.
- [14] E. Rajasekar, A. Murugesan, R. Subramanian, and N. Nedunchezian, "Review of NO_x reduction technologies in CI engines fuelled with oxygenated biomass fuels.pdf," *Renew. Sustain. Energy Rev.*, vol. 14, pp. 2113–2121, 2010.
- [15] W. Tutak, "Bioethanol E85 as a fuel for dual fuel diesel engine," *Energy Convers. Manag.*, vol. 86, pp. 39–48, 2014.
- [16] Y. S. Jang, A. Malaviya, C. Cho, J. Lee, and S. Y. Lee, "Butanol production from renewable biomass by clostridia," *Bioresour. Technol.*, vol. 123, pp. 653–663, 2012.
- [17] M. Iranmanesh, J. P. Subrahmanyam, and M. K. G. Babu, "Application of diethyl ether to reduce smoke and NO_x emissions simultaneously with diesel and biodiesel fueled engines," in *Proceedings of IMECE2008, Volume 3: Combustion Science and Engineering*, 2008, no. 3, pp. 77–83.
- [18] N. L. Jain, S. L. Soni, M. P. Poonia, D. Sharma, A. K. Srivastava, and H. Jain, "Performance and emission characteristics of preheated and blended thumba vegetable oil in a compression ignition engine," *Appl. Therm. Eng.*, vol. 113, pp. 970–979, 2017.
- [19] Z. H. Zhang and R. Balasubramanian, "Influence of butanol addition to diesel-biodiesel blend on engine performance and particulate emissions of a stationary diesel engine," *Appl. Energy*, vol. 119, pp. 530–536, 2014.
- [20] A. Atmanli, B. Yuksel, and E. Ileri, "Experimental investigation of the effect of diesel-cotton oil-n-butanol ternary blends on phase stability, engine performance

- and exhaust emission parameters in a diesel engine,” *Fuel*, vol. 109, pp. 503–511, 2013.
- [21] M. M. Rahman, S. Stevanovic, R. J. Brown, and Z. Ristovski, “Influence of different alternative fuels on particle emission from a turbocharged common-rail diesel engine,” *Procedia Eng.*, vol. 56, pp. 381–386, 2013.
- [22] G. Chen, W. Yu, Q. Li, and Z. Huang, “Effects of n-butanol addition on the performance and emissions of a turbocharged common-rail diesel engine,” *SAE Tech. Pap. 2012-01-0852*, 2012.
- [23] S. Kumar, J. H. Cho, J. Park, and I. Moon, “Advances in diesel-alcohol blends and their effects on the performance and emissions of diesel engines,” *Renew. Sustain. Energy Rev.*, vol. 22, pp. 46–72, 2013.
- [24] Y. Putrasaria, A. Nura, and A. Muharama, “Performance and emission characteristic on a two cylinder DI diesel engine fuelled with ethanol-diesel blends,” *Energy Procedia*, vol. 32, pp. 21–30, 2013.
- [25] M. Lapuerta, O. Armas, and J. M. Herreros, “Emissions from a diesel-bioethanol blend in an automotive diesel engine,” *Fuel*, vol. 87, no. 1, pp. 25–31, 2008.
- [26] C. Sayin, “Engine performance and exhaust gas emissions of methanol and ethanol-diesel blends,” *Fuel*, vol. 89, no. 11, pp. 3410–3415, 2010.
- [27] C. Sayin, A. N. Ozsezen, and M. Canakci, “The influence of operating parameters on the performance and emissions of a DI diesel engine using methanol-blended-diesel fuel,” *Fuel*, vol. 89, no. 7, pp. 1407–1414, 2010.
- [28] O. Can, I. Celikten, and N. Usta, “Effects of ethanol addition on performance and emissions of a turbocharged indirect injection diesel engine running at different injection pressures,” *Energy Convers. Manag.*, vol. 45, no. 15–16, pp. 2429–2440, 2004.
- [29] S. M. Palash, H. H. Masjuki, M. A. Kalam, B. M. Masum, A. Sanjid, and M. J. Abedin, “State of the art of NO_x mitigation technologies and their effect on the performance and emission characteristics of biodiesel-fueled compression ignition engines,” *Energy Convers. Manag.*, vol. 76, pp. 400–420, 2013.
- [30] R. Mohsin, Z. A. Majid, A. H. Shihnan, N. S. Nasri, and Z. Sharer, “Effect of biodiesel blends on engine performance and exhaust emission for diesel dual fuel

- engine,” *Energy Convers. Manag.*, vol. 88, pp. 821–828, 2014.
- [31] R. J. H. Klein-Douwel *et al.*, “Soot and chemiluminescence in diesel combustion of bio-derived, oxygenated and reference fuels,” *Proc. Combust. Inst.*, vol. 32, no. 2, pp. 2817–2825, 2009.
- [32] H. Bayindir, M. Zerrakki Isik, and H. Aydın, “Evaluation of combustion, performance and emission indicators of canola oil-kerosene blends in a power generator diesel engine,” *Appl. Therm. Eng.*, vol. 114, pp. 234–244, 2017.
- [33] A. Corsini, A. Marchegiani, F. Rispoli, F. Sciulli, and P. Venturini, “Vegetable oils as fuels in diesel engine. Engine performance and emissions,” *Energy Procedia*, vol. 81, pp. 942–949, 2015.
- [34] D. Agarwal and A. K. Agarwal, “Performance and emissions characteristics of Jatropha oil (preheated and blends) in a direct injection compression ignition engine,” *Appl. Therm. Eng.*, vol. 27, no. 13, pp. 2314–2323, 2007.
- [35] E. Rajasekar, A. Murugesan, R. Subramanian, and N. Nedunchezian, “Review of NOx reduction technologies in CI engines fuelled with oxygenated biomass fuels,” *Renew. Sustain. Energy Rev.*, vol. 14, pp. 2113–2121, 2010.
- [36] C. Y. Choi and R. D. Reitz, “Experimental study on the effects of oxygenated fuel blends and multiple injection strategies on DI diesel engine emissions,” *Fuel*, vol. 78, no. 11, pp. 1303–1317, 1999.
- [37] S. D, V. T, and T. M, “Experimental analysis of combustion and emissions characteristics of CI engine powered with diethylether blended diesel as fuel,” *Res. J. Eng. Sci.*, vol. 1, no. 4, pp. 41–47, 2012.
- [38] A. K. Agarwal, “Biofuels (alcohols and biodiesel) applications as fuels for internal combustion engines,” *Prog. Energy Combust. Sci.*, vol. 33, no. 3, pp. 233–271, 2007.
- [39] F. K. Forson, E. K. Oduro, and E. Hammond-Donkoh, “Performance of jatropha oil blends in a diesel engine,” *Renew. Energy*, vol. 29, no. 7, pp. 1135–1145, 2004.
- [40] A. S. Ramadhas, S. Jayaraj, and C. Muraleedharan, “Use of vegetable oils as I.C. engine fuels - A review,” *Renew. Energy*, vol. 29, no. 5, pp. 727–742, 2004.
- [41] J. Narayana Reddy and A. Ramesh, “Parametric studies for improving the performance of a Jatropha oil-fuelled compression ignition engine,” *Renew.*

- Energy*, vol. 31, no. 12, pp. 1994–2016, 2006.
- [42] D. Agarwal, L. Kumar, and A. Kumar, “Performance evaluation of a vegetable oil fuelled compression ignition engine,” vol. 33, pp. 1147–1156, 2008.
- [43] R. N. Singh, D. K. Vyas, N. S. L. Srivastava, and M. Narra, “SPRERI experience on holistic approach to utilize all parts of *Jatropha curcas* fruit for energy,” *Renew. Energy*, vol. 33, no. 8, pp. 1868–1873, 2008.
- [44] S. K. Haldar, B. B. Ghosh, and A. Nag, “Studies on the comparison of performance and emission characteristics of a diesel engine using three degummed non-edible vegetable oils,” *Biomass and Bioenergy*, vol. 33, no. 8, pp. 1013–1018, 2009.
- [45] N. R. Banapurmath, P. G. Tewari, and R. S. Hosmath, “Performance and emission characteristics of a DI compression ignition engine operated on Honge, *Jatropha* and Sesame oil methyl esters,” *Renew. Energy*, vol. 33, no. 9, pp. 1982–1988, 2008.
- [46] S. P. Chincholkar, S. Saurabh, A. Rehman, S. Dixit, and A. Lanjewar, “Biodiesel as an alternative fuel for diesel engines,” *Asian J. Exp. Sci.*, vol. 19, no. 2, pp. 13–22, 2005.
- [47] S. K. Jain, S. Kumar, and A. Chaube, “Technical sustainability of biodiesel and its blends with diesel in C. I. engines : a review,” *Int. J. Chem. Eng. Appl.*, vol. 2, no. 2, pp. 102–109, 2011.
- [48] M. Lapuerta, O. Armas, and J. Rodriguez-Fernandez, “Effect of biodiesel fuels on diesel engine emissions,” *Prog. Energy Combust. Sci.*, vol. 34, no. 2, pp. 198–223, 2008.
- [49] G. Dwivedi and M. P. Sharma, “Impact of cold flow properties of biodiesel on engine performance,” *Renew. Sustain. Energy Rev.*, vol. 31, pp. 650–656, 2014.
- [50] B. Kegl, “Effects of biodiesel on emissions of a bus diesel engine,” vol. 99, pp. 863–873, 2008.
- [51] B. Baiju, M. K. Naik, and L. M. Das, “A comparative evaluation of compression ignition engine characteristics using methyl and ethyl esters of *Karanja* oil,” *Renew. Energy*, vol. 34, no. 6, pp. 1616–1621, 2009.
- [52] J. A. Yamin, N. Sakhnini, A. Sakhrieh, and M. A. Hamdan, “Environmental and

- performance study of a 4-Stroke CI engine powered with waste oil biodiesel,” *Sustain. Cities Soc.*, vol. 9, pp. 32–38, 2013.
- [53] G. L. N. Rao, S. Sampath, and K. Rajagopal, “Experimental studies on the combustion and emission characteristics of a diesel engine fuelled with used cooking oil methyl ester and its diesel blends,” *Eng. Technol.*, vol. 4, no. 2, pp. 64–70.
- [54] D. Ramesh, A. Sampathrajan, and T. Nadu, “Investigations on performance and emission characteristics of diesel engine with Jatropha biodiesel and its blends,” *Agric. Eng. Int. CIGR Ejournal*, vol. 10, pp. 1–13, 2008.
- [55] G. V. Subbaiah, K. R. Gopal, S. A. Hussain, B. D. Prasad, K. T. Reddy, and A. Pradesh, “Rice bran oil biodiesel as an additive in diesel-ethanol blends for diesel engines,” *Int. J. Recent Res. Appl. Stud.*, vol. 3, no. June, pp. 334–342, 2010.
- [56] R. Li, Z. Wang, P. Ni, Y. Zhao, M. Li, and L. Li, “Effects of cetane number improvers on the performance of diesel engine fuelled with methanol/biodiesel blend,” *Fuel*, vol. 128, pp. 180–187, 2014.
- [57] E. A. Ajav, B. Singh, and T. K. Bhattacharya, “Experimental study of some performance parameters of a constant speed stationary diesel engine using ethanol-diesel blends as fuel,” *Biomass and Bioenergy*, vol. 17, no. 4, pp. 357–365, 1999.
- [58] A. C. Hansen, Q. Zhang, and P. W. L. Lyne, “Ethanol-diesel fuel blends - A review,” *Bioresour. Technol.*, vol. 96, no. 3, pp. 277–285, 2005.
- [59] R. L. Cole, R. B. Poola, R. Sekar, J. E. Schaus, and P. McPartlin, “Effect of ethanol fuel additive on diesel emissions,” Argonne, Illinois, 2000.
- [60] A. C. Hansen, P. W. L. Lyne, and Q. Zhang, “Ethanol-diesel blends: a step towards a bio-based fuel for diesel engines,” in *ASAE Meeting paper No. 01-6048*, St. Joseph, Mich.: ASAE, 2001.
- [61] M. M. Rahman, S. Stevanovic, R. J. Brown, and Z. Ristovski, “Influence of different alternative fuels on particle emission from a turbocharged common-rail Diesel engine,” *Procedia Eng.*, vol. 56, pp. 381–386, 2013.
- [62] N. Yilmaz, F. M. Vigil, A. B. Donaldson, and T. Darabseh, “Investigation of CI engine emissions in biodiesel – ethanol – diesel blends as a function of ethanol concentration,” pp. 10–13, 2013.

- [63] G. Labeckas, S. Slavinskas, and M. Maz, "The effect of ethanol-diesel- biodiesel blends on combustion, performance and emissions of a direct injection diesel engine," vol. 79, pp. 698–720, 2014.
- [64] C. Jin, M. Yao, H. Liu, C. F. F. Lee, and J. Ji, "Progress in the production and application of n-butanol as a biofuel," *Renew. Sustain. Energy Rev.*, vol. 15, no. 8, pp. 4080–4106, 2011.
- [65] B. Choi *et al.*, "Effect of diesel fuel blend with n-butanol on the emission of a turbocharged common rail direct injection diesel engine," *Appl. Energy*, vol. 146, pp. 20–28, 2015.
- [66] D. Bharti, A. Agrawal, A. N. Shrivastava, and B. Koshti, "Experimental investigation and performance parameter on the effect of n-butanol diesel blends on an single cylinder four stroke diesel engine," *Int. J. Sci. Res. Publ.*, vol. 2, no. 8, pp. 1–8, 2012.
- [67] N. Yilmaz, F. M. Vigil, K. Benalil, S. M. Davis, and A. Calva, "Effect of biodiesel-butanol fuel blends on emissions and performance characteristics of a diesel engine," *Fuel*, vol. 135, pp. 46–50, 2014.
- [68] O. Armas, R. Garcia-Contreras, and A. Ramos, "Pollutant emissions from New European Driving Cycle with ethanol and butanol diesel blends," *Fuel Process. Technol.*, vol. 122, pp. 64–71, 2014.
- [69] E. G. Giakoumis, C. D. Rakopoulos, A. M. Dimaratos, and D. C. Rakopoulos, "Exhaust emissions with ethanol or n-butanol diesel fuel blends during transient operation: A review," *Renew. Sustain. Energy Rev.*, vol. 17, pp. 170–190, 2013.
- [70] D. C. Rakopoulos, C. D. Rakopoulos, and E. G. Giakoumis, "Impact of properties of vegetable oil , bio-diesel , ethanol and n -butanol on the combustion and emissions of turbocharged HDDI diesel engine operating under steady and transient conditions," *Fuel*, vol. 156, pp. 1–19, 2015.
- [71] G. Tuccar, T. Ozgur, and K. Aydin, "Effect of diesel-microalgae biodiesel-butanol blends on performance and emissions of diesel engine," *Fuel*, vol. 132, no. 2014, pp. 47–52, 2014.
- [72] Z. H. Zhang and R. Balasubramanian, "Physicochemical and toxicological characteristics of particulate matter emitted from a non-road diesel engine:

- Comparative evaluation of biodiesel-diesel and butanol-diesel blends,” *J. Hazard. Mater.*, vol. 264, pp. 395–402, 2014.
- [73] O. Dogan, “The influence of n-butanol/diesel fuel blends utilization on a small diesel engine performance and emissions,” *Fuel*, vol. 90, no. 7, pp. 2467–2472, 2011.
- [74] N. Qureshi, B. C. Saha, B. Dien, R. E. Hector, and M. A. Cotta, “Production of butanol (a biofuel) from agricultural residues: Part I - Use of barley straw hydrolysate,” *Biomass and Bioenergy*, vol. 34, no. 4, pp. 559–565, 2010.
- [75] D. C. Rakopoulos, C. D. Rakopoulos, E. G. Giakoumis, A. M. Dimaratos, and D. C. Kyritsis, “Effects of butanol-diesel fuel blends on the performance and emissions of a high-speed di diesel engine,” *Energy Convers. Manag.*, vol. 51, no. 10, pp. 1989–1997, 2010.
- [76] D. C. Rakopoulos, C. D. Rakopoulos, D. T. Hountalas, E. C. Kakaras, E. G. Giakoumis, and R. G. Papagiannakis, “Investigation of the performance and emissions of bus engine operating on butanol/diesel fuel blends,” *Fuel*, vol. 89, no. 10, pp. 2781–2790, 2010.
- [77] C. D. Rakopoulos, K. A. Antonopoulos, and D. C. Rakopoulos, “Experimental heat release analysis and emissions of a HSDI diesel engine fueled with ethanol-diesel fuel blends,” *Energy*, vol. 32, no. 10, pp. 1791–1808, 2007.
- [78] C. D. Rakopoulos, D. C. Rakopoulos, E. G. Giakoumis, and D. C. Kyritsis, “The combustion of n -butanol / diesel fuel blends and its,” vol. 225, pp. 289–308, 2010.
- [79] D. C. Rakopoulos, C. D. Rakopoulos, R. G. Papagiannakis, and D. C. Kyritsis, “Combustion heat release analysis of ethanol or n-butanol diesel fuel blends in heavy-duty di diesel engine,” *Fuel*, vol. 90, no. 5, pp. 1855–1867, 2011.
- [80] C. D. Rakopoulos, A. M. Dimaratos, E. G. Giakoumis, and D. C. Rakopoulos, “Study of turbocharged diesel engine operation, pollutant emissions and combustion noise radiation during starting with bio-diesel or n-butanol diesel fuel blends,” *Appl. Energy*, vol. 88, no. 11, pp. 3905–3916, 2011.
- [81] C. D. Rakopoulos, A. M. Dimaratos, E. G. Giakoumis, and D. C. Rakopoulos, “Investigating the emissions during acceleration of a turbocharged diesel engine operating with bio-diesel or n-butanol diesel fuel blends,” *Energy*, vol. 35, no. 12,

pp. 5173–5184, 2010.

- [82] G. Valentino, F. E. Corcione, S. E. Iannuzzi, and S. Serra, “Experimental study on performance and emissions of a high speed diesel engine fuelled with n-butanol diesel blends under premixed low temperature combustion,” *Fuel*, vol. 92, no. 1, pp. 295–307, 2012.
- [83] Z. Chen, Z. Wu, J. Liu, and C. Lee, “Combustion and emissions characteristics of high n-butanol/diesel ratio blend in a heavy-duty diesel engine and EGR impact,” *Energy Convers. Manag.*, vol. 78, pp. 787–795, 2014.
- [84] S. Yamamoto, Y. Agui, N. Kawaharada, H. Ueki, D. Sakaguchi, and M. Ishida, “Comparison of diesel combustion between ethanol and butanol blended with gas oil,” *SAE Tech. Pap. 2012-32-0020*, 2012.
- [85] A. F. Lopez, M. Cadrazco, A. F. Agudelo, L. A. Corredor, J. A. Velez, and J. R. Agudelo, “Impact of n-butanol and hydrous ethanol fumigation on the performance and pollutant emissions of an automotive diesel engine,” *Fuel*, vol. 153, pp. 483–491, 2015.
- [86] M. Zoeldy, A. Hollo, and A. Thernesz, “Butanol as a diesel extender option for internal combustion engines,” *SAE Tech. Pap. 2010-01-0481*, 2010.
- [87] Z. Sahin and O. N. Aksu, “Experimental investigation of the effects of using low ratio n-butanol/diesel fuel blends on engine performance and exhaust emissions in a turbocharged DI diesel engine,” *Renew. Energy*, vol. 77, pp. 279–290, 2015.
- [88] Sahin, Zehra, O. Durgun, and O. N. Aksu, “Experimental investigation of n-butanol/diesel fuel blends and n-butanol fumigation - evaluation of engine performance, exhaust emissions, heat release and flammability analysis,” *Energy Convers. Manag.*, vol. 103, pp. 778–789, 2015.
- [89] S. S. Merola, C. Tornatore, S. E. Iannuzzi, L. Marchitto, and G. Valentino, “Combustion process investigation in a high speed diesel engine fuelled with n-butanol diesel blend by conventional methods and optical diagnostics,” *Renew. Energy*, vol. 64, pp. 225–237, 2014.
- [90] L. Siwale *et al.*, “Combustion and emission characteristics of n-butanol/diesel fuel blend in a turbo-charged compression ignition engine,” *Fuel*, vol. 107, pp. 409–418, 2013.

- [91] K. Fushimi, E. Kinoshita, and Y. Yoshimoto, "Effect of butanol isomer on diesel combustion Characteristics of butanol / gas oil blend," *SAE Tech. Pap. 2013-32-9097*, 2013.
- [92] Z. Chen, J. Liu, Z. Han, B. Du, Y. Liu, and C. Lee, "Study on performance and emissions of a passenger-car diesel engine fueled with butanol-diesel blends," *Energy*, vol. 55, pp. 638–646, 2013.
- [93] Z. H. Zhang, S. M. Chua, and R. Balasubramanian, "Comparative evaluation of the effect of butanol-diesel and pentanol-diesel blends on carbonaceous particulate composition and particle number emissions from a diesel engine," *Fuel*, vol. 176, pp. 40–47, 2016.
- [94] A. Ibrahim, "Performance and combustion characteristics of a diesel engine fuelled by butanol-biodiesel-diesel blends," *Appl. Therm. Eng.*, vol. 103, pp. 651–659, 2016.
- [95] H. Liu, S. Li, Z. Zheng, J. Xu, and M. Yao, "Effects of n-butanol, 2-butanol, and methyl octynoate addition to diesel fuel on combustion and emissions over a wide range of exhaust gas recirculation (EGR) rates," *Appl. Energy*, vol. 112, no. x, pp. 246–256, 2013.
- [96] M. Zheng, T. Li, and X. Han, "Direct injection of neat n-butanol for enabling clean low temperature combustion in a modern diesel engine," *Fuel*, vol. 142, pp. 28–37, 2015.
- [97] H. Huang, Q. Liu, R. Yang, T. Zhu, R. Zhao, and Y. Wang, "Investigation on the effects of pilot injection on low temperature combustion in high-speed diesel engine fueled with n-butanol-diesel blends," *Energy Convers. Manag.*, vol. 106, pp. 748–758, 2015.
- [98] N. Zhou, M. Huo, H. Wu, K. Nithyanandan, C. fon F. Lee, and Q. Wang, "Low temperature spray combustion of acetone-butanol-ethanol (ABE) and diesel blends," *Appl. Energy*, vol. 117, pp. 104–115, 2014.
- [99] A. Atmanli, E. Ileri, and B. Yuksel, "Experimental investigation of engine performance and exhaust emissions of a diesel engine fueled with diesel–n-butanol–vegetable oil blends," *Energy Convers. Manag.*, vol. 81, pp. 312–321, 2014.

- [100] A. Atmanli, E. Ileri, B. Yuksel, and N. Yilmaz, "Extensive analyses of diesel-vegetable oil-n-butanol ternary blends in a diesel engine," *Appl. Energy*, vol. 145, pp. 155–162, 2015.
- [101] A. Atmanli, E. Ileri, and B. Yuksel, "Effects of higher ratios of n-butanol addition to diesel-vegetable oil blends on performance and exhaust emissions of a diesel engine," *J. Energy Inst.*, vol. 88, no. 3, pp. 209–220, 2015.
- [102] A. Atmanli, "Comparative analyses of diesel-waste oil biodiesel and propanol, n-butanol or 1-pentanol blends in a diesel engine," *Fuel*, vol. 176, pp. 209–215, 2016.
- [103] S. Imtenan, H. H. Masjuki, M. Varman, I. M. Rizwanul Fattah, H. Sajjad, and M. I. Arbab, "Effect of n-butanol and diethyl ether as oxygenated additives on combustion-emission-performance characteristics of a multiple cylinder diesel engine fuelled with diesel-jatropha biodiesel blend," *Energy Convers. Manag.*, vol. 94, pp. 84–94, 2015.
- [104] M. A. Fayad, A. Tsolakis, D. Fernandez-Rodriguez, J. M. Herreros, F. J. Martos, and M. Lapuerta, "Manipulating modern diesel engine particulate emission characteristics through butanol fuel blending and fuel injection strategies for efficient diesel oxidation catalysts," *Appl. Energy*, vol. 190, pp. 490–500, 2017.
- [105] M. Z. Isik, H. Bayındır, B. Iscan, and H. Aydın, "The effect of n-butanol additive on low load combustion, performance and emissions of biodiesel-diesel blend in a heavy duty diesel power generator," *J. Energy Inst.*, vol. 90, no. 2, pp. 174–184, 2017.
- [106] M. Vojtisek-Lom *et al.*, "Blends of butanol and hydrotreated vegetable oils as drop-in replacement for diesel engines: Effects on combustion and emissions," *Fuel*, vol. 197, pp. 407–421, 2017.
- [107] N. Nabi, A. Zare, F. M. Hossain, T. A. Bodisco, Z. D. Ristovski, and R. J. Brown, "A parametric study on engine performance and emissions with neat diesel and diesel-butanol blends in the 13-Mode European Stationary Cycle," *Energy Convers. Manag.*, vol. 148, pp. 251–259, 2017.
- [108] S. Saravanan, B. R. Kumar, A. Varadharajan, D. Rana, B. Sethuramasamyraja, and G. L. Narayana, "Optimization of DI diesel engine parameters fueled with iso -

- butanol / diesel blends – Response surface methodology approach,” *Fuel*, vol. 203, pp. 658–670, 2017.
- [109] H. Huang, Q. Liu, W. Teng, and Q. Wang, “The potentials for improving combustion performance and emissions in diesel engines by fueling n- butanol / diesel / PODE 3-4 blends,” *Energy Procedia*, vol. 105, pp. 914–920, 2017.
- [110] A. Nayyar, D. Sharma, S. Lal, and A. Mathur, “Characterization of n-butanol diesel blends on a small size variable compression ratio diesel engine : Modeling and experimental investigation,” *Energy Convers. Manag.*, vol. 150, no. x, pp. 242–258, 2017.
- [111] A. Nayyar, D. Sharma, S. Lal, and A. Mathur, “Experimental investigation of performance and emissions of a VCR diesel engine fuelled with n-butanol diesel blends under varying engine parameters,” *Environ. Sci. Pollut. Res.*, 2017.
- [112] G. Yanfeng, L. Shenghua, G. Hejun, H. Tiegang, and Z. Longbao, “A new diesel oxygenate additive and its effects on engine combustion and emissions,” *Appl. Therm. Eng.*, vol. 27, no. 1, pp. 202–207, 2007.
- [113] H. J. Curran *et al.*, “Detailed chemical kinetic modeling of diesel combustion with oxygenated fuels,” *SAE Tech. Pap. 2001-01-0653*, 2001.
- [114] M. Shahabuddina, H. H. Masjuki, M. A. Kalam, M. Mofijur, M. A. Hazrat, and A. M. Liaquat, “Effect of additive on performance of C.I. engine fuelled with bio diesel,” *Energy Procedia*, vol. 14, no. 2011, pp. 1624–1629, 2012.
- [115] C. Y. Lin and J. C. Huang, “An oxygenating additive for improving the performance and emission characteristics of marine diesel engines,” *Ocean Eng.*, vol. 30, no. 13, pp. 1699–1715, 2003.
- [116] G. Chen, Y. Shen, Q. Zhang, M. Yao, Z. Zheng, and H. Liu, “Experimental study on combustion and emission characteristics of a diesel engine fueled with 2,5-dimethylfuran-diesel, n-butanol-diesel and gasoline-diesel blends,” *Energy*, vol. 54, pp. 333–342, 2013.
- [117] H. Liu, J. Xu, Z. Zheng, S. Li, and M. Yao, “Effects of fuel properties on combustion and emissions under both conventional and low temperature combustion mode fueling 2,5-dimethylfuran/diesel blends,” *Energy*, vol. 62, no. 215–223, 2013.

- [118] R. Vallinayagam *et al.*, “Impact of ignition promoting additives on the characteristics of a diesel engine powered by pine oil-diesel blend,” *Fuel*, vol. 117, pp. 278–285, 2014.
- [119] E. Khalife, M. Tabatabaei, A. Demirbas, and M. Aghbashlo, “Impacts of additives on performance and emission characteristics of diesel engines during steady state operation,” *Prog. Energy Combust. Sci.*, vol. 59, pp. 32–78, 2017.
- [120] M. N. Nabi *et al.*, “Influence of fuel-borne oxygen on european stationary cycle: diesel engine performance and emissions with a special emphasis on particulate and NO emissions,” *Energy Convers. Manag.*, vol. 127, pp. 187–198, 2016.
- [121] C. He *et al.*, “Size-segregated particulate matter emission characteristics of a heavy-duty diesel engine with oxygenated fuels,” *Appl. Therm. Eng.*, vol. 125, pp. 1173–1180, Oct. 2017.
- [122] P. R. Shah and A. Ganesh, “A comparative study on influence of fuel additives with edible and non-edible vegetable oil based on fuel characterization and engine characteristics of diesel engine,” *Appl. Therm. Eng.*, vol. 102, pp. 800–812, 2016.
- [123] R. R. Raine and H. Thorwarth, “Performance and combustion characteristics of a glow-ignition two-stroke engine,” *SAE Tech. Pap. 2004-01-1407*, 2004.
- [124] A. Ambekar, R. Bhangale, R. Chatterjee, C. Kulkarni, S. Kumar, and A. Chowdhury, “Glow-plug-assisted combustion of nitromethane sprays in a constant volume chamber,” *Appl. Therm. Eng.*, vol. 76, pp. 462–474, 2015.
- [125] Q. Zhang, W. Li, D. Lin, N. He, and Y. Duan, “Influence of nitromethane concentration on ignition energy and explosion parameters in gaseous nitromethane / air mixtures,” *J. Hazard. Mater.*, vol. 185, no. 2–3, pp. 756–762, 2011.
- [126] M. Saei Moghaddam and A. Zarringhalam Moghaddam, “Performance and exhaust emission characteristics of a CI engine fueled with diesel-nitrogenated additives,” *Chem. Eng. Res. Des.*, vol. 92, no. 4, pp. 720–726, 2014.
- [127] V. Pirouzfard, A. Zarringhalam, and B. Mirza, “Physicochemical properties and combustion performance of gas oil-fuel additives,” *J. Energy Resour. Technol.*, vol. 134, no. 4, 2012.
- [128] F. Ommi, K. Nekofar, and V. Pirozfar, “Emission and properties characteristics

- using additive- ethanol-diesel fuel blends on a diesel engine,” *J. Eng. Ann. Fac. Eng. Hunedoara*, vol. 7, no. 2, pp. 35–42, 2009.
- [129] A. Fayyazbakhsh and V. Pirouzfard, “Investigating the influence of additives-fuel on diesel engine performance and emissions: Analytical modeling and experimental validation,” *Fuel*, vol. 171, pp. 167–177, 2016.
- [130] A. Fayyazbakhsh and V. Pirouzfard, “Determining the optimum conditions for modified diesel fuel combustion considering its emission, properties and engine performance,” *Energy Convers. Manag.*, vol. 113, pp. 209–219, 2016.
- [131] C. G. McCreath and F. Technology, “The effect of fuel additives on the exhaust emissions from diesel engines,” *Combust. Flame*, vol. 17, no. 3, pp. 359–366, 1971.
- [132] H. Ma, K. Kar, R. Stone, R. Raine, and H. Thorwarth, “Analysis of combustion in a small homogeneous charge compression assisted ignition engine,” *Int. J. Engine Res.*, vol. 7, no. 3, pp. 237–253, 2006.
- [133] Y. Ren *et al.*, “Combustion and emissions of a DI diesel engine fuelled with diesel-oxygenate blends,” *Fuel*, vol. 87, no. 12, pp. 2691–2697, 2008.
- [134] Y. Di, C. S. Cheung, and Z. Huang, “Experimental investigation of particulate emissions from a diesel engine fueled with ultralow-sulfur diesel fuel blended with diglyme,” *Atmos. Environ.*, vol. 44, no. 1, pp. 55–63, 2010.
- [135] P. Baskar, K. Nanthagopal, and T. Elango, “The effect of two oxygenates on diesel engine emissions,” *ARPJ. Eng. Appl. Sci.*, vol. 6, no. 3, pp. 55–60, 2011.
- [136] O. Purchase and P. Export, “The potential of dimethylether (DME) as an alternative fuel for compression ignition-engines A review,” no. 4, pp. 10–13.
- [137] M. Pugazhivadivu and S. Rajagopan, “Investigations on a diesel engine fuelled with biodiesel blends and diethyl ether as an additive,” *Indian J. Sci. Technol.*, vol. 2, no. 5, pp. 31–35, 2009.
- [138] B. Bailey, J. Eberhardt, S. Goguen, and J. Erwin, “Diethyl ether (DEE) as a renewable diesel fuel,” *SAE Tech. Pap. 972978*, 1997.
- [139] I. Sezer, “Thermodynamic, performance and emission investigation of a diesel engine running on dimethyl ether and diethyl ether,” *Int. J. Therm. Sci.*, vol. 50, no. 8, pp. 1594–1603, 2011.

- [140] D. H. Qi, H. Chen, L. M. Geng, and Y. Z. Bian, "Effect of diethyl ether and ethanol additives on the combustion and emission characteristics of biodiesel-diesel blended fuel engine," *Renew. Energy*, vol. 36, no. 4, pp. 1252–1258, 2011.
- [141] C. Cinar, O. Can, F. Sahin, and H. S. Yucesu, "Effects of premixed diethyl ether (DEE) on combustion and exhaust emissions in a HCCI-DI diesel engine," *Appl. Therm. Eng.*, vol. 30, no. 4, pp. 360–365, 2010.
- [142] D. C. Rakopoulos, C. D. Rakopoulos, E. G. Giakoumis, and A. M. Dimaratos, "Studying combustion and cyclic irregularity of diethyl ether as supplement fuel in diesel engine," *Fuel*, vol. 109, pp. 325–335, 2013.
- [143] D. C. Rakopoulos, C. D. Rakopoulos, E. G. Giakoumis, and A. M. Dimaratos, "Characteristics of performance and emissions in high-speed direct injection diesel engine fueled with diethyl ether/diesel fuel blends," *Energy*, vol. 43, no. 1, pp. 214–224, 2012.
- [144] D. C. Rakopoulos, "Combustion and emissions of cottonseed oil and its bio-diesel in blends with either n-butanol or diethyl ether in HSDI diesel engine," *Fuel*, vol. 105, pp. 603–613, 2013.
- [145] M. L. Jesu, V. E. Geo, D. K. Jebo, and B. Nagalingam, "A comparative analysis of different methods to improve the performance of cotton seed oil fuelled diesel engine," *Fuel*, vol. 102, pp. 372–378, 2012.
- [146] R. Anand and N. V Mahalakshmi, "Simultaneous reduction of NO_x and smoke from a direct-injection diesel engine with exhaust gas recirculation and diethyl ether," *Proc. Inst. Mech. Eng. Part-D, J. Automob. Eng.*, vol. 221, no. 1, pp. 109–116, 2007.
- [147] N. Kapilan, P. Mohanan, and R. P. Reddy, "performance and emission studies of diesel engine using diethyle ether as oxygenated fuel additive," *SAE Tech. Pap. 2008-01-2466*, 2008.
- [148] P. Mohanan, N. Kapilan, and R. P. Reddy, "Effect of diethyle ether on the performance and emission of a 4-s DI diesel engine," *SAE Tech. Pap. 2003-01-0760*, 2003.
- [149] S. Lee and T. Y. Kim, "Performance and emission characteristics of a DI diesel engine operated with diesel/DEE blended fuel," *Appl. Therm. Eng.*, vol. 121, pp.

- 454–461, 2017.
- [150] Y. Ren *et al.*, “Effect of the addition of diglyme in diesel fuel on combustion and emissions in a compression-ignition engine,” *Energy and Fuels*, vol. 21, no. 5, pp. 2573–2583, 2007.
- [151] D. C. Rakopoulos, C. D. Rakopoulos, E. G. Giakoumis, and A. M. Dimaratos, “Studying combustion and cyclic irregularity of diethyl ether as supplement fuel in diesel engine,” *FUEL*, vol. 2, pp. 1–11, 2013.
- [152] R. J. Moffat, “Describing the uncertainties in experimental results,” *Exp. Therm. Fluid Sci.*, vol. 1, no. 1, pp. 3–17, 1988.
- [153] D. C. Rakopoulos, C. D. Rakopoulos, and D. C. Kyritsis, “Butanol or DEE blends with either straight vegetable oil or biodiesel excluding fossil fuel : Comparative effects on diesel engine combustion attributes , cyclic variability and regulated emissions trade-off,” *Energy*, vol. 115, pp. 314–325, 2016.
- [154] E. G. Giakoumis, C. D. Rakopoulos, A. M. Dimaratos, and D. C. Rakopoulos, “Exhaust emissions with ethanol or n-butanol diesel fuel blends during transient operation: A review,” *Renew. Sustain. Energy Rev.*, vol. 17, pp. 170–190, 2013.
- [155] Y. Jian-guang, Z. Wu-gao, and H. Zhen, “Effect of cetane number improver on heat release rate and emissions of high speed diesel engine fueled with ethanol – diesel blend fuel,” *Fuel*, vol. 83, no. 2004, pp. 2013–2020, 2013.
- [156] N. Nabi and J. Einar, “Experimental investigation of engine emissions with marine gas oil-oxygenate blends,” *Sci. Total Environ.*, vol. 408, no. 16, pp. 3231–3239, 2010.
- [157] D. Y. Chang and J. H. V. Gerpen, “Determination of particulate and unburned hydrocarbon emissions from diesel engines fueled with biodiesel,” *SAE Tech. Pap. No. 982527*, 1998.
- [158] T. C. Zannis, D. T. Hountalas, and D. . Kouremenos, “Experimental investigation to specify the effect of oxygenated additive content and type on DI diesel engine performance and emissions,” *SAE Tech. Pap. 2004-01-0097*, 2004.
- [159] S. S. Gill, A. Tsolakis, J. M. Herreros, and A. P. E. York, “Diesel emissions improvements through the use of biodiesel or oxygenated blending components,” *Fuel*, vol. 95, pp. 578–586, 2012.

- [160] F. Xin *et al.*, “Comprehensive investigations of biobutanol production by a non-acetone and 1,3-propanediol generating clostridium strain from glycerol and polysaccharides,” *Biotechnol. Biofuels*, vol. 9, pp. 1–12, 2016.
- [161] B. Ndaba, I. Chiyanzu, and S. Marx, “N-Butanol derived from biochemical and chemical routes: A review,” *Biotechnol. Reports*, vol. 8, pp. 1–9, 2015.
- [162] D. E. Ramey, “Butanol : The other alternative fuel,” 2007.
- [163] P. H. Pfromm, V. Amanor-Boadu, R. Nelson, P. Vadlani, and R. Madl, “Bio-butanol vs. bio-ethanol: A technical and economic assessment for corn and switchgrass fermented by yeast or clostridium acetobutylicum,” *Biomass and Bioenergy*, vol. 34, no. 4, pp. 515–524, 2010.
- [164] N. Qureshi and H. P. Blaschek, “ABE production from corn: a recent economic evaluation.,” *J. Ind. Microbiol. Biotechnol.*, vol. 27, no. 5, pp. 292–7, 2001.
- [165] N. Qureshi, B. C. Saha, M. A. Cotta, and V. Singh, “An economic evaluation of biological conversion of wheat straw to butanol: A biofuel,” *Energy Convers. Manag.*, vol. 65, pp. 456–462, 2013.

Appendix-A

$$\text{Calorific value of blend, } C_v \text{ (kJ/kg)} = \frac{\left(\frac{v_1}{v} \times \rho_1 \times C_{v1}\right) + \left(\frac{v_2}{v} \times \rho_2 \times C_{v2}\right) + \dots + \left(\frac{v_i}{v} \times \rho_i \times C_{vi}\right)}{\left(\frac{v_1}{v} \times \rho_1\right) + \left(\frac{v_2}{v} \times \rho_2\right) + \dots + \left(\frac{v_i}{v} \times \rho_i\right)}$$

$$\text{Cetane number of blends, } CN = \left(\frac{v_1}{v} \times CN_1\right) + \left(\frac{v_2}{v} \times CN_2\right) + \dots + \left(\frac{v_i}{v} \times CN_i\right)$$

$$\text{Brake Power, } BP \text{ (kW)} = \frac{T(2\pi N)}{(60 \times 1000)}$$

$$\text{Brake Thermal Efficiency, } BTE \text{ (\%)} = \frac{BP \times 3600}{(m_f \times C_v)} \times 100$$

$$\text{Brake Specific Fuel Consumption, } BSEC \text{ (kg/kW-h)} = \frac{m_f \times C_v}{BP}$$

Where:

C_v = Calorific value of blend (kJ/kg), $C_{v1}, C_{v2}, \dots, C_{vi}$ = calorific value blended fuels (kJ/kg),

v_1, v_2, \dots, v_i = volume percentage blended fuels, $v = v_1 + v_2 + \dots + v_i$

$\rho_b, \rho_1, \dots, \rho_i$ = density of blended fuels (kg/m^3),

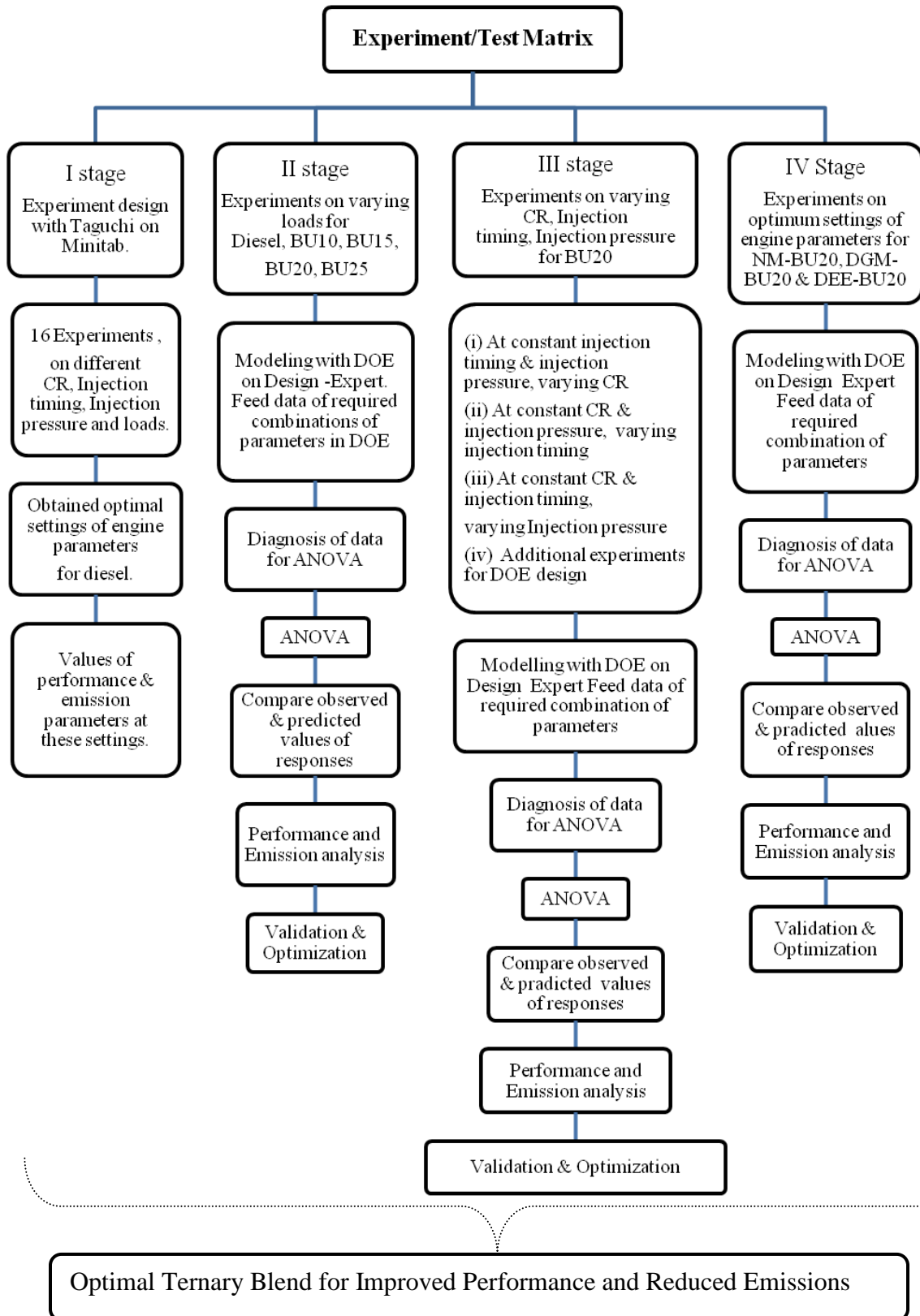
CN = Cetane number of blends

CN_1, CN_2, \dots, CN_i = Cetane number of blended fuels

T = Brake torque (i.e. load) (Nm), N = r.p.m.

m_f = mass of fuel consumption (kg/h),

Appendix-B



Appendix-C

Calorific value and Cetane number of n-butanol-diesel blends

S.No.	Fuel/Blend	Calorific value (kJ/kg)	Cetane number
1.	BU10	42039	52.5
2.	BU15	41556	50.9
3.	BU20	41071	49.4
4.	BU25	40585	47.9

Calorific value of nitromethane-n-butanol-diesel blends

S.No.	Fuel/Blend	Calorific value (kJ/kg)
1.	NM1BU20	40655
2.	NM2BU20	40241
3.	NM3BU20	39831

Calorific value and Cetane number of diglyme-n-butanol-diesel blends

S.No.	Fuel/Blend	Calorific value (kJ/kg)	Cetane number
1.	DGM5BU20	40143.7	53.2
2.	DGM10BU20	39228.0	57.1
3.	DGM15BU20	38323.7	60.9
4.	DGM20BU20	37430.4	64.7

Calorific value and Cetane number of diethylether-n-butanol-diesel blends

S. No.	Fuel/Blend	Calorific value (kJ/kg)	Cetane No.
1.	DEE5BU20	40761.4	53.2
2.	DEE10BU20	40447.2	57.0
3.	DEE15BU20	40128.5	60.7
4.	DEE20BU20	39805.2	64.5

Brief bio-data

Ashish Nayyar was born on 26th August, 1977 to Mr. S.M. Nayyar and Suman Nayyar. He passed his Bachelor of Engineering in Mechanical Engineering in 2002 from M.B.M Engineering College, Jodhpur. He is working in the field of education since last 15 years. He completed his M. Tech. (Mechanical Engineering) with specialization in Energy Engineering from MNIT, Jaipur in 2009.

Presently he is working as an Associate Professor in Department of Mechanical Engineering, Swami Keshvanand Institute of Technology, Management and Gramothan, Jaipur. He is a member of SAEINDIA, ASME, Institution of Engineers (India), ISTE and reviewer of two Journals (Environmental Science and Pollution Research & International Energy Journal). Recently, in June, 2017 he has presented his research paper in ASME-Power and Energy Conference held at Charlotte, NC, USA. He was awarded with Travel Grant from All India Council for Technical Education (AICTE), New Delhi and Department of Science and Technology, Rajasthan, India for participation in this conference. He has organized several National and one International conference. He has also received grant to organize conference from Ministry of New and Renewable Energy, India and for development of laboratory under MODROB scheme of AICTE. He has been completed doctoral degree from Malaviya National Institute of Technology Jaipur in April, 2018.

Publications

Papers published in international journals

1. A. Nayyar, D. Sharma, S. Lal, and A. Mathur, “Characterization of n-butanol diesel blends on a small size variable compression ratio diesel engine : Modeling and experimental investigation,” *Energy Convers Manag*, vol. 150, pp. 242–258, 2017.
2. A. Nayyar, D. Sharma, S. Lal, and A. Mathur, “Experimental investigation of performance and emissions of a VCR diesel engine fuelled with n-butanol diesel blends under varying engine parameters,” *Environ Sci Pollut Res*, vol. 24, no. 25, pp. 20315–20329, 2017.

Papers presented/published in international conferences:

1. A. Nayyar, D. Sharma, S. L. Soni, and A. Mathur, “POWER-ICOPE2017-3236, Experimental study of performance and exhaust emissions of a VCR diesel engine fuelled with oxygenated additives” in ASME online, 2017, pp. 1–10.<http://proceedings.asmedigitalcollection.asme.org/proceeding.aspx?articleid=2653575>
2. A. Nayyar, D. Sharma, and S. L. Soni, “Opportunity of Using Additives Diesel Fuel Blends in C. I. Engines : A Review,” in ICEMS 2016, JNU, Jaipur, pp. 224–225.